

Detailed Seismic Assessment

Revised C8 – Unreinforced Masonry Buildings For Non-Earthquake Prone Building Purposes

AUGUST 2025
PUBLIC COMMENT DRAFT

Foreword

The Joint Committee for Seismic Assessment and Retrofit of Existing Buildings is responsible for the joint oversight of the system used to assess, communicate, manage and mitigate seismic risk in existing buildings. It reviews how the guidelines are functioning in practice, identifies areas that require further input and development, and either advises on or assists in the development of proposals for work programmes that contribute towards these objectives. The Joint Committee includes representatives from The Natural Hazards Commission Toka Tū Ake, the Ministry of Business, Innovation & Employment, and the technical societies (NZGS, NZSEE, SESOC).

The Joint Committee's Vision is that:

- Seismic retrofits are being undertaken when necessary to reduce our seismic risk over time while limiting unnecessary disruption, demolitions and carbon impacts, promoting continued use or re-use of buildings.
- Decisions on retrofitting are informed by an appropriate understanding of seismic risk and are aligned with longer term asset planning.
- Seismic assessment and retrofit guidelines help engineers focus on the most critical vulnerabilities in a building, serve the needs of the market and regulation, and evolve through a stable ongoing cycle allowing new knowledge and improvements to be included in a predictable manner, including the consideration of objectives beyond life safety.
- Engineers are supported in the implementation of Seismic Assessment and Retrofit Guidelines through a range of training and information sharing strategies, including tools for risk communication to manage unnecessary vacating of buildings.
- Society is informed about the level of risk posed by existing buildings.

Acknowledgements

This document was prepared by the Joint Committee, including:

Joint Committee

Nic Brooke	SESOC
Dave Brunsdon	SESOC
Alistair Cattanach	SESOC
Caleb Dunne	NHC
Ken Elwood	MBIE
Rob Jury	NZSEE
Stuart Palmer	NZGS
Mark Ryburn	MBIE
Henry Tatham	NZSEE
Merrick Taylor	NZGS
Andy Thompson	NZSEE

Technical review group

Jason Ingham (Chair)
Yuni Azhari
Alistair Cattanach
Hossein Derakhshan
Francisco Galvez
Hamish Tocher
Nicki Vance

Version Record

Version	Date	Purpose/ Summary of changes
1	17 July 2017	Initial release
2 (Draft)	August 2025	Revision with additional information (see summary on page iv) Release for Public Comment only

This document is managed by the Joint Committee for Seismic Assessment and Retrofit of Existing Buildings.

Refer to the following pages for a summary of the key changes from previous versions.

Please submit any feedback to nonEPBguidanceconsultation@engineeringnz.org

Copyright

The copyright owner authorises reproduction of this work, in whole or in part, so long as no charge is made for the supply of copies and the integrity and attribution of the contributors and publishers of the document is not interfered with in any way.

Where the material is being published or issued to others, the source and copyright status should be acknowledged.

The permission to reproduce copyright material does not extend to any material in this report that is identified as being the copyright of a third party. Authorisation to reproduce such material should be obtained from the copyright holders.

Disclaimer

This document is intended as a guideline only. This document is intended for use by trained practitioners under appropriate supervision and review. Practitioners must exercise professional skill and judgement in its application.

This document has not been released under Section 175 of the Building Act. While care has been taken in preparing this document, it should not be used as a substitute for legislation or legal advice.

It is not mandatory to use the information in this document, but if used:

- This document does not relieve any person or consenting authority of the obligation to conduct their own professional enquiries, research or assessments, and to exercise their own independent judgement, according to the circumstances of the particular case;
- Consenting authorities are not bound to accept the information as demonstrating compliance with any relevant Acts, Codes or Standards.

Neither the Joint Committee, nor any of its member organisations, nor any of their respective employees, is responsible for any actions taken on the basis of information in this document, or any errors or omissions.

Users of information from this publication assume all liability arising from such use.

By continuing to use the document, a user confirms that they agree to these terms

This section is part of the *Non-EPB (Earthquake-Prone Building) Seismic Assessment Guidelines* which constitute a proposed technical revision to the 1 July 2017 EPB Seismic Assessment Guidelines. The *Non-EPB Seismic Assessment Guidelines* may be used for general commercial Detailed Seismic Assessments for non-EPB purposes. It is to be used in conjunction with Part A of the *EPB Seismic Assessment Guidelines*.

Engineers engaged to assess buildings identified by a territorial authority as being potentially earthquake prone in accordance with the *EPB Methodology* must continue to use *EPB Seismic Assessment Guidelines* (1 July 2017) as these are referenced in the Methodology.

Summary of Key Changes from Version 1

This 2025 update to C8 has included:

- Expanded details regarding the treatment of cavity walls
- Greater discussion regarding the selection of boundary conditions for out-of-plane wall response
- A procedure for the detailed assessment of masonry gables, including the preparation of charts to facilitate the assessment process
- Expanded clarification for how to select an equivalent frame when assessing the in-plane response of a penetrated unreinforced masonry wall
- Expanded details on horizontally-spanning masonry walls, including advice on strongbacks
- Corrections to the charts in Appendix C8C
- A significant number of worked examples.

Other sections where less extensive modification have been introduced include:

- Reference to section C11 for the consideration of reinforced concrete masonry
- Considerations when assessing a registered heritage building
- Brief comments on how to assess unreinforced masonry parts that are found in building types that are not predominantly of unreinforced masonry construction.
- Brief comments on how to subdivide a complex URM building into more macroelements
- Procedure when an unreinforced masonry wall is a basement and subjected to soil pressures
- Aspects to consider when a concrete ring beam or bond beam is present.
- Further advice on aspects related to toe crushing.

In most cases the new information is providing expanded clarification or is addressing an identified omission in the 2015 issue of C8.

Several changes in the 2025 issue of C8 will influence the calculated %NBS score. These changes are:

1. Criteria for rocking displacement have been relaxed. This change was consistent with changes made to more recent releases from ACSE-41 which is the source document for the criteria. This change will elevate %NBS scores in a small number of cases where overall response is dictated by the rocking limit.
2. Errors were identified and have been corrected in the charts for face-loaded walls. There was no error in the guidance formulas and text, so this error only impacts assessments that used the charts. This correction will elevate the evaluated %NBS score when using the new charts.
3. Errors were identified and have been corrected in the charts for the out-of-plane response of vertical cantilevers (parapets and some one-storey walls). There were no errors in the guidance formulas and text, so this error only impacts assessments that used the charts. Feedback indicates that most assessors code the formulation into spreadsheets, so only a subset of all assessments relied only on the charts.

The error identified in Item 3 is unconservative and is the only change that will potentially result in a lower calculated %NBS score. There is a narrow range of parapet configurations which would have previously exceeded 33% using the old charts and would now score below 33% using the corrected charts. For example, for a 2-leaf parapet and soil class C, the parapet height would have the range shown in the table below.

Seismic Zone	Low	Medium	High
Parapet height (mm)	700-1600	450-700	250

Most parapets would be over 250mm and typically in High zone would have braced regardless of assessment outcomes or would have restraint from the likes of gutters or flashings if lower than 250mm,. Few Medium zone parapets are likely to be at this height: parapets are most commonly less than 450 mm or more than 1200 mm high. Low zone parapets represent the greatest residual risk. This risk only exists if the charts were used to assess parapet stability rather than the mathematical formulation (which engineers often carry out by standard spreadsheet).

Contents

C8. Unreinforced Masonry Buildings.....C8-1

C8.1 General.....	C8-1
C8.1.1 Background	C8-1
C8.1.2 Scope	C8-3
C8.1.3 Basis of this section.....	C8-4
C8.1.4 How to use this section	C8-5
C8.1.5 Definitions and acronyms	C8-5
C8.1.6 Notation, symbols and abbreviations	C8-8
C8.2 Typical URM Building Practices in New Zealand	C8-14
C8.2.1 Consideration of heritage features	C8-14
C8.2.2 Building forms.....	C8-15
C8.2.2.1 Ornamental features and appendages.....	C8-18
C8.2.2.2 URM components in non-URM Buildings.....	C8-19
C8.2.2.3 Subdivision of complex URM buildings into macroelements	C8-19
C8.2.3 Foundations.....	C8-20
C8.2.4 Solid and Cavity Walls.....	C8-21
C8.2.4.1 Typical wall thickness.....	C8-24
C8.2.4.2 Cavity ties	C8-25
C8.2.4.3 Masonry bond pattern and cross sections	C8-26
C8.2.5 Constituent materials.....	C8-30
C8.2.5.1 Bricks.....	C8-30
C8.2.5.2 Mortar	C8-30
C8.2.5.3 Timber	C8-30
C8.2.5.4 Concrete block	C8-30
C8.2.6 Floor/roof diaphragms	C8-30
C8.2.6.1 Timber floors	C8-31
C8.2.6.2 Reinforced concrete slabs.....	C8-31
C8.2.6.3 Roofs	C8-32
C8.2.7 Diaphragm seating and connections.....	C8-33
C8.2.8 Wall to wall connections	C8-36
C8.2.9 Damp-proof course (DPC).....	C8-36
C8.2.10 Built-in timber	C8-37
C8.2.11 Concrete ring beams or bond beams.....	C8-38
C8.2.12 Bed-joint reinforcement	C8-40
C8.2.13 Lintels	C8-40
C8.2.14 Secondary structure and critical non-structural items	C8-41
C8.2.15 Seismic strengthening methods used to date	C8-41
C8.3 Observed Seismic Behaviour of URM Buildings.....	C8-47
C8.3.1 General.....	C8-47
C8.3.2 Building configuration	C8-48
C8.3.3 Diaphragms	C8-49
C8.3.4 Connections	C8-50
C8.3.4.1 General.....	C8-50
C8.3.4.2 Wall to wall connections	C8-50

C8.3.4.3	Wall to floor/wall to roof connections.....	C8-51
C8.3.5	Walls subjected to face loads.....	C8-54
C8.3.6	Walls subjected to in-plane loads.....	C8-56
C8.3.7	Secondary members/elements	C8-60
C8.3.8	Pounding	C8-61
C8.3.9	Foundations and geotechnical failure	C8-62
C8.4	Factors Affecting Seismic Performance of URM Buildings	C8-63
C8.4.1	Number of cycles and duration of shaking	C8-63
C8.4.2	Other key factors	C8-64
C8.4.2.1	General.....	C8-64
C8.4.2.2	Building form	C8-64
C8.4.2.3	Unrestrained components	C8-64
C8.4.2.4	Connections	C8-64
C8.4.2.5	Wall slenderness	C8-64
C8.4.2.6	Diaphragm deficiency.....	C8-65
C8.4.2.7	In-plane walls	C8-65
C8.4.2.8	Foundations.....	C8-65
C8.4.2.9	Redundancy	C8-65
C8.4.2.10	Quality of construction and alterations	C8-65
C8.4.2.11	Maintenance	C8-66
C8.5	Assessment Approach.....	C8-66
C8.5.1	General.....	C8-66
C8.5.2	Assessment process	C8-68
C8.5.3	Assessment of strengthened buildings	C8-73
C8.5.3.1	Wall-to-diaphragm anchors	C8-73
C8.5.3.2	Diaphragm continuity.....	C8-74
C8.5.3.3	Deformation compatibility	C8-74
C8.5.4	Assessment of URM row buildings	C8-75
C8.5.4.1	General performance	C8-76
C8.5.4.2	Building interconnection	C8-76
C8.6	On-site Investigations	C8-77
C8.6.1	General.....	C8-77
C8.6.2	Form and configuration	C8-77
C8.6.3	Diaphragm and connections	C8-77
C8.6.4	Load-bearing walls	C8-78
C8.6.5	Non-loadbearing walls.....	C8-79
C8.6.6	Concrete	C8-79
C8.6.7	Foundations.....	C8-79
C8.6.8	Geotechnical and geological hazards	C8-80
C8.6.9	Secondary elements.....	C8-80
C8.6.10	Seismic separation	C8-80
C8.6.11	Previous strengthening.....	C8-80
C8.7	Material Properties and Weights.....	C8-85
C8.7.1	General.....	C8-85
C8.7.2	Clay bricks and mortars.....	C8-86
C8.7.3	Compressive strength of masonry	C8-87
C8.7.4	Tensile strength of masonry	C8-88
C8.7.5	Diagonal tensile strength of masonry.....	C8-88

C8.7.6	Modulus of elasticity and shear modulus of masonry	C8-88
C8.7.7	Timber diaphragm material properties	C8-89
C8.7.8	Material unit weights.....	C8-89
C8.8	Assessment of Member/Element Capacity	C8-89
C8.8.1	General.....	C8-89
C8.8.2	Strength reduction factors	C8-89
C8.8.3	Diaphragms	C8-89
C8.8.3.1	General.....	C8-89
C8.8.3.2	Diaphragm deformation limits to provide adequate support to face-loaded walls.....	C8-90
C8.8.3.3	Timber diaphragms	C8-91
C8.8.3.4	Rigid diaphragms	C8-96
C8.8.4	Connections	C8-96
C8.8.4.1	General.....	C8-96
C8.8.4.2	Embedded anchors	C8-96
C8.8.4.3	Plate anchors	C8-98
C8.8.4.4	Capacity of wall between connections	C8-99
C8.8.5	Wall elements subjected to face (out-of-plane) loading	C8-99
C8.8.5.1	General.....	C8-99
C8.8.5.2	Vertical spanning walls.....	C8-101
C8.8.5.3	Vertical cantilevers	C8-110
C8.8.5.4	Gables	C8-111
C8.8.5.5	Horizontal and vertical-horizontal spanning panels	C8-115
C8.8.6	Walls subjected to in-plane load	C8-117
C8.8.6.1	General.....	C8-117
C8.8.6.2	In-plane capacity of URM walls and pier elements	C8-118
C8.8.6.3	URM spandrel capacity	C8-126
C8.8.6.4	Analysis methods for penetrated walls.....	C8-132
C8.8.7	Other items of a secondary nature	C8-136
C8.9	Assessment of Global Capacity	C8-137
C8.9.1	General.....	C8-137
C8.9.2	Global capacity of basic buildings	C8-140
C8.9.3	Global capacity of complex buildings	C8-142
C8.9.4	Global analysis	C8-142
C8.9.4.1	Selection of analysis methods.....	C8-142
C8.9.4.2	Mathematical modelling.....	C8-143
C8.9.4.3	Fundamental period	C8-143
C8.9.4.4	Seismic mass	C8-144
C8.9.4.5	Stiffness of URM walls and wall piers subject to in-plane actions ...	C8-144
C8.10	Assessment of Earthquake Force and Displacement Demands	C8-145
C8.10.1	General.....	C8-145
C8.10.2	Primary lateral structure	C8-145
C8.10.2.1	General	C8-145
C8.10.2.2	Basic buildings	C8-146
C8.10.3	Secondary and critical non-structural items	C8-148
C8.10.4	Vertical demands.....	C8-148
C8.10.5	Flexible diaphragms	C8-148
C8.10.5.1	General	C8-148

C8.10.5.2 Timber diaphragms	C8-149
C8.10.6 Rigid diaphragms	C8-150
C8.10.7 Connections providing support to face-loaded walls	C8-150
C8.10.8 Connections transferring diaphragm shear loads	C8-150
C8.11 Assessment of %NBS	C8-150
C8.12 Improving Seismic Performance of URM Buildings	C8-150
C8.13 References	C8-151
C8.13.1 Suggested Reading	C8-156

Appendix C8A : On-site Testing C8-1

C8A.1 General Considerations	C8-1
C8A.2 Masonry Assemblage (Prism) Material Properties	C8-1
C8A.2.1 Masonry compressive strength	C8-1
C8A.2.2 Masonry modulus of elasticity	C8-2
C8A.2.2.1 Laboratory calibrated displacement measurement	C8-2
C8A.2.2.2 In situ deformability test incorporating flat jacks	C8-2
C8A.2.3 Masonry flexural bond strength	C8-3
C8A.2.4 Masonry bed-joint shear strength	C8-4
C8A.3 Constituent Material Properties	C8-5
C8A.3.1 Brick compressive strength	C8-5
C8A.3.2 Brick modulus of rupture	C8-6
C8A.3.3 Mortar compressive strength	C8-6
C8A.4 Proof Testing of Anchor Connections	C8-7
C8A.4.1 Anchors loaded in tension	C8-8
C8A.4.2 Anchors loaded in shear	C8-8
C8A.5 Investigation of Collar Joints and Wall Cavities	C8-9
C8A.6 Cavity Tie Examination	C8-9

Appendix C8B : Derivation of Instability Deflection and Fundamental Period for Face-Loaded Masonry Walls C8-11

C8B.1 General Considerations and Approximations	C8-11
C8B.2 Vertically Spanning Walls	C8-13
C8B.2.1 General formulation	C8-13
C8B.2.2 Limiting deflection for static instability	C8-14
C8B.2.3 Equation of motion for free vibration	C8-16
C8B.2.4 Period of free vibration	C8-17
C8B.2.5 Maximum acceleration for vertically spanning walls	C8-19
C8B.2.6 Participation factor for vertically spanning walls	C8-20
C8B.2.7 Simplifications for regular vertically spanning walls	C8-20
C8B.2.8 Approximate displacements for static instability of regular vertically spanning walls	C8-20
C8B.2.9 Approximate expression for period of vibration of regular vertically spanning walls	C8-21
C8B.2.10 Participation factor of regular vertically spanning walls	C8-21
C8B.2.11 Maximum acceleration of regular vertically spanning walls	C8-21

C8B.2.12 Adjustments required for vertically spanning walls when inter-storey displacement is large.....	C8-22
C8B.3 Vertical Cantilevers	C8-22
C8B.3.1 General formulation.....	C8-22
C8B.3.2 Limiting deflection of cantilever for static instability	C8-24
C8B.3.3 Period of vibration of cantilever.....	C8-25
C8B.3.4 Participation factor for cantilever.....	C8-26
C8B.3.5 Maximum acceleration of cantilever.....	C8-27
C8B.3.6 Pediment cantilever worked example 1	C8-27
C8B.3.7 Pediment cantilever worked example 2	C8-30
C8B.4 Gable Walls.....	C8-32
C8B.4.1 Vertical cantilever gables	C8-33
C8B.4.1.1 Vertical cantilever gable worked example.....	C8-34
C8B.4.1.2 Return wall separation cantilever worked example.....	C8-37
C8B.4.2 Vertically spanning gables.....	C8-41
C8B.4.2.1 Symmetrical (isosceles) gable configuration.....	C8-41
C8B.4.2.2 Vertical spanning symmetrical (isosceles) gable worked example.....	C8-43
C8B.4.2.3 Non-symmetrical (scalene) gable configuration.....	C8-45
C8B.4.2.4 Secured sawtooth gable worked example	C8-47
C8B.4.3 Vertical-horizontal spanning gables	C8-49
C8B.4.3.1 Vertical-horizontal spanning gable worked example.....	C8-55
C8B.5 Cavity Walls.....	C8-62
C8B.5.1 Identification of cavity walls	C8-62
C8B.5.2 Cavity wall boundary conditions.....	C8-62
C8B.5.3 Cavity tie types and definitions.....	C8-63
C8B.5.4 Assessment of cavity wall in as-built state	C8-63
C8B.5.5 Connection of cavity wall at roof/floor level	C8-63
C8B.5.6 Assessment of cavity walls with flexible ties	C8-64
C8B.5.7 Assessment of cavity walls with rigid shear-transferring ties	C8-65
C8B.5.8 Rocking Method for assessment of cavity walls with rigid shear-transferring ties.....	C8-65
C8B.5.9 Flexural Method for Assessment of cavity walls with rigid shear-transferring ties.....	C8-69
C8B.5.10 Flexural method worked examples	C8-70
C8B.6 Horizontally Spanning Walls	C8-75
C8B.6.1 Flexural response assumptions	C8-76
C8B.6.2 Flexural response calculation.....	C8-77
C8B.6.3 Tables of horizontal span values.....	C8-78
C8B.6.4 Rigid strongbacks.....	C8-80
C8B.6.5 Flexible strongbacks.....	C8-80
C8B.6.6 Worked examples.....	C8-82
C8B.7 Boundary Conditions Worked Examples	C8-86
C8B.7.1 Two-storey building worked example: Lower wall with upper wall and parapet above	C8-86
C8B.7.2 Two-storey building worked example: Lower wall with upper wall and parapet above	C8-87
C8B.7.3 Two-storey building worked example: Upper wall with parapet above.....	C8-88
C8B.7.4 Two-storey building worked example: Upper cavity wall with parapet above (stiff L1 floor).....	C8-89

C8B.7.5 Two-storey building worked example: Lower cavity wall with upper wall and parapet above	C8-90
C8B.7.6 Two-storey building worked example: Upper cavity wall with parapet above (flexible floor).....	C8-91
C8B.7.7 Single-storey building worked example: Wall with unsecured parapet above.....	C8-91
C8B.7.8 Single-storey building worked example: Wall with secured parapet above.....	C8-92
C8B.8 Axial Load Position Worked Examples	C8-93
C8B.8.1 Roof load on cantilever wall worked example: Stiffly tied by truss.....	C8-93
C8B.8.2 Roof load on cantilever wall worked example: Flexibly tied.....	C8-93
C8B.8.3 Post-tensioned parapet worked example.....	C8-94

Appendix C8C : Charts for Assessment of Out-of-Plane Masonry Walls C8-96

C8C.1 General Considerations and Approximations	C8-96
C8C.2 One-way Vertically Spanning Face-Loaded Walls	C8-96
C8C.2.1 Explanatory calculations.....	C8-97
C8C.3 Vertical Cantilevers	C8-99

C8. Unreinforced Masonry Buildings

C8.1 General

C8.1.1 Background

This section was first released in 2015 as a revision to Section 10 of the unreinforced masonry (URM) section in the “Assessment and Improvement of the Structural Performance of Buildings in Earthquakes” (“the 2006 guidelines”, NZSEE, 2006). The 2015 release drew on key observations from the 2010/11 Canterbury earthquake sequence and on the significant quantity of research conducted in recent years at the University of Auckland, University of Canterbury and further afield. New sections in the 2015 release included revised information on materials characterisation, a new method for diaphragm assessment, a new approach to the treatment of in-plane pier capacity based on failure modes, and the introduction of spandrel models.

This 2025 release has included:

- Expanded details regarding the treatment of cavity walls
- Greater discussion regarding the selection of boundary conditions for out-of-plane wall response
- A procedure for the detailed assessment of unreinforced masonry gables, including the preparation of charts to facilitate the assessment process
- Expanded clarification for how to select an equivalent frame when assessing the in-plane response of a penetrated unreinforced masonry wall
- Expanded details on horizontally-spanning masonry walls, including advice on strongbacks
- Corrections to the charts in Appendix C8C
- A significant number of worked examples.

Other sections where less extensive modification have been introduced include:

- Reference to section C11 for the consideration of reinforced concrete masonry buildings
- Considerations when assessing a registered heritage building
- Brief comments on how to assess unreinforced masonry parts that are found in building types that are not predominantly of unreinforced masonry construction.
- Brief comments on how to subdivide a complex URM building into more macroelements
- Procedure when an unreinforced masonry wall is a basement and subjected to soil pressures
- Aspects to consider when a concrete ring beam or bond beam is present
- Further advice on aspects related to toe crushing.

URM construction can be vulnerable to earthquake shaking because of its high mass, lack of integrity between elements and lack of deformation capability. The most hazardous features of URM buildings are inadequately restrained elements at height (such as façades, chimneys, parapets and gable-end walls), face-loaded walls, and their connections to

diaphragms and return walls. These **elements** can present a significant risk to occupants as well as people **located** within a relatively wide zone from the building (see Figure C8.1).



Figure C8.1: Collapsed masonry façade causing fatalities in the Canterbury earthquakes

Assessing the performance of these buildings can be complex as potential failure mechanisms are different from those occurring in other building types. Performance tends to be limited to out-of-plane wall behaviour, relative movement of different elements attached to flexible diaphragms, and tying of parts. This **behaviour** conflicts with the more typical idealisation of a building acting as one unified mass, but is essential to understand in order to assess these structures reliably.

The seismic capacity of URM bearing wall buildings is also difficult to quantify and may result in margins against collapse that are small for the following reasons:

- URM walls and piers may have limited nonlinear deformation capability depending on their configuration, material characteristics, vertical stresses and potential failure modes.
- They rely on friction and overburden from supported loads and wall weights.
- They often have highly variable material properties.
- Their strength and stiffness degrade with each additional cycle of greater displacement of inelastic response to shaking. Therefore, **URM walls** are vulnerable to incremental damage, especially in larger-magnitude, longer-duration earthquakes with multiple aftershocks.

Unlike other construction materials covered by these guidelines URM has not been permitted to contribute to the building lateral load resisting system in new buildings since 1964. Therefore, there is no standard for new URM buildings which could be used to compare to the standard achieved for an existing building. New building standard (*NBS*) and *%NBS* as it relates to URM buildings is therefore assumed to be defined by the requirements set out in this section.

If buildings have undergone damage in an earthquake, much of the cyclic capacity may have already been used by the main event. Assessment of these buildings after an earthquake should consider this damaged state. As a result, their seismic capacity could be significantly lower than in their undamaged or repaired state. This **potential reduction in capacity** is the important rationale for interim shoring for URM buildings (refer to **Figure C8.2**) to mitigate further damage as an important part of building conservation. These techniques typically provide tying (rather than strengthening) to prevent further dilation of rocking or sliding planes, and to relieve stresses at areas of high concentration.

Note:

These guidelines recommend considering selective strengthening of URM buildings as a first step before proceeding to a detailed assessment, particularly in high seismicity areas. Improvement of diaphragm to wall connections, for example, will almost certainly be required to provide the building with any meaningful capacity as the as-built details will provide almost no support.

Using sound engineering judgement when assessing URM buildings is also important **because** the engineer may **otherwise** end up with an economically non-viable solution, with the result **being** that **building** demolition may appear to be the only option.



Figure C8.2: Temporary securing of a mildly damaged solid masonry URM building (Dunning Thornton/Heartwood Community)

C8.1.2 Scope

This section sets out guidelines for assessing:

- **unreinforced solid clay brick masonry buildings;** constructed of rectangular units in mortar, laid in single or multi-wythe walls, and in forms of bond such as common bond, English bond, running bond and Flemish bond.

These guidelines are valid for:

- **walls in good condition**; with negligible mortar joint cracking, brick splitting, settlement or similar factors
- walls **subjected to face loading and attached to rigid or flexible diaphragms**
- brick veneers **subjected to face loading**
- stone masonry where the stones are layered.

These **guidelines** can also be applied, with some additional requirements, to:

- unreinforced stone masonry that is well coursed and laid in running bond
- **unreinforced hollow clay brick masonry**
- **unreinforced** hollow or solid **concrete** block masonry. Refer to Section C7 for assessment of brick or block infill masonry walls in framed construction and refer to Section C11 for assessment of reinforced concrete masonry
- rubble stone masonry: the failure modes of these structures may be other than those covered here, including the possibility of delamination
- cobble stone masonry: assessment of face-loaded capacity is not covered by these guidelines.

Not in scope

This section does not cover:

- earthquake-damaged masonry buildings
- reinforced partially filled and fully filled **concrete** block masonry (refer to Section C11).

Note:

Although the strengthening of URM buildings is outside the scope of this section, brief comments on this topic have been included in Section C8.12.

C8.1.3 Basis of this section

This section is largely based on experimental and analytic studies undertaken at the University of Auckland, University of Canterbury and in Australia, and on the research undertaken by Magenes and Calvi (1997) and Blaikie (1999, 2002). The section also draws on ASCE 41-13 (2014).

Most of the default **material property** values have been adopted from tests undertaken at the University of Auckland (Lumantarna et al., 2014a; Lumantarna et al., 2014b) and from other sources including FEMA 306 (1998), ASCE 41-13 (2014), Kitching (1999) and Foss (2001).

Procedures for assessing face-loaded walls spanning vertically in one direction are based on displacement response that includes strongly nonlinear effects. These procedures have been verified by research (Blaikie, 2001, 2002) using numerical integration time history analyses and by laboratory testing that included testing on shake tables. This research extended the preliminary conclusions reached in Blaikie and Spurr (1993). Other research has been conducted elsewhere, some of which is listed in studies including Yokel and Dikkers (1971), Fattal and Gattaneo (1976), Hendry (1973, 1981) Haseltine et al. (1977), West et al. (1977), Sinha (1978), ABK Consultants (1981), Kariotis (1986), Drysdale and Essawy (1988), Lam et al. (1995) and La Mendola et al. (1995). More recent research has been conducted by Derakhshan et al (2013a, 2013b, 2014a, 2014b).

Other useful information on materials, inspection and assessments is contained in FEMA 306 (1998) and ASCE 41-13 (2014).

C8.1.4 How to use this section

This section is set out as follows.

Understanding URM buildings (Sections C8.2 to C8.4)

These sections provide important context on the characteristics of URM buildings, typical building practices in New Zealand, and observed behaviour in earthquakes. **Because** URM is a non-engineered construction, and given the learnings about its seismic performance **in past earthquakes in New Zealand**, the engineer should review this information carefully before proceeding to the assessment.

Assessing URM buildings (Sections C8.5 to C8.11)

These sections explain how to approach the assessment depending on what is being asked and the type of building that is being assessed. Given the nature of URM construction and the number of previous strengthening techniques used on these buildings, on-site investigation is particularly important. These sections provide a checklist of what to look for on-site as well as probable material properties, before setting out the detailed assessment methods.

Improving URM buildings (Section C8.12)

Although formally outside scope, this section includes some brief comments on improving seismic performance of existing URM buildings. This is an introduction only to a broad field of techniques which is under continual development and research.

C8.1.5 Definitions and acronyms

Action	Set of concentrated or distributed forces acting on a structure (direct action), or deformation imposed on a structure or constrained within it (indirect action). The term 'load' is also often used to describe direct actions.
Adhesion	Bond between masonry unit and mortar.
Basic building	Building of up to two storeys in height with flexible diaphragms where there is little expected interaction between parallel lines of seismic resistance.
BCA	Building Consent Authority.
Beam	A member subjected primarily to loads producing flexure and shear. See also Spandrel.
Bearing wall	A wall that carries (vertical) gravity loads due to floor and roof weight.
Bed joint	The horizontal layer of mortar on which a brick or stone is laid.
Bond	The pattern in which masonry units are laid.
Brittle	A brittle material or structure is one that fails or breaks suddenly once its probable strength capacity has been reached. A brittle structure has very little tendency to deform before it fails, and it very quickly loses lateral load carrying capacity once failure is initiated.
Cavity wall	A cavity wall consists of two 'skins' (or leaves) separated by a hollow space (cavity). The skins are commonly both masonry, such as brick or concrete block, or one skin could be concrete. The cavity is constructed to provide ventilation and moisture control in the wall.

Cohesion	Bond between mortar and brick.
Collar joint	A vertical longitudinal space between wythes of masonry or between an outer masonry wythe and another backup system. This space is often specified to be filled solid with mortar or grout, but sometimes collar-joint treatment is left unspecified.
Cornice	A decorative band of masonry at or near the top of the wall, typically having a horizontal projection that extends out from the exterior plane of the wall.
Course	A course refers to a horizontal row of masonry units, with multiple courses stacked on top of one another.
Critical structural weakness (CSW)	The lowest scoring structural weakness determined from a DSA. For an ISA all structural weaknesses are considered to be potential CSWs.
Cross wall	An interior wall that extends from the floor to the underside of the floor above or to the ceiling, securely fastened to each and capable of resisting lateral forces.
Dead load	The weight of the building materials that make up a building, including its structure, enclosure and architectural finishes. The dead load is supported by the structure (walls, floors and roof).
Design strength	The nominal strength multiplied by the appropriate strength reduction factor.
Diaphragm	A horizontal (or approximately horizontal) structural element (usually suspended floor or ceiling or a braced roof structure) that is connected to the vertical elements around it and distributes earthquake lateral forces to vertical elements, such as walls, of the lateral force-resisting system. Diaphragms can be classified as flexible or rigid.
Dimension	When used alone to describe masonry units, means nominal dimension.
Ductile/ductility	Describes the ability of a structure to sustain its load carrying capacity and dissipate energy when it is subjected to cyclic inelastic displacements during an earthquake.
Earthquake-Prone Building (EQP)	A legally defined category which describes a building that has been assessed as likely to have its ultimate limit state capacity exceeded in moderate earthquake shaking (which is defined in the regulations as being one third of the size of the shaking that a new building would be designed for on that site). A building having seismic capacity less than 34%NBS.
Earthquake Risk Building (ERB)	A building that falls below the threshold for acceptable seismic risk, as recommended by NZSEE (i.e. <67%NBS or two thirds new building standard).
Face-loaded walls	Walls subjected to out-of-plane inertial forces. Also see Out-of-plane load.
Finial	A distinctive ornament typically located on and above the parapet
Flexible diaphragm	A diaphragm which for practical purposes is considered so flexible that it is unable to transfer the earthquake loads to shear walls even if the floors/roof are well connected to the walls. Floors and roofs constructed of timber, and/or steel bracing in a URM building fall in this category.
Gravity load	The load applied in a vertical direction, including the weight of building materials (dead load), environmental loads such as snow, and building contents (live load).
Gross area	The total cross-sectional area of a section through a member bounded by its external perimeter faces without reduction for the area of cells and re-entrant spaces.
In-plane load	Load acting along the wall length.
In-plane wall	Wall loaded along its length. Also referred as in-plane loaded wall.
Irregular building	A building that has an irregularity that could potentially affect the way in which it responds to earthquake shaking. A building that has a sudden change in its plan shape is considered to have a horizontal irregularity. A

	building that changes shape up its height (such as one with setbacks or overhangs) or that is missing significant load-bearing elements is considered to have a vertical irregularity. Structural irregularity is as defined in NZS 1170.5:2004.
Lateral load	Load acting in the horizontal direction, which can be due to wind or earthquake effects.
Leaf	See Wythe.
Load	See Action.
Load path	A path through which vertical or seismic forces travel from the point of their origin to the foundation and, ultimately, to the supporting soil.
Low-strength masonry	Masonry laid in weak mortar, such as weak cement/sand or lime/sand mortar.
Masonry	Any construction in units of clay, stone or concrete laid to a bond and joined together with mortar.
Masonry unit	A preformed unit intended for use in masonry construction, e.g. brick, concrete block.
Mortar	The cement/lime/sand mix in which masonry units are bedded.
Mullion	A vertical member of stone, metal or wood located between the separate panes of a window, or the like.
Net area	The gross cross-sectional area of the wall less the area of un-grouted areas or penetrations.
Out-of-plane load	Load acting at right angles to the wall surface. Walls subjected to out-of-plane shaking are referred to as face-loaded walls.
Parapet	A section of wall that extends above the roof level.
Partition	A non-loadbearing wall which is separated from the primary lateral structure.
Party wall	A party wall (occasionally party-wall or parting wall) is a dividing wall between two adjoining structures providing support for either or both.
Pediment	The elevated section of a parapet, usually on the street frontage and often of a triangular or approximately triangular geometry.
Pier	A vertical portion of wall located horizontally between doors, windows or similar structures. See also Spandrel.
Pointing (masonry)	Troweling mortar into a masonry joint after the masonry units have been laid. Higher quality mortar is used than for the brickwork. See also Repointing.
Primary element	An element which is part of the primary lateral structure.
Probable strength	The expected or estimated mean strength of a member/element, calculated using the section dimensions as detailed and the probable material strengths as defined in these guidelines.
Rake	The sloped edge of a gable or pitched roof, extending from the eave to the ridge
Regular building	A building that is not an irregular building.
Repointing	The process of replacing deteriorated mortar in the joints of a masonry wall with new mortar.
Required strength	The strength of a member/element required to resist combinations of actions for ultimate limit states as specified in AS/NZS 1170.0:2002.
Return wall	A short wall usually perpendicular to, and connected to a wall orientated in the direction of loading to increase its structural stability.

Rigid diaphragm	A suspended floor, roof or ceiling structure that is able to provide effective transfer of lateral loads to walls. Floors or roofs made from reinforced concrete, such as reinforced concrete slabs, fall into this category.
Running or stretcher bond	The unit set out when the units of each course overlap the units in the preceding course by between 25% and 75% of the length of the units.
Seismic hazard	The potential for damage caused by earthquakes. The level of hazard depends on the magnitude of probable earthquakes, the type of fault, the distance from faults associated with those earthquakes, and the type of soil at the site.
Seismic system	That portion of the structure which is considered to provide the earthquake resistance to the entire structure.
Shear wall	A wall which resists lateral loads along its primary axis (also known as an in-plane wall).
SLaMA	Simple Lateral Mechanism Analysis (refer to Section C2).
Spandrel	Horizontal section of wall located between the top of a window and the sill of the window above. See also Pier.
Special study	A procedure for justifying a departure from these guidelines or determining information not covered by them. Special studies are outside the scope of these guidelines.
Stack bond	The unit set out (bond pattern) when the units of each course do not overlap the units of the preceding course by the amount specified for running or stretcher bond.
Structural element	Combinations of structural members that can be considered to work together; e.g. the piers and spandrels in a penetrated wall, or beams and columns in a moment resisting frame.
Through stone	A long stone (header unit) that connects two wythes together in a stone masonry wall. It is also known as bond stone. Contrary to its name, a through stone can also be a concrete block, a wood element, or steel bars with hooked ends embedded in concrete that perform the same function.
Transom	A transverse horizontal structural element of wood, steel, stone or concrete.
Transverse wall	See Cross wall.
Unreinforced masonry (URM) wall	A wall comprising masonry units connected together with mortar and containing no steel, timber, cane or other reinforcement.
Veneer	See Wythe.
Wall	A vertical element which because of its position and shape contributes to the rigidity and strength of a structure.
Wall tie	The tie in a cavity wall, used to tie the internal and external walls (or wythes), constructed of wires, steel bars or straps.
Wythe	A continuous vertical section of masonry one unit in thickness. A wythe may be independent of, or interlocked with, the adjoining wythe(s). A single wythe is also referred to as a veneer or leaf.

C8.1.6 Notation, symbols and abbreviations

Symbol	Meaning
A	Angular deflection (rotation) of the top and bottom parts of a wall panel relative to a line through the top and bottom restraints, radian. The angle is in radians. It is measured as if there were no inter-storey deflection.
$A_{d, gross}$	Gross plan area of diaphragm

Symbol	Meaning
$A_{d,net}$	Net plan area of diaphragm excluding any penetration, m^2
A_h	Angular deflection (rotation) for the homogeneous equation used to solve for period of the part
\ddot{A}_h	Angular acceleration for the homogeneous equation used to solve for period of the part
\ddot{A}_{max}	Max acceleration
$A_{n,wall}$	Net plan area of masonry wall, mm^2
$A_{n,web}$	Area of net mortared/grouted section of the wall web, mm^2
A_p	Angular deflection (rotation) for the particular equation used to solve for period of the part
a	Parameter given by equation
B	Depth of diaphragm, m
b	Parameter given by equation
c	Masonry bed-joint probable cohesion, N/mm^2 . The ability of the mortar to work in conjunction with the bricks. This property is related to moisture absorption in the bricks. It depends less on the absorption qualities of individual brick types and is not greatly influenced by keying of the brick surface (e.g. holes, lattices or patterning). Cohesion is relevant to the primary decision of whether to use cracked or un-cracked masonry properties for the analyses.
$C(0)$	Elastic site hazard spectrum for horizontal loading at fundamental period of 0 sec
$C(T_1)$	Elastic site hazard spectrum for horizontal loading
$C(T_d)$	Seismic coefficient at required height at period T_d
$C_h(0)$	Spectral shape factor for relevant soil determined from Clause 3.1.1, NZS 1170.5:2004, g
$C_h(T_1)$	Spectral shape factor for relevant site subsoil type and period T_1 as determined from Section 3, NZS 1170.5:2004, g
$C_{hc}(T_p)$	Spectral shape factor for site subsoil type C and period T_p as determined from Section 3, NZS 1170.5:2004, g
C_{Hi}	Floor height coefficient for level i as defined in NZS 1170.5:2004
$C_i(T_p)$	Part spectral shape factor
C_m	Value of the seismic coefficient, applied uniformly to the entire panel, that would cause a mechanism to just form, g
$C_p(0.75)$	Seismic coefficient for parts at 0.75 sec. Value of the seismic coefficient that would cause a mechanism to just form, g
$C_p(T_p)$	Design response coefficient for parts as defined by Section 8, NZS 1170.5:2004, g
D	Dimensional (e.g. two dimensional or three dimensional)
D_{ph}	Displacement response (demand) for a wall panel subject to an earthquake shaking as specified by Equation C8.18, mm
e	Eccentricity
E_m	Young's modulus of masonry, MPa
e_b	Eccentricity of the pivot at the bottom of the panel measured from the centroid of W_b , mm

Symbol	Meaning
e_o	Eccentricity of the mid height pivot measured from the centroid of W_b , mm
e_p	Eccentricity of P measured from the centroid of W_t , mm
e_t	Eccentricity of the mid height pivot measured from the centroid of W_t , mm
F	Applied load on timber lintel
F_i	Equivalent static horizontal force at the level of the diaphragm (level i)
f'_b	Probable compressive strength of bricks measured on the flat side, MPa
f'_j	Probable mortar compressive strength, MPa
f'_{ji}	Measured irregular mortar compressive strength, MPa
f'_m	Probable masonry compressive strength, MPa
f'_r	Modulus of rupture of bricks, MPa
f'_t	Probable tensile strength of masonry, MPa
$f_{t,eff}$	Equivalent tensile strength of masonry spandrel, MPa
f_a	Axial compression stress on masonry due to gravity load, MPa
f_{bt}	Probable brick tensile strength, MPa. May be taken as 85% of the stress derived from splitting tests or as 50% of the stress derived from bending tests.
f_{dt}	Probable diagonal tensile strength of masonry, MPa
f_{hm}	Probable compression strength of the masonry in the horizontal direction ($0.5f'_m$), MPa
g	Acceleration due to gravity, m/sec^2
G'_d	Reduced diaphragm shear stiffness, kN/m
$G'_{d,eff}$	Effective diaphragm shear stiffness, kN/m
G_d	Shear stiffness of straight sheathed diaphragm, kN/m
G_m	Shear modulus of masonry, MPa
h	Free height of a cantilever wall from its point of restraint, or height of wall in between restraints in case of a simply-supported face-loaded wall. The clear height can be taken at the centre-to-centre height between lines of horizontal restraint. In the case of concrete floors, the clear distance between floors will apply.
h'	Height of pier between penetrations as defined in Figure C8.88 and used in Equation C8.48
\bar{H}	Storey height. See Figure C8.88 and Equation C8.48
h_{eff}	Effective height of wall or pier between resultant forces
h_i	Height of attachment of the part
H_1	Height of wall below diaphragm, m
h_n	Height from the base to the uppermost seismic weight or mass of the primary structure
h_{sp}	Height of spandrel excluding depth of timber lintel if present
h_{tot}	Total height of spandrel

Symbol	Meaning
H_u	Height of wall above diaphragm, m
I_g	Moment of inertia for the gross section representing uncracked behaviour
I_{xx}	Mass moment of inertia about x-x axis, kgm^2
I_{yy}	Mass moment of inertia about y-y axis, kgm^2
J	Rotational inertia of the wall panel and attached masses, kgm^2
J_{anc}	Rotational inertia of ancillary masses, kgm^2
J_{bo}	Rotational mass moment of inertia of the bottom part of the wall about its centroid, kgm^2
J_{to}	Rotational mass moment of inertia of the top part of the wall about its centroid, kgm^2
k	In-plane stiffness of walls and piers, N/mm
K_R	Seismic force reduction factor for in-plane seismic force
L	Span of diaphragm, m
l	Length of header
l_{sp}	Clear length of spandrel between adjacent wall piers
L_w	Length of wall or length of pier
M	Moment capacity of the wall
M_1, M_i, M_n	Moment imposed on wall/pier elements
m	Mass, kg
m_i	Seismic mass at the level of the diaphragm (level i)
$N(T_1, D)$	Near fault factor determined from Clause 3.1.6, NZS 1170.5:2004
n	Number of recesses
N_1, N_i, N_n	Axial loads on pier elements
P	Superimposed dead load applied to the top of wall/pier
p	Depth of mortar recess, mm
$P - \Delta$	P-delta
p_p	Mean axial stress due to superimposed and dead load in the adjacent wall piers
p_{sp}	Axial stress in the spandrel
P_{Tot}	Total roof load acting on parapet
P_w	Self-weight of wall and pier
P_1, P_2	Separate (total) roof loads acting on the two halves of a gable
Q	Live load
Q_1, Q_i, Q_n	Shear in pier element
R	Return period factor, R_u determined from Clause 3.1.5, NZS 1170.5:2004
r_a	Rise of arch (refer to Figure C8.83)

Symbol	Meaning
r_i	Radius of intrados (lower side) of arch (refer to Figure C8.83)
r_o	Radius of extrados (upper side) of arch (refer to Figure C8.83)
R_p	Risk factor for parts as defined in NZS 1170.5:2004
R_u	Return period factor for ultimate limit state as defined in NZS 1170.5:2004
S_i	Sway potential index
S_p	Structural performance factor in accordance with NZS 1170.5:2004
t	Effective thickness, which may vary with position, mm
t_h	Depth of header
T_1	Fundamental period of the building, sec
T_d	Fundamental period of diaphragm, sec
t_{gross}	Overall thickness of wall, which may vary with position, mm
t_l	Effective thickness of walls below the diaphragm, m
t_{nom}	Nominal thickness of wall excluding pointing, which may vary with position, mm
T_p	Effective period of parts, sec
t_u	Effective thickness of walls above the diaphragm, m
V	Probable shear strength capacity
V_b	Horizontal base shear
V_{dpc}	Probable capacity of a slip plane for no slip
V_{dt}	Probable in-plane diagonal tensile strength capacity of pier and wall
V_{fl}	Shear induced in spandrel due to peak flexural strength of spandrel
$V_{fl,r}$	Shear induced in spandrel due to residual flexural strength of spandrel
$(V_{prob})_{global,base}$	Probable base shear capacity of building
$(V_{prob})_{line,i}$	Probable shear capacity of wall along line i
$(V_{prob})_{wall1}$	Probable shear capacity of wall 1
V_r	Probable in-plane rocking strength capacity of pier and wall
V_s	Probable in-plane bed-joint shear strength capacity of pier and wall
V_{s1}	Probable peak shear strength of spandrel
V_{s2}	Probable peak shear strength of spandrel
$V_{s,r}$	Probable residual spandrel shear strength capacity or probable residual wall sliding shear strength capacity
V_{tc}	Probable in-plane toe crushing strength capacity of pier and wall
$V_{tc,r}$	Residual in-plane toe crushing strength capacity of pier and wall
W	Weight of the wall and pier
W_b	Weight of the bottom part of the wall
W_i	Seismic weight at level i

Symbol	Meaning
W_{strong}	Share of seismic load from wall out-of-plane assigned to flexible strongback
W_t	Weight of the top part of the wall
W_{Tot}	Total weight of gable
W_{trib}	Uniformly distributed tributary weight
y_b	Height of the centroid of W_b from the pivot at the bottom of the wall
y_t	Height from the centroid of W_t to the pivot at the top of the wall
Z	Hazard factor as defined in NZS 1170.5:2004
α_a	Arch half angle of embrace
α_{ht}	h/t ratio correction factor
α_{tl}	t/l ratio correction factor
α_w	Diaphragm stiffness modification factor taking into account boundary walls
β	Factor to correct nonlinear stress distribution
β_i	The ratio of the applied shear at level i to the shear at the base of the line under consideration
β_s	Spandrel aspect ratio
β_{sp}	Width of spandrel
γ	Participation factor for rocking system relating the deflection at the mid height hinge to that obtained from the spectrum for a simple oscillator of the same effective period and damping
Δ	Horizontal displacement, mm
Δ_d	Horizontal displacement of diaphragm
Δ_i	Deflection that would cause instability of a face-loaded wall under forces W_b , W_t and P only
Δ_m	An assumed maximum useful deflection = $0.6\Delta_i$ and $0.3\Delta_i$ for simply-supported and cantilever walls respectively used for calculating deflection response capacity
Δ_t	An assumed maximum useful deflection = $0.6\Delta_m$ and $0.8\Delta_m$ for simply-supported and cantilever walls respectively used for calculating fundamental period of face-loaded rocking wall
$\Delta_{tc,r}$	Deformation at the onset of toe crushing
Δ_y	Yield displacement
θ	Chord rotation of spandrel measured parallel to the displaced wall, relative to pier, radian
θ_y	Yield rotation of the spandrel
κ	Term used in the solution to the homogeneous equation of free vibration
μ	Structural ductility factor in accordance with NZS 1170.5:2004
μ_{dpc}	DPC coefficient of friction
μ_f	Probable coefficient of friction of masonry
μ_p	Ductility of part (wall)
ρ	Density (mass per unit volume)

Symbol	Meaning
τ	Time. Term used to evaluate the period of the rocking part
ξ_{sys}	Equivalent viscous damping of the system
$\Sigma V_{u,\text{Pier}}^*$	Sum of the 100%NBS shear force demands on the piers above and below the joint calculated using $K_R = 1.0$
$\Sigma V_{n,\text{Pier}}$	Sum of pier capacities above and below the joint
$\Sigma V_{u,\text{Spandrel}}^*$	Sum of the 100%NBS shear force demands on the spandrels to the left and right of the joint calculated using $K_R = 1.0$
$\Sigma V_{n,\text{Spandrel}}$	Sum of the spandrel capacities to the left and right of the joint
ϕ	Strength or capacity reduction factor
ψ	The maximum inter-storey slope which may need to be measured between diaphragms which includes both inter-storey and diaphragm deflection, radian

C8.2 Typical URM Building Practices in New Zealand

Most of New Zealand's URM buildings were constructed during a relatively narrow window of time; between the late 1870s and 1940s (Russell and Ingham, 2010a). As a result, construction methods are relatively uniform nationwide with only a few variations reflecting the origins of the stonemasons and the customary stones ("hard rock" or "soft rock") that they used for laying. However, these buildings vary substantially in their structural configuration and layout.

C8.2.1 Consideration of heritage features

In general terms, preservation and if required, structural strengthening of buildings can result in a positive heritage outcome when it enables a building to be retained in a sustainable long-term use. Demolition, and removal of significant portions of heritage fabric (for example, parapets, pediments or ornaments), can result in significant and negative effects. The overall approach is, therefore to retain elements that are likely to have the greatest heritage values. Records of significant features can be found in a listing by a Territorial Authority, and/or if applicable, Heritage NZ, and in some cases a building's Conservation Management Plan. Advice should be sought where an engineer is unsure of the relative merits of various features.

Design principles, if interventions are required, include:

- Taking into consideration the properties of traditional building materials such as brick and stone.
- Selecting designs that minimise changes to key architectural or design features.
- Maximising and augmenting existing strength/load paths, rather than creating new ones
- Minimising the visibility of interventions when viewed from public places. Preserving existing grids and existing primary circulation paths.
- Designing retrofit for modularity and removability, for example, so that parapet braces can be removed and reinstated in a future re-roofing project. Designing for reversibility so that interventions could be removed if best-practice changes.

Ensuring that waterproofing/weathertightness is maintained through all detailing, especially around roofs and gutters.

C8.2.2 Building forms

The range of typical URM buildings is set out in Table C8.1 together with some common characteristics for each type. Note that:

- most smaller **URM** buildings are cellular in nature, combining internal masonry or timber walls with the perimeter masonry façade to provide an overall rigid unit
- many smaller commercial URM buildings have **highly penetrated** street façades at ground level and high bottom storeys
- larger buildings tend to have punched wall frames (refer to **Figure C8.3**) and open plan areas where floors and roofs are supported by timber, cast iron or steel posts
- large, complex buildings such as churches are particularly vulnerable to earthquake shaking as they tend to have irregular plans, tall storey heights, offset roofs, few partitions and many windows.

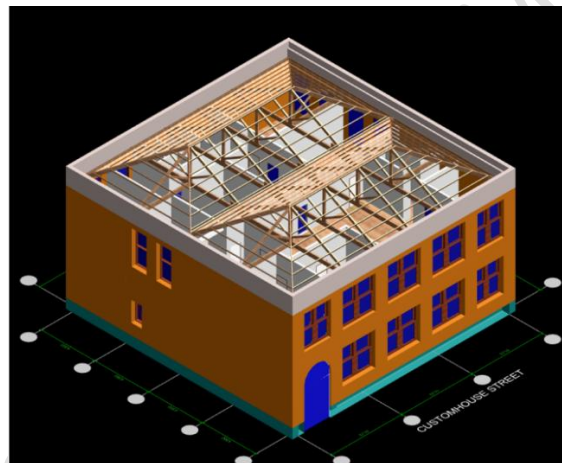
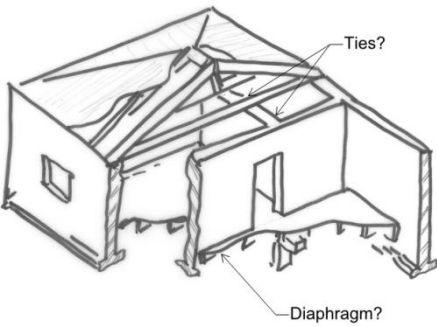
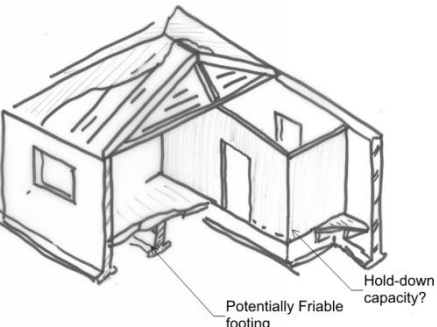

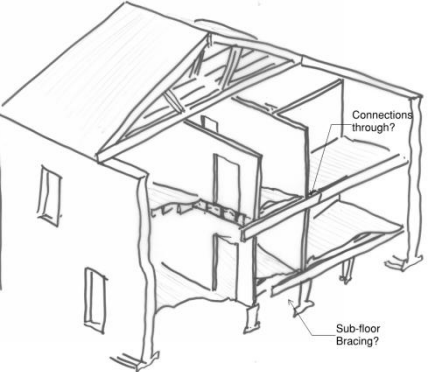


Figure C8.3: URM building with punched wall

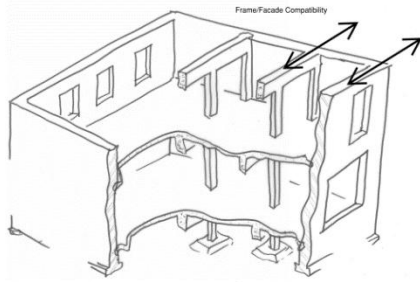
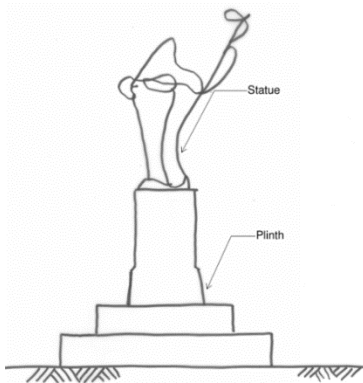
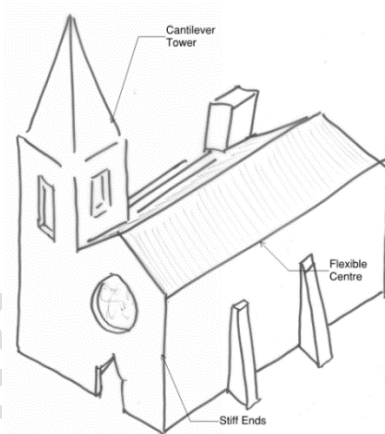
In these guidelines smaller **URM** buildings (i.e. less than or equal to two storeys in height), including small churches and halls, are categorised as *basic buildings* to distinguish them from more complex buildings. Basic buildings are only those with flexible diaphragms where there is little interaction between parallel lines of seismic resistance. Simplified approaches, particularly associated with determining material properties and analysis, and ignoring the effects of torsion or transfer of load in plan between floors, are possible when assessing buildings with these characteristics. These **topics** are covered in the appropriate sections below.

The interaction of buildings constructed with common boundary or party walls is discussed in more detail in Section C8.5.4.

Table C8.1: Building forms

Form	Illustration	Particular issues
1 storey cellular: Masonry internal walls <i>Bracing predominantly from in-plane walls cantilevering from ground level</i>		<ul style="list-style-type: none"> Bonding at wall intersections Plan regularity – diaphragm demand if irregular Relative stiffness/strength from varying wall lengths Subfloor height and level of fixity Ground floor diaphragm/bracing
1 storey cellular: Timber internal walls <i>Bracing predominantly from walls loaded in-plane cantilevering from ground level</i>		<ul style="list-style-type: none"> Connection to masonry at intersections Stiffness compatibility with masonry – wall geometry Stiffness compatibility with masonry – materiality (plaster/lath, fibrous plaster) Flexibility of strapping/lining with respect to masonry Timber wall foundation bracing capacity
>1 storey cellular: Masonry internal walls <i>Bracing predominantly from walls loaded in-plane with interaction over doorways and between floors</i>		<p>As for 1 Storey plus:</p> <ul style="list-style-type: none"> Wall coupling over doorways Change in wall thickness at first floor
>1 storey cellular: Timber internal walls <i>Bracing predominantly from walls loaded in-plane with interaction over doorways and between floors</i>		<p>As for 1 Storey plus:</p> <ul style="list-style-type: none"> Hold-down of upper walls to lower walls Hold-down and bracing of lower walls to piles

Form	Illustration	Particular issues
1 storey open: <i>Bracing predominantly from walls loaded out-of-plane cantilevering from ground level</i>		<ul style="list-style-type: none"> • End walls and differential stiffness • Ground conditions and foundations critical • Wall connection with ground floor slab if present
>1 storey open: <i>Bracing predominantly from walls loaded out-of-plane cantilevering from ground level, with contributions from end walls</i> Most common town centre commercial structures		<ul style="list-style-type: none"> • Diaphragm stiffness • Diaphragm strength • Ancillary structures forming bracing • Contribution of shop front beams/frame • Plan regularity
Multi-storey open <i>Bracing predominantly from perimeter walls loaded in-plane</i>		<ul style="list-style-type: none"> • Wall-to-diaphragm connection demands high for out-of-plane wall loads • Diaphragm stiffness important for out-of-plane wall analysis • Diaphragm strength demands often high • Holes in diaphragms • Punched walls in-plane analysis can be complex
Multi-storey with internal structures <i>Bracing from combination of internal walls and perimeter walls loaded in-plane</i>		<ul style="list-style-type: none"> • Wall-to-diaphragm connection demands high • Compatibility between flexible internal and stiff external structures • Punched walls in-plane analysis can be complex

Form	Illustration	Particular issues
Multi-storey frame/wall <i>Bracing from combination of internal walls and perimeter walls loaded in-plane</i>		<ul style="list-style-type: none"> • Often heavyweight floors: stiff but strength difficult to ascertain • Internal frame stiffness vs perimeter punched wall stiffness • High shear demands on in-plane connection to perimeter elements
Monumental – single form <i>Bracing predominantly from cantilever action, single degree of freedom</i> Statues, towers, chimneys and the like		<ul style="list-style-type: none"> • Often rocking governed – can be beneficial • Foundation stability critical • Combination of materials forming masonry unit • Damping
Monumental – multiple forms <i>Multiple degrees of freedom with different stiffnesses/periods</i> Most churches and larger civic structures		<ul style="list-style-type: none"> • Highly complex interaction between elements • Special study • Peer review recommended

C8.2.2.1 Ornamental features and appendages

Many URM buildings have an ornamental front façade that requires particular care when undertaking a site inspection: additional information on size, alignment and condition is likely required for assessment. Consider if there is evidence of past features that may have caused damage. This could be heavy signage or canopies which may have prised the brickwork outward. Similarly, the residual metalwork could have corroded; the expansion of the corroded metal can cause structural distress.

Assessment requires consideration of loss of stability, and whether the dislodged component is a Significant Life Safety Hazard. Any loss of stability will cause damage and so its vulnerability should be discussed with the Client as to repair or retrofit. However, the object needs to be sufficiently large and fall a sufficient distance to be a Significant Life Safety Hazard (SLSH) and govern the %NBS – refer Section A of the Guidelines.



Figure C8.4: Ornamental features

C8.2.2.2 URM components in non-URM Buildings

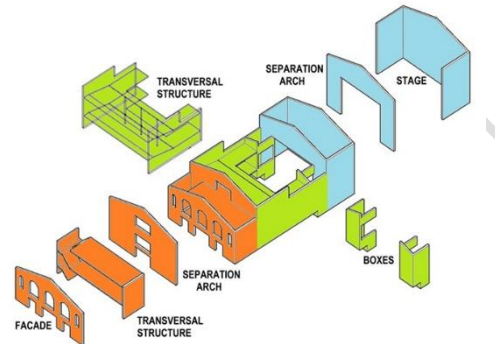
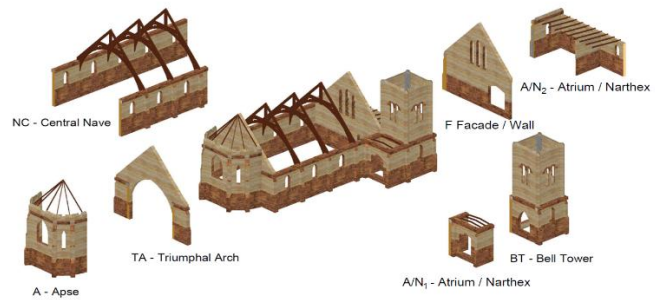
URM components such as large chimneys and brick party walls in lightweight timber buildings can dominate the actions of those buildings due to the mass of the URM. The assessment should consider the relative stiffness. Flexible URM elements such as party walls out of plane will rely on the lightweight structure for bracing (C9) but the minor contribution from the masonry base fixity to the ground if appropriate can be considered if deformations are appropriately controlled. Stiff URM elements such as large chimneys may instead dominate the buildings response: they will provide significant capacity, but the contribution of other timber elements must consider how much of their capacity is mobilised at the limiting displacement of the URM component.

In many lightweight buildings, the URM component inside the building is encapsulated in framing and does not provide gravity support to the structure (for example the remnant of a chimney taken down to ceiling level). Although the likelihood this component could cause damage should be reported, in many cases the component will not pose a SLSSH and therefore not govern the %NBS – refer Section A of the Guidelines.

URM parts in other buildings should be assessed using Parts loadings, and whether it poses a SLSSH should be assessed. Masonry infill walls should be assessed using Section C7.

C8.2.2.3 Subdivision of complex URM buildings into macroelements

Although these guidelines are primarily intended for basic 1-storey and 2-storey URM buildings it has been established (Lagomarsino and Cattari, 2015) that more complex URM buildings such as churches, theatres, town halls and train stations often exhibit the same local failure mechanisms (for example, out-of-plane wall failure) such that complex URM buildings can be subdivided into more basic macroelements to facilitate assessment. Care is required to correctly attribute demand to each macroblock based upon mass and stiffness attributes and the presence or absence of reliable connections, and numerical modelling may be required to confirm the suitability of the selected macroelements. Furthermore, macroelement assessment can be useful not only as a substitute for complex computational methods, but also as a means to validate the computational outputs as a first-principles sanity check to ensure that results from advanced modelling remain physically reasonable and consistent with observed behaviour.



(a) Complex URM building

(b) Subdivision into macroelements

Figure C8.5: Subdivision of complex URM buildings into macroelements (Galvez et al., 2018)

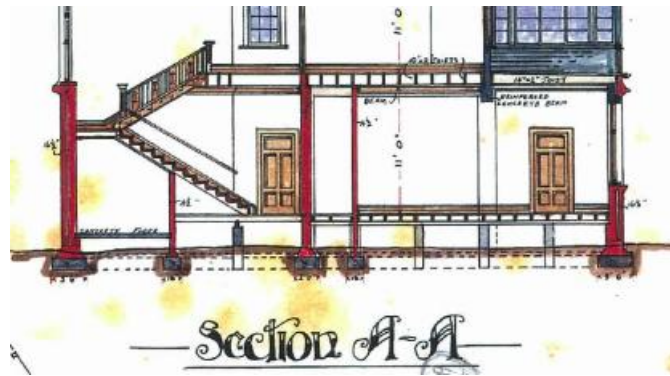
C8.2.3 Foundations

Foundations for URM buildings were typically shallow strip footings (refer to [Figure C8.6\(a\)](#)), including under openings in punched walls or facades. Bricks were typically placed transverse to the wall to give a half-to-one brick-thickening, although larger multi-stepped thickenings were used in large structures. The bricks were typically protected from direct contact with the ground with a layer of concrete. In smaller buildings, this concrete layer was often thin and unreinforced.

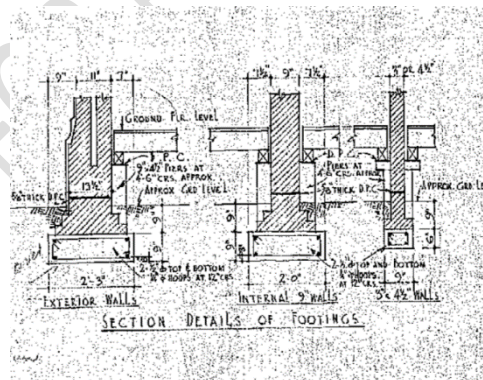
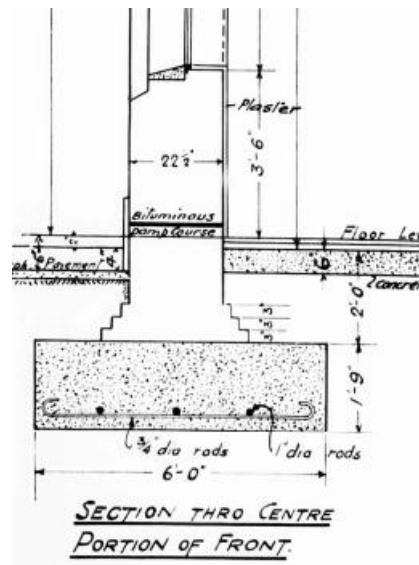
Deeper concrete strips (refer to [Figure C8.6\(b\)](#)) for larger buildings were often nominally reinforced with plain reinforcing bars, flats, or train/tram rails. In extremely poor ground or where the foundation formed a sea wall or wharf, these reinforced concrete strips generally spanned between driven timber or sometimes between steel or precast piles. The design was often rudimentary, with the depth of the concrete at least half that of the span regardless of reinforcement.

As the widening of the foundation was often nominal, some settlement was common in poorer ground either during or after construction. Settlement during construction could often be “built in” so would not be visible. Larger industrial buildings with timber, steel or cast iron posts were often founded on large, isolated pads. As these pads were sized for the “live” actions, they are often lightly loaded so are an excellent indicator of settlement.

In some cases, URM forms basement walls. Assessment should consider C(0) seismic actions on both the wall and the backfill combined. Capacity shall be the static capacity based on the axial load on the cross section only, with no tension from the mortar bed. Pay particular attention to the condition of the mortar and masonry if there has been moisture ingress.



(a) Typical foundation details



(b) Examples of cross sections of URM building foundations

Figure C8.6: URM building foundations

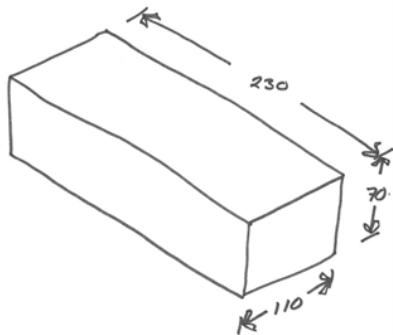
C8.2.4 Solid and Cavity Walls

Both solid walls and cavity walls were common types of wall construction:

- Solid walls were generally used for industrial buildings and for buildings located on the outskirts of town, and for party walls and walls either not visible or in lower storeys.
- Cavity walls were used in buildings to control moisture ingress. Cavity walls also allow the use of different quality bricks on the interior and exterior, usually where a better architectural finish was required on the exterior.

New Zealand clay bricks are generally consistent in geometry with dimensions as shown in Figure C8.7(a). Because of the modular nature of masonry construction it is relatively easy to match the wall thickness and the cross-sectional attributes of the wall. A collar joint thickness of 10 mm can be assumed, such that for solid walls a single leaf wall has a thickness of 110 mm, a 2-leaf wall has a thickness of 230 mm, and a 3-leaf wall has a thickness of 350 mm. For cavity construction a cavity width of 50 mm can be assumed such that a single-single cavity wall has a thickness of 270 mm, a double-single cavity wall has a thickness of 390 mm, etc. Tall multi-storey masonry construction is uncommon in New Zealand but for such cases the number of leaves used in the solid wall thickness may be substantially greater than 3 leaves as shown in Figure C8.7(b).

Regional variations in brick module dimensions can occur, resulting in different brick sizes those given in Figure C8.7(a), with resulting changes in wall thickness. While 50 mm (2") cavities are the most common, cavities of 38 mm (1½") can also be found.



(a) Typical geometry of a regular clay brick



(b) Ground floor of the 7-storey Manchester Courts building demolished after the 2010 Darfield earthquake

Figure C8.7: Brick geometry and example of multi-leaf solid clay brick wall

In cavity walls, the exterior masonry wythes act as an architectural finish. If cavity walls are not recognised in assessment, an unconservative assumption can be made for the structural thickness of these walls. It was common to provide an outer wythe that was continuous over the full height of the wall, with an inner structural wall that often had a single-wythe thickness for the top storey and a thickness of two or more wythes for the lower storeys (refer to Figure C8.8). Construction quality was usually better for visible walls and veneers than in hidden areas or at the rear of buildings.

As can be seen in Figure C8.8, a cavity wall often results in an uneven distribution of top load into the inner and outer leaves of a wall, leading to a difference in the capacity of the inner and outer leaves.



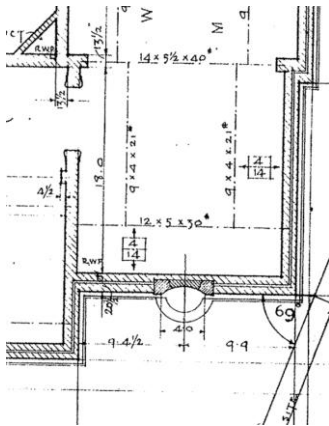
Figure C8.8: Change in cross section of brick wall (Holmes NZ LP)

The presence of cavity walls may be indicated by one or more of the following signs:

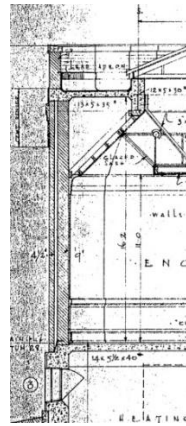
- A wall thickness that is not a wythe multiple (refer C8.2.4.1 for typical solid and cavity wall thicknesses).
- Walls shown in original building drawings as double lines or with multiple thickness call-ups for the same wall segment (refer Figure C8.9 for cavity walls shown as 9" and 4 ½").
- Airbricks / vent bricks (although these can be present in solid walls too).
- Weep holes created by the regularly-spaced absence of head joints (the vertical mortar joints between bricks). The weep holes will often be located towards the bottom of a wall section, on the exterior face, and can be present at more than one level. Weep holes are intended to allow moisture to vent out of the cavity.
- An absence of header bricks in the exterior face of a wall which is thicker than one wythe may indicate that the wall is a veneer.

Drilling investigation holes through mortar or bricks may be the most accurate and simplest method to confirm the presence of a suspected cavity wall.

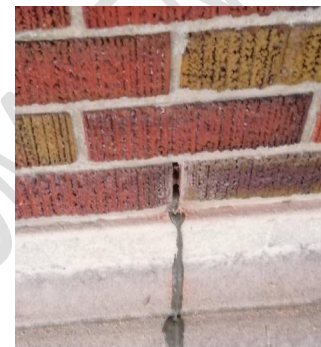
Often a cavity wall, which was originally on the exterior of the building, has become an interior wall following subsequent alteration.



(a) Typical plan and section showing cavity wall



(b) Vent brick



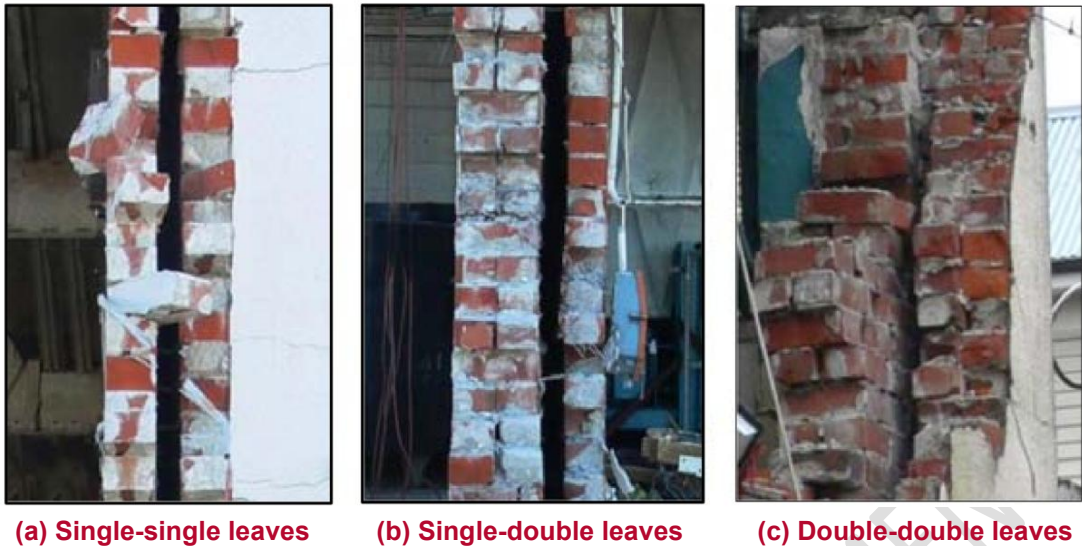
(c) Weep holes

Figure C8.9: Cavity wall indicators (Holmes NZ LP)

C8.2.4.1 Typical wall thickness

The commonly used nominal thicknesses of **solid** brick walls in New Zealand are 230 mm (9", two wythes), 350 mm (14", three wythes) and **470 mm** (18", four wythes). These **dimensions are** in addition to any outer veneer of 110 mm (4½", one wythe).

Giaretton et al. (2015) noted three types of cavity wall cross-sections identified in the Christchurch area: single-single masonry leaves, single-double masonry leaves, and double-double masonry leaves (see Figure C8.10). Assuming a cavity spacing of approximately two inches (50 mm) these walls would have thicknesses of approximately 270 mm, 390 mm, and 510 mm respectively.



(a) Single-single leaves

(b) Single-double leaves

(c) Double-double leaves

Figure C8.10: Typical cavity wall sections (Giairetton)

C8.2.4.2 Cavity ties

In cavity walls, outer wythes were usually tied to the inner wythe or main structural wall with #8 ties, sometimes with a kink in the middle, or with flat pieces of tin generally at spacings of **approximately** 900 mm (3') horizontally and every fifth or sixth course vertically (refer to **Figure C8.11**). Cast steel, wrought steel or mild steel toggles were sometimes used at similar spacings.



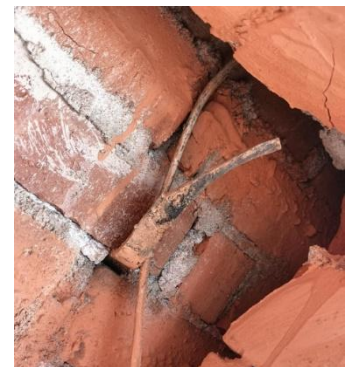
(a) Common wire ties



(b) Double hook ties



(c) Butterfly ties

(d) V-drip flat fishtailed wall tie
(tie has been bent upward)**Figure C8.11: Commonly observed wall ties (Dizhur, Dunning Thornton)**

C8.2.4.3 Masonry bond pattern and cross sections

A number of different bond patterns have been used for URM buildings, as described below. The bond pattern is an important feature of URM buildings: it determines how the masonry units in a wall are connected and has a significant effect on both the wall strength and how its components act together as a complete structural member/element.

Stretcher units, or stretchers, are bricks laid in the plane of the wall. Header units, or headers are bricks laid across the wall joining the masonry wythes **or leaves** together.

In cross section, a wall three units thick is a three wythe wall. To act as **a single multi-wythe wall**, each wythe should be adequately connected to the adjoining wythe with headers at appropriate intervals.

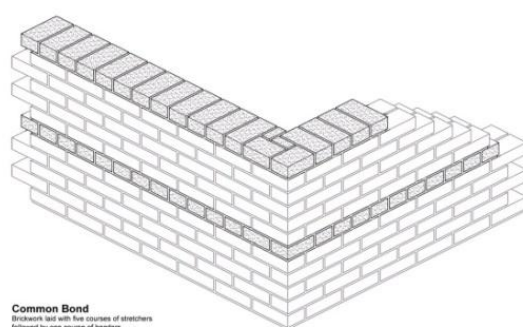
Note that sometimes fake headers are incorporated into a wythe that do not cover two adjoining wythes. These can disguise the presence of a cavity wall where there is a cavity void between the inner and outer wythes.

Clay brick masonry

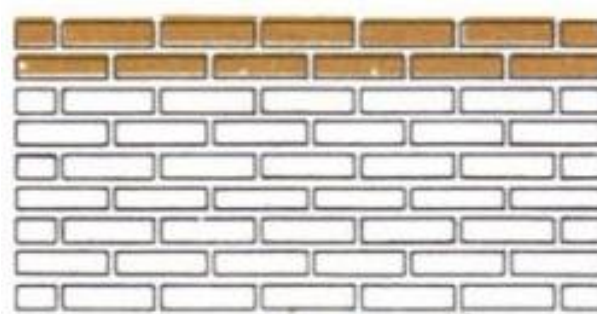
Most New Zealand URM buildings were constructed with either common bond, which is the most frequently occurring bond pattern, or English bond, which is often found on the bottom (ground) storey.

Common bond is sometimes referred to as American bond or English garden wall bond. **Common bond** has layers of stretchers, and headers **positioned** every three to six courses (refer to **Figure C8.12(a)**). These headers can be **located** at different levels in different buildings, and sometimes even within the same building. For example, the headers may be every second course at the bottom of the ground storey but every fourth course near the top of the third storey. Header courses may be irregular and made to fit in at ends of walls and around drainpipes with half widths and other cut bricks.

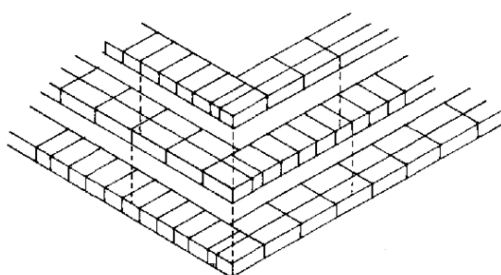
English bond has alternating header and stretcher courses (refer to **Figure C8.12(c)**).



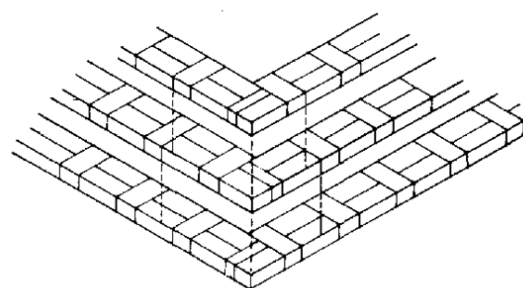
(a) Common bond



(b) Running bond



(c) English bond



(d) Flemish bond

Figure C8.12: Different types of brick masonry bond patterns

Other bond patterns used in New Zealand include Running bond (refer to [Figure C8.12\(b\)](#)) and Flemish bond (refer to [Figure C8.12\(d\)](#)). Running bond (stretcher courses only) often indicates the presence of a cavity wall. Flemish bond (alternating headers and stretchers in every course) is the least common bond pattern and is generally found between openings on an upper storey; for example, on piers between windows.

Stone masonry

Stone masonry buildings in New Zealand are mainly built with igneous rocks such as basalt and scoria, or sedimentary rocks such as limestone. Greywacke, which is closely related to schist, is also used in some parts of the country. Trachyte, dolerite, and combinations of these are also used.

Wall texture

Wall texture describes the disposition of the stone courses and vertical joints. There are three different categories (refer to [Figure C8.13](#)): ashlar (squared stone); rubble (broken stone); and cobble stones (field stone), which is less common.

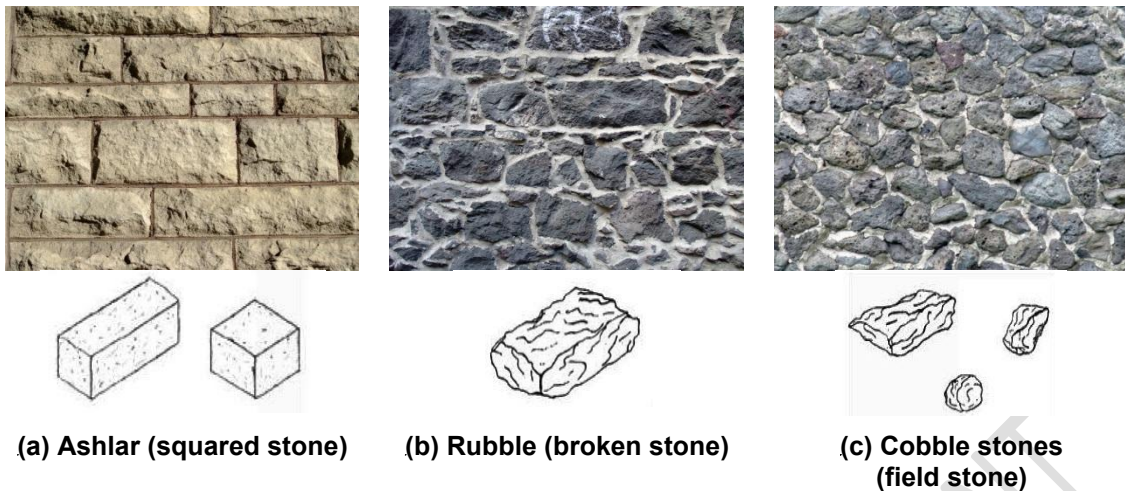


Figure C8.13: Classification of stone units (Giarretton)

Ashlar (dressed or undressed) is stonework cut on four sides so that the adjoining sides will be **oriented** at right angles to each other (refer to Figure C8.13(a)). Ashlar is usually laid as either coursed ashlar, which is in regular courses with continuous joints (refer to Figure C8.14(a)), or block-in-course ashlar (refer to Figure C8.14(b)). Ashlar may also appear as broken courses (which describes the broken continuity of the bed and head joints) of either random-course ashlar (refer to Figure C8.14(c)), or broken ashlar (refer to Figure C8.14(d)).

All ashlar should have straight and horizontal bed joints, and the vertical joints should be kept plumb. This type of stone can also be found in coursed rubble; in which case it may be considered as a hybrid between rubble and ashlar stonework.

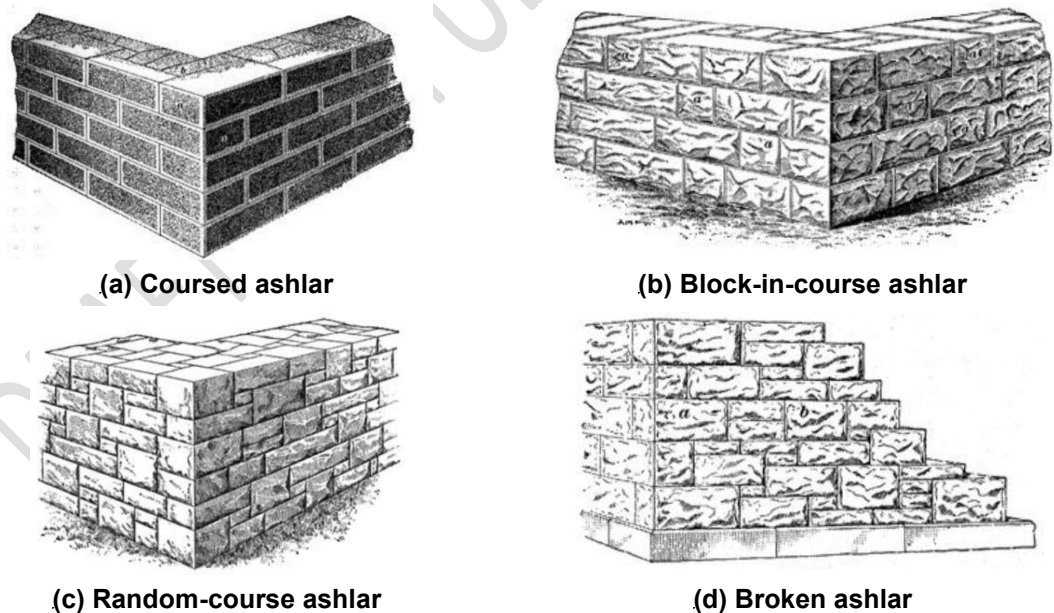


Figure C8.14: Schematic of different forms of Ashlar bond (Lowndes, 1994)

Rubble stonework consists of stones in which the adjoining sides are not required to be at right angles (refer to Figure C8.13(b)). This form of masonry was often used for rough masonry such as foundations and backing, and frequently consists of common, roughly dressed field stone.

Wall cross section

It is usually not possible to establish the **cross-section** characteristics of a stone masonry wall from the bond pattern. More detailed inspection is required to identify any connections between the wythes; to determine what material the core is composed of; and to locate any voids, a cavity, or the presence of other elements such as steel ties. All of these **details** contribute to determining the wall's structural properties.



(a) Dressed stone in outer leaves and “rubble” fill



(b) Stone facing and brickwork backing



(c) Stone facing and concrete core

Figure C8.15: Stone masonry cross sections in New Zealand. Representative cases observed in Christchurch after the Canterbury earthquakes (Giarretton)

Concrete block masonry

Although solid concrete masonry was used in New Zealand from the 1880s, hollow concrete block masonry was not used widely until the late 1950s. **Concrete block masonry** was usually constructed in running bond, but stacked bond was sometimes used for architectural effect.

From the 1960s onwards, **concrete block** masonry was usually constructed with one wythe 190 mm thick, although the **width** was sometimes 140 mm thick. Cavity construction, involving two wythes with a cavity between, was mostly used for residential or commercial office construction but occasionally for industrial buildings. The external wythe was usually 90 mm thick and the interior wythe was either 90 mm or 140 mm. Cavity construction was often used for infills, with a bounding frame of either concrete or encased steelwork.

To begin with, reinforcement in concrete masonry was usually quite sparse, with vertical bars tending to be placed at window and door openings and wall ends, corners and intersections, and horizontal bars at sill and heads and the tops of walls or at floor levels. Early on, it was common to fill just the reinforced cells. Later, when the depressed web open-ended bond beam blocks became more available, more closely spaced vertical reinforcement became more practicable. When the depressed web open-ended bond beam blocks (style 20.16) became available without excessive distortion from drying shrinkage, these **units** tended to replace the standard hollow blocks for construction of the whole wall (with specials at ends, lintels and the like).

Wire reinforcement formed into a ladder structure (“Bloklok” or a similar proprietary product) was common in cavity construction. Two wires ran in the mortar in bed joints, joined across the cavity by another wire at regular centres and acting as cavity ties.

C8.2.5 Constituent materials

C8.2.5.1 Bricks

New Zealand brick sizes are based on imperial size. The most common nominal size of clay bricks used in masonry buildings is 230 mm x 110 mm x 70 mm (9"x 4½"x 3½').

C8.2.5.2 Mortar

Mortar is usually soft due to factors including inferior initial construction, ageing, weathering and leaching (refer to [Figure C8.16](#)). Both the type and proportions of mortar constituents varied significantly throughout the country. Until early last century, lime-sand mortar was common but cement-lime-sand mortar and cement-sand mortar were also used.

Note:

While the lime in lime mortars will continue to absorb moisture and “reset”, over time it will leach and this leads to deterioration of the mortar.



Figure C8.16: Soft mortar. Note the delaminated mortar from bricks in the background (Ingham and Griffith, 2011)

C8.2.5.3 Timber

Totara, rimu, matai (black pine) and kahikatea (white pine) were the most commonly used timber species in URM buildings.

C8.2.5.4 Concrete block

From the beginning, hollow concrete blocks were manufactured by the Besser process, where lean mix concrete was compacted into moulds using vibration. Concrete strength was usually 30 MPa or greater. [Further details are provided in Section C11.](#)

C8.2.6 Floor/roof diaphragms

Floors of URM buildings were usually made from timber and sometimes from reinforced concrete slabs.

C8.2.6.1 Timber floors

Timber floor diaphragms are usually constructed of 19-25 mm thick tongue and groove (T&G) membrane nailed to timber joists that are supported by timber or steel beams. Matai and rimu were commonly used for the floor diaphragm membrane. These timbers may have hardened from a century of drying and be “locked up” from long use. The diaphragm may also have been damaged by insect infestation or decay from moisture ingress. As well as the timber characteristics, the response of these diaphragms during an earthquake is dictated by the behaviour of the nail joints. It should be recognised that the nails in use a century ago were much softer than those used today. Resistance comes primarily from friction between the boards, complemented by “vierendeel” action from the pairs of nails in a board. A further complication is that the response of timber diaphragms is different for each direction, recognising that joists and boards span in different directions. Hence, diaphragm in-plane stiffness and strength should be assessed for earthquake loading oriented both parallel and perpendicular to the orientation of the joists.

C8.2.6.2 Reinforced concrete slabs

Reinforced concrete slabs were usually monolithic to brick walls and form a rigid diaphragm. While they may have been reinforced with bars, as is commonly the case for modern construction, these bars were often round or of a roughness pattern that provides significantly less bond than expected today. As a result, the presence of termination details (such as hooks, thickenings or threads/nuts) will have a marked effect on the load carrying capacity. Other types of reinforcement included expanded metal lath (refer to [Figure C8.17](#)) and even train rails.



Figure C8.17: Concrete slab with expanded metal lath reinforcement. Corrosion of the lath from carbonation of the concrete over time has caused the concrete to spall

Portland cement gradually became available throughout New Zealand from the 1890s to the late 1920s, which was the time of much URM construction. Non-Portland cement concretes (often called “Clinker” concretes, as they were produced from only a single firing of lime products) are significantly weaker and should be assessed with caution. Similarly, as concrete was a relatively expensive material during these times, voids or ribs were often formed in slabs using hollow ceramic tiles.

Note:

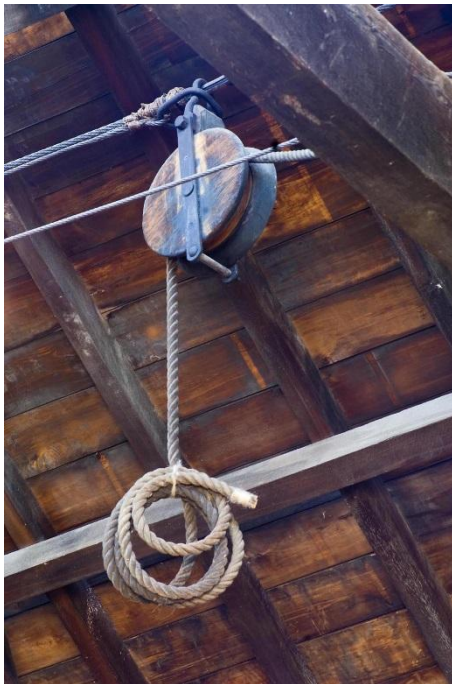
Take care when making assumptions relating to the concrete strength. Intrusive investigation is essential to understand the makeup of the original slab construction and its constituents properly if forces greater than nominal are to be transferred.

C8.2.6.3 Roofs

The roof structure is usually provided with straight sarking (refer to **Figure C8.18**) or diagonal sarking (refer to **Figure C8.19**) nailed to purlins supported by timber trusses. Straight sarking has similar action to flooring, but boards are often square edged so they do not have the stiffness and strength of the high-friction tongue and groove connection. Diagonal sarking is naturally stiffer and stronger than rectangular sarking because the boards provide the diagonal “truss” members between the rafters and purlins. However, the ductility and displacement capacity of diagonal sarking will be less than for rectangular sarking as movements will cause direct shearing of the fixings along the lines of the boards.

Note:

Refer to Section C8.8.3 for the capacities of these types of systems. Further information is also provided in Section C9.



(a) Typical horizontal roof sarking



(b) Roof diaphragm with vertical sarking

Figure C8.18: Typical timber diaphragms – straight sarking

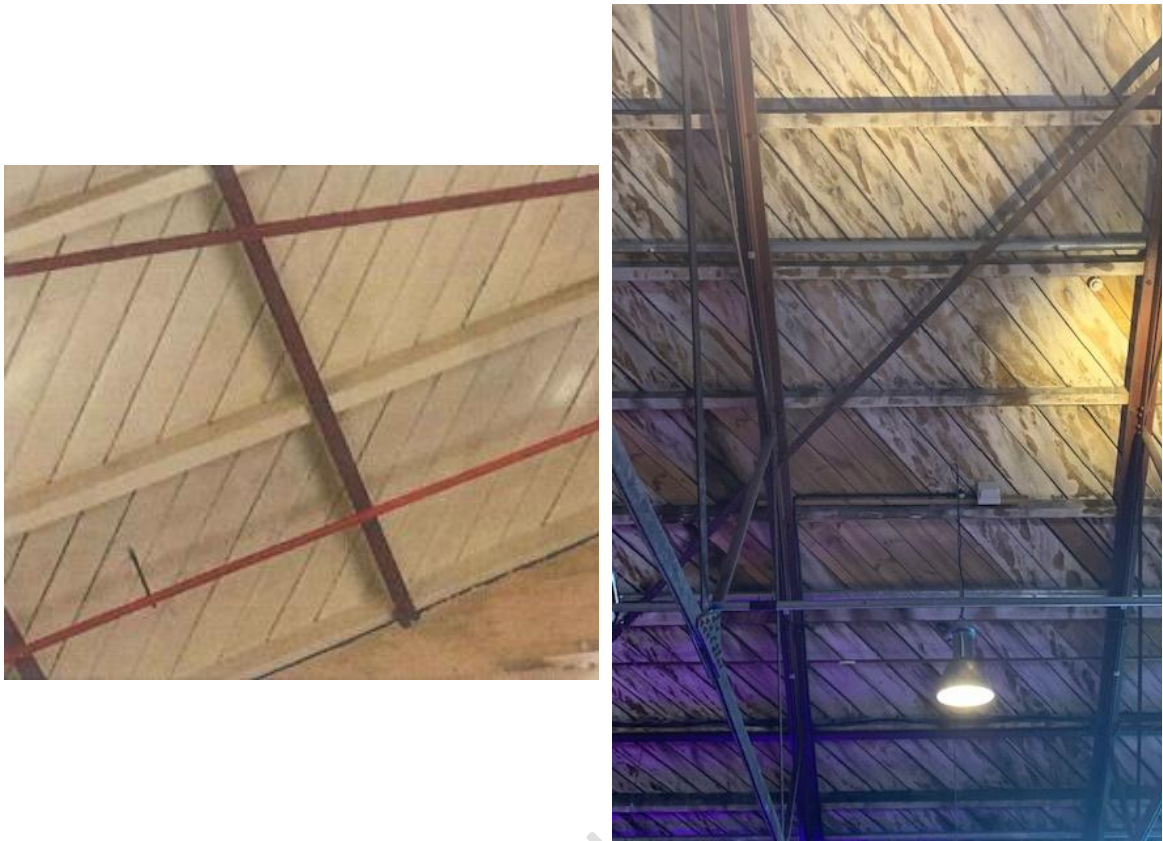


Figure C8.19: Typical timber diaphragms – diagonal sarking

The strength of both floor and roof diaphragms is complemented by the ceiling sheathing material. Common types of ceilings that provide structural capacity are timber lath-and-plaster, fibrous plaster, steel lath-and-plaster, and pressed metal. More modern additions of plywood boards and plasterboard may have also occurred over time.

C8.2.7 Diaphragm seating and connections

URM buildings are characterised by absent or weak connections between various structural components. Often, walls parallel to the joists and rafters are not tied to the floors and roof respectively (refer to [Figure C8.20](#)), except in a few cases depending on the design architect. Wall-diaphragm anchor plates, sometimes referred to as rosettes or washers, have been used to secure diaphragms to walls since the late 19th century (refer to [Figure C8.21](#)). If these **elements** are present in a building **then** they may have been installed during the original construction or at any time since as a remediation measure.



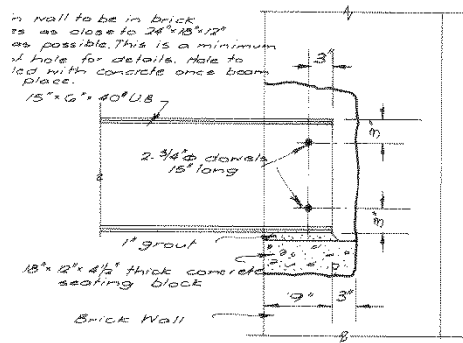
Figure C8.20: A lack of connection of the walls parallel to joist and rafters with diaphragms and return walls leading to collapse of wall **due to face loading**



Figure C8.21: 1896 image showing anchor plate connections installed in early URM construction (National Library of New Zealand)

Even where walls are carrying beams, joists or rafters, they are not always secured to these elements. Connections made of steel straps tying the beams, joists or rafters to walls have been observed (refer to [Figure C8.22](#) and [Figure C8.23](#)), sometimes with a fish-tail cast into concrete pockets.

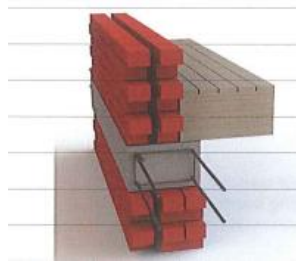
Another common feature is a gap on either side of the timber joists and beams to avoid moisture transfer from brickwork to timber. With such connections, horizontal shear cannot be transferred from walls to joists. However, if the joists are set tightly in the pocket **then** they can be effective in horizontal shear transfer between the wall and floor structure.



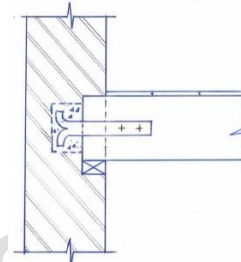
(a) Steel beam to wall pocketed connection



(b) Floor joist to wall connection. Note presence of steel strap (Matt Williams)



(c) Floor seating arrangement

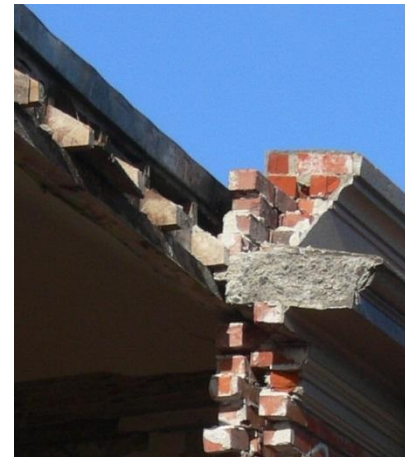


(d) Fish-tail connection between wall and joist

Figure C8.22: Typical connection between masonry walls and joist



(a) Wall to roof truss connection
(Miyamoto International)



(b) Roof seating arrangement and
parapet wall **with flared cornice**
(Dizhur)



(c) Wall to roof truss connection. Note truss is seated on a concrete padstone
(Miyamoto International)

Figure C8.23: Typical wall to roof connections

C8.2.8 Wall to wall connections

In most cases there are no mechanical connections provided to tie orthogonal walls together. Concrete bands may be provided but may not be tied together at corners as it is possible that they were built by different teams **of masons** at different stages. If **orthogonal walls** are jointed **then** it may just be with intermittent steel ties, or bricks pocketed into the abutting walls which have very little tie or shear capacity.

C8.2.9 Damp-proof course (DPC)

Most traditional buildings incorporate a damp-proof course (DPC) in the masonry between foundations and ground floor level. This **DPC** can be made from galvanised metal, lead, slate, thick bitumen or bitumen fabric.

The DPC layer usually forms a slip plane (refer to **Figure C8.24(a)**) which is weaker than the surrounding masonry for sliding. **The DPC** also forms a horizontal discontinuity which can affect bond for face loading or hold-down of walls for in-plane loading. Sliding on the DPC layer has been recorded, as shown in **Figure C8.24(b)**.

Consideration of the DPC layer is an important part of establishing the capacity of the wall: refer to Section C8.8.6 for details.



(a) DPC below timber – Chest Hospital, Wellington



(b) Bitumen DPC and sliding evident after the 2013 Cook Strait earthquakes

Figure C8.24: Common DPC materials

C8.2.10 Built-in timber

Most traditional URM buildings incorporate built-in timbers (refer to Figure C8.25) for:

- fixing of linings, skirting, cornices and dado/picture rails
- plates supporting intermediate floor joists
- forming header connections between wall layers, and
- top plates for affixing rafters or trusses.



Figure C8.25: 12 mm timber built into every eighth course for fixing linings

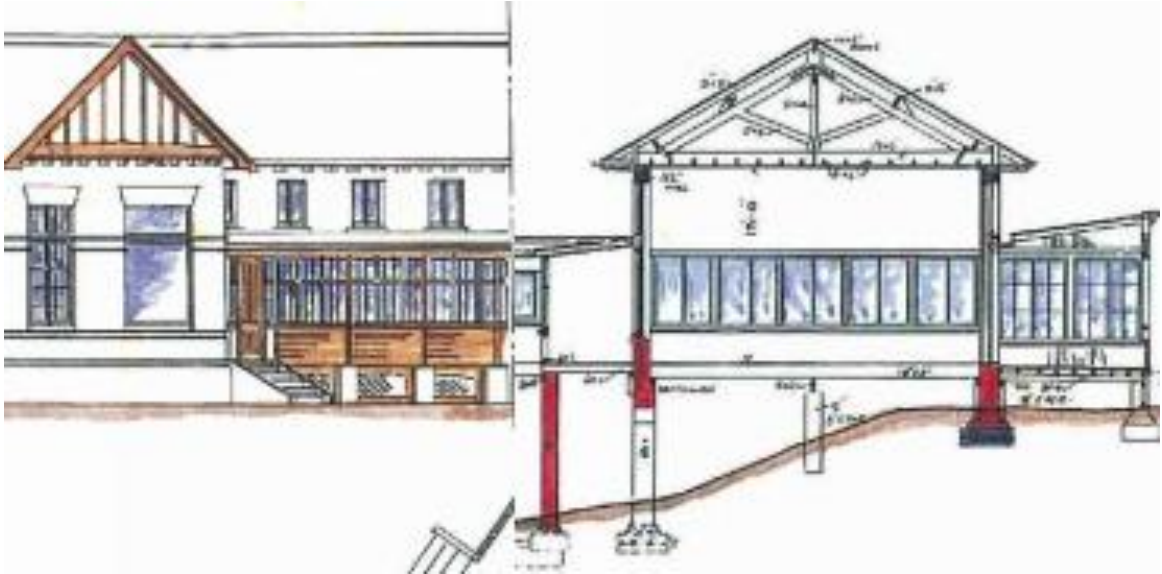
Degradation of these items is common, which causes localised stresses or bowing of walls. This **deterioration** will typically be more severe on the south side of buildings or nearer the ground level. Timber also shrinks, particularly perpendicular to the grain, and such timbers are often not in full contact with the surrounding masonry. In the case of continuous timber plates, engagement with the masonry is often limited to localised timber blocks notched into the walls.

C8.2.11 Concrete ring beams or bond beams

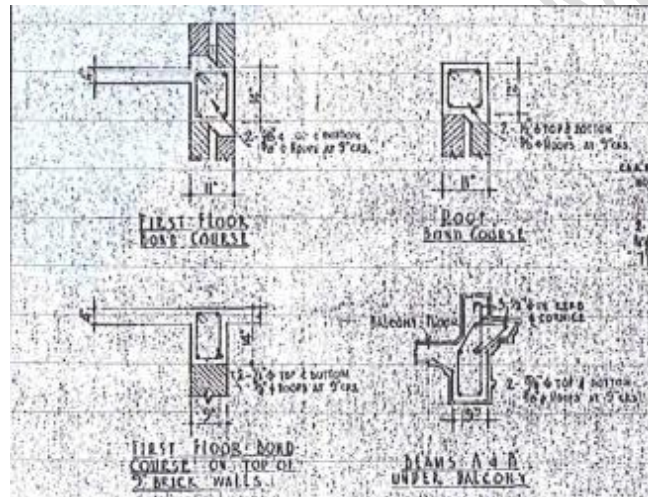
Ring beams, bond beams or perimeter tie beams (refer to **Figure C8.22(c)** and **Figure C8.26**) were typically constructed of reinforced concrete, plain concrete or timber. These **elements** can provide significant benefits to the performance of masonry buildings, including:

- providing a larger, often stronger substrate for the attachment of fixings and thereby providing better load distribution
- distributing diaphragm loads along the length of a wall
- tying **leaves** together in cavity construction (refer to **Figure C8.22(c)** and **Figure C8.26(b)**), provided that the bond beam is laid over both wythes
- providing coupling between wall panels for in-plane loads
- providing longitudinal tying to spandrel beams, and
- providing out-of-plane stability to face-loaded walls.

Depending on the age of the structure, there may be poor/no hook or termination details in reinforced concrete bond beams, so concentrated loads near the ends of such bond beams should be avoided. **Similarly care should be taken when using bond beams as diaphragm chords because the (round) reinforcement may not be adequately lapped to provide sufficient capacity for high cyclic tie loads.** Stirrup reinforcement in these beams is often nominal – if present at all – so care should be taken when shear loads are being applied to these elements.



(a) Bond beam in cavity wall also forming lintel – Chest Hospital, Wellington (Dunning Thornton)



(b) Typical lintel detail (Dizhur)

Figure C8.26: Bond beams

The presence of a concrete band provides no surety that reinforcement is present. Figure C8.27 shows a concrete capping beam that is obviously not reinforced. See also Figure C8.23(b).

The reinforcement in the beam may also have degraded or may soon degrade if carbonation/chloride attack has penetrated into the concrete to the depth of the reinforcement. When severe, corrosion deposits will split the concrete.



Figure C8.27: The wide cracks through bond beams indicate a lack of reinforcement in the beam (Dizhur)

C8.2.12 Bed-joint reinforcement

Bed-joint reinforcement (course reinforcement) varies in type and application. It can include:

- single wires or pairs of wires laid in mortar courses to augment in-plane performance
- single wires or pairs of wires laid in mortar courses to act as lintels or ties to soldier courses
- prefabricated/welded lattices laid in multi-wythe walls to ensure bond
- prefabricated/welded lattices laid across cavity walls to form cavity ties
- cast iron oversize cavity ties laid in multi-wythe walls to ensure bond, and
- chicken mesh.

Bed-joint reinforcement is often small in size relative to a fairly massive wall. **Bed-joint reinforcement** adds robustness but usually does not add significant structural strength.

This type of reinforcement is not usually apparent from a visual inspection. However, the requirement for bed-joint reinforcement was often noted in the original masonry specifications and has been observed in brick buildings.

C8.2.13 Lintels

Lintels commonly comprise:

- reinforced concrete beams over the full width of the wall
- reinforced concrete beams behind a decorative facing course, with this facing course supported on cavity ties or a steel angle
- steel angles
- steel flats (shorter spans)
- timber piece
- soldier course arches or flat arches, and
- stone lintels.

Arches or flat arches add a permanent outward thrust to a building which can destabilise walls in plane. This thrust along with any other forces should be resisted by ties in the building.

Reinforced concrete beams can contribute to in-plane pier/wall behaviour as they effectively reinforce the spandrel. However, they concentrate bearing loads at their supports and, if such frames dilate, can be points of overloading or destabilisation. They are also useful components for attachments for diaphragms (if the window heads are sufficiently high) as they provide a robust, blocky element to connect to.

C8.2.14 Secondary structure and critical non-structural items

Parapets are commonly placed on top of the perimeter walls. Parapets are frequently positioned off centre from the wall beneath, and capping stones or other ornamental features are then attached to the street side. Roof flashings are often chased into the brickwork on the external face just above roof level, creating a potential weak point in the masonry where rocking can occur.

Note:

Parapets, chimneys, pediments, cornices and signage (refer to Figure C8.28) on street frontages present a significant hazard to the public. The Ministry of Business, Innovation and Employment has issued a determination (2012/043) clarifying that external hazards such as these must be included in the seismic assessment rating of a building.

Heavy partition walls are potentially critical non-structural (or secondary structural) items which are usually not tied to the ceiling diaphragm and can pose a serious threat to life safety.



Figure C8.28: Secondary elements (Miyamoto International)

C8.2.15 Seismic strengthening methods used to date

Many URM buildings have been strengthened over the years either because of legislative requirements (e.g. earthquake-prone building legislation) or post-earthquake reconstruction (e.g. following the 1942 Wairarapa earthquake).

A number of strengthening techniques have been used (Ismail, 2012). The main principles were to tie unrestrained elements, such as chimneys and parapets, to the main load-bearing

structure and to tie various building elements together so the building could act globally as a box with the intention that the available lateral capacity of the building could be fully mobilised even though it may not always have been increased.

Note:

Before 2004, seismic strengthening requirements for URM buildings were very low. In addition, in most strengthening projects the material properties were not verified by testing, anchors were mostly untested, and they were installed without documented quality assurance procedures. **In the Canterbury earthquakes it was observed that many adhesive anchors performed poorly (see Figure C8.29).**



Figure C8.29: Anchor failure from the Canterbury earthquakes (University of Auckland)

Assessment of previously retrofitted buildings requires an understanding of the retrofit measures that historically have been carried out and the likely effect these would have on the seismic performance.

Techniques used historically for strengthening different structural mechanisms include:

- **chimneys:** internal post-tensioning and steel tube reinforcement, concrete filling, external strapping and bracing, removal and replacement (see Figure C8.30 and Figure C8.55b)



Figure C8.30: Performance of braced chimneys in the Canterbury earthquakes (University of Auckland)

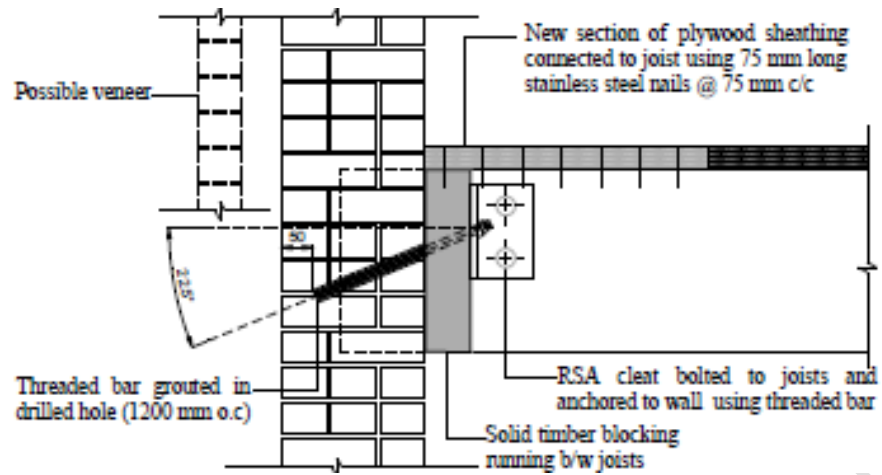
- **parapets:** vertical steel mullions, raking braces, steel capping, post-tensioning, internal bonded reinforcement, near surface mounted (NSM) composite strips
- **face-loaded walls:** vertical steel or timber mullions, horizontal transoms, post-tensioning, internal bonded reinforcement, composite fibre overlay, NSM composite strips, reinforced concrete or cementitious overlay, grout saturation/injection, horizontal and vertical reinforced concrete bands.
- **wall-diaphragm connections:** steel angle or timber joist/ribbon plate with either grouted bars or bolts/external plate, blocking between joists notched into masonry, external pinning to timber beam end or to concrete beam or floor, through rods with external plates, new isolated padstones, new bond beams
- **diaphragm strengthening:** plywood overlay floor or roof sarking, plywood ceiling, plywood/light gauge steel composite, plasterboard ceiling, thin concrete overlay/topping, elastic cross bracing, semi-ductile cross bracing (e.g. Proving ring), replacement floor over/below with new diaphragm
- **in-plane wall strengthening/new primary strengthening elements:** sprayed concrete overlay, vertical post-tensioning, internal horizontal reinforcement or external horizontal post-tensioning, bed-joint reinforcement, composite reinforced concrete boundary or local reinforcement elements, composite fibre reinforced (FRP) boundary or local reinforcement elements, nominally ductile concrete walls or punched wall/frame or reinforced concrete masonry walls, nominally ductile steel concentric or cross bracing, limited ductility steel moment frame or concrete frame or concrete walls or timber walls, ductile eccentrically braced frame/K-frames, ductile concrete coupled or rocking walls, or tie to new adjacent (new) structure, structural plaster
- **reinforcement at wall intersections in plan:** removal and rebuilding of bricks with inter-bonding, bed-joint ties, drilled and grouted ties, metalwork reinforcing internal corner, grouting of crack

- **foundation strengthening:** mass underpinning, grout injection, concentric/balanced re-piling, eccentric re-piling with foundation beams, mini piling/ground anchors
- **cavity ties:** helical steel mechanical engagement – small diameter, steel mechanical engagement – medium diameter, epoxied steel rods/gauze sleeve, epoxied composite/non-metallic rods, brick header strengthening
- **canopies:** reinforcement or recast of existing hanger embedment, new steel/cast iron posts, new cantilevered beams, deck reinforcement to mitigate overhead hazard, conversion to accessible balcony, base isolation.

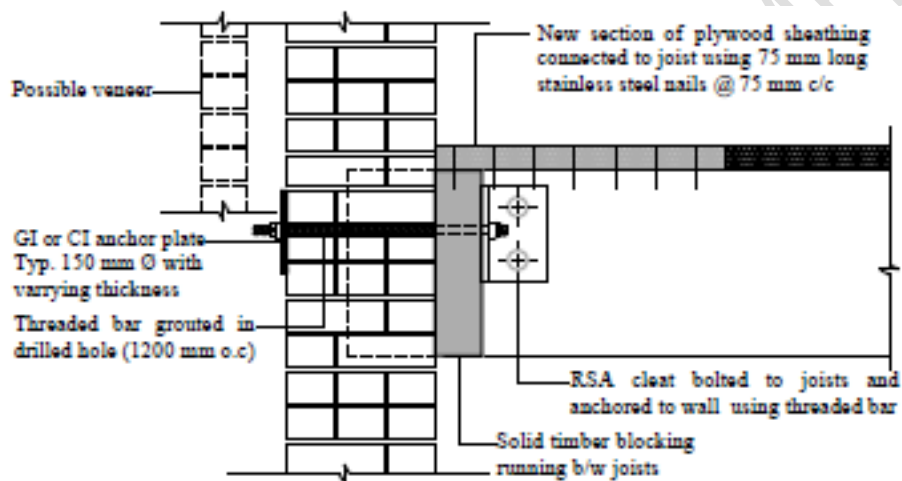
Figure C8.31 to Figure C8.35 illustrate some of these techniques. Also refer Table C8.2 in Section C8.6.11, which lists common strengthening techniques and particular features or issues to check for each method.



Figure C8.31: Bracing of wall against face load (Dunning Thornton)



(a) Bent adhesive anchor



(b) Through anchor with end plate (plate anchor)

Figure C8.32: Wall-diaphragm connections (Ismail, 2012)



Figure C8.33: New plywood diaphragm (Holmes NZ LP)



(a) Concentric steel frame (Beca)



(b) Steel frame (Dizhur)



(c) FRP overlay



(d) Steel frame (Dunning Thornton)

Figure C8.34: Improving in-plane capacity of URM walls

Strengthening of parapets is often carried out using racking braces, with one end tied to the timber roof structure (refer to [Figure C8.35](#)). However, issues with this method include a lack of vertical tie-down to counter the vertical force component of brace and ground shaking, or the flexibility of the roof amplifying shaking of the parapet.

Note:

When strengthening parapets, it is essential to make a robust connection down to the wall below and back into the structure. The danger of non-robust strengthening is that the parapet still fails, but collapses in larger, more dangerous pieces.



Figure C8.35: Parapet bracing. Note a lack of vertical tie-up of the parapet (Dizhur)

C8.3 Observed Seismic Behaviour of URM Buildings

C8.3.1 General

When assessing and retrofitting existing URM buildings it is important to understand the potential seismic deficiencies and failure hierarchy of these buildings and their components.

The most hazardous of these deficiencies are inadequately restrained elements located at height, such as street-facing façades, unrestrained parapets, chimneys, ornaments and gable end walls. These are usually the first elements to fail in an earthquake and are a risk to people in a zone extending well outside the building perimeter.

The next most critical elements are face-loaded walls and their connections to diaphragms and return walls. Even though their failure may not lead to the building's catastrophic collapse, they could pose a severe threat to life safety.

However, when building members/elements are tied together and out-of-plane failure of walls is prevented, the building will act as a complete entity and in-plane elements will come under lateral force action.

Failures of URM buildings (summarised in Figure C8.36) can be broadly categorised as:

- **local failures** – these include the toppling of parapets, walls not carrying joists or beams under face load, and materials falling from damaged in-plane walls. These local failures could cause significant life-safety hazards, although buildings may still survive these failures.
- **global failures** – these include failure modes leading to total collapse of a building due to such factors as loss of load path and deficient configuration.

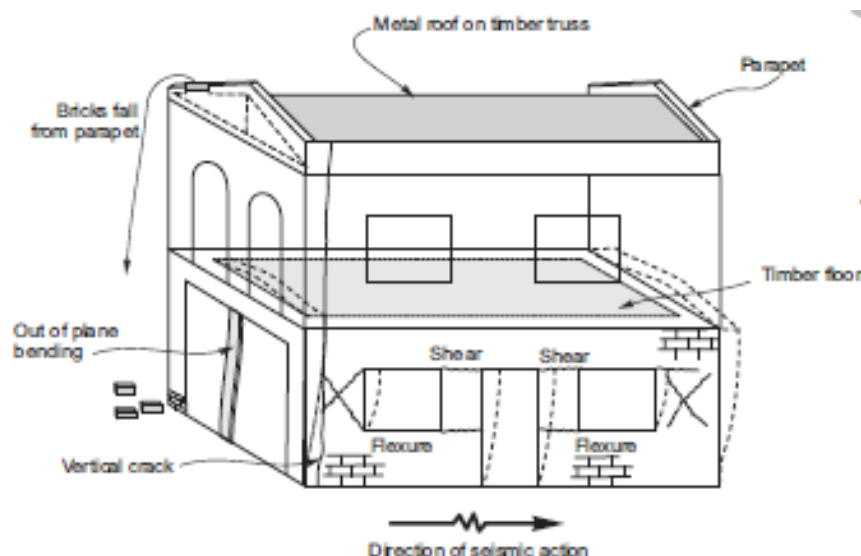


Figure C8.36: Failure modes of URM buildings

In URM buildings, in-plane demands on walls decrease up the height of the walls. In-plane capacity also decreases with height as the vertical load decreases. In contrast, out-of-plane demands are greatest at the upper level of walls (refer to Figure C8.37), but out-of-plane capacity is lowest in these areas due to a lack of vertical load on them. Hence, the toppling of walls starts from the top unless these walls are tied to the diaphragm.

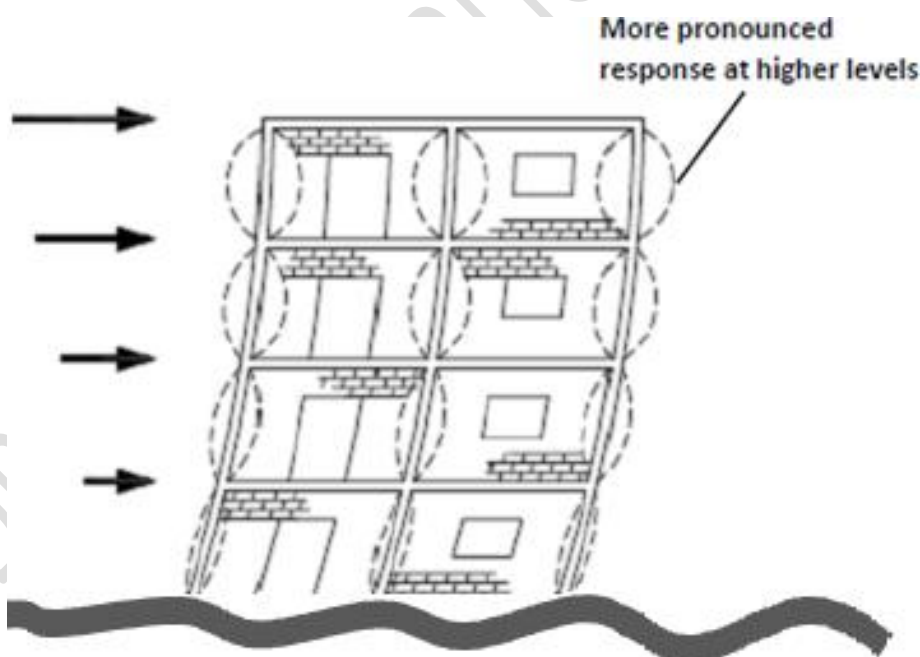


Figure C8.37: Out-of-plane deformation of masonry walls is most pronounced at the top floor level (adapted from Tomazevic, 1999)

C8.3.2 Building configuration

Building configuration tends to dictate the nature of URM failures. Cellular type buildings act as stiff structures, attracting high accelerations and therefore force-governed failure of their parts. Collapse of walls subjected to face loading and spanning vertically and

horizontally between floors and abutting walls respectively tends to be independent for each cell, depending on the angle of loading and the wall configuration.

Buildings where the span or flexibility of the diaphragm is an order of magnitude **greater** than the wall **dimensions** tend to have more displacement-related failures. Walls and parapet collapse initiates from the mid-span of the diaphragm where **deformations** are greatest (but accelerations are not necessarily as high).

Taller buildings may exhibit less damage at low levels than shorter buildings (refer to **Figure C8.38**), as the confinement of the masonry from the weight above provides significant strength. In larger buildings, the weaker elements (usually spandrels) fail first from bottom up (as shown later in this section, in **Figure C8.54**). This results in period lengthening of the structure and reduces the ability to transmit forces up the building.

As with all structures, the behaviour of URM buildings with a more regular configuration is generally more predictable. Buildings with irregular plan configurations, such as those on street corners (especially with an acute angle corner), suffer high displacements on their outer points. Shop fronts similarly experience high drifts, but these are often masked by “buttressing” from adjacent buildings in a “row” effect. This effect also disguises a vertical irregularity in which stiff façades tend to move as a solid element above the flexible open shop front.



Figure C8.38: Reduction of damage towards base of building as axial load increases (Dunning Thornton)

C8.3.3 Diaphragms

The timber diaphragms commonly used in URM buildings are generally flexible, which may result in large diaphragm displacements during an earthquake. These will impose large displacement demand on the adjoining face-loaded walls, which could lead them to fail (refer to **Figure C8.39**).



Figure C8.39: Out-of-plane wall failure due to excessive roof diaphragm movement (Dizhur et al., 2011)

Figure C8.40 shows a photograph of delamination of plaster due to interaction between wall and ceiling due to shear transfer.



Figure C8.40: Lath and plaster ceiling. Note that stresses where shears are transmitted to the wall have caused the plaster to delaminate from the timber lath

In some cases, diaphragm and shear-wall accelerations can increase with the flexibility of the diaphragm (Tena-Colunga and Abrams, 1996).

C8.3.4 Connections

C8.3.4.1 General

The following types of damage to wall-diaphragm connections have been postulated (Campbell et al., 2012) – the first four were actually observed during the 2010/11 Canterbury earthquake sequence:

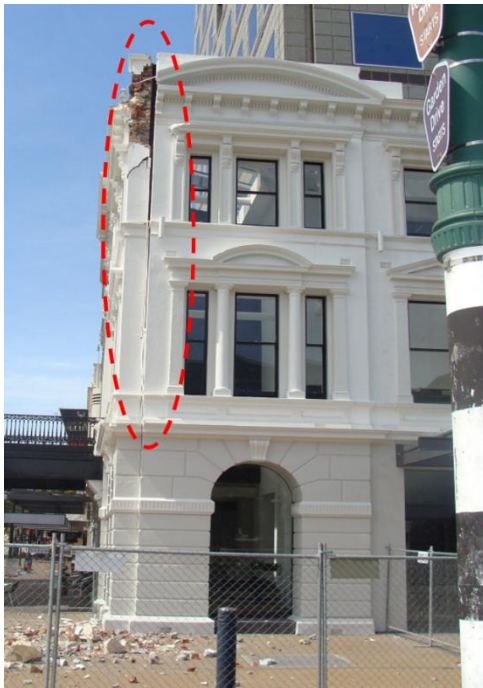
- punching shear failure of masonry
- yield or rupture of connector rod
- rupture at join between connector rod and joist plate
- splitting of joist or stringer
- failure of fixing at joist
- splitting or fracture of anchor plate
- yield or rupture at threaded nut.

C8.3.4.2 Wall to wall connections

Connections between the face-loaded and return walls will open (i.e. there is return wall separation) after a few initial cycles of shaking (refer to Figure C8.41) because of stiffness incompatibility between stiff in-plane and flexible face-loaded walls and a natural dilation

of a wall and pier assembly working in plane. This leads to loss of flange effect and softening of the building, resulting in a change in dynamic characteristics of the walls and piers. The integrity of connection between wall at junctions and corners depends on bonding between orthogonal walls.

While return wall separation can cause significant damage to the building fabric it does not necessarily constitute significant structural damage. This is provided the wall elements have adequate out-of-plane capacity to span vertically and there are enough wall diaphragm ties.



(a) Vertical cracks (Dizhur)



(b) Corner vertical splitting where walls are poorly keyed in together

Figure C8.41: Damage to in-plane and face-loaded wall junctions

C8.3.4.3 Wall to floor/wall to roof connections

Failure of rosettes, rupture of anchor bars and punching shear failure of the wall was commonly observed following the 2010/11 Canterbury earthquake sequence (refer to [Figure C8.42](#)). This failure mode is characterised by failure of the mortar bed and head joints in a manner that traces a failure surface around the perimeter of the anchor plate. For multi-wythe walls the head joints will not be in alignment and, as for a concrete punching shear failure, it is possible that the failure surface on the interior surface of the wall may cover a broader area.



Figure C8.42: Plate anchor on verge of punching shear failure (Dizhur et al., 2011)

Testing at the University of Auckland (Campbell et al., 2012) has shown that anchor plates may exhibit a variety of different failure modes (refer to [Figure C8.43](#) and [Figure C8.44](#) for examples) so their condition should be considered carefully.

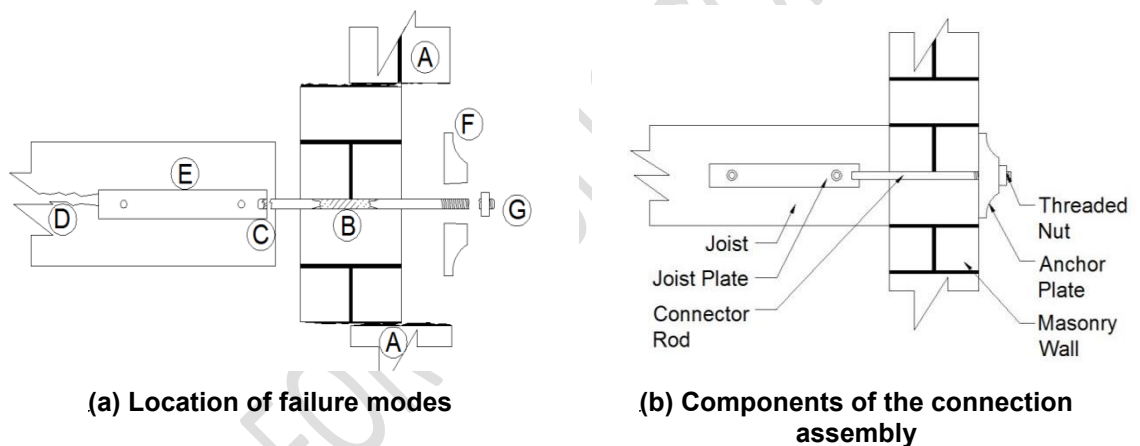


Figure C8.43: Observed failure modes from tensile test series (Campbell et al., 2012)



Figure C8.44: Observed failure modes from tensile test series (Campbell et al., 2012)

Adhesive anchorages have been a popular form of anchorage for many years. These typically involve a threaded rod being chemically set into a drilled hole using either grout or epoxy adhesive. Unfortunately, there have been numerous observations of failed adhesive anchorages following the 2010/11 Canterbury earthquake sequence (refer to [Figure C8.45](#)). Reasons for this include:

- their use in regions expected to be loaded in flexural tension during an earthquake (such as on the rear surface of a parapet that may topple forward onto the street) – the brick work was likely to crack in the vicinity of the anchorages and cause them to fail, even if the adhesive had been placed effectively
- incorrect installation – examples included cases of insufficient or absent adhesive, where the drilled hole had not been sufficiently cleared of brick dust from the drilling operation so there was inadequate bond to the brick surface, or where the inserted anchorage was of insufficient length
- anchors that were adequately set into a brick but the secured brick had failed in bed-joint shear around its perimeter. As a result, only the individual brick was left connected to the anchorage, while the remainder of the brickwork had failed.



Figure C8.45: Failed adhesive brick anchors (Dizhur et al., 2013)

C8.3.5 Walls subjected to face loads

Out-of-plane wall collapse under face load is one of the major causes of destruction of masonry buildings, particularly when a timber floor and roof are supported by these walls. The seismic performance of the URM face-loaded walls depends on the type of diaphragm, performance of wall-diaphragm connections and the wall-wall connection. Figure C8.46 illustrates the response of face-loaded walls to the type of diaphragm and wall-diaphragm connections.

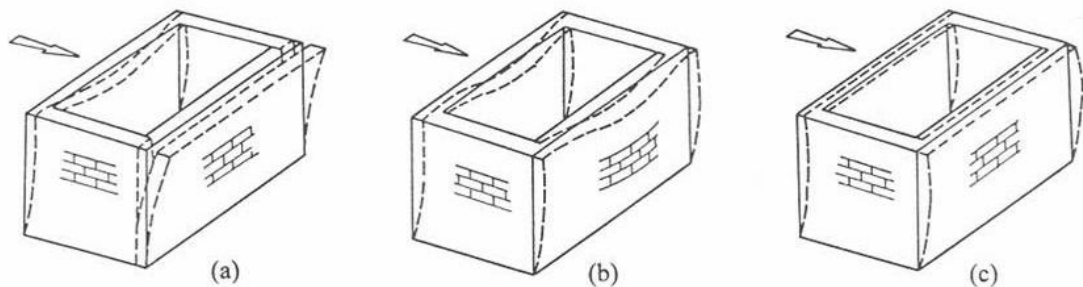


Figure C8.46: Effect of types of diaphragm on face-loaded walls – a) inferior wall-to-wall connection and no diaphragm, b) good wall-to-wall connection and ring beam with flexible diaphragm, c) good wall-to-wall connection and rigid diaphragm

Figure C8.47 and Figure C8.48 show images of damage to masonry buildings due to collapse of walls under face load.



Figure C8.47: Out-of-plane instability of wall under face load due to a lack of ties between the face-loaded wall and the rest of the structure (Sharpe)

Gable end walls sit at the top of walls at the end of buildings with pitched roofs. If this triangular portion of the wall is not adequately attached to the roof or ceiling, it will rock as a free cantilever (similar to a chimney or parapet) so is vulnerable to collapse. This is one of the common types of out-of-plane failure of gable walls (refer to [Figure C8.48](#)).



Figure C8.48: Collapse of gable wall. Note a secured gable end that survived earthquake loading and a companion failed gable end that was not secured (Ingham and Griffith, 2011)

Cavity wall construction can be particularly vulnerable to face-loading. Severe structural damage and major collapse of URM buildings with this type of construction was observed during the 2010/2011 Canterbury earthquake inspections (refer to [Figure C8.49](#)) and their performance was significantly worse than solid URM construction in resisting earthquake forces.



Figure C8.49: Failure of URM cavity walls (Dizhur)

The veneers of cavity wall construction also have the potential to topple during earthquake shaking (refer to [Figure C8.49](#)). Toppling is typically attributed to the walls' high slenderness ratio, deteriorated condition of the ties, overly flexible ties, pull-out of ties from the mortar bed joints due to weak mortar (refer to [Figure C8.11](#)), or a total absence of ties.

In multi-storey buildings the out-of-plane collapse of walls is more pronounced at the top floor level. This is due to the lack of overburden load on the walls and amplification of the earthquake shaking there (refer to [Figure C8.37](#)).

C8.3.6 Walls subjected to in-plane loads

Damage to URM walls due to in-plane seismic effects (in the direction of the wall length) is less significant than damage due to out-of-plane seismic effects. In addition, the stocky elements in URM (walls, piers and spandrels) usually make these structures more forgiving of distress in individual elements than the skeletal structures of modern framed buildings; principally, because the spectral displacements are small compared to the member dimensions. Nevertheless, some failure modes are less acceptable than others.

In general, the preferred failure modes are rocking or sliding of walls or individual piers. These modes have the capacity to sustain high levels of resistance during large inelastic straining. For example, sliding displacements at the base of a wall can be tolerated because the wall is unlikely to become unstable due to the shear displacements.

Masonry walls are either unpenetrated or penetrated. A penetrated wall consists of piers between openings plus a portion below openings (sill masonry) and above openings (spandrel masonry). When subjected to in-plane earthquake shaking, masonry walls and piers may demonstrate diagonal tension cracking, rocking, toe crushing, sliding shear, or a combination of these. Similarly, the spandrels may demonstrate diagonal tension cracking, unit cracking or joint sliding. [Figure C8.50](#) shows the potential failure mechanisms for unpenetrated and penetrated walls.

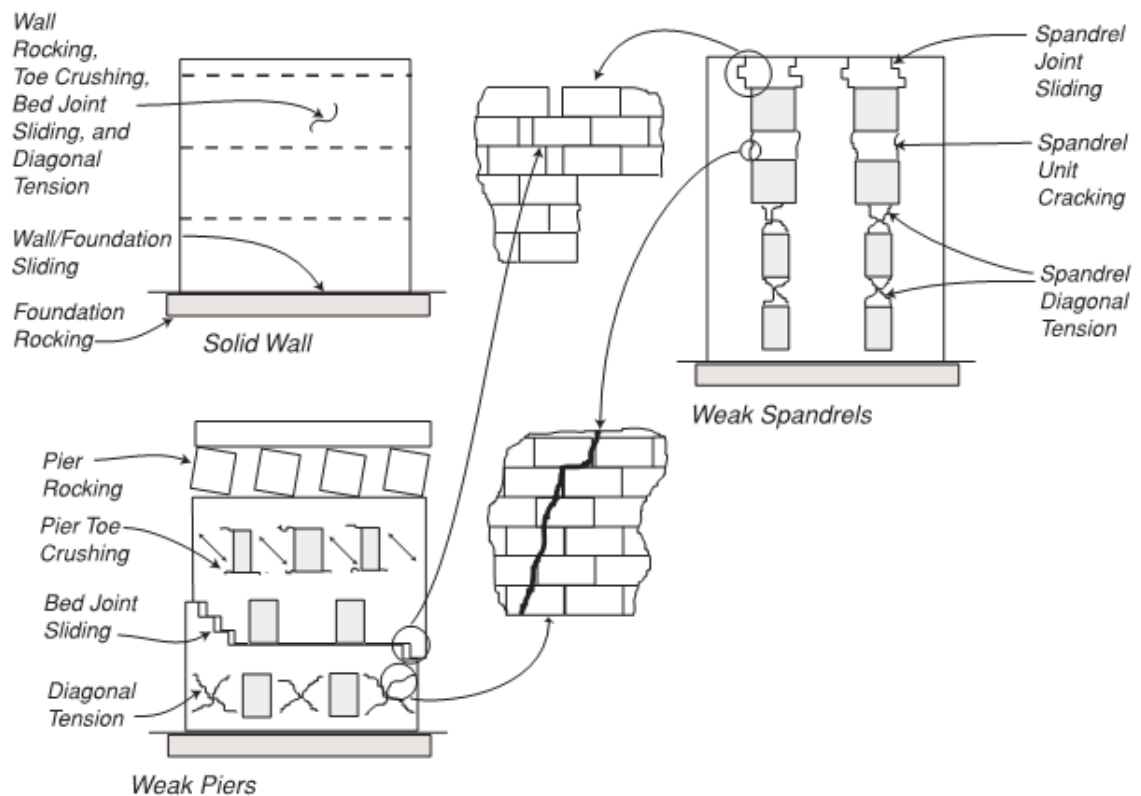


Figure C8.50: In-plane failure modes of URM wall (FEMA 306, 1998)

Rocking of URM piers may result in the crushing of pier end zones and, under sustained cyclic loading, bricks could delaminate if the mortar is weak. An example of this is shown in [Figure C8.51](#), where the damage to the building is characterised by the rotation of entire piers.



Figure C8.51: Rocking and delamination of bricks of a one-storey unreinforced brick masonry building with reinforced concrete roof slab (Bothara and Hıçyılmaz, 2008)

Sliding shear can occur along a distinctly defined mortar course (refer to [Figure C8.52\(a\)](#)) or over a limited length of several adjacent courses, with the length that slides increasing

with height (refer to [Figure C8.52\(b\)](#)). This can often be mistaken for diagonal tension failure, which is less common in walls with moderate to low axial forces.



(a) Sliding shear failure along a defined plane at first floor level (Dunning Thornton)



(b) Stair-step crack sliding, in walls with low axial loads (Bothara)

Figure C8.52: Sliding shear failure in a brick masonry building

Alternatively, masonry piers subjected to shear forces can experience diagonal tension cracking, also known as X-cracking (refer to [Figure C8.53](#)). Diagonal cracks develop when tensile stresses in the pier exceed the masonry tensile strength, which is inherently very low. This type of damage is typically observed in long and squat piers and on the bottom storey of buildings, where gravity loads are relatively large and the mortar is excessively strong.



(a) **Diagonal tension** cracks to a brick pier. Note splitting of bricks (Dizhur)



(b) **Diagonal tension** cracks to brick masonry. Note splitting of bricks, indicative of mortar stronger than bricks (Russell, 2010)

Figure C8.53: Diagonal tension cracking

In the penetrated walls, where spandrels are weaker than piers, the spandrel may suffer catastrophic damage (refer to [Figure C8.54](#)). This could turn squat piers into tall piers, resulting in a reduction in the overall wall capacity and an increase in expected deflections. The increase in deflection will increase the fundamental period of the building and reduce the demands which may be a mitigating effect. In any event, the consequences of failure of the spandrels and the resulting effect on life safety needs to be considered.

As noted in Section C8.2.9, sliding on the DPC layer has also been observed (refer to [Figure C8.24](#) in that section).



Figure C8.54: Failure of spandrels. Also note rocking of upper piers and corner cracking of the parapet (Dizhur)

C8.3.7 Secondary members/elements

The instability of parapets and chimneys is caused by these elements acting as rocking cantilevers which can topple when sufficiently accelerated (refer to [Figure C8.55](#)). Braced chimneys and parapets also failed during the 2010/11 Canterbury earthquake sequence (Ismail, 2012). Possible reasons include:

- bracing to the roof caused coupling with the vertical response modes of the roof trusses where the roof structure was flexible
- ties tying the parapets to the wall below the diaphragm level did not exist or were deficient
- strengthening standards were low (until 2004 the general requirement was to strengthen URM buildings to two thirds of NZSS 1900.8:1965)
- spacing between lateral support points was too large
- high vertical accelerations
- lack of deformation compatibility between support points (refer to [Figure C8.55\(b\)](#)).



(a) Out-of-plane instability of parapet (Beca)



(b) Chimney at onset of falling (Dizhur)

Figure C8.55: Secondary members/elements

Canopies can be both beneficial and detrimental in relation to life safety (refer to **Figure C8.56**):

- They are often hung off the face of the buildings so columns supporting their outer edge do not obstruct the footpath or roadway. When subject to vertical loads, these diagonal hangers act to pry the outer layers of brick off the face of the building at the connection point.
- However, if they are sufficiently robust in their decking and fixings or if they are propped, they can provide overhead protection by taking at least the first impact of any falling objects.



Figure C8.56: Face-load failure of URM façade exacerbated by outward loadings from downward force on canopy. Note the adjacent propped canopy did not collapse. (Dunning Thornton)

C8.3.8 Pounding

This failure mechanism only occurs in row-type construction (refer to Section C8.5.4) where there is insufficient space between adjacent buildings **such that** they pound into each other when **deforming** laterally during an earthquake. Many examples of pounding damage to URM buildings were observed following the 2010/11 Canterbury earthquake sequence (refer to **Figure C8.57** and Cole et al., 2012).

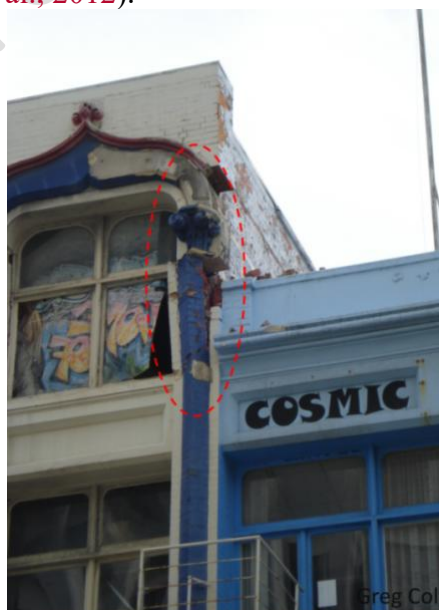


Figure C8.57: Pounding failure (Cole)

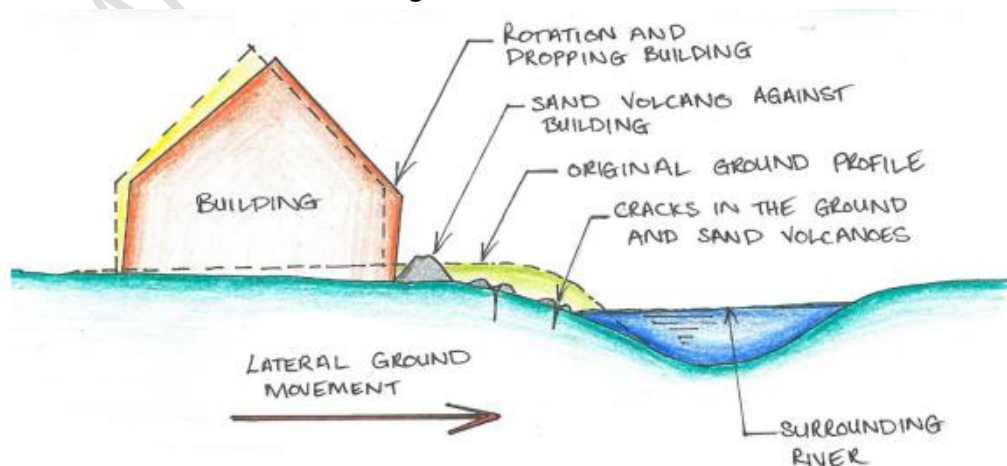
The severity of damage due to pounding depends upon the floor alignment between adjacent buildings, the difference in stiffness between the adjacent buildings, the pounding interface, floor weights, overall height variation between adjacent buildings, wall opening configurations, and the clearance of structural separation between adjacent buildings if separation is provided. Buildings with greater stiffness and lower overall height than their neighbours are prone to experience more detrimental pounding effects in terms of amplified seismic responses and damage propagating from the pounding interface. The extent of pounding damage may also be influenced by torsional actions due to irregular geometry that are particularly (although not exclusively) common for buildings located on the ends of a row. The potential for pounding effects should be carefully considered in URM row buildings where dynamic incompatibility between adjacent buildings may exist (Maison and Kasai, 1992; Kasai and Mason, 1997).

C8.3.9 Foundations and geotechnical failure

Foundation damage that can be seen by inspection is commonly from lateral spreading and differential settlement. URM buildings typically have no tying capacity at foundation level, so they split at the weakest point along a wall. “Failure” is often an extremely large displacement (refer to [Figure C8.58](#)). However, given the slower and non-cyclic nature of lateral spreading, this is less likely to induce actual collapse until extreme displacements are reached.



(a) Large diagonal cracks and lateral movement of the access ramp caused by ground movement



(b) Settlement and lateral spread towards river

Figure C8.58: Earthquake-induced geotechnical damage to URM buildings (Neill et al., 2014)

C8.4 Factors Affecting Seismic Performance of URM Buildings

C8.4.1 Number of cycles and duration of shaking

The strength and stiffness of URM degrades rapidly with an increasing number of cycles and the duration of ground shaking (refer to [Figure C8.59](#)). In general, a number of cycles of moderate acceleration sustained over time can be much more difficult for an URM building to withstand than a single, much larger peak acceleration (FEMA 454, 2006). Similarly, damage from higher acceleration, shorter period ground shaking from shallow earthquakes could be considerably greater than from deep earthquakes. This could affect stiffer URM buildings far more than flexible frame and timber structures.



(a) Post-September 2010 event – minor visible damage



(b) Post-February 2011 event – wall section on verge of failure



(c) Post-June 2011 event – wall collapse

Figure C8.59: Progressive damage and effect of shaking duration – 2010/11 Canterbury earthquake sequence (Dizhur)

Note:

The assessment of damaged buildings is outside the scope of these guidelines, and therefore progressive deterioration after the main event is not considered. It is assumed that the building will have been appropriately stabilised if this had been required after the main event.

C8.4.2 Other key factors

C8.4.2.1 General

Other key factors affecting the seismic performance of URM buildings include:

- building form
- unrestrained components
- connections
- wall slenderness
- diaphragm deficiency
- in-plane walls
- foundations
- redundancy
- quality of construction and alterations, and
- maintenance.

C8.4.2.2 Building form

A structurally irregular building suffers more damage than a regular building because of the concentration of both force and displacement demands on certain elements. An example of this is buildings along urban streets where the façades facing the street can be highly penetrated, with relatively narrow piers between openings, and the bottom storey could be totally open. This configuration could impose significant torsional demand and soft/weak storey mechanism. This can result in increased displacement demand and may lead to collapse.

C8.4.2.3 Unrestrained components

Instability of parapets and chimneys is caused by their low bending strength and high imposed accelerations. When subject to seismic actions, they rock on their supports at the roof line and can topple over when sufficiently accelerated by an earthquake.

C8.4.2.4 Connections

URM buildings can show significant resilience to seismic shaking as long as the building and its components can maintain their integrity. The wall-diaphragm anchors serve to reduce the vertical slenderness of a wall and also to make the building elements work together as a whole, rather than as independent parts. However, one of the most significant deficiencies in URM buildings in New Zealand is the lack of adequate connections; particularly those between walls and diaphragms.

C8.4.2.5 Wall slenderness

Unreinforced face-loaded masonry walls are weak in out-of-plane bending so are susceptible to out-of-plane failures. The earthquake vulnerability of a URM wall to out-of-plane bending is predominantly dictated by its slenderness (the ratio between thicknesses to span of wall). Cavity walls are especially vulnerable as the steel ties connecting the exterior wythes to the backing wall can be weakened by corrosion.

C8.4.2.6 Diaphragm deficiency

Diaphragms act as a lid to a box and are essential for tying the walls together and ensuring that lateral loads are transferred to the lateral load resisting elements. If diaphragms are too flexible, their ability to do this is compromised. Excessive diaphragm displacement imposes large displacement demand on walls, particularly on face-loaded walls, which could result in wall collapse.

C8.4.2.7 In-plane walls

These walls provide global strength and stiffness against earthquake load. Their seismic performance is defined by: the slenderness of walls and piers; vertical load; size and location of penetrations; relative strength between mortar and masonry units; and presence of bond beams, built-in timber and DPC.

C8.4.2.8 Foundations

Foundation flexibility and deformation affect the local and global earthquake response of URM buildings. However, foundations tend to be quite tolerant to deformations and building failure is rarely caused by ground settlement unless the ground underneath the building liquefies or suffers lateral spreading. Foundation effects or soil-structure interaction tend to reduce the force demand on the primary lateral-force-resisting elements, such as stiff in-plane loaded walls. At the same time, ground deformation can pose an additional rotational demand on the bottom storey wall under face load. The base fixity of the wall needs to be considered carefully as do the conditions at the wall base that have accumulated over the building's life (such as undermining by broken drains, clay heave or alteration of the surrounding soil or levels), and if these have changed with earthquake-induced liquefaction.

Existing high bearing pressures require careful consideration with respect to possible liquefaction-induced settlements. Settlement of long solid walls is often not a critical consideration for a URM building as the upper floors and roof frame into the walls with pin connections. However, careful consideration of the induced damage to any perpendicular/abutting walls is essential. For taller walls, ratcheting down with cyclic in-plane actions may be a consideration (refer Section C4). With little or no reinforcement in the footings (or ground slabs if present), there will be little resistance to lateral spreading or ground lurch, so vulnerability to these induced displacements should be assessed.

C8.4.2.9 Redundancy

The redundancy of a building refers to the alternative load paths able to add to resistance. The ability to redistribute demands through a secondary load path is an important consideration, as a building with low redundancy will be susceptible to total collapse if only one of its structural elements fails.

C8.4.2.10 Quality of construction and alterations

URM buildings in New Zealand represent an old building stock which has gone through many changes of occupancy. As a result, there may have been a number of structural modifications at different times which may not have been well considered, such as opening new penetrations in walls and diaphragms, removing existing components and adding new components. Such alterations will affect seismic performance.

C8.4.2.11 Maintenance

Older buildings that have been insufficiently maintained will have reduced material strength due to weathering (refer to [Figure C8.60](#)), corrosion of cavity ties (refer to [Figure C8.61](#)), rotting of timber and other processes that weaken masonry, connection capability, timber and reinforced concrete members. Similarly, water penetration in lime-based masonry will lead to leaching of lime from the mortar.



Figure C8.60: Severely degraded bricks and mortar due to moisture ingress (Ingham and Griffith, 2011)

The metallic cavity ties used in the original construction of URM cavity walls typically have no corrosion protection so are prone to severe deterioration (refer to [Figure C8.61](#)).



Figure C8.61: Metal cavity ties in rusted condition (Dizhur et al., 2011)

C8.5 Assessment Approach

C8.5.1 General

The assessment of a URM building requires an understanding of the likely behaviour of a number of building components and how these are likely to interact with each other.

The nature of the construction of this type of building means that each one is unique in terms of construction, quality of the original workmanship and current condition.

Therefore, it is important that the engineer has an appreciation of how the building was constructed, its current condition, the observed behaviour of similar buildings in previous earthquakes and a holistic view of the factors likely to affect its seismic performance. These issues are discussed in Sections C8.2, C8.3 and C8.4, which are considered to be essential reading prior to progressing through the assessment processes outlined in this section.

It is a general recommendation of these guidelines that the capacity of a building should be considered independently from the demands (imposed inertial loads and displacements) placed on it, bringing both together only in the final step of the assessment process. This is no different for URM buildings and is the basis behind the recommended assessment processes outlined below.

Past observations in earthquakes indicate that some components of URM buildings are particularly vulnerable to earthquake shaking and a hierarchy in vulnerability can be identified that can be useful in guiding the assessment process. Figure C8.62 shows a capacity “chain” for a typical URM building, with component vulnerability decreasing from left to right on the chain. The capacity of the building will be limited by the capacity of the weakest link in the chain, and the ability of each component to fully develop its capacity will typically be dependent on the performance of components to the left of it on the chain. This suggests that the assessment of component capacities should also proceed from left to right in Figure C8.62.

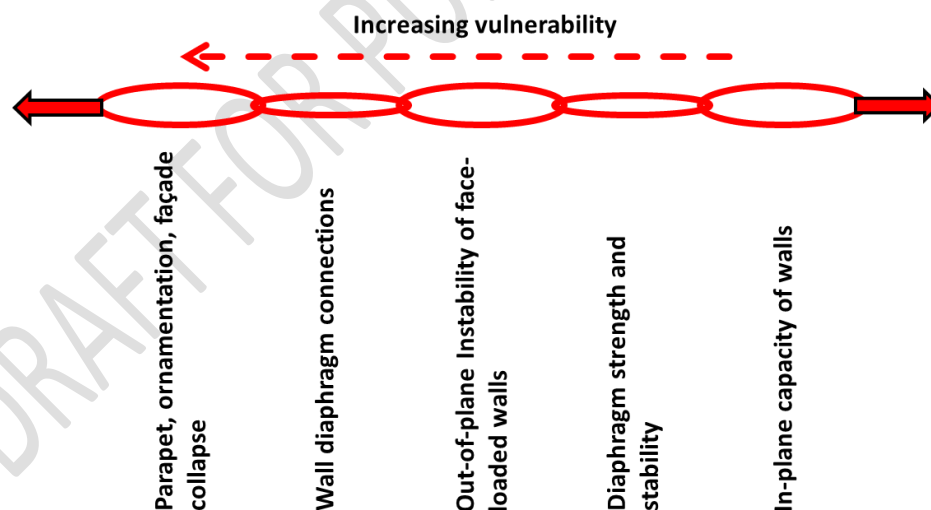


Figure C8.62: The capacity “chain” and hierarchy of URM building component vulnerability

While the critical structural weakness in a structural system will often be readily apparent (e.g. lack of any positive ties from brick walls to floors/roof) it will generally be necessary to evaluate the capacity of each link in the chain to fully inform on the components that require retrofit and the likely cost of this.

URM buildings come in different configurations, sizes and complexity. While complex buildings may require a first principles approach to the assessment of element capacity and internal actions within elements, simplifications are possible for more basic structures. Guidance is provided for both the detailed complete solutions and basic solutions for common simple buildings.

In Section C8.5.2 the assessment process, as it applies to URM buildings, is discussed with particular emphasis on how the approach might be varied depending on the complexity of the building. The assessment approach will also be influenced by any previous strengthening (refer to Section C8.5.3), and its location (including when it is a row building (refer to Section C8.5.4)).

C8.5.2 Assessment process

Key steps involved in the assessment of URM buildings are shown in and described below.

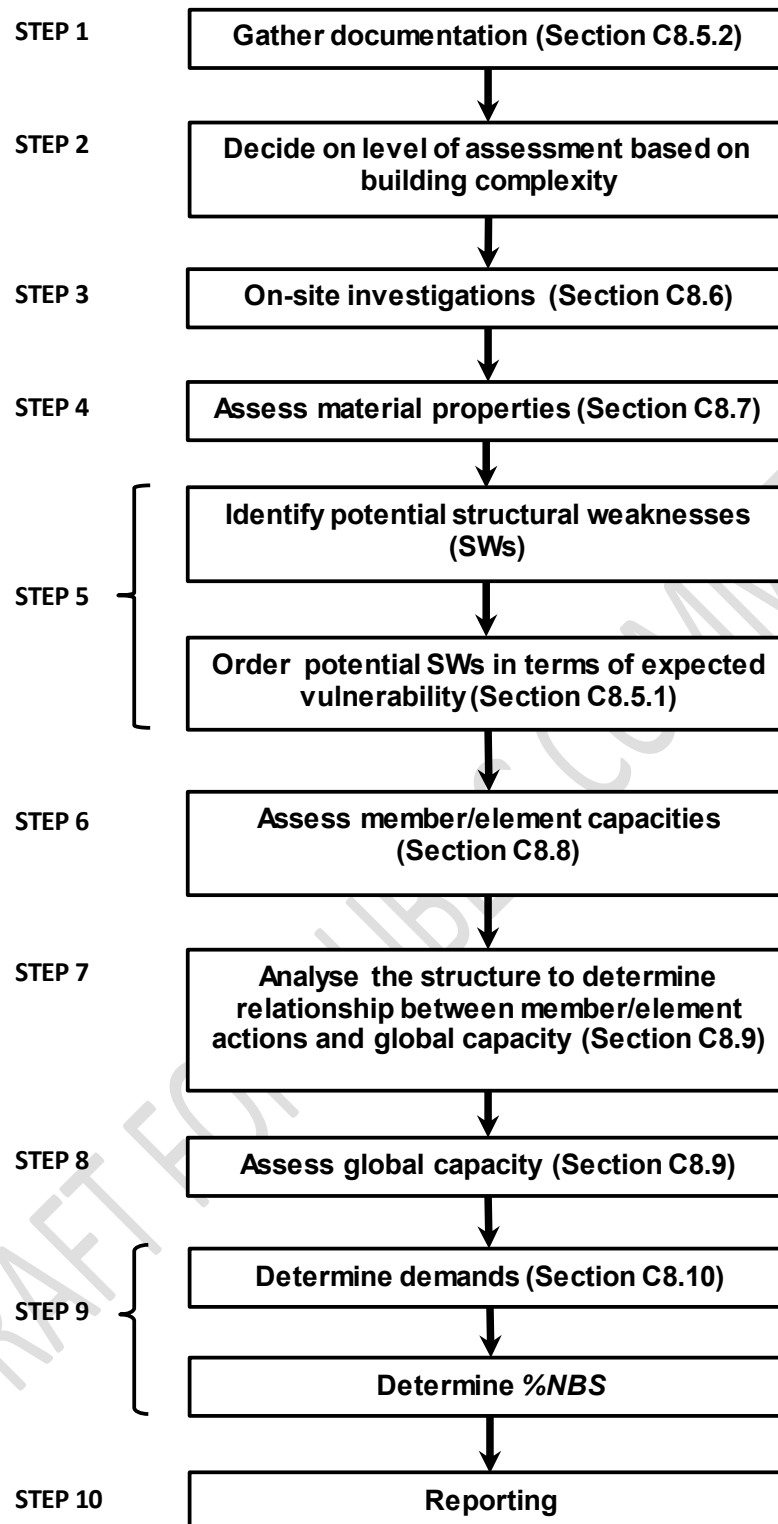


Figure C8.63: Assessment process for URM buildings

Step 1 Gather documentation

Collect relevant information and documents about the building including drawings, design feature reports, calculations and specifications, and any historical material test results and inspection reports (if available).

If the building has been previously altered or strengthened, collect all available drawings, calculations and specifications of this work.

Study this information before proceeding with the on-site investigation.

Step 2 Consider building complexity

Determine an assessment strategy based on an initial appraisal of the complexity of the building. This can be reviewed as the assessment progresses.

Although all aspects will need to be considered for all buildings, simplifications can be made for basic buildings e.g. one or two storey commercial, rectangular in plan. For these buildings the default material strengths are expected to be adequate without further consideration so that on-site testing, other than scratch testing of the bed joints to ascertain mortar type and quality, is not considered necessary. Foundation rotations are also not expected to have a significant effect so can be ignored.

Concentration of effort should be on assessing the score for face-loaded walls, connections from the walls to the diaphragms and the diaphragms (lateral deflection between supported walls). The score for the walls in plane will depend on the ability (stiffness) of the diaphragm to transfer the shears but the calculations required are likely to be simple irrespective of whether the diaphragms are rigid (concrete) or flexible (timber, steel braced). Behaviour can be assumed to be linear-elastic (i.e. ignore any nonlinear behaviour).

Complexity is likely to be increased if a building has previously been retrofitted. Not all issues with the building will necessarily have been addressed in historical retrofits. Stiffness compatibility issues will often not have been considered or fully addressed.

Step 3 Investigate on-site

Refer to Section C8.6.

Evaluate how well the documentation describes the “as constructed” and, where appropriate, the “as strengthened” building.

Carry out a condition assessment of the existing building.

Complete any on-site retrieval of samples and test these.

Identify any site conditions that could potentially affect the building performance (refer to Section C4).

Step 4 Assign material properties

Start by using the probable material properties that are provided in Section C8.7, or establish actual probable values through intrusive testing (the engineer may come back to this step depending on the outcome of the assessment).

Recognise that for basic buildings obtaining building-specific material strengths through testing may not be necessary to complete an assessment.

Step 5 Identify potential structural weaknesses and relative vulnerability

First, identify all of the various components in the building, and then identify potential structural weaknesses (SWs) related to these.

The identification of potential SWs in this type of building requires a good understanding of the issues discussed in Sections C8.2, C8.3 and C8.4.

Early recognition of SWs and their relative vulnerability and interdependence is likely to reduce assessment costs and focus the assessment effort.

Prior experience is considered essential when identifying the SWs in complex buildings.

Separate the various members/elements into those that are part of the primary lateral load resisting system and those that are not (secondary structural). Some elements may be categorised as having both a primary lateral load resisting function (e.g. in-plane walls and shear connections to diaphragms) and a secondary structural function (e.g. face-loaded walls and supporting connections).

The relative vulnerability of various elements in typical URM buildings is likely to be as follows (refer also [Figure C8.62](#)):

- **Inadequately restrained elements located at height:** e.g. street-facing façades, unrestrained parapets, chimneys, ornaments and gable end walls. Collapse of these elements may not lead to building collapse but they are potential life safety hazards and therefore their performance must be reflected in the overall building score.
- **Inadequate connection between face-loaded walls and floors/roof:** little or no connection capacity will mean that the walls will not be laterally supported when the inertial wall forces are in a direction away from the building. It can then be easily concluded that the walls and/or connections will be unlikely to score above 34%NBS, except perhaps in low-seismic regions. If observations indicate reasonable diaphragm action from the floors and/or roof, adequate connections will mean that the out-of-plane capacity of the face-loaded walls may now become the limiting aspect.
- **Out-of-plane instability of face-loaded walls:** if the wall capacity is sufficient to meet the requirements set out for face-loaded walls, then the capacity of the diaphragms becomes important as the diaphragms are required to transfer the seismic loads from the face-loaded walls into the in-plane walls.
- **The in-plane capacity of walls:** these are usually the least vulnerable elements.

Step 6 Assess element capacities

Calculate the seismic capacities from the most to the least vulnerable element in turn. There may be little point in expending effort on refining existing capacities only to find that the capacity is significantly influenced by a more vulnerable item that will require addressing to meet earthquake-prone requirements or target performance levels. Connections from brick walls to floors/roof diaphragms are an example of this. Lack of ties in moderate to high seismic areas will invariably result in an earthquake-prone status for the masonry wall and therefore it may be more appropriate and useful to assess the wall as < 34%NBS and also calculate a capacity assuming ties are in place. This will inform on the likely effect of retrofit measures.

An element may consist of a number of individual members. For example, the capacity of a penetrated wall (an element) loaded in-plane will need to consider the likely behaviour of

each of the piers and the spandrel regions between and above and below the openings respectively (the elements). For some elements the capacity will be a function of the capacity of individual members and the way in which the members act together. Therefore, establishing the capacity of an element may require structural analysis of the element to determine the manner in which actions in the members develop.

For each member/element assess whether or not exceeding its capacity (this may be more easily conceptualised as failure for these purposes) would lead to a significant life safety hazard, (refer to Part A and Section C1 for discussion of what constitutes a significant life safety hazard). If it is determined that it will not, then that member/element can be neglected in the assessment of the expected seismic performance of the structure. The same decisions may need to be made regarding the performance of members within an element.

Step 7 Analyse the global structure

In general, the complexity and extent of the analysis should reflect the complexity of the building.

Start with analyses of low sophistication, progressing to greater sophistication only as necessary.

An analysis of the primary lateral load resisting structure will be required to determine the relationship between the global capacity and the individual member/element actions.

The analysis undertaken will need to recognise that the capacity of members/elements will not be limited to consideration of elastic behaviour. Elastic linear analysis will likely be the easiest to carry out but the engineer must recognise that restricting to elastic behaviour will likely lead to a conservatively low assessment score.

The analysis will need to consider the likely impacts of plan eccentricities (mass, stiffness and/or strength).

Step 8 Assess global capacity

From the structural analyses determine the global capacity of the building. This will be the capacity of the building as a whole determined at the point that the most critical member/element of the primary lateral load resisting system reaches its determined capacity.

It may also be useful to determine the global capacity assuming successive critical members/elements are addressed (retrofitted). This will inform on the extent of retrofit that would be required to achieve a target score. A member/element will not be critical if its failure does not lead to a significant life safety hazard.

Step 9 Determine the demands and %NBS

Determine the global demand for the building from Section C3 and assess the global %NBS (global capacity/global demand x 100).

Assess the demands on secondary structural items and parts of the building and assess %NBS for each (capacity/demand x 100).

List the %NBS values in a table.

The critical structural weakness (CSW) will be the item in the table with the lowest %NBS score and that %NBS becomes the score for the building.

Review the items in the %NBS table to confirm that all relate to elements, the failure of which would lead to a significant life safety hazard. If not, revise the assessment to remove the non-significant life safety elements from consideration.

Step 10 Reporting

Refer to Part A and Section C1.

C8.5.3 Assessment of strengthened buildings

Seismic assessment of URM buildings that previously have been strengthened is similar to that undertaken for un-strengthened structures except that the performance of previously installed strengthening members/elements has to be taken into account. (Table C8.2 in Section C8.6 provides a detailed list of strengthening techniques used in URM buildings and associated features.)

Issues requiring consideration include the capacity of the installed elements, diaphragm continuity, and deformation compatibility between the original and installed strengthening elements.

C8.5.3.1 Wall-to-diaphragm anchors

The effectiveness of existing wall-to-diaphragm anchors needs to be verified. Examples of poorly performing anchors that are known to have been used in previous strengthening projects include:

- **Shallow embedment grouted anchors:** anchors installed with low embedment depths (i.e. less than half the wall thickness) were observed to perform poorly under face loads (Moon et al., 2011).
- **Grouted plain round bar anchors:** plain round bars have a low bond strength compared with threaded bar or deformed reinforcing bar anchors.
- **Mechanical expansion anchors:** mechanical anchors do not generally perform well in URM due to the low tensile capacity of masonry and the limited embedment depths that can be achieved with available mechanical anchors.

The default connector strengths detailed in Section C8.8.4 can be used for existing wall to diaphragm anchors that are in good condition and are known to have been installed and tested in accordance with the requirements of Appendix C8A.

Existing non-headed wall anchors of unknown construction should be proof tested in accordance with the test procedures detailed in Appendix C8A.

Existing headed wall anchors should be tested if there is evidence of significant corrosion or if anchor capacities greater than the default values detailed in Section C8.8.4 are required.

Existing wall-to-diaphragm anchor connections that rely on cross-grain bending of boundary joists should be reviewed. Cross-grain bending will occur in the boundary joist when face-loaded walls pull away from supporting floor diaphragms for the case when wall anchor brackets are not provided (refer [Figure C8.64](#)). Timber has low cross-grain bending capacity and, in many instances, has been found to be inadequate to resist the necessary seismic loads

in past earthquakes (ICBO, 2000). Capacity is greatly improved if the ribbon board or solid blocking is well connected to the joists. Where the connection is to a boundary joist, the presence of solid blocking between one or more pairs of joists should be checked, with adequate connection to the joists.

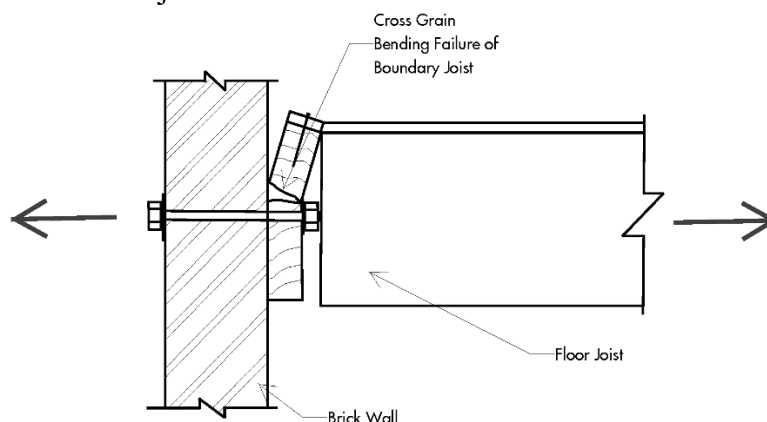


Figure C8.64: Out-of-plane loading cross grain bending failure mechanism (Oliver, 2010)

C8.5.3.2 Diaphragm continuity

Detailing of existing strengthened diaphragms should be reviewed to ensure that reliable load paths exist to transfer the inertia loads from the face-loaded URM walls into the body of the diaphragm.

Existing nailed plywood sheathing joints should not be relied upon to transfer tension forces unless adequate detailing is provided at the joint locations (ICBO, 2000). The sub-diaphragm design methodology can be used to assess existing diaphragm strengthening continuity (Oliver, 2010), with checks then made to assess if those discontinuous diaphragms that arise when continuity is not realised or is lost can continue to fulfil the role of structural diaphragms, even if originally not intended to be discontinuous.

C8.5.3.3 Deformation compatibility

Flexible lateral load resisting systems, such as structural steel or reinforced concrete moment resisting frames, have been used to strengthen URM buildings (refer to [Figure C8.34\(a\)](#)).

When assessing the effect of strengthening measures such as this, deformation compatibility between the stiff URM structure and the more flexible lateral load resisting system needs to be considered.

An understanding of the nonlinear strength-deformation relationship for each strengthening element will be required so that this can be compared with the relationships determined for the URM elements and other structural systems that may be present.

Often it will not be possible to mobilise the full capacity of a flexible strengthening element before the deformation capacity of the URM is exceeded. If so, one option available is to delete the URM from the primary seismic resisting system (assuming there is confidence that a significant life safety hazard does not arise from the failure of the masonry) and reassess the capacity.

C8.5.4 Assessment of URM row buildings

URM row buildings are buildings of similar structural form arranged side by side with insufficient seismic gaps to their neighbours, often with common boundary (party) walls: i.e. there is interaction between the individual buildings during a seismic shaking such that they cannot be considered in isolation. Buildings interconnected across boundaries should be considered as one building for the purposes of assessment, (refer to Part A).

Note:

The guidance below has been inferred from observed building damage only.

The effect of seismic shaking on row buildings is complex but also one of the least researched topics, particularly for URM buildings. It requires a special study which is outside the scope of these guidelines.

The effects of seismic shaking due to a lack of seismic gap can be both favourable (for the building within the row) and unfavourable (for the buildings on the ends of the row) provided the buildings are similar. Both of these effects should be accounted for when assessing the building's overall seismic performance. The building or structure within a row could become an end building if adjacent buildings are demolished.

Favourable effects include the potential for the whole block of row buildings to act as one unit and share seismic loads, and buttressing of central buildings by adjacent buildings in a row or an isolated building.

Unfavourable effects include pounding (knee effect and impact) on vertical load-bearing elements; the loss of which could potentially lead to loss of the gravity load path.

Buildings at the ends of rows suffer from two significant additional effects. First, they can be subject to the inertia/pounding effects of not just the adjacent building but some accumulation of effects along the row. Second and more importantly, forces tend to be almost unidirectional, pushing the end buildings off the row. This ratcheting effect is particularly detrimental to masonry structures where strains/crack widths accumulate much more quickly than when elements are able to complete a full return cycle. Therefore, the standard procedures for the assessment of buildings at the ends of rows should be used with care and consideration for these effects.

Note:

These guidelines recommend that all row effects on a particular building from the overall structure are described as part of its analysis and the vulnerabilities recorded. A “building” may be being assessed as if it is on one title, but the building from a structural connectivity point of view may extend for the whole block. The connectivity of the parts should be brought to the Building Consent Authority's (BCA's) attention throughout the assessment or retrofit consent process. Strengthening one “building” as part of a row will reduce the hazard in that section, but the seismic capacity of the overall building may still remain low due to the capacities in the remainder of the structure. The legal and compliance effects of row buildings should be discussed and agreed with owners and BCAs as part of any assessment process.

C8.5.4.1 General performance

The performance of row buildings depends primarily on the alignment (or otherwise) of:

- floor diaphragms
- façades
- primary transverse bracing elements, when situated against the boundary, and
- common walls.

The extent of misalignment of floors increases the bending effect on structures that are common to both buildings. When the extent of misalignment is greater than the depth of the wall, shear failure can also be induced.

Often, even if floors are misaligned, the façades are in the same plane (this is common in URM buildings). As a large proportion of the mass of the building is in the façade, it will not participate in the pounding action between the misaligned floors.

The effect of pounding damage to masonry buildings is generally less than for a frame or rigid diaphragm building as it tends to be more localised. Because of the high stiffness and often low height of these buildings, the impact forces are high frequency and associated with small displacements, and therefore carry less energy. Façades and other walls in the same alignment pound in their strong direction. Pounding between parallel walls where the pounding energy is dispersed over a large area will have a smaller effect than localised punching.

In addition to the above, most URM buildings have timber floors which have little mass to cause pounding. Similarly, with flexible diaphragms the impact energy is absorbed over a larger displacement. However, it is important to consider that URM is a brittle material and is sensitive to impact. Therefore, the engineer should consider whether the damage caused is likely to lead to loss of significant vertical load-carrying elements.

C8.5.4.2 Building interconnection

If row buildings share common walls but are not reliably tied together they are considered as one building with interconnected structures (refer to Part A). However, the length of dependable seating of the floors, or roof elements on the common wall will need to be assessed against the relative displacement of each building section.

If they are tied, note that the performance of elements that provide tying between the buildings (and similarly retrofit ties) can be classified into three types: rigid, elastic unbonded, and ductile. Rigid and elastic unbonded elements transfer force without dissipation of energy. For elastic unbonded elements, if there is sufficient stretch to allow the relative movement of the two structures their different stiffnesses will interact and will interrupt each other's resonances. Some force will also be lost through pounding as the elements return together. Where floors align, the ties may take the form of simple rods or beams. Where floors misalign, these rods/beams will be coupled to a vertical column element which will (elastically) transfer the floor force across the offset.

C8.6 On-site Investigations

C8.6.1 General

The engineer will need to conduct a detailed building inspection in order to assess existing building strength and before preparing any strengthening proposal.

This on-site investigation should cover the whole building, paying particular attention to the rear of the building and any hidden areas. It should include, but not be limited to, the following aspects.

C8.6.2 Form and configuration

Verify or establish the form and configuration of the building and its various components, including load paths between members, elements, and systems. As URM buildings may have had many changes of occupancy, there may be significant differences between available documentation and the actual building. Record this if so.

Note the number of storeys, building dimensions and year of construction. The notes of building dimensions should include opening locations and their dimensions, and should identify any discontinuities in the structural system.

Note the structural system and material description, including vertical lateral force-resisting system, basement and foundation system.

Also note any architectural features that may affect earthquake performance, including unrestrained items such as parapets or chimneys.

Note adjacent buildings and any potential for pounding and falling hazards. (Also refer to Section C8.5.4 for specific implications for row buildings.)

C8.6.3 Diaphragm and connections

Note the diaphragm types. For timber diaphragms, investigate the timber type, joist and beam spacing, and their connections, membrane and cladding type.

Note the presence of floor and roof diagonal bracing systems and the dimensions of these elements.

Examine wall-diaphragm connections and anchorage types (mechanical, adhesive and plate) to identify details and condition. Removal of floor or ceiling tiles may be required to investigate connections and anchorage types. Record the condition of these connections, any variation in connection types and other features such as any alterations or deterioration.

Note:

If adhesive anchors are used, these warrant careful investigation. In some cases, a visual inspection will not be sufficient and an on-site testing programme should be considered.

A dribble of epoxy on the wall can indicate that the anchor hole was filled properly. However, it may also indicate that there are voids between segments of adhesive along the length of the anchor; or that the anchor was inserted, taken out and reinserted.

For pocket type connections, check if the joists/rafters/beams are tightly packed by masonry on both sides or if there is a gap on both sides of the joists/rafters/beams.

When inspecting the diaphragm, note the location and size of the penetration accommodating stair or elevator access. Studies have shown that when penetrations are less than 10% of the diaphragm area it is appropriate to reduce in-plane diaphragm stiffness and strength in proportion to the reduction in diaphragm area. However, for larger diaphragm penetrations a special study should be undertaken to establish their influence on diaphragm response.

Note if the diaphragm has previously been re-nailed at every nail joint using modern nails placed by a nail gun or if it has been varnished.

The assessment should also consider the quality of the fixings from any sheathing to the supporting structure to transfer the loads and prevent buckling of the diaphragm. Plaster, especially if cementitious, will act to protect the fixings. However, rusting of nails and screws can cause splitting of timber which can drastically reduce the strength of a sarking board of the supporting framing. These guidelines encourage careful examination for rusting or signs of leaks, especially in roof cavities if these are accessible.

C8.6.4 Load-bearing walls

Record the walls' general condition including any deterioration of materials, damage from past earthquakes, or alterations and additions that could affect earthquake performance.

For multi-wythe construction, record the number of wythes, the distance between wythes, placement of inter-wythe ties, and the condition and attachment of wythes. Note that cavity walls will appear thicker than the actual structural wall (refer C8.2.4).

Record the bond type of the masonry, including the presence and distribution of headers. If possible, confirm that the bond bricks (headers) are not fake and cover more than one wythe. Check if the collar joint is filled.

Check any unusual characteristics, such as a mix of walling units or unusual crack patterns.

Record the type and condition of the mortar and mortar joints (for example, any weathering, erosion or hardness of the mortar) and the condition of any pointing or repointing, including cracks and internal voids. It is important to establish the mortar strength relative to the bricks as stronger mortar can lead to a brittle mode of failure. Investigation of existing damage to masonry walls can reveal their relative strength. Damage to bricks indicates a stronger mortar and weaker brick.

Note:

Visual inspection and simple scratching of the bricks and mortar may be sufficient to investigate the quality of masonry constituents. To be fully effective, the visual inspection should include both faces of the masonry.

Note that the mortar used for pointing is usually far better than the actual main body of the mortar, so scrape the point to full depth to investigate this.

The extent to which detailed testing of the materials should be considered will depend on the importance of the building and the likely sensitivity of the material properties to the assessment result.

Check any damp areas and the rear part of the building to investigate the quality and deterioration of the masonry and its constituents. **Look for signs of current (or removed) plant growth. Plants will often grow roots in mortar joints which as they expand de-stabilise the walls. If the plants are removed the remaining roots will decay and can cause instability.**

Note any horizontal cracks in bed joints, vertical cracks in head joints and masonry units, or diagonal cracks near openings.

Record the presence of bond beams and their locations, and covered walls. Signs of cracking or decay should be investigated and, where appropriate, include chemical testing. Refer to Section C5 for further information on concrete testing.

Examine and record any rotting and insect infestation of timber. Investigate timber in contact with masonry, particularly in damp areas.

Record the presence of any DPC layers.

Identify any vertical member/elements that are not straight. Bulging or undulations in walls should be observed. Note any separation of exterior wythes, out-of-plumb walls, and leaning parapets or chimneys. Check URM party walls and partitions and investigate whether these are tied to the structural system.

If opening up is permitted, include areas with built-in timbers (described in Section C8.2.10) so allowance can be made during the analysis. This analysis should allow for the brick capacity only, with no beneficial support from the timber unless specific investigations can prove otherwise. Existing bowing of walls and a lack of vertical load path where timber plates have shrunk can severely reduce face load capacity.

C8.6.5 Non-loadbearing walls

Record the material and construction details of the non-loadbearing walls. These walls may stiffen the floor diaphragm and brace the main loading walls. Their weight could be a significant portion of the total weight.

Check any unusual wall plaster construction.

C8.6.6 Concrete

Take care when making assumptions relating to the concrete strength and detailing. Intrusive investigation is essential to understand the makeup of the original construction and its constituents properly if any greater than nominal forces are to be transferred.

C8.6.7 Foundations

Note the type, material and structure of the foundation system.

Check if the bricks are in contact with the soil. Degradation can occur depending on the extent to which the bricks were fired when originally produced, and/or if the soil is damp.

C8.6.8 Geotechnical and geological hazards

Carefully investigate any foundation settlement or deterioration due to vegetation. In particular, check around drains and slopes.

Note any geological site hazards such as susceptibility to liquefaction and conditions for slope failure and surface fault rupture. Look for past signs of ground movement.

C8.6.9 Secondary elements

Record the details of secondary elements such as parapets, ornamentation, gable walls, lift wells, heavy equipment, canopies and chimneys. Include details of their dimensions and location. Also check for the presence of capping stones or other ornamental features as these create additional mass and eccentricity.

In particular, check if parapets are positioned off-centre to the wall beneath. Inspect parapets to estimate the location of the rocking pivot.

C8.6.10 Seismic separation

Investigate seismic separation with adjacent buildings. (Note that an apparent presence of a structural separation is not necessarily an indication that pounding will not occur unless the entire length of the separation is clear of any obstructions between the two buildings (Cole et al., 2011).

C8.6.11 Previous strengthening

Verify any strengthening systems that have been used against available drawings and documentation. Record any variations and deterioration observed. Check as-built accuracy and note the type of anchors used, their size and location. Use Table C8.2 to check for particular issues that can arise with different strengthening techniques: record any relevant observations. Also refer to Section C8.5.3 for additional considerations for strengthened buildings, including deformation compatibility between the original and installed strengthening elements.

Table C8.2: Historical techniques used for URM buildings and common features

Structural mechanism	Technique	Comments/issues
Chimneys	Internal post-tensioning	Requires well-mapped, understood and not degraded vertical load-path
	Internal steel tube reinforcement	Wrap-around/tie reinforcement to connect to tube important
	Concrete filling	Adds mass Adhesion to surrounding brick often insufficient to tie
	External strapping	Inward collapse needs to be checked, especially if mortar degraded on inside

Structural mechanism	Technique	Comments/issues
		Geometry often means external frames step outward: changes in angle need full resolution not to apply stress concentrations to masonry
	External bracing	Raking braces should have all vertical components of load resolved at each end Compatibility of stiff braced chimney with a flexible diaphragm must be checked
	Removal and replacement with lightweight	Heritage and weathering implications
Parapets (durability and weathering of particular concern)	Vertical steel mullions	Robust attachment to upper levels of brick with little wall/weight above critical Weathering through roof
	Raking braces	Robust attachment to upper levels of brick with little wall/weight above critical Interaction with roof modes can destabilise Vertical tie-down required to raking braces
	Steel capping spanning between abutting frames or walls	Anchorage depth down into mass of parapet to clamp down loose upper bricks
	Internal post-tensioning	Anchorage depth down into mass of parapet to clamp down loose upper bricks
	External post-tensioning	Anchorage depth down into mass of parapet to clamp down loose upper bricks
	Internal bonded reinforcement	Anchorage depth down into mass of parapet to clamp down loose upper bricks
	Near Surface Mounted (NSM) composite strips	Parapet responds differently to different directions of load UV degradation
Face-loaded walls	Vertical steel mullions (refer to Figure C8.31)	Stiffness vs out-of-plane rocking/displacement capability important Regularity/robustness of attachment to wall is important
	Vertical timber mullions	Stiffness vs out-of-plane rocking/displacement capability important Regularity/robustness of attachment to wall is important
	Horizontal transoms spanning between abutting frames or walls	Stiffness and attachment requirements need to consider wall above which gives clamping action to masonry at level of attachment
	Internal post-tensioning	Durability Anchorage level and fixity Level of pre-stress to allow rocking without brittle crushing
	External post-tensioning	As above
	Internal bonded reinforcement	Maximum quantity to ensure ductile failure Anchorage beyond cracking points, and consider short unbonded lengths
	Composite fibre overlay	Preparation to give planar surface very involved
	Near Surface Mounted (NSM) composite strips	Wall responds differently to different directions of load Bond important if in-plane capacity is not to be weakened

Structural mechanism	Technique	Comments/issues
	Reinforced concrete overlay	Wall responds differently to different directions of load
	Reinforced cementitious overlay	Wall responds differently to different directions of load Ductility of reinforcement important for deflection capacity
	Grout saturation/injection	Elastic improvement only: more suitable for low seismic zones and very weak materials
Connection of walls to diaphragms	Steel angle with grouted bars (refer to Figure C8.32(a))	Bar anchorage Diaphragm/bar eccentricity must be resolved
	Steel angle with bolts/external plate (refer to Figure C8.32(b))	Diaphragm/bar eccentricity must be resolved
	Timber joist/ribbon plate with grouted bars	Bar anchorage Diaphragm/bolt eccentricity causes bending of timber across grain - a potential point of weakness
	Timber joist/ribbon plate with bolts/external plate	Diaphragm/bolt eccentricity causes bending of timber across grain - a potential point of weakness
	Blocking between joists notched into masonry	Joist weak axis bending must be checked Tightness of fit of joists into pockets Degradation of joists
	External pinning to timber beam end	Quality assurance/buildability of epoxy in timber Concentrated localised load Development in masonry (external plate preferred for high loads)
	External pinning to concrete beam or floor	Development in masonry (external plate preferred for high loads) Concrete floor type (hollow pots, clinker concrete)
	Through rods with external plates	Elastic elongation Concentrated localised load
	New isolated padstones	Tightness of fit Resolution of eccentricity between masonry bearing and diaphragm connection
	New bond beams	High degree of intervention
Diaphragm strengthening	Plywood overlay floor or roof sparking (refer to Figure C8.33)	Flexibility Requires continuous chord members and primary resistance elements
	Plywood ceiling	As above, plus existing ceiling battening/fixings may not be robust or may be decayed
	Plywood/light gauge steel composite	Stiffer but less ductile than ply-only Eccentricities between thin plate and connections must be resolved
	Plasterboard ceiling	As ply ceiling but less ductile Prevention of future modification/removal
	Thin concrete overlay/topping	Thickness for adequate reinforcement Additional mass

Structural mechanism	Technique	Comments/issues
		Ductility capacity of non-traditional reinforcement Buckling restraint/bond to existing structure
	Elastic cross bracing	Stiffness relative to wall out-of-plane capacity Edge distribution members and chords critical Concentration of loads at connections
	Semi-ductile cross bracing (e.g. Proving ring)	As elastic Energy absorption benefit is not easily quantified without sophisticated analysis
	Replacement floor over/below with new diaphragm	Design as new structure
In-plane wall strengthening New primary strengthening elements (refer to Figure C8.34)	Sprayed concrete overlay	Restraint to existing floor/roof structure Out-of-plane capacity of wall Ductility capacity if used very dependent on aspect ratio Chords Foundation capacity needs to be checked (uplift/rocking)
	Internal vertical post-tensioning	Ensure pre-stress limited to ensure no brittle failure See out-of-plane issues also
	External vertical post-tensioning	Ensure pre-stress limited to ensure no brittle failure See out-of-plane issues also
	Internal horizontal reinforcement	Coring/drilling difficult Stressing horizontally requires good vertical (perpendicular) mortar placement and quality
	External horizontal post-tensioning	Stressing horizontally requires good vertical (perpendicular) mortar placement and quality
	Bed-joint reinforcement	Workmanship critical Low quantities of reinforcement only possible
	Composite reinforced concrete boundary or local reinforcement elements	Development at ends/nodes Bond to existing
	Composite FRP boundary or local reinforcement elements	As above plus stiffness compatibility with existing
	Nominally ductile concrete walls or punched wall/frame	High foundation loads result
	Nominally ductile reinforced concrete masonry walls	Stiffness compatibility considering geometry (including foundation movement) important
	Nominally ductile steel concentric or cross bracing	Stiffness compatibility assessment critical considering element flexibility, plan position and diaphragm stiffness Drag beams usually required
	Limited ductility steel moment frame	Flexibility/stiffness compatibility very important

Structural mechanism	Technique	Comments/issues
	Limited ductility concrete frame	Flexibility/stiffness compatibility important
	Limited ductility concrete walls	Assess effectiveness of ductility, including foundation movements Ensure compatibility with any elements cast against Drag beams often required
	Limited ductility timber walls	Flexibility/stiffness compatibility very important Drag beams often required
	Ductile EBF/K-frames	Element ductility demand vs building ductility assessment important Drag beams usually required
	Ductile concrete coupled or rocking walls	Element ductility demand vs building ductility assessment important Ensure compatibility with any elements cast against drag beams often required
	Tie to new adjacent (new) structure	Elastic elongation and robustness of ties to be considered Higher level of strengthening likely to be required
Reinforcement at wall intersections in plan	Removal and rebuilding of bricks with inter-bonding	Shear connection only with capacity reduced considering adhesion and tightness of fit Disturbance of bond to adjacent bricks
	Bed-joint ties	Small reinforcement only practical but can be well distributed Care with resolving resultant thrust at any bends
	Drilled and grouted ties	Tension only: consider shear capacity Depth to develop capacity typically large Compatibility with face-load spanning of wall
	Metalwork reinforcing internal corner	Attachment to masonry Small end-distance in abutting wall can mean negligible tension capacity
	Grouting of crack	Shear friction only: tension mechanism also required Stabilises any dilation but does not allow recovery
Foundation strengthening	Mass underpinning	Creates hard point in softer/swellable soils Even support critical
	Grout injection	Creates hard point in softer/swellable soils Difficult to quantify accurately
	Concentric/balanced re-piling	Localised “needles” through walls must provide sufficient bearing for masonry
	Eccentric re-piling with foundation beams	Stiffness of found beams important to not rotate walls out-of-plane
	Mini piling/ground anchors	Cyclic bond less than static bond Testing – only static practical Vulnerable to bucking if liquefaction
	Pile type: vertical stiffness and pre-loading	Pre-loading dictates load position

Structural mechanism	Technique	Comments/issues
		Pre-loading important if new foundations less stiff than existing Dynamic distribution between new and old likely different than static Effects of liquefaction must be considered: may create limiting upper bound to strengthening level
Façade wythe ties	Helical steel mechanical engagement – small diameter	Low tension capacity, especially if cracked
	Steel mechanical engagement – medium diameter	Some vierendeel action between wythes Durability
	Epoxied steel rods/gauze sleeve	Some vierendeel action between wythes
	Epoxied composite/non-metallic rods	Stiffness
	Brick header strengthening	Additional new headers still brittle: can become overstressed under thermal/seasonal or foundation loadings in combination
Canopies	Reinforce or recast existing hanger embedment	Degradation of steel Depth of embedment to ensure sufficient mass of bricks to prevent pull-out
	New steel/cast iron posts	Propping of canopy can mitigate hazard from masonry falling to pavement Props in addition to hangers are not so critical with regard to traffic damage
	New cantilevered beams	Co-ordination with clerestory/bressumer beam Backspan reaction on floor
	Deck reinforcement to mitigate overhead hazard	Sacrificial/crushable layer to mitigate pavement hazard
	Conversion to accessible balcony	Likely to achieve all of the above objectives for canopies and also has natural robustness as designed for additional live load. Hazard still exists for balcony occupants
Base isolation		A lack of sufficient gap around the building Vertically re-founding the building

C8.7 Material Properties and Weights

C8.7.1 General

This section provides default probable material properties for clay brick masonry and other associated materials.

These values can be used for assessment of URM buildings in the absence of a comprehensive testing programme (refer to Appendix C8A for details). However, to arrive at any reliable judgement, some on-site testing such as scratching, etc. as discussed in this section is recommended.

Note:

Before proceeding to on-site intrusive testing it is important to sensibly understand what information will be collected from any investigation, how this information would be used, and what value it would add to the reliability of the assessment. Sensitivity analyses can be used to determine the influence of any material parameter on the assessment outcome and therefore whether testing to refine that material parameter beyond the default values given in this section is warranted.

When assessing the material characteristics of the building, survey the entire building to ensure that the adopted material properties are representative. It may be appropriate to assign different material properties to different masonry walls depending on variations in age, weathered condition or other aspects.

C8.7.2 Clay bricks and mortars

Recommended probable default material properties for clay bricks and lime/cement mortar, correlated against hardness, are given in C8.3 and C8.4. The descriptions in these tables are based on the use of a simple scratch test but there are a variety of similar, simple on-site tests the engineer can use.

To ensure that the test is representative of the structural capability of the materials, remove any weathered or remediated surface material prior to assessing the hardness characteristics. This requirement is particularly important for establishing mortar material properties where the surface mortar is either weathered or previously remediated and may not be representative of the mortar at depth. One recommended technique to establish whether the mortar condition is uniform across the wall thickness is to drill into the mortar joint and inspect the condition of the extracted mortar dust as the drill bit progresses through the joint.

Table C8.3: Probable strength parameters for clay bricks (Almesfer et al., 2014)

Brick hardness	Brick description	Probable brick compressive strength, f'_b (MPa)	Probable brick tensile strength, f_{bt} (MPa)
Soft	Scratches with aluminium pick	14	1.7
Medium	Scratches with 10 cent copper coin	26	3.1
Hard	Does not scratch with above tools	35	4.2

Table C8.4: Probable strength parameters for lime/cement mortar (Almesfer et al., 2014)

Mortar hardness	Mortar description	Probable mortar compressive strength, f'_j (MPa)	Probable Cohesion, c (MPa)	Probable coefficient of Friction, μ_f^Ψ
Very soft	Raked out by finger pressure	0-1	0.1	0.3
Soft	Scratches easily with fingernails	1-2	0.3	
Medium	Scratches with fingernails	2-5	0.5	0.6
Hard	Scratches using aluminium pick	To be established from testing	0.7	0.8
Very hard†	Does not scratch with above tools	To be established from testing		

Note:

† When very hard mortar is present it can be expected that walls subjected to in-plane loads and failing in diagonal shear will form diagonal cracks passing through the bricks rather than a stair-stepped crack pattern through the mortar head and bed joints. Such a failure mode is non-ductile. Very hard mortar typically contains cement.

Ψ Values higher than 0.6 may be considered with care/investigation depending upon the nature/roughness of the brick material and the thickness of the mortar with respect to the brick roughness.

Values for adhesion may be taken as half the cohesion values provided in Table C8.4.

In cases where the probable modulus of rupture of clay bricks cannot be established from testing, the following value may be used (Almesfer et al., 2014):

$$f'_r(\text{MPa}) = 0.12f'_b \quad \dots\text{C8.1}$$

C8.7.3 Compressive strength of masonry

In cases where the compressive strength of masonry cannot be established from the testing of extracted masonry prisms, the probable masonry compressive strength, f'_m , can be established using Equation C8.2 (Lumantarna et al., 2014b). Table C8.5 presents probable compressive strength values of clay brick masonry based on this equation using the brick and mortar probable compressive strength values from C8.3 and C8.4.

$$f'_m(\text{MPa}) = \begin{cases} 0.75f'_b{}^{0.75} \times f'_j{}^{0.3} & \text{for } f'_j \geq 1 \text{ MPa} \\ 0.75f'_b{}^{0.75} & \text{for } f'_j < 1 \text{ MPa} \end{cases} \quad \dots\text{C8.2}$$

Table C8.5: Probable compressive strength of clay brick masonry, f'_m

Probable mortar strength, f'_j (MPa)	Probable brick compressive strength, f'_b (MPa)		
	14	26	35
0	5.4	8.6	10.8
1	5.4	8.6	10.8
2	6.7	10.6	13.3
5	8.8	14.0	17.5
8	10.1	16.1	20.1

C8.7.4 Tensile strength of masonry

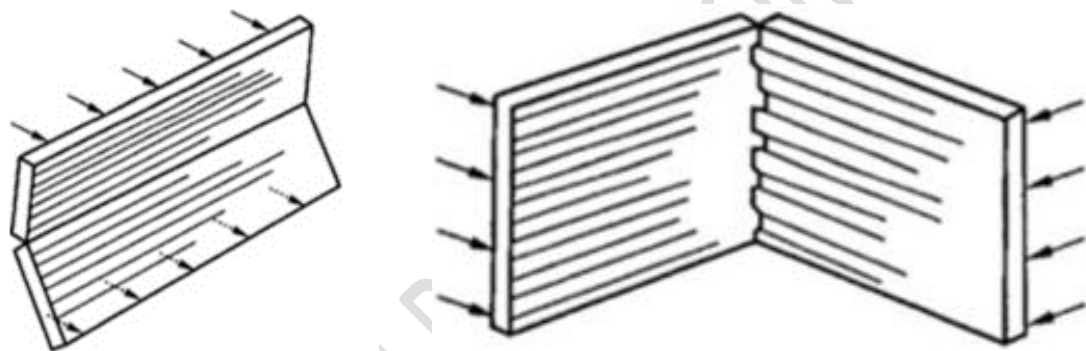
The tensile strength of masonry in both horizontal and vertical directions, including any cement rendering and plaster, should be assumed to be zero for walls that can be subjected to face load, except when the requirements given in Section C8.8.5.2 for elastic analysis are satisfied for vertical spanning face-loaded walls.

When assessing the tensile strength of spandrels refer to Section C8.8.6.3.

Note:

When the requirements of Section C8.8.5.2 are met values of 0.2 MPa and 0.4 MPa would seem appropriate for f'_t when the failure plane is parallel and perpendicular to the bed joints respectively (refer to Figure C8.65). Where there is a high likelihood of low adhesion between the masonry units and the mortar (e.g. when lime mortar has leached), zero tensile strength of masonry should be assumed.

These values should be used for assessing the probable capacity of elements/members whenever tension develops in the masonry.



(a) Plane of failure parallel to bed joint

(b) Plane of failure perpendicular to bed joint

Figure C8.65: Tensile failure planes

C8.7.5 Diagonal tensile strength of masonry

Where specific material testing is not undertaken to determine probable masonry diagonal tension strength, this may be taken as:

$$f_{dt}(\text{MPa}) = 0.5c + f_a\mu_f \quad \dots\text{C8.3}$$

where:

c	=	masonry bed-joint cohesion
μ_f	=	masonry co-efficient of friction
f_a	=	axial compression stress due to gravity loads calculated at the mid height of the wall/pier (MPa).

C8.7.6 Modulus of elasticity and shear modulus of masonry

The masonry modulus of elasticity, E_m , can be calculated by using the masonry probable compressive strength in accordance with Equation C8.4 (Lumantarna et al., 2014b). Note

that this value of modulus of elasticity has been established as a chord modulus of elasticity between $0.05f'_m$ and $0.7f'_m$ in order to represent the elastic stiffness appropriate up to maximum strength.

Young's modulus of clay brick masonry can be taken as:

$$E_m(MPa) = 300f'_m \quad \dots C8.4$$

Shear modulus of clay brick masonry can be taken as (ASCE 41-13, 2014):

$$G_m(MPa) = 0.4 E_m \quad \dots C8.5$$

C8.7.7 Timber diaphragm material properties

Refer to Section C9 for timber diaphragm material properties.

C8.7.8 Material unit weights

The engineer can use the unit weights given in Table C8.6 as default values if more reliable measurements are not available.

Table C8.6: Unit weights

Material	Unit weight (kN/m ³)
Brick masonry	18
Oamaru stone masonry	16
Timber	5-6

C8.8 Assessment of Member/Element Capacity

C8.8.1 General

This section covers the assessment of the capacity of the various members and elements that make up a masonry building.

In the displacement-based procedure for face-loaded walls that is presented, the assessment of the demand is an integral part of the procedure.

C8.8.2 Strength reduction factors

The assessment procedures in these guidelines are based on probable strengths and, therefore, the strength reduction factor, ϕ , should be set equal to 1.0. The probable strength equations and recommended default probable capacities in this section assume ϕ equals 1.0.

C8.8.3 Diaphragms

C8.8.3.1 General

Diaphragms in URM buildings fulfil two principal functions: (1) They provide support to the walls oriented perpendicular to the direction of loading, and (2) if they are stiff enough,

they have the potential to allow shears to be transferred between walls in any level, to resist the storey shear and the torsion due to any plan eccentricities.

The relative lateral stiffness of the diaphragms to the walls providing lateral support is often quite low due to the high stiffness of the walls, particularly for diaphragms constructed of timber or steel bracing.

Flexibility in a diaphragm, if too high, can reduce the ability of the diaphragm to provide adequate support to walls and thus affect the response of these walls, or render the ability of the diaphragm to transfer storey shears to minimal levels, although this will not generally be an issue if recognised and appropriately allowed for in the global analysis of the building. Therefore, considering the effects of diaphragm flexibility is essential for proper understanding of both in-plane and out-of-plane response of the walls.

When assessing the capacity of diaphragms it is necessary to consider both their probable strength and their deformation capacity.

The probable strength capacity should be determined in accordance with the requirements in these guidelines that relate to the particular construction material of the diaphragm.

The deformation capacity will be that for which the strength capacity can be sustained.

The deformation capacity is also limited to that which it is expected will result in detrimental behaviour of supported walls or of the building as a whole.

The diaphragm deformations should be included when determining the inter-storey deflections for checking overall building deformations against the NZS 1170.5:2004 limit of 2.5%.

In the sections below recommendations are provided for diaphragm deformation limits to ensure adequate support for face-loaded walls and for flexible (timber) and rigid diaphragms. Rigid diaphragms would typically need to be constructed of concrete to achieve the necessary relative stiffness with the walls.

C8.8.3.2 Diaphragm deformation limits to provide adequate support to face-loaded walls

In order to ensure that the face-loaded walls are adequately supported, the maximum diaphragm in-plane displacement measured with respect to the diaphragm support walls should not exceed 50% of the thickness of the supported (face-loaded) walls (refer to Figure C8.66). For cavity construction with adequate cavity ties installed, the inner masonry leaf is usually the load-bearing leaf and this criterion will require the maximum acceptable diaphragm displacement to be limited to 50% of the thickness of the inner leaf.

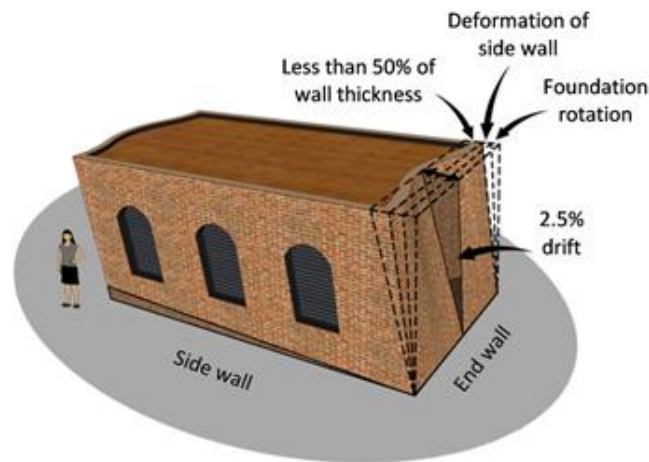


Figure C8.66: Mid-span diaphragm displacement limit for URM building on a flexible foundation

C8.8.3.3 Timber diaphragms

General

Most URM buildings in New Zealand have flexible timber floor and ceiling diaphragms. Their in-plane deformation response is strongly influenced by the characteristics of the nail connections (Wilson et al., 2013a) and their global response is most adequately replicated as a shear beam (Wilson et al., 2013b). Responses can be separated into directions either parallel or perpendicular to the orientation of the joists (Wilson et al., 2013c), as illustrated in **Figure C8.67**. They are significantly influenced by the presence of any floor or ceiling overlay, the degradation of the diaphragm due to aspects such as moisture or insect damage, and any prior remediation such as re-nailing or varnishing (Giongo et al., 2013). If the diaphragms have had epoxy coatings that have penetrated into the joints between the flooring, this has been observed to result in substantial stiffening. Therefore, these guidelines recommend undertaking a sensitivity analysis, recognising that the effective diaphragm stiffness could be more than given here by an order of magnitude or greater.

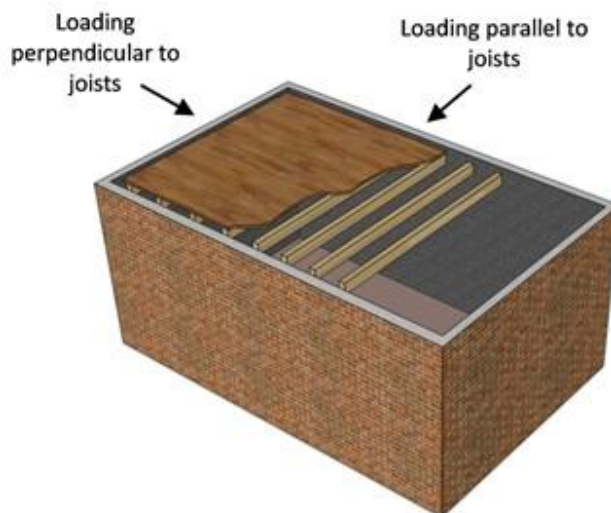


Figure C8.67: Orthogonal diaphragm response due to joist orientation

It is assumed here that the diaphragm is adequately secured to all perimeter walls via pocketing and/or anchorages to ensure that diaphragm deformation occurs rather than global sliding of the diaphragm on a ledge. It is also assumed that the URM boundary walls deform out-of-plane in collaboration with deformation of the flexible timber diaphragm. For non-rectangular diaphragms, use the mean dimensions of the two opposing edges of the diaphragm to establish the appropriate dimensions of an equivalent rectangular diaphragm.

Note:

Timber roofs of URM buildings were often built with both a roof and ceiling lining. As a result, roof diaphragms are likely to be significantly stiffer than the mid height floor diaphragms if there are no ceilings on the mid-floors. Diagonal sarking in the roof diaphragm will also further increase its relative stiffness compared to the floor diaphragms.

If the diaphragm being assessed has an overlay or underlay (e.g. of plywood or pressed metal sheeting), consult the stiffness and strength criteria for improved diaphragms. The engineer will still need to consider stiffness and ductility compatibility between the two. For example, it is likely that a stiff, brittle timber lath-and-plaster ceiling will delaminate before any straight sarking in the roof above can be fully mobilised.

While the flooring, sarking and sheathing provide a shear load path across the diaphragm, it is necessary to consider the connections to the surrounding walls (refer to Section C8.8.4) and any drag or chord members. A solid URM wall may be able to act as a chord as it has sufficient in-plane capacity to transfer the chord loads directly to the ground. However, a punched URM wall with lintels only over the openings will have little tension capacity and may be the critical element in the assessment. Timber trusses and purlins, by their nature, only occur in finite lengths: their connections/splices designed for gravity loads may have little tie capacity.

Strength and stiffness need to be adjusted for sloping diaphragms (typically roofs). Ensure that the resultant forces in the chords at changes in diaphragm slope are resolved into the framing or walls supporting that diaphragm.

Probable strength capacity

The probable strength capacity of a timber diaphragm should be assessed in accordance with Section C9 of these guidelines.

Probable deformation capacity

Deformations in timber diaphragms should be assessed using the effective diaphragm stiffness defined below.

The probable deformation capacity should be taken as the lower of the following, assessed for each direction:

- $L/33$ for loading oriented perpendicular to the joists or $L/53$ for loading oriented parallel to the joists
- deformation limit to provide adequate support to face-loaded walls. Refer Section C8.8.3.2.

- deformation required to meet global inter-storey drift limit of 2.5% in accordance with NZS 1170.5:2004. Refer Section C8.8.3.1.

Effective diaphragm stiffness

To determine the effective stiffness of a timber diaphragm, first assess the condition of the diaphragm using the information in Table C8.7.

Table C8.7: Diaphragm condition assessment criteria (Giongo et al., 2014)

Condition rating	Condition description
Poor	Considerable borer; floorboard separation greater than 3 mm; water damage evident; nail rust extensive; significant timber degradation surrounding nails; floorboard joist connection appears loose and able to wobble
Fair	Little or no borer; less than 3 mm of floorboard separation; little or no signs of past water damage; some nail rust but integrity still fair; floorboard-to-joist connection has some but little movement; small degree of timber wear surrounding nails
Good	Timber free of borer; little separation of floorboards; no signs of past water damage; little or no nail rust; floorboard-to-joist connection tight, coherent and unable to wobble

Next, select the diaphragm stiffness using Table C8.8 and accounting for both loading orientations.

Note:

While other diaphragm characteristics such as timber species, floor board width and thickness, and joist spacing and depth are known to influence diaphragm stiffness, their effects on stiffness can be neglected for the purposes of this assessment.

Pre-testing has indicated that re-nailing vintage timber floors using modern nail guns can provide a 20% increase in stiffness.

Table C8.8: Shear stiffness values[†] for straight sheathed vintage flexible timber floor diaphragms (Giongo et al., 2014)

Direction of loading	Joist continuity	Condition rating	Shear stiffness [†] , G_d (kN/m)
Parallel to joists	Continuous or discontinuous joists	Good	350
		Fair	285
		Poor	225
Perpendicular to joists ^{††}	Continuous joists, or discontinuous joists with reliable mechanical anchorage	Good	265
		Fair	215
		Poor	170
	Discontinuous joists without reliable mechanical anchorage	Good	210
		Fair	170
		Poor	135

Note:

† Values may be amplified by 20% when the diaphragm has been renailed using modern nails and nail guns

†† Values should be interpolated when there is mixed continuity of joists or to account for continuous sheathing at joist splice

For diaphragms constructed using other than straight sheathing, multiply the diaphragm stiffness by the values given in Table C8.9. If roof linings and ceiling linings are both assumed to be effective in providing stiffness, add their contributions.

Table C8.9: Stiffness multipliers for other forms of flexible timber diaphragms (derived from ASCE 41-13, 2014)

Type of diaphragm sheathing		Multipliers to account for other sheathing types
Single straight sheathing		x 1.0
Double straight sheathing	Chorded	x 7.5
	Unchorded	x 3.5
Single diagonal sheathing	Chorded	x 4.0
	Unchorded	x 2.0
Double diagonal sheathing or straight sheathing above diagonal sheathing	Chorded	x 9.0
	Unchorded	x 4.5

For typically-sized diaphragm penetrations (usually less than 10% of gross area) the reduced diaphragm shear stiffness, G'_d , is given by Equation C8.6:

$$G'_d(kN/m) = \frac{A_{d,net}}{A_{d,gross}} G_d \quad \dots C8.6$$

where $A_{d,net}$ and $A_{d,gross}$ refer to the net **diaphragm plan area** and the gross diaphragm plan area respectively (in square metres).

For non-typical sizes of diaphragm penetration, a special study should be undertaken to determine the influence of diaphragm penetration on diaphragm stiffness and strength.

The effective diaphragm stiffness should be modified further to account for stiffness of the URM boundary walls deforming in collaboration with the flexible timber diaphragm.

Hence:

$$G'_{d,eff}(kN/m) = \alpha_w G'_d \quad \dots C8.7$$

where α_w may be determined using any rational procedure to account for the stiffness and incompatibility of deformation modes arising from collaborative deformation of the URM walls displacing out-of-plane as fixed end flexure beams and the diaphragm deforming as a shear beam.

In lieu of a special study, prior elastic analysis has suggested that Equation C8.8 provides adequate values for α_w :

$$\alpha_w \cong 1 + \left(t_\ell^3 / H_\ell^3 + t_u^3 / H_u^3 \right) L^2 E_m / B G'_d \quad \dots C8.8$$

where:

t_ℓ	=	effective thickness of walls below the diaphragm, m
t_u	=	effective thickness of walls above the diaphragm, m
H_ℓ	=	height of wall below diaphragm, m
H_u	=	height of wall above diaphragm, m
E_m	=	Young's modulus of masonry, MPa
B	=	depth of diaphragm, m
L	=	span of diaphragm perpendicular to loading, m.
G'_d	=	reduced diaphragm shear stiffness, kN/m

Refer to **Figure C8.68** for definition of the above terms.

For scenarios where the URM end walls are likely to provide no supplementary stiffness to the diaphragm, $\alpha_w = 1.0$ should be adopted.

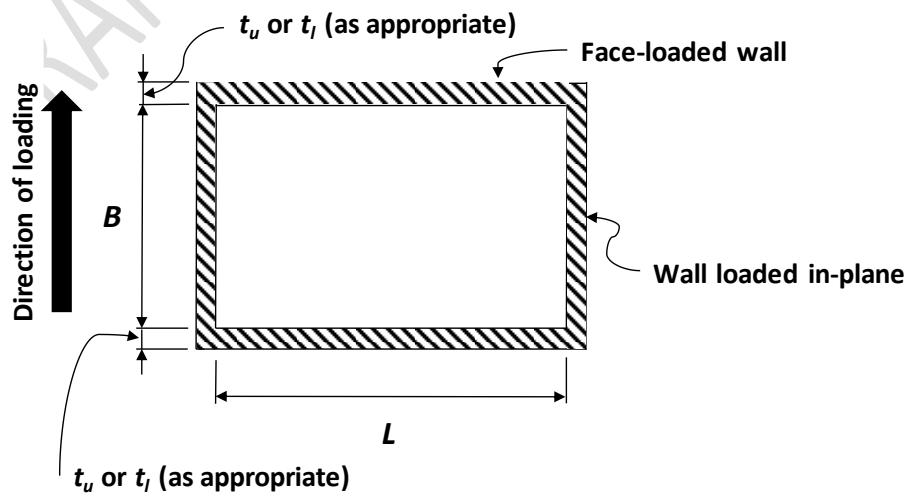


Figure C8.68: Schematics showing dimensions of diaphragm

C8.8.3.4 Rigid diaphragms

When considering rigid diaphragms, the engineer can use a “strut-and-tie” method. However, investigate the presence of termination details (hooks, thickenings, threads/nuts) carefully as their ability to transfer the loads at the strut-and-tie nodes is likely to govern the diaphragm capacity.

Rigid diaphragms can be assumed to have minimal effect on the response of out-of-plane walls.

C8.8.4 Connections

C8.8.4.1 General

The probable capacity of diaphragm to wall connections is taken as the lowest probable capacity of the failure modes listed below:

- punching shear failure of masonry
- yield or rupture of connector rod in tension or shear
- rupture at join between connector rod and joist plate
- splitting of joist or stringer
- failure of fixing at joist
- splitting or fracture of anchor plate
- yield or rupture at threaded nut.

Suggested default probable capacities for embedded and plate bearing anchors are provided below. Guidance on specific assessment of capacities is also provided.

C8.8.4.2 Embedded anchors

The engineer can use the probable capacities provided in C8.10 and C8.11 in lieu of specific testing provided that:

- the capacity should not be taken greater than the probable capacities of the anchor itself or the anchor to grout or grout to brick bond
- when the embedment length is less than four bolt diameters or 50 mm, the pull-out strength should be taken as zero
- the minimum edge distance to allow full shear strength to be assumed should be 12 diameters
- shear strength of anchors with edge distances equal to or less than 25 mm should be taken as zero.

Linear interpolation of shear strength for edge distances between these bounds is permitted (ASCE 41-13, 2014).

Simultaneous application of shear and tension loads need not be considered when using the values from C8.10 and C8.11.

Table C8.10: Default anchor probable shear strength capacities for anchors into masonry units only¹

Anchorage type	Rod size	Probable shear strength capacity ² (kN)
Bolts/steel rods fixed through and bearing against a timber member ^{1,2}	M12	8.5
	M16	15
	M20	18.5
Bolts/steel rods fixed through a steel member (washer) having a thickness of 6 mm or greater	M16	20
Note: <ol style="list-style-type: none"> 1. Anchors into mortar bed joints will have significantly lower shear capacities 2. Timber member to be at least 50 mm thick and MSG8 grade or better 3. For adhesive connectors embedment should be at least 200 mm into solid masonry 		

The values in Table C8.11 are based on the pull-out of a region of brick, assuming cohesion or adhesion strength of the mortar on the faces of the bricks perpendicular to the application of the load factored by 0.5 and friction on the top and/or bottom faces (refer to [Figure C8.69](#)), depending on the height of wall above the embedment as follows:

- 0 m (i.e. at the top of the wall) – adhesion only on the bottom and side faces.
- ≥ 0.3 m but < 3 m – adhesion on the top, bottom and side faces, friction on the top and bottom faces.
- ≥ 3 m – cohesion on the top, bottom and side faces, friction on the top and bottom faces.

A factor of 0.5 has been included in these values to reflect the general reliability of mechanisms involving cohesion/adhesion and friction.

Table C8.11: Default anchor probable tension pull-out capacities for 0 m, ≥ 0.3 m and ≥ 3 m of wall above the embedment²

Mortar hardness	Single-wythe wall (kN)			Embedment 160 mm ¹ into two-wythe wall (kN)			Embedment 250 mm ¹ into three-wythe wall (kN)		
	0	≥ 0.3 m ⁽³⁾	≥ 3 m	0	≥ 0.3 m ⁽³⁾	≥ 3 m	0	≥ 0.3 m ⁽³⁾	≥ 3 m
Very soft	0.3	0.5	1	1	1.5	4	1.5	3	8
Soft	1	1.5	3	2.5	4	9	5	8	18
Medium	1.5	2.5	6	4	6.5	15	8	14	31
Hard	2.5	3.5	8	6	9	21	11	19	43
Very hard	$>2.5^{(4)}$	$>4^{(4)}$	$>8^{(4)}$	$>6^{(4)}$	$>10^{(4)}$	>21	$>11^{(4)}$	$>20^{(4)}$	$>43^{(4)}$

Notes:

1. Representative value only: assumes drilling within 50 mm of far face of wall.
2. Simultaneous application of tension and shear loading need not be considered.
3. These values are intended to be used until there is ≥ 3 m of wall above the embedment.
4. Values for very hard mortar may be substantiated by calculation but can be assumed to be at least those shown.

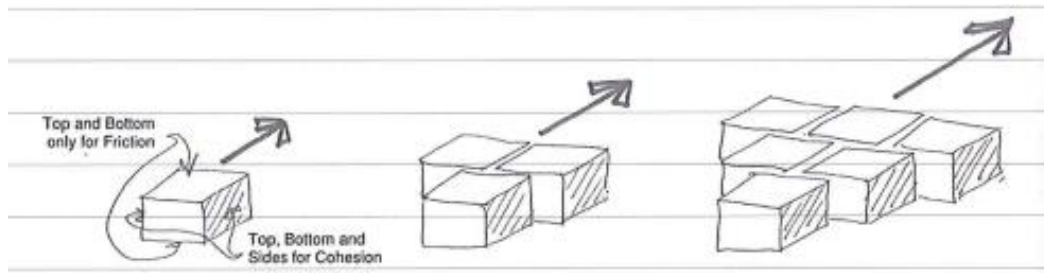


Figure C8.69: Basis for embedded anchor capacity estimation

The designer should select a bar diameter and tested epoxy system that will develop the required bond directly to the bricks and grout system as appropriate. Alternatively, cement mortars can be used but the capacity should be substantiated by site pull-out tests, using the grouting and cleanout methodology proposed by relevant standards/specifications.

For coarse thread screws, use the manufacturer's data for the direct bond to bricks, taking account of the brick compressive strength and ensuring that fixings are into whole bricks rather than mortar courses.

When assessing the capacity of straight or bent adhesive anchors, refer to the product specification and the methodology prescribed by the anchor manufacturer.

For inclined embedded anchors, the horizontal force capacity should be reduced to the horizontal vector component, and checks made for an adequate load path for the vertical component. If the inclination is less than 22.5 degrees these effects can be considered insignificant and the full capacity of the anchor can be assumed.

Note:

For regular rectangular URM buildings the usual procedure is to design embedded anchors for the calculated tension demand to secure out-of-plane loaded walls and then check the design for shear demand arising from earthquake demand in the perpendicular direction, as long as shear actions do not cause the engaged bricks to be prised/rotated out of the wall.

C8.8.4.3 Plate anchors

For plate anchors, postulate the potential failure surface to estimate its capacity.

A wall punching shear model is shown in [Figure C8.70](#).

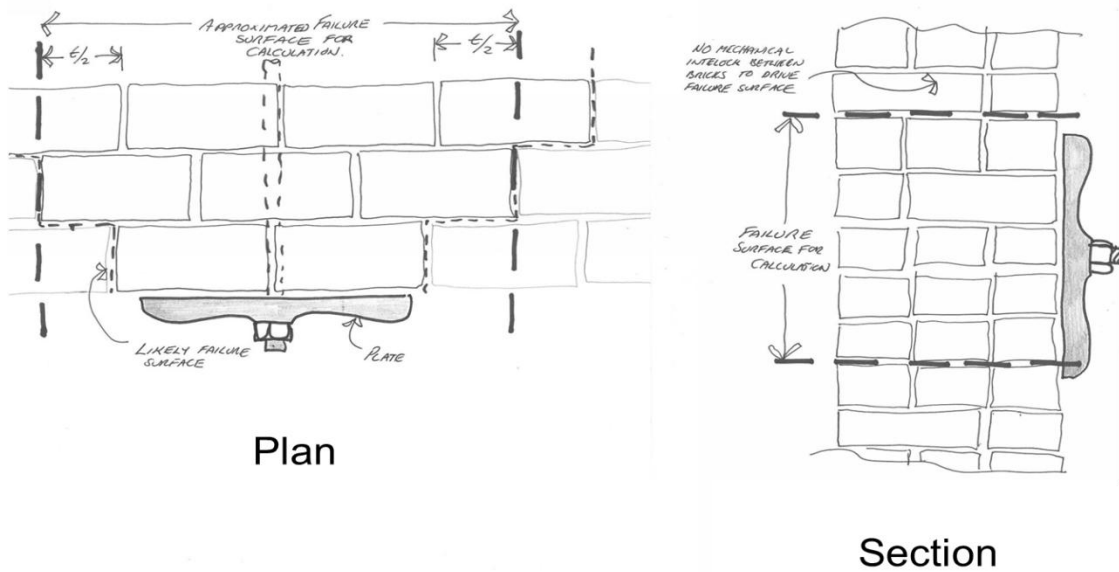


Figure C8.70: Failure surfaces for plate anchors

C8.8.4.4 Capacity of wall between connections

Where the lateral spacing of connections used to resist the wall anchorage force is greater than four times the wall thickness, measured along the length of the wall, check the section of wall spanning between the anchors to resist the local out-of-plane bending caused by the lateral force (FEMA P-750, 2009). This check might be undertaken allowing for arching in the masonry; for example, through the compressive membrane forces that develop when a conical “yield line” pattern develops in the brick around the anchor.

For most applications involving bearing plates, it should be sufficiently accurate to assume a cylinder with a cross section the same shape as the bearing plate but lying outside it all round by half the thickness of the wall. Cohesion may be considered to be acting on the sides of this cylinder.

C8.8.5 Wall elements subjected to face (out-of-plane) loading

C8.8.5.1 General

This section provides both force-based (assuming elastic behaviour) and displacement-based inelastic methods for assessing face-loaded walls. The force-based methods utilising the direct tensile capacity of the masonry are only appropriate if all of the criteria listed in Section C8.8.5.2 are met.

Note:

The procedures in some earlier versions of these guidelines (such as the 1995 “Red Book” (NZSEE, 1995)) that were based on the concept of equating total energy (strain energy of deformation plus potential energy due to shifts of weights) of the rocking wall to that for an elastic oscillator have since been shown to be deficient. These procedures give inconsistent results and are potentially unsafe; particularly where walls are physically hinged at floor levels (i.e. when they are supported on a torsionally flexible beam with no wall underneath) or made of stiff (high modulus of elasticity) masonry.

The 2015 update used the same formulations as the 2006 guidelines (NZSEE, 2006) but accommodated some of the more significant recent research findings. These updates were based on work carried out at the University of Auckland and University of Adelaide (Derakhshan et al., 2013a and 2013b; Derakhshan et al., 2014a and 2014b). However, these guidelines do not include all of the detailed procedures set out in this research (Derakhshan et al., 2014a) because there were some simplifying assumptions that made these procedures less suitable for thicker walls.

Procedures given for assessing face-loaded walls spanning one-way horizontally, or two-way horizontally and vertically, are based on response assuming only weak nonlinear effects (i.e. assumption of elastic or nominally elastic response). These are based on less rigorous research and are not as well developed as procedures for walls spanning vertically. Caution is therefore required when using these recommendations.

For walls spanning vertically in one direction between a floor and another floor or the roof, or vertically cantilevered (as in partitions and parapets), assure the lateral restraint of the floors and the roof for all such walls. If this restraint cannot be assured, the methods presented here for one-way vertically spanning walls cannot be used. However, it might still be possible to assess such walls by analysing them as spanning horizontally between other walls, columns or other elements, or as two-way assemblages.

Header courses are typically provided every four to six courses in common bond. This configuration would normally suffice for walls loaded out-of-plane. These header courses would normally pass through the whole wall, with bricks lapping in the interior as required. For example, in triple brick walls the header course on the inside will be either one brick higher or lower than the header course on the outside to allow lapping over the central wythe.

If headers are sparse (header rows spaced wider than every six courses), investigate the sufficiency of the available header courses by assuming a vertical shear acting on the centreline of the lower wall equal to $P + W_t + 0.5W_b$. This shear needs to be resisted by header bricks crossing the centreline. For this purpose, the engineer can assume each header brick contributes a shear resistance of $2f_r b t_h^2 / l$, where b , t_h and l are the breadth, depth and length of the header and f_r is its modulus of rupture of brick in bending.

For stone masonry walls, for example those having two fair faces and rubble infill, there may be no practical shear load path between the faces. The internal and external faces of such walls should be treated as acting independently.

If a wythe is not integral with the main structural wall, refer to the guidance in Appendix C8B.5 for a suggested procedure for assessment.

Non-structural masonry (usually single-wythe partitions, acoustic linings or fire linings) should be considered as a mass within the building and the risks for face-load collapse evaluated.

Internal walls with floors on both sides can be assumed to be supported at floor levels but checks on the diaphragms (strength and deformation) and perpendicular walls will still be required.

Walls should be assessed in every storey and for both directions of response (inwards and outwards). Set the rating of the wall at the least value found, as failure in any one storey for either direction of loading will lead to progressive failure of the whole wall.

C8.8.5.2 Vertical spanning walls

General

When using an elastic analysis to determine the capacity of a wall section, the direct tensile strength of the masonry should be ignored unless:

- the capacity so determined is halved and the available ductility is assumed to be 1
- an inspection of the wall reveals no signs of cracking at that section, and
- the in-plane calculations indicate cracking of the brickwork is not expected.

If a displacement-based approach is adopted, the maximum out-of-plane displacement should be limited to 0.6 times the instability displacement for simply supported walls and 0.3 times the instability displacement for cantilever walls; e.g. parapets.

In the case of walls supported against face load, deflection of the supports will need to meet minimum requirements to ensure the walls can respond as assumed. In these guidelines, limits on the deflection of diaphragms are considered a diaphragm capacity issue and are defined in Section C8.8.3.2. These deflection limits should also apply to any other supports to face-loaded walls; for example, the support that may be provided by steel portal or steel bracing retrofits.

Elastic analysis

A simple bending analysis may be performed for the seismic assessment of face-loaded walls using Equation C8.9 provided that the criteria given in Section C8.8.5.2 are met. Equation C8.9 is applicable for a unit wall length.

$$M = \frac{t_{\text{nom}}^2}{6} (f'_t + \frac{P}{A_{\text{n,wall}}}) \quad \dots\text{C8.9}$$

where:

- P = load applied to top of wall (N)
 $A_{\text{n,wall}}$ = net plan area of masonry wall (mm²)
 M = moment capacity of the wall (Nmm)
 t_{nom} = nominal thickness of wall excluding pointing (mm)

$$t_{\text{nom}} = t_{\text{gross}} - np \quad \dots\text{C8.10}$$

where:

- f'_t = probable tensile strength
 p = depth of mortar recess (in mm) as shown in Figure C8.71
 t_{gross} = overall thickness of wall (in mm)
 n = number of recesses.

$n = 2$ if recesses are provided on both sides; $n = 1$ otherwise.

If the recess is less than 6 mm, it can be ignored.

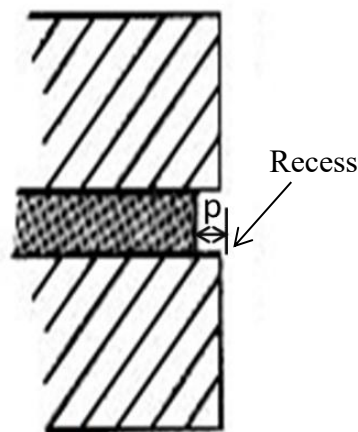


Figure C8.71: Pointing with recess

The imposed moment may be assumed critical at:

- mid height of walls restrained at the top and bottom, or
- at the base of cantilever walls.

The direct tensile strength, f'_t , should be ignored in capacity calculations unless there is no sign of pre-cracking in the wall at the section being considered and cracking of the brickwork in the region of the section is not expected for loading in-plane and the strength capacity calculated assuming tensile strength has been factored by 0.5. The ductile capability of the should be taken as 1.

Inelastic displacement-based analysis for walls spanning vertically between supports

Follow the steps below to assess the displacement response capability and displacement demand in order to determine the adequacy of the walls.

Note:

Appendix C8B provides some guidance on methods for determining key parameters. Refer to Figure C8B.1 for the notation employed.

Some **simplifications** have been provided which can be used (these are listed after these steps **and in Table 8.12**) if wall panels are uniform within a storey (approximately rectangular in vertical and horizontal section and without openings). **In addition, some “approximations” have been provided that have validity only in certain conditions, e.g. Equation C8.23 for a wall with very high aspect ratio.**

Charts are provided in Appendix C8C that allow assessment of %NBS for regular walls (vertically spanning and vertical cantilever) in terms of height to thickness ratio of the wall, gravity load on the wall, and parameters defining the demand on the wall. **These charts exclude any approximation and are based on exact expressions that are found in this section.**

The wall panel is assumed to form hinge lines at the points where effective horizontal restraint is assumed to be applied. The centre of compression on each of these hinge lines is assumed to form a pivot point. The height between these pivot points is the effective **wall** height h (in mm). At mid height between these pivots, height $h/2$ from either, a third pivot point is assumed to form.

The recommended steps for assessment of walls following the displacement-based method are discussed below:

Step 1

Divide the wall panel into two parts: a top part bounded by the upper pivot and the mid height between the top and bottom pivots; and a bottom part bounded by the mid height pivot and the bottom pivot.

Note:

This division into two parts is based on the assumption that a significant crack will form at the mid height of the wall, where an effective hinge will form. The two parts are then assumed to remain effectively rigid. While this assumption is not always correct, the errors introduced by the resulting approximations are not significant.

One example is that significant deformation occurs in the upper part of top-storey walls. In particular, where the tensile strength of the mortar is small the third hinge will not necessarily form at the mid height.

Step 2

Calculate the weight of the wall parts: W_b (in N) of the bottom part and W_t (in N) of the top part, and the weight acting at the top of the storey, P (in N).

Note:

The weight of the wall should include any render and linings, but these should not be included in t_{nom} or t (in mm) unless the renderings are integral with the wall. The weight acting on the top of the wall should include all roofs, floors (including partitions and ceilings and the seismic live load) and other features that are tributary to the wall.

Step 3

From the nominal thickness of the wall, t_{nom} , calculate the effective thickness, t .

Note:

The effective thickness is the actual thickness minus the depth of the equivalent rectangular stress block. The reduction in thickness is intended to reflect that the walls will not rock about their edge but about the centre of the compressive stress block.

The depth of the equivalent rectangular stress block should be calculated with caution, as the depth determined for static loads may increase under earthquake excitation. Appendix C8B suggests a reasonable value based on experiments, $t = t_{nom}$ (0.975-0.025 P/W). The thickness calculated by this formula may be assumed to apply to any type of mortar, provided it is cohesive. For weaker (and softer) mortars, greater damping will compensate for any error in the calculated t .

Step 4

Assess the maximum distance, e_p , from the centroid of the top part of the wall to the line of action of P . Refer to Figure C8B.1 for definition of e_b , e_t and e_o . Usually, the eccentricities

e_b and e_p will each vary between 0 and $t/2$ (where t is the effective thickness of the wall). Exceptionally they may be negative; i.e. where P promotes instability due to its placement.

When considering the restraint available from walls on foundations assume the foundation is the same width as the wall and use the following values for e_b :

- 0 if the factor of safety for bearing under the foundation, for dead load only (FOS), is equal to 1
- $t/3$ if FOS = 3 (commonly the case)
- $t/4$ if FOS = 2.

Note:

Figure C8B.2 shows the positive directions for the eccentricities for the assumed direction of rotation (angle A at the bottom of the wall is positive for anti-clockwise rotation).

The walls do not need to be rigidly attached or continuous with a very stiff section of wall beyond to qualify for an assumption of full flexural restraint.

Care should be taken not to assign the full value of eccentricity at the bottom of the wall if the foundations are indifferent and may themselves rock at moments less than those causing rocking in the wall. In this case, the wall might be considered to extend down to the supporting soil where a cautious appraisal should then establish the eccentricity. The eccentricity is then related to the centroid of the lower block in the usual way.

Step 5

Calculate the mid height deflection, Δ_i , that would cause instability under static conditions. The following formula may be used to calculate this deflection.

$$\Delta_i = \frac{bh}{2a} \quad \dots C8.11$$

where:

$$b = W_b e_b + W_t(e_o + e_b + e_t) + P(e_o + e_b + e_t + e_p) - \Psi(W_b y_b + W_t y_t) \quad \dots C8.12$$

and:

$$a = W_b y_b + W_t(h - y_t) + Ph \quad \dots C8.13$$

Note:

The deflection that would cause instability in the walls is most directly determined from virtual work expressions, as noted in Appendix C8B.

For guidance on the selection of assumptions for the values of Ψ and e_p , see commentary in Appendix C8B.2.2.

Step 6

Assign the maximum usable deflection, Δ_m (in mm), as $0.6 \Delta_i$.

Note:

The lower value of the deflection for calculation of instability limits reflects that response predictions become difficult as the theoretical limit is approached. In particular, the response becomes overly dependent on the characteristics of the earthquake, and minor perturbances lead quickly to instability and collapse.

Step 7

Calculate the period of the wall, T_p , as four times the duration for the wall to return from a displaced position measured by Δ_t (in mm) to the vertical. The value of Δ_t is less than Δ_m . Research indicates that $\Delta_t = 0.6\Delta_m = 0.36\Delta_i$ for the calculation of an effective period for use in an analysis using a linear response spectrum provides a close approximation to the results of more detailed methods. The period may be calculated from the following equation:

$$T_p = 4.07 \sqrt{\frac{J}{a}} \quad \dots C8.14$$

where J is the rotational inertia of the masses associated with W_b , W_t and P and any ancillary masses, and is given by the following equation:

$$J = J_{bo} + J_{to} + \frac{1}{g} \left\{ W_b [e_b^2 + y_b^2] + W_t [(e_o + e_b + e_t)^2 + y_t^2] + P [(e_o + e_b + e_t + e_p)^2] \right\} + J_{anc} \quad \dots C8.15$$

where J_{bo} and J_{to} are mass moment of inertia of the bottom and top parts about their centroids, and J_{anc} is the inertia of any ancillary masses, such as veneers, that are not integral with the wall but that contribute to the inertia.

When treating cavity walls, [refer to the guidance in Appendix C8B.5](#).

Note:

The equations are derived in Appendix C8B. The method in this Appendix can be used to assess less common configurations as necessary.

Step 8

Calculate the design response coefficient $C_p(T_p)$ in accordance with Section 8 of NZS 1170.5:2004 taking $\mu_p = 1$ and substituting $C_i(T_p)$:

$$C_i(T_p) = C_{hc}(T_p) \quad \dots C8.16$$

where:

$C_{hc}(T_p)$ = the spectral shape factor ordinate, $C_h(T_p)$, from NZS 1170.5:2004 for Ground Class C and period T_p provided that, solely for the purpose of calculating $C_{hc}(T_p)$, T_p need not be taken less than 0.5 sec.

Note:

When calculating C_{Hi} from NZS 1170.5:2004:

- (1) For walls spanning vertically and held at the top, h_i should be taken as the average of the heights of the points of support (typically these will be at the heights of the diaphragms).
- (2) In the case of vertical cantilevers, h_i should be measured to the point from which the wall is assumed to cantilever.
- (3) If the wall is sitting on the ground and is laterally supported above, then h_i may be taken as half of the height to the point of support.
- (4) If the wall is sitting on the ground and is not otherwise attached to the building it should be treated as an independent structure, not as a part. This will involve use of the appropriate ground spectrum for the site.

Note:

The above substitution for $C_i(T_p)$ has been necessary because the use of the tri-linear function given in NZS 1170.5:2004 (Equations 8.4(1), 8.4(2) and 8.4(3)) does not allow appropriate conversion from force to displacement demands. The revised $C_i(T_p)$ converts to the following, with the numerical numbers available from NZS 1170.5:2004 Table 3.1.

$$\begin{aligned}
 C_i(T_p) &= 2.0 \quad \text{for } T_p < 0.5 \text{ sec} \\
 &= 2.0(0.5/T_p)^{0.75} \quad \text{for } 0.5 < T_p < 1.5 \text{ sec} \\
 &= 1.32/T_p \quad \text{for } 1.5 < T_p < 3 \text{ sec} \\
 &= 3.96/T_p^2 \quad \text{for } T_p > 3 \text{ sec}
 \end{aligned}$$

Only 5% damping should be applied. Experiments show that expected levels of damping from impact are not realised: the mating surfaces at hinge lines tend to simply fold onto each other rather than impact.

Step 9

Calculate γ , the participation factor for the rocking system. This factor may be taken as:

$$\gamma = \frac{(W_b y_b + W_t y_t) h}{2gJ} \quad \dots \text{C8.17}$$

Note:

The participation factor relates the response deflection at the mid height of the wall to the response deflection for a simple oscillator of the same period and damping.

Step 10

From $C_p(T_p)$, T_p , R_p and γ calculate the displacement response, D_{ph} (in mm) as:

$$D_{ph} = \gamma (T_p/2\pi)^2 C_p(T_p) \cdot R_p \cdot g \quad \dots \text{C8.18}$$

where:

$$\begin{aligned}
 C_p(T_p) &= \text{the design response coefficient for face-loaded walls (refer to Step 8 above, and for more details refer to Section C8.10.3)} \\
 T_p &= \text{period of face-loaded wall, sec} \\
 R_p &= \text{the part risk factor as given by Table 8.1, NZS 1170.5:2004} \\
 C_p(T_p) \cdot R_p &\leq 3.6.
 \end{aligned}$$

Note that with T_p expressed in seconds, the multiplied terms $(T_p/2\pi)^2 \times C_p(T_p) \times g$ may be closely approximated in metres by:

$$(T_p/2\pi)^2 \times C_p(T_p) \times g = \text{MIN}(T_p/3, 1) \quad \dots\text{C8.19}$$

Step 11

Calculate

$$\%NBS = 100 \times \Delta_m / D_{ph} = 60(\Delta_i / D_{ph}) \quad \dots\text{C8.20}$$

Note:

The 0.6 factor applied to Δ_i reflects that response becomes very dependent on the characteristics of the earthquake for deflections larger than $0.6\Delta_i$.

The 2006 guidelines allowed a 20% increase in %NBS calculated by the above expression. However that is not justified now that different displacements are used for capacity and for the period and the subsequent calculation of demand.

The following Steps 12 to 14 are only required for anchorage design.

Step 12

Calculate the horizontal accelerations that would just force the rocking mechanism to form. The acceleration may be assumed to be constant over the height of the **wall**, reflecting that it is associated more with acceleration imposed by the supports than with accelerations associated with the wall deflecting away from the line of the supports. Express the acceleration as a coefficient, C_m , by dividing by g .

Note:

Again, virtual work proves the most direct means for calculating the acceleration. Appendix C8B shows how and derives the following expression for C_m , in which the ancillary masses are assumed part of W_b and W_t .

$$C_m = \frac{b}{(W_b y_b + W_t y_t)} \quad \dots\text{C8.21}$$

Note:

To account for the initial enhancement of the capacity of the rocking mechanism due to tensile strength of mortar and possible rendering, we recommend that C_m be cautiously assessed when mortar and rendering are present or in the case where the wall is intended to be retrofitted. The value of C_m may also be too large to use for the design of connections. Accordingly, it is recommended that C_m need not be taken greater than the maximum part coefficient determined from Section 8 of NZS 1170.5:2004 setting R_p and $\mu_p = 1.0$.

Step 13

Calculate $C_p(0.75)$, which is the value of $C_p(T_p)$ for a part with a short period from NZS 1170.5:2004, and define a seismic coefficient for the connections which is the lower of C_m , $C_p(0.75)$ or 3.6.

Note:

$C_p(0.75)$ is the short period ordinate of the design response coefficient for parts from NZS 1170.5:2004, and 3.6 g is the maximum value of $C_p(T_p)$ required to be considered by NZS 1170.5:2004 when R_p and $\mu_p = 1.0$.

Step 14

Calculate the required support reactions using the contributing weight of the walls above and below the connection (for typical configurations this will be the sum of W_b and W_t for the walls above and below the support accordingly) and the seismic coefficient determined in Step 13.

Step 15

Calculate

$$\%NBS = \frac{\text{Capacity of connection from Section C8.8.4} \times 100}{\text{Required support reaction from Step 14}} \quad \dots \text{C8.22}$$

Note:

If supports to face-loaded walls are being retrofitted, we recommend that the support connections are made stronger than the wall(s) and not less than required using a seismic coefficient of $C_p(0.75)$; i.e. do not take advantage of a lower C_m value.

Simplifications for regular *vertically spanning* walls

The following approximations can be used if wall panels are uniform within a storey (approximately rectangular in vertical and horizontal section and without openings) and the inter-storey deflection does not exceed 1% of the storey height. The results are summarised in Table C8.12.

The steps below relate to the steps for the general procedure set out above.

- Step 1 Divide the wall as before.
- Step 2 Calculate the weight of the wall, W (in N), and the weight applied at the top of the storey, P (in N).
- Step 3 Calculate the effective thickness as before, noting that it will be constant.
- Step 4 Calculate the eccentricities, e_b , e_t and e_p . Each of these may usually be taken as either $t/2$ or 0.
- Step 5 Calculate the instability deflection, Δ_i from the formulae in Table C8.12 for the particular case.
- Step 6 Assign the maximum usable deflection, Δ_m , for capacity as 60% of the instability deflection.
- Step 7 Calculate the period, which may be taken as $4.07\sqrt{(J/a)}$, where J and a are given in Table C8.12. Alternatively, where the wall is fairly thin (h/t is large), the period may be approximated as:

$$T_p = \sqrt{\frac{0.28h}{(1+2P/W)}} \quad \dots C8.23$$

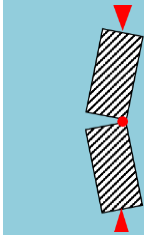
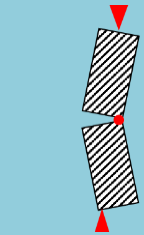
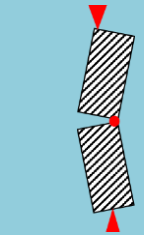
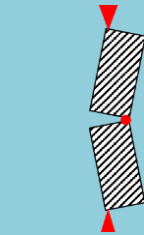
in which h is expressed in metres.

- Step 8 Calculate $C_p(T_p)$ following Equation C8.16.
- Step 9 Calculate the participation factor as for the general method, with the numerator of the expression expanded to give $g = Wh^2/8Jg$. This may be taken at the maximum value of 1.5 or may be assessed by using the simplified expression for J shown in Table C8.12.
- Step 10 Calculate D_{ph} from $C_p(T_p)$, T_p and γ in the same manner as for the general method.
- Step 11 Calculate %NBS in the same manner as for the general method.

Note:

Charts are provided in Appendix C8C that allow the %NBS to be calculated directly for various boundary conditions for regular walls spanning vertically, given h/t_{Gross} for the wall, gravity load on the wall and factors defining the demand.

Table C8.12: Static instability deflection for uniform walls – various boundary conditions

Boundary condition number	0	1	2	3
				
e_p	0	0	$t/2$	$t/2$
e_b	0	$t/2$	0	$t/2$
b	$(W/2 + P)t$	$(W + 3P/2)t$	$(W/2 + 3P/2)t$	$(W + 2P)t$
a	$(W/2 + P)h$	$(W/2 + P)h$	$(W/2 + P)h$	$(W/2 + P)h$
$\Delta_i = bh/(2a)$	$t/2$	$\frac{(2W + 3P)t}{(2W + 4P)}$	$\frac{(W + 3P)t}{(2W + 4P)}$	t
J	$\left\{ \left(\frac{W}{12} \right) [h^2 + 7t^2] + Pt^2 \right\} / g$	$\left\{ \left(\frac{W}{12} \right) [h^2 + 16t^2] + 9Pt^2/4 \right\} / g$	$\left\{ \left(\frac{W}{12} \right) [h^2 + 7t^2] + 9Pt^2/4 \right\} / g$	$\left\{ \left(\frac{W}{12} \right) [h^2 + 16t^2] + 4Pt^2 \right\} / g$
C_m	$(2 + 4P/W)t/h$	$(4 + 6P/W)t/h$	$(2 + 6P/W)t/h$	$4(1 + 2P/W)t/h$

Note:

1. The boundary conditions of the piers shown above are for clockwise potential rocking.
2. The top eccentricity, e_t , is not related to a boundary condition, so is not included in the table. The top eccentricity, e_t , is the horizontal distance from the central pivot point to the centre of mass of the top block which is not related to a boundary condition.
3. The eccentricities shown in the sketches and the simplified equations are for the positive sense. Where an eccentricity is in the other sense, these equations are not useful. Similar simplified expressions can be developed by entering the eccentricities as negative number(s) in respective expressions, e.g. in Equation C8.15.

Refer to Appendix C8B2.9 for additional guidance for assessing boundary conditions.

C8.8.5.3 Vertical cantilevers

Parameters for assessing vertical cantilevers, such as partitions and parapets, are derived in Appendix C8B. Please consult this appendix for general cases. Examples of how to consider the position of imposed top load are given in C8B3.6.

For parapets of uniform rectangular cross section, the following approximations can be used. These steps relate to the steps set out earlier for the general procedure for walls spanning between vertical diaphragms.

- Step 1 There is no need to divide the parapet. Only one pivot is assumed to form: at the base.
- Step 2 The weight of the parapet is W (in N). P (in N) is zero.
- Step 3 The effective thickness is t (in mm) $= 0.98t_{\text{nom}}$.
- Step 4 Only e_b is relevant and it is equal to $t/2$. However, if the wall is supported on the ground, refer to Step 4 of the general procedure for walls spanning vertically between diaphragms

- Step 5 The instability deflection measured at the top of the parapet $\Delta_i = t$.
- Step 6 The maximum usable deflection measured at the top of the parapet $\Delta_m = 0.3\Delta_i = 0.3t$.
- Step 7 The period may be calculated from the assumption that $\Delta_t = 0.8\Delta_m = 0.24\Delta_i$.

$$T_p = \sqrt{0.65h \left[1 + \left(\frac{t}{h} \right)^2 \right]} \quad \dots C8.24$$

in which h , the height of the parapet above the base pivot, and t , the thickness of the wall, are expressed in metres. The formulation is valid for $P = 0$, $e_b = t/2$, $y_b = h/2$ and approximating $t = t_{nom}$.

- Step 8 Calculate $C_p(T_p)$ (refer to Step 8 of the general procedure for walls spanning vertically between diaphragms).
- Step 9 Calculate $\gamma = 1.5/[1 + (t/h)^2] \leq 1.5$...C8.25
- Step 10 Calculate D_{ph} from $C_p(T_p)$, T_p and γ as before.
- Step 11 Calculate %NBS as for the general procedure for walls spanning between a floor and an upper floor or roof, from;

$$\%NBS = 100 \Delta_m/D_{ph} = 30 \Delta_i/D_{ph} = 30 t/D_{ph}. \quad \dots C8.26$$

Note:

The following Steps 12 to 14 are only required for anchorage design.

- Step 12 Calculate $C_m = t/h$...C8.27
- Step 13 Calculate $C_p(0.75)$ which is the value of $C_p(T_p)$ for a part with a short period from NZS 1170.5:2004 and define a seismic coefficient for the connections which is the lower of C_m , $C_p(0.75)$ and 3.6.
- Step 14 Calculate the base shear from W , C_m and $C_p(0.75)$. This base shear adds to the reaction at the roof level restraint.

Note:

Charts are provided in Appendix C8C that allow the %NBS to be calculated directly for various boundary conditions for regular walls cantilevering vertically, given h/t_{Gross} for the wall, gravity load on the wall and factors defining the demand.

C8.8.5.4 Gables

Gables merit specific consideration because they are located at the uppermost elevations of the building and therefore are subjected to the greatest amplification of seismic input due to their height, and because their performance during an earthquake is highly dependent on their boundary conditions. Furthermore, due to their triangular geometry it is inappropriate to consider their response on a per unit length basis as can be done for a regular vertical spanning wall or a regular cantilever. Instead, their complete geometry must be considered.

Note:

This section describes the characteristics of gable failure mechanisms and the factors that contribute to the selection of the appropriate gable failure mechanism. The numerical procedures used to evaluate the %NBS score for gables are reported in Appendix C8B.4.

Special attention must be given to the correct identification of the total weight of the gable (W_{Tot}) and the total overburden (P_{Tot}) acting on the gable from roof loading. As illustrated in Figure C8.72, the analysis procedure involves the consideration of gables having a triangular geometry, but because gables (and triangles) can occur in a variety of configurations, care is necessary when applying the procedures presented in Appendix C8B.4 to ensure that the correct W and the correct P are used in calculations.

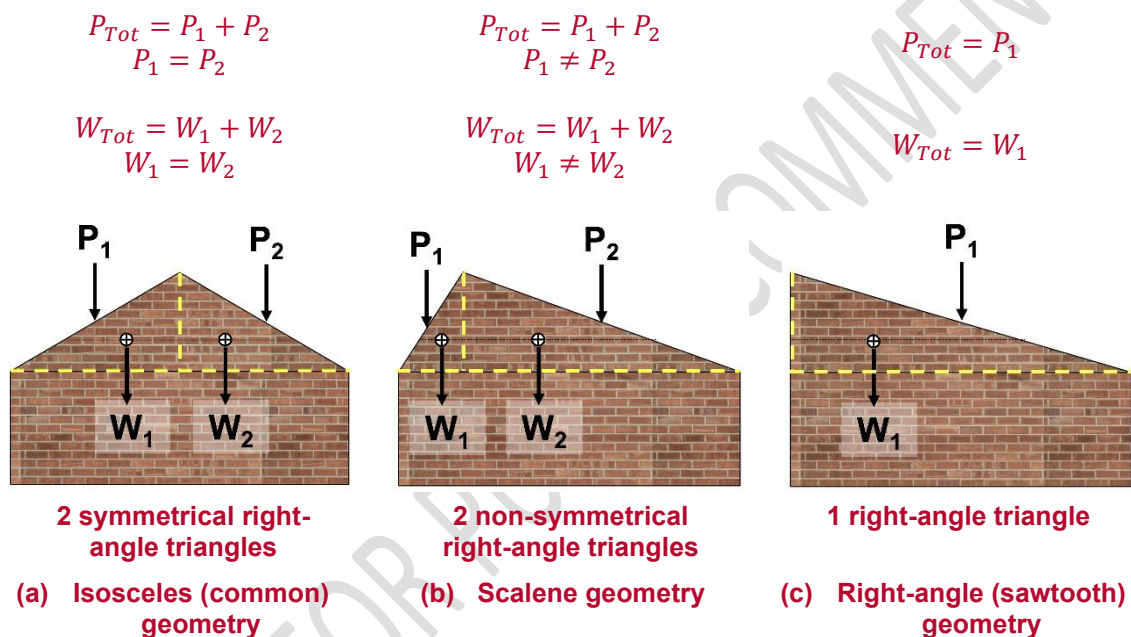


Figure C8.72: Gable geometric variations

Note:

It is useful to recall the well-known relationship for a triangle: $\text{Area} = \frac{1}{2} \times \text{base} \times \text{height}$.

In Figure C8.72 it is noted that W_{Tot} is common to all three configurations shown because both the base and height dimensions are common. However, the total roof load P_{Tot} will have minor variations depending on the gable geometry.

Three general cases can be identified for gables as illustrated in Figure C8.73, Figure C8.74, and Figure C8.75. This delineation is based on the degree of fixity provided by the roof, by the ceiling diaphragm, and by the perpendicular return walls. A reduction in wall thickness at the height of the gable where the diaphragm is supported may also be a contributing factor, as may any openings and associated concrete lintels or concrete ring beams present in the gable or in the wall directly below the gable.

Case 1: Vertical cantilever gables

Gables failing as triangular vertical cantilevers are triggered by a discontinuity at the base of the gable. This failure mode may result from a change of wall thickness between the gable and the wall below the gable or by the presence of detailing such as a well-connected ceiling diaphragm, a reinforced concrete lintel, or a concrete bond beam. Additionally, this failure mode requires that there be no evidence that the gable is adequately fixed to the roof structure. This scenario may also arise when the wall below the gable has thickenings or buttresses that terminate at the base of the gable. These conditions cause a rotational weakness to occur at the base of the gable, which becomes the hinge point for the cantilevered failure. This failure mode was frequently observed in the Canterbury earthquakes, with examples shown in Figure C8.73.

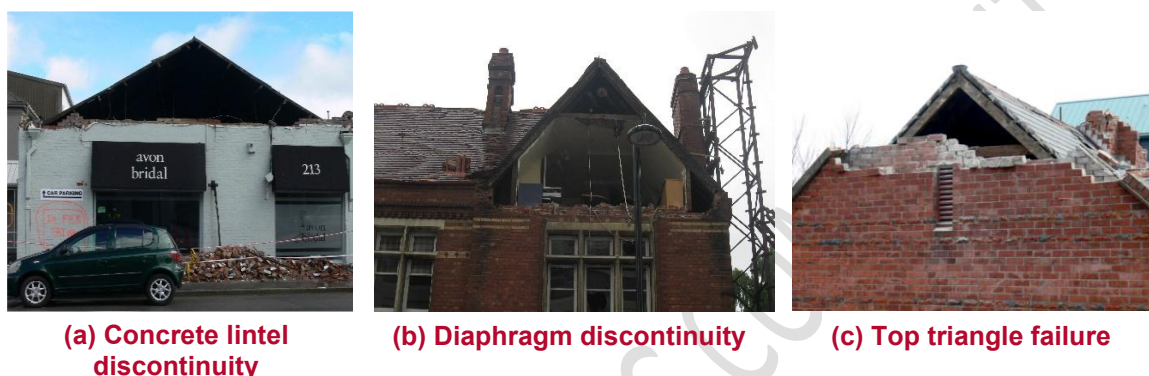


Figure C8.73: Gables failing as vertical cantilevers

Note:

A variation of Case 1 arises when there is some evidence that the gable may fail by forming a horizontal crack at approximately the mid-height of the gable, resulting in the overturning of a smaller triangle at the gable top (this variation is illustrated in Figure C8.73c). The same formulation as for Case 1 can be used, but with a reduced effective height. While it can be difficult to determine when to prioritise the full gable failure mode or this localised failure mode, certain factors can trigger the latter, such as existing mid-height anchorages, openings in the gable, or thickenings/buttresses projecting up to mid-height of the gable. Note that higher mode effects may also contribute to the formation of this mechanism but that such modal contributions have been neglected here because of their complexity.

Case 2: Vertically spanning gables

Vertically spanning gable failure is associated with fully restrained boundary conditions where reliable fixity is provided around the full perimeter of the gable triangle having a symmetrical isosceles geometry (see Figure C8.74c). The mechanism also occurs for the scenario of a sawtooth gable with a free vertical edge as shown in Figure C8.74b. This failure mode is triggered by discontinuities similar to Case 1 at the base of the gable and by the top edge of the gable being well-connected to the roof.

- For a half gable with a free vertical edge, a diagonal crack forms to divide the gable into two equal triangular wall panels as seen in Figure C8.74a.
- For a full triangular gable, three wall panels are formed with diagonal cracks meeting at the centre of the gable and a vertical crack reaching the apex to form a symmetrical inverted Y mechanism, as seen in Figure C8.74c,d.

This failure mechanism (and the associated boundary conditions) occurs less often when compared to other gable failure mechanisms. It is noted that this failure mechanism can be difficult to identify from post-earthquake damage observations.

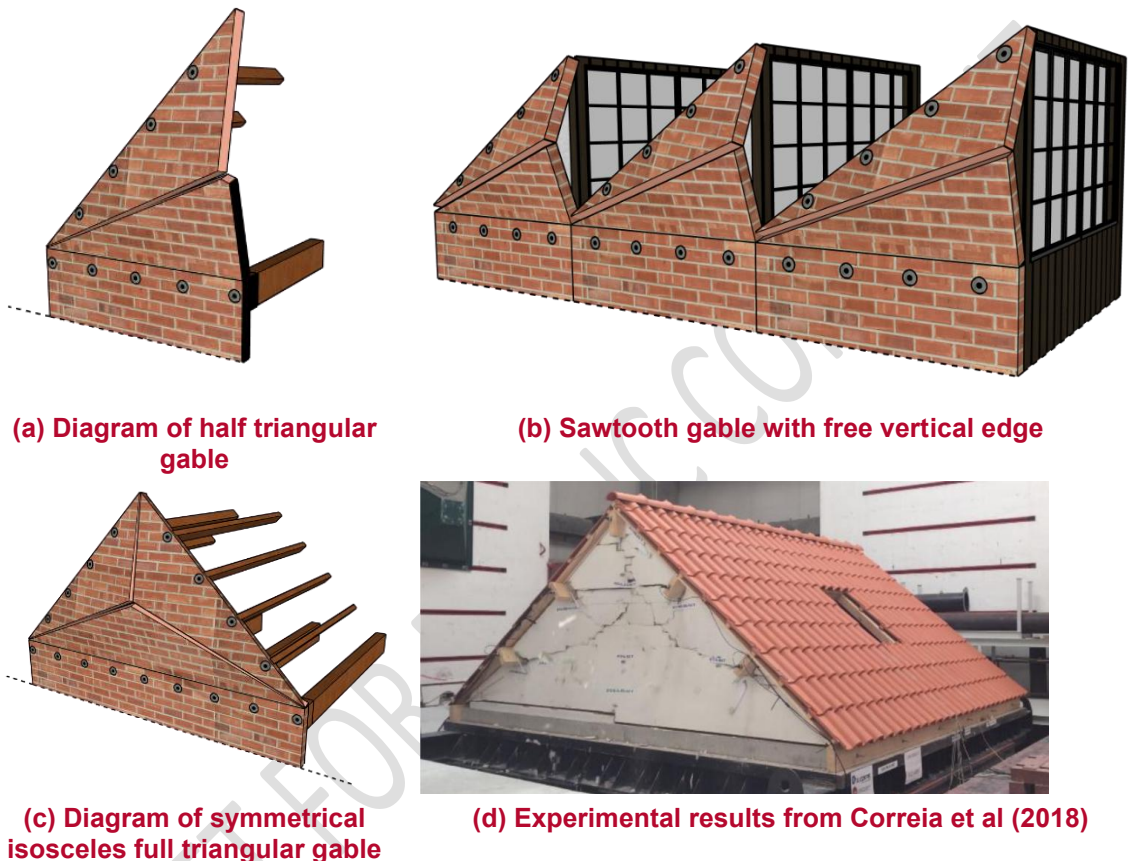


Figure C8.74: Vertically spanning gable failure

Note:

The current formulation for the Case 2 scenario is based on the symmetrical failure mechanism illustrated in Figure C8.74c, with the mathematics assuming the boundary conditions shown in Figure C8.74c. This situation only occurs for isosceles triangular configurations (see Figure C8.72) having a fully restrained condition around the entire perimeter of the gable or for the condition of a right-angle triangular configuration with a free vertical edge, such as may be assumed when the vertical face of a sawtooth gable (right-angle triangle configuration) is predominantly composed of windows to allow natural lighting into the building interior (see Figure C8.74b).

Case 3: Vertical-horizontal spanning gables

Vertical-horizontal spanning gable failure occurs when neither the roof nor the ceiling diaphragm provides suitable fixity, or when the gable does not have a ceiling diaphragm that

provides constraint at the base of the gable. In this case the complete gable overturns along with a portion of the wall below, and the base of the failure mechanism has a curved shape.

The specific geometry of the failure mechanism is dictated by the distance between the return walls and the wall height below the gable. It is uncommon for the full height of the wall below the gable to fail except for cases where the distance between return walls is several times greater than the height of the wall below the gable or cases where the wall below the gable is highly penetrated with openings. This case was observed moderately often in the Canterbury earthquakes as seen in Figure C8.75a,c.



Figure C8.75: Vertical-horizontal spanning gables failure mechanism

Note:

For gable failure mechanism case 3 and when stretcher, running or common bond pattern is used, if $\frac{h+t}{l+t} \geq 2 \frac{H}{L}$ (where H and L are the height and length of the wall, and h and l are the height and length of the brick, with t being the mortar joint thickness) then the gable should be treated as a vertical cantilever wall because the horizontal boundary conditions have limited supporting effect (see Figure C8.75c). From Figure C8.7(a) it can be established that typical values are $h = 70$ mm, $l = 230$ mm and $t = 10$ mm such that the wall can be treated as a vertical cantilever when $L \geq 6H$. In cases of irregular, Flemish, or stack bond patterns the wall can be treated as a vertical cantilever when $L \geq 4H$.

When the gable wall is treated as a cantilever the effective height of the composite structure should be taken as the wall height plus half the gable height because the triangular gable section has half the mass moment of inertia of a rectangular section such that the triangular gable is equivalent to a rectangle of the same width and half the mass.

C8.8.5.5 Horizontal and vertical-horizontal spanning walls

Advice on approaches to assessment of horizontal one-way spanning walls is given in Appendix C8B.6, for use in limited and specific contexts. Some tables of acceptable span values are provided.

Past earthquakes have shown that URM walls can act as a two-way spanning wall showing yield line patterns (refer to Figure C8.76) similar to those that occur in a two-way spanning slab if the walls are attached to the supports on four sides. However, a special study is recommended if two-way spanning is to be assumed. This study should take into account different elastic properties, displacement compatibility, and any detrimental effects resulting from the expected behaviour of the wall in the orthogonal direction.

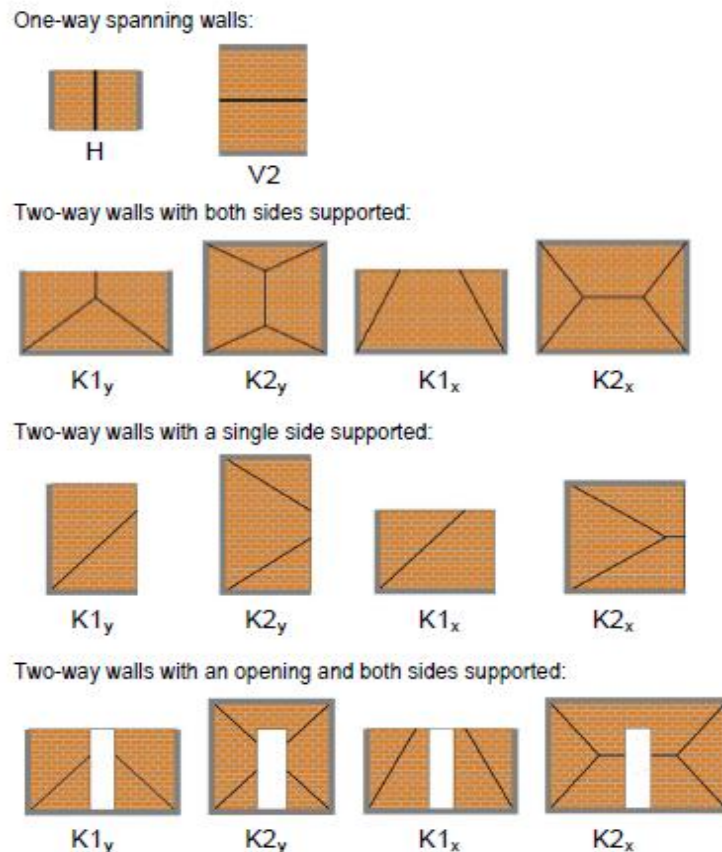


Figure C8.76: Idealised cracking patterns for masonry walls

Note:

Computationally intensive analytical methodologies such as finite element analysis have been shown to predict the out-of-plane strength of two-way spanning URM walls with good reliability. However, their reliance on knowing the precise values of material properties, the high computational effort and the high analytical skill required of the user makes them unsuitable for everyday design use.

The approach prescribed by the Australian masonry code AS 3700:2011 (AS, 2011) for ultimate strength design of two-way spanning walls is the so-called virtual work method, developed by Lawrence and Marshall (1996). This is a form of rigid plastic analysis which assumes that, at the point of ultimate strength, the load resistance of the wall is obtained from contributions of moment capacities along vertical and diagonal crack lines in two-way bending mechanisms (refer to Figure C8.76). Comparisons of strength predictions with a large experimental data set have been shown to be largely favourable in the sources mentioned before, in spite of numerous shortcomings of the moment capacity expressions used within the method which are still currently prescribed in AS 3700:2011 (AS, 2011).

More recently, Willis et al. (2004) and Griffith et al. (2007) have developed alternative expressions for calculating the moment capacities which incorporate significant improvements over the AS 3700 expressions as they are based on more rational mechanical models, account for the beneficial effects of vertical compression, and are dimensionally consistent. Furthermore, Willis et al. (2004) demonstrated that the expressions perform favourably in predicting the ultimate load capacity when implemented into the virtual work approach.

The currently available research is not sufficient for assessing two-way walls in a typical design office environment. However, significant progress has been made into the behaviour of walls of this kind, e.g. Vaculik (2012), and this research progress is likely to be translated into procedures suitable for design office use and routine assessment in a future update of these guidelines.

C8.8.6 Walls subjected to in-plane load

C8.8.6.1 General

The capacity of wall members/elements will typically be limited by their horizontal shear capacity.

Wall members/elements under in-plane load can be broadly categorised into two main groups: walls without penetration and walls with penetrations. Beware of hidden penetrations or weaknesses in walls, such as existing or removed fireplaces, and old door or window openings subsequently covered over or filled in.

The capacity of a wall element without penetrations should be assessed as outlined in Section C8.8.6.2.

The recommended approach to assessing the capacity of a wall element with penetrations is as follows:

- Step 1: Divide the wall element into individual “members” consisting of the “piers” between the penetrations and “spandrel” members above and below the penetrations.
- Step 2: Carry out a plane frame lateral load analysis of the wall to determine the relationship between the earthquake lateral load and the actions in the piers (including axial load) and the spandrels.
- Step 3: Determine the capacity of the piers in a similar manner to walls in accordance with Section C8.8.6.2. This will be a function of axial load on the pier (tension and/or compression).
- Step 4: Determine the capacity of the spandrels in accordance with Section C8.8.6.3.
- Step 5: Determine if the capacity of the penetrated wall is governed by spandrel or pier capacity. This will need to be evaluated for each spandrel to pier connection, and the effect of the potential axial load in the piers will need to be considered. A sway index as defined in Section C8.8.6.4 can be used to do this.
- Step 6: Based on the sway index, determine if the capacity of each pier element is governed by the pier itself or the abutting spandrel element.
- Step 7: Carry out an analysis of the wall element to determine its capacity based on the capacity of the individual piers (including the effects of axial load) acting in series (refer to Section C8.8.6.4).

Note:

For basic buildings, when assessing the capacity of the wall element the effect of the spandrels may be ignored and the piers assumed to extend over the full height of the wall

as cantilevers. This will avoid the need to assess the effect of lateral load induced axial loads, but larger displacements may be predicted.

The degree to which a wall on a single line, but extending over several storeys, should be broken down into individual members will depend on the method of analysis used to establish the building's global capacity. This is discussed further in Section C8.9. Typically it is expected that it will be necessary to assess the capacity for each wall line between each storey in the building.

C8.8.6.2 In-plane capacity of URM walls and pier elements

The in-plane strength capacity of URM walls and pier elements should be taken as the lower of the assessed diagonal tensile, toe crushing, in-plane rocking or bed-joint sliding strength capacities as determined below. This then becomes the mode of behaviour and the basis for the calculation of the deformation capacity. Where DPC layers are present these may also limit the shear that can be resisted.

For the purposes of assessing the wall or pier capacities for each mechanism the yield displacement, Δ_y , may be taken as the sum of the flexural and shear in-plane displacements (making allowance for cracking, i.e. the effective modulus of elasticity and shear modulus, etc., as recommended in Section C8.7.6) when the element is subjected to a lateral shear consistent with achieving the shear strength for that mechanism as given below. Refer also to Section C8.9.4.5.

Diagonal tensile capacity

This is one of the most important checks to be carried out.

The maximum diagonal tensile strength of a wall, pier or spandrel without flanges (or where the engineer has decided to ignore them) can be calculated using Equation C8.28 (ASCE 41-13, 2014). Otherwise, refer to the relevant reference to account for the effect of flanges.

$$V_{dt} = f_{dt} A_{n,web} \beta \sqrt{1 + \frac{f_a}{f_{dt}}} \quad \dots C8.28$$

where:

- β = factor to correct nonlinear stress distribution (refer to Table C8.13)
- $A_{n,web}$ = area of net mortared/grouted section of the wall web, mm²
- f_{dt} = masonry diagonal tension strength (refer to Equation C8.3), MPa
- f_a = axial compression stress due to gravity loads calculated at mid height of the wall/pier, MPa.

Table C8.13: Shear stress factor, β , for Equation C8.30

Criterion			β
Slender piers, where $h_{eff}/l > 1.5$			0.67
Squat piers, where $h_{eff}/l < 1.0$			1.00
Note:			
Linear interpolation is permitted for intermediate values of h_{eff}/l			

Refer to **Figure C8.77** for the definition of h_{eff} .

This failure mode occurs when the diagonal tensile strength of a wall or pier is exceeded by the principal stresses. It is one of the undesirable failure modes as it causes a rapid degradation in strength and stiffness after the formation of cracking, ultimately leading to loss of load path. For this reason a deformation limit of Δ_y for this failure mode is recommended.

This failure mode is more common where axial stresses are high, piers are squatter and the tensile strength of masonry is low.

Diagonal tension failure leads to formation of an inclined diagonal crack that commonly follows the path of bed and head joints through the masonry, because of the lower strength of mortar compared to brick. However, cracking through brick is also possible if the mortar is stronger. In New Zealand masonry, the crack pattern typically follows the mortar joint.

For conditions where axial stresses on walls or piers are relatively low and the mortar strengths are also low compared to the splitting strengths of the masonry units, diagonal tension actions may be judged not to occur prior to bed-joint sliding. However, there is no available research to help determine a specific threshold of axial stress and relative brick and mortar strengths that differentiates whether cracking occurs through the units or through the mortar joints (ASCE 41-13, 2014).

Toe crushing capacity

The probable toe crushing strength, V_{tc} , of a wall, pier or spandrel can be calculated using Equation C8.29 if no flanges are present or if the engineer has decided to ignore them. If flanges are to be accounted for, refer to the relevant reference.

$$V_{\text{tc}} = (\alpha P + 0.5 P_w) \left(\frac{L_w}{h_{\text{eff}}} \right) \left(1 - \frac{f_a}{0.7 f'_m} \right) \quad \dots \text{C8.29}$$

where:

- α = factor equal to 0.5 for fixed-free cantilever wall/pier, or equal to 1.0 for fixed-fixed wall/pier
- P = superimposed and dead load at top of the wall/pier
- P_w = self-weight of wall/pier
- L_w = length of the wall/pier, mm
- h_{eff} = height to resultant of seismic force (refer to **Figure C8.77**), mm
- f_a = axial compression stress due to gravity loads at the base of the wall/pier, MPa
- f'_m = masonry compression strength, MPa (refer to Section C8.7.3).

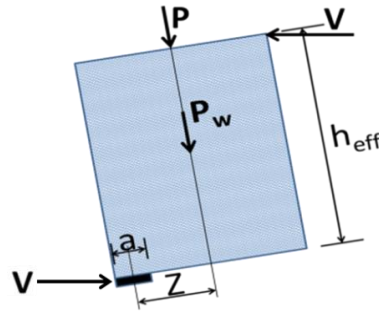


Figure C8.77: A rocking pier

A deformation limit of Δ_y or ϕ_y is recommended for this failure mode for walls/piers and spandrels respectively.

A toe crushing failure mode is not an expected failure mode of low-rise New Zealand walls or piers during in-plane loading. However, it still needs to be assessed; particularly when the walls have been retrofitted with un-bonded post-tensioning or a seismic intervention that inhibits the diagonal tension failure mode.

Allowance for toe crushing can enable a form of limited redistribution of in-plane load between piers of differing length, provided that these piers are adjacent and along the same line. For example, if one squat pier is in line with four more slender piers (see Figure C8.78) then allowing toe crushing of the squat pier (therefore resulting in effective shortening of the pier length) will result in the more slender piers attracting greater load (because the effective stiffnesses of all the piers is then more similar) and therefore global capacity may improve.

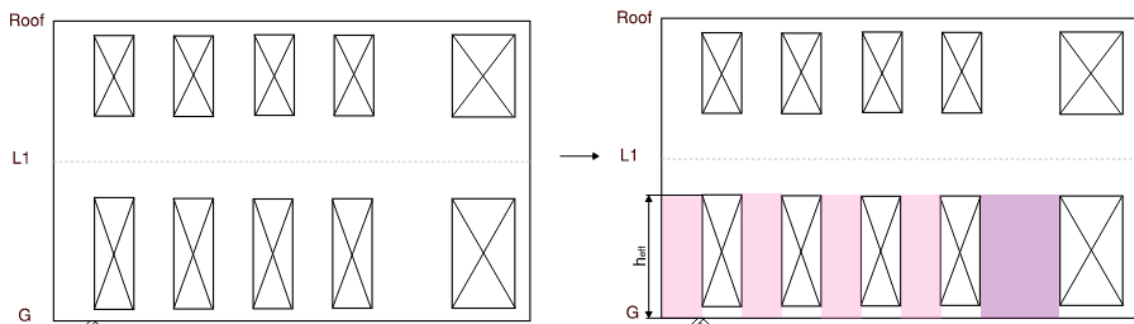


Figure C8.78: Example URM punched wall, and ground floor pier idealisation

The wall shown in Figure C8.78 is idealised as shown in Figure C8.79. Originally the squat pier takes the majority of shear, but allowing for toe crushing of the squat pier leads to a more even distribution of resistance.

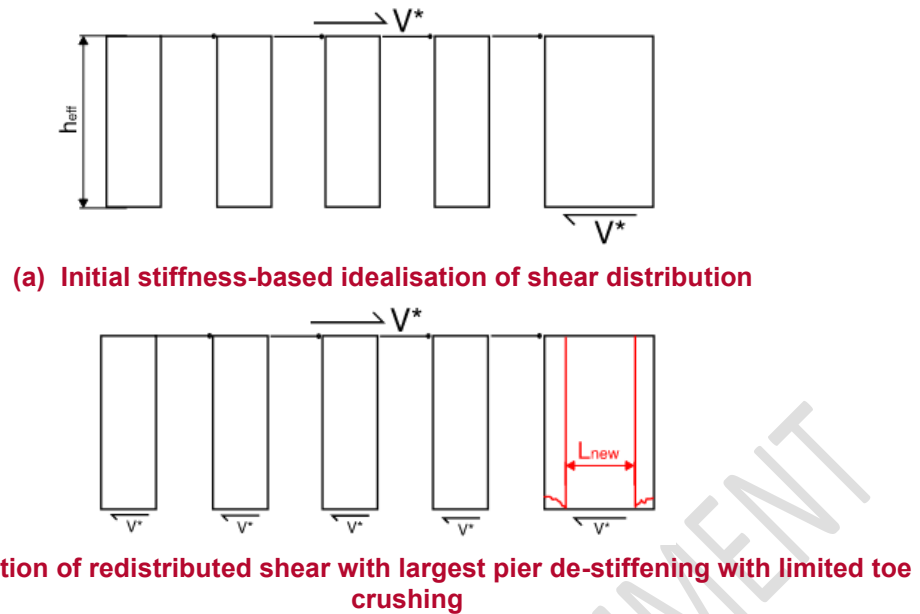


Figure C8.79: Idealisation of pier loads when accounting for toe crushing

‘New’ squat piers needs to be re-assessed for all failure modes for its new length (ie reconsider diagonal tension failure, rocking capacity). This includes assessment of strong pier-weak beam mechanism if previously assumed for the squat pier. The ‘amount’ of toe crushing can vary subject to the following limits:

- Net capacity of all walls along the line is *greater* than the capacity of the original assessed capacity (ie the just the squat wall alone)
- $L_{new} > 0.7L_{original}$
- The building must have sufficient tie capacity such that a load equal to the full *original* squat pier capacity can reach the squat pier ie the full original squat pier capacity must be provided as a tie capacity even in the reduced length case.

Note that ‘toe crushing’ may appear physically as loss of bricks locally to the ends of the pier, rather than physical decrease in unit height.

Rocking capacity

Rocking failure is one of the stable modes of failure. Experimental investigations undertaken by Knox (2012), Anthoine et al. (1995), Costley and Abrams (1996), Franklin et al. (2001), Magenes and Calvi (1995), Moon et al. (2006), Bruneau and Paquette (2004), Xu and Abrams (1992), and Bothara et al. (2010) have confirmed that URM elements exhibiting rocking behaviour have substantial deformation capacity past initial cracking but also exhibit very low levels of hysteretic damping.

A generalised relationship between strength and deformation for the rocking mechanism is shown in **Figure C8.80**.

The maximum probable rocking strength of a wall (considered over one level) or pier, V_r , can be calculated using Equation C8.30.

$$V_r = 0.9 (\alpha P + 0.5P_w) \frac{L_w}{h_{eff}} \quad \dots \text{C8.30}$$

where:

V_r	=	strength of wall or wall pier based on rocking
α	=	factor equal to 0.5 for fixed-free cantilever wall, or equal to 1.0 for fixed-fixed wall pier
P	=	superimposed and dead load at the top of the wall/pier under consideration
P_w	=	self-weight of the wall/pier
L_w	=	length of wall or pier, mm
h_{eff}	=	height to resultant of seismic force (refer to Figure C8.77), mm.

When assessing the capacity of walls without openings for the full height of the building, Equation C8.30 will need to be adjusted to account for the different location of the lateral force. This can be assumed to be applied at two thirds of the height of the building from the point of fixity.

Nonlinear response of rocking URM piers is generally characterised by a negative post-yield slope due to P-delta effects but will be limited by toe crushing, as the effective bearing area at the toe of the rocking pier reduces to zero under increasing lateral displacement (refer to Figure C8.80). This latent toe crushing differs from that discussed above as it typically occurs at larger rotations and lower shears.

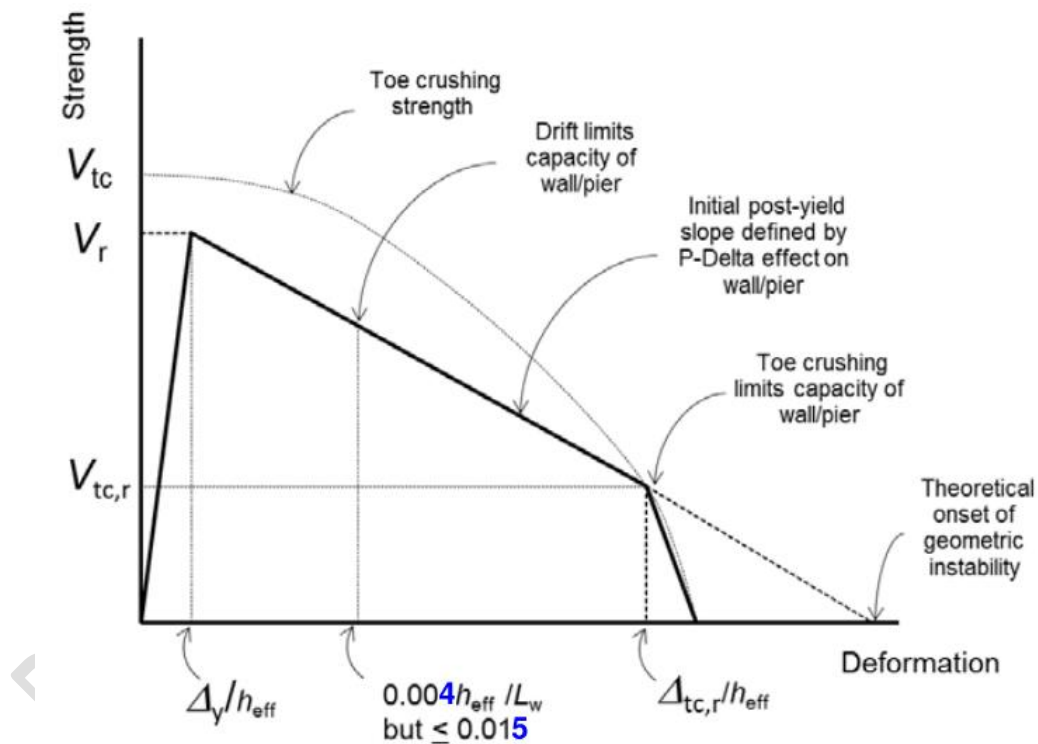


Figure C8.80: Generalised force-deformation relationship for rocking of unreinforced masonry walls or piers (ASCE 41-21, 2014)

Deformation associated with the onset of toe crushing, $\Delta_{tc,r}/h_{eff}$, should be calculated using a moment-curvature or similar analytical approach and a maximum usable strain at the compression fibre of 0.0035. The axial compressive stress on the toe due to gravity loads should be based on an equivalent compression zone of the effective net section of the rocking pier that is in bearing.

Under rare conditions, the geometric stability of the rocking pier due to P-delta effects may govern the ultimate deformation capacity. In the absence of substantiating test results, assume elastic unloading hysteretic characteristics (no degradation of resistance with displacement) for rocking URM in-plane walls and wall piers assessed within the deformation limits of this guideline.

Note:

It is recommended that the capacity of a rocking wall/pier is limited to that consistent with a wall/pier lateral drift equal to the lower of $0.4\%h_{\text{eff}}/L_w$ ($= 0.004h_{\text{eff}}/L_w$) or 1.5% ($= 0.015$). These criteria are adopted from the ASCE 41-23 nonlinear acceptance criteria for Life safety (Table 11-4 of ASCE 41-23). The lateral performance of a rocking wall is considered to be less reliable and not to provide the level of resilience considered appropriate when the deflections exceed these values. Wall/pier elements that are not part of the seismic resisting system and which have a thickness greater than 350 mm (3 wythes) are expected to be able to provide reliable vertical load carrying capacity at higher deflections approaching twice the limits given above. These greater limits can also be used for all wall/pier elements when cyclic stiffness and strength degradation are included in the analysis method used. Such an analysis will automatically include redistribution of the lateral loads between elements when this is necessary.

Assumption of fixity or cantilever action depends on the stiffness and overall integrity of the spandrels above and below the rocking pier and on how effectively spandrels can transmit vertical shears and bending. Conversely, wall spandrels that are weak relative to adjacent piers may not provide fixity at the tops and bottoms of piers and may result in piers acting as cantilevers. In general, deep spandrels could provide fixed-fixed boundary conditions.

Note that if the self-weight of the pier is large and boundary conditions are fixed-fixed, Equation C8.30 may overestimate the rocking capacity.

This behaviour mode is common where axial stresses are low, walls or piers are slender (height to length ratio > 2) and mortar strength are relatively better.

Bed-joint sliding shear capacity

Bed-joint sliding failure is one of the stable modes of failure. Investigations undertaken by various researchers have confirmed that URM elements exhibiting bed-joint sliding behaviour have substantial deformation capacity past initial cracking.

The recommended generalised force-deformation relationship for URM walls and wall piers governed by bed-joint sliding or sliding stair-stepped failure modes is illustrated in Figure C8.81. A simplified form of the ASCE 41-13 (2014) force-deformation relationship has been adopted.

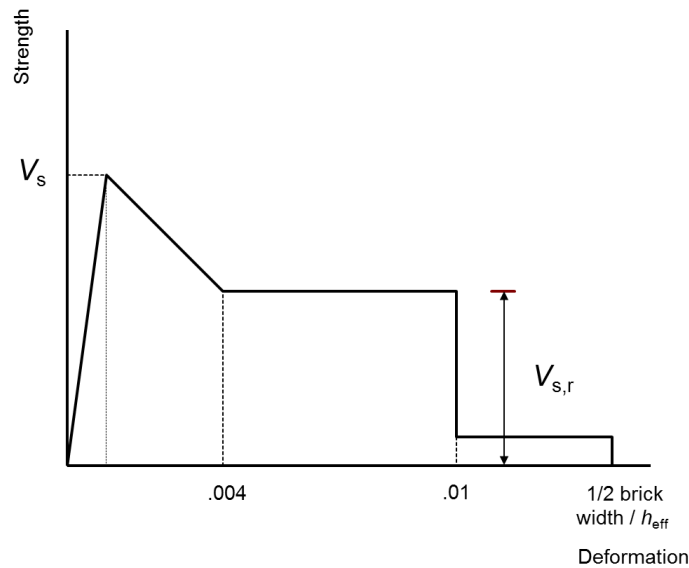


Figure C8.81: Generalised force-deformation relationship for unreinforced masonry walls or piers governed by bed-joint sliding or stair-stepped sliding

The maximum probable sliding shear strength, V_s , can be found from Equation C8.31.

$$V_s = 0.7(t_{\text{nom}}L_w c + \mu_f(P + P_w)) \quad \dots\text{C8.31}$$

where:

- μ_f = masonry coefficient of friction
- P = superimposed and dead load at top of the wall/pier
- P_w = self-weight of wall/pier above the sliding plane being considered.

The 0.7 factor is to reflect the overall reliability of the sliding mechanism calculation.

The capacity for bed-joint sliding in masonry elements is a function of bond and frictional resistance. Therefore, Equation C8.31 includes both factors. However, with increasing cracking, the bond component is progressively degraded until only the frictional component remains. The probable residual wall sliding shear capacity, $V_{s,r}$, is therefore found from Equation C8.31 setting the cohesion, c , equal to 0.

Note:

It is recommended that bed-joint sliding be checked at the base of the pier unless there is a site condition (such as the presence of a DPC layer or a change of masonry type) that may suggest the formation of a slip plane at a different level.

Note:

It is recommended that the bed-joint sliding capacity of a rocking wall/pier is limited to a lateral drift of 0.003. The lateral performance of a wall/pier is considered to be unreliable and not able to provide the level of resilience considered appropriate when the deflections exceed this value. Wall/pier elements that are not part of the seismic resisting system are expected to be able to provide reliable vertical load carrying capacity at higher drifts, approaching 0.0075. These greater limits can also be used for all wall/pier elements when

cyclic stiffness and strength degradation are included in the analysis method used. Such an analysis will automatically include redistribution of the lateral loads between elements when this is necessary.

Slip plane sliding

A DPC layer, if present, will be a potential slip plane, which may limit the capacity of a wall.

The probable shear capacity of a slip plane for no slip can be found from Equation C8.32:

$$V_{\text{dpc}} = \mu_{\text{dpc}} (P + P_w) \quad \dots \text{C8.32}$$

where:

μ_{dpc} = DPC coefficient of friction. Typical values are 0.2-0.5 for bituminous DPC, 0.4 for lead, and higher (most likely governed by the mortar itself) for slate DPC.

Other terms are as previously defined.

Note:

Where sliding of a DPC layer is found to be critical, testing of the material in its current/in-situ state may be warranted. Alternatively, parametric checks, where the effects of low/high friction values are assessed, may show that the DPC layer is not critical in the overall performance.

Sliding on a DPC slip plane does not necessarily define the deformation capacity of this behaviour mode.

Evaluating the extent of sliding may be calculated using the Newmark sliding block (Newmark, 1965) or other methods. However, exercise caution around the sensitivity to different types of shaking and degradation of the masonry above/below the sliding plane. Where sliding is used in the assessment to give a beneficial effect, this should be subject to peer review.

Effect of wall and pier flanges

It is common practice to ignore the effects of flanges on the walls or piers while assessing the in-plane capacity of walls and piers. However, experimental research undertaken by Costley and Abrams (1996), Bruneau and Paquette (2004), Moon et al. (2006), Yi et al. (2008), and Russell and Ingham (2010b) has shown that flanges have the potential to influence the response of in-plane walls. Flanged walls can have considerably higher strength and stiffness than those without flanges. The assessment could be particularly non-conservative where estimated rocking, sliding shear, or stair-step cracking strength (which are stable modes of failure) is close to the diagonal tensile strength of pier and walls. The recommended approach is to assess how much flange is required for diagonal tension to be the critical behaviour mode and, based on this, determine if further investigation is required.

Note:

One of the preconditions for taking into account the effect of the flanges is that they should remain integral with the in-plane piers and walls during the seismic shaking. Therefore, the integrity of the connections must be ascertained before ignoring or including them.

If flanges are taken into account, it is common to assume that the lengths of flanges acting in compression are the lesser of six times the thicknesses of the in-plane walls or the actual lengths of the flanges. It is also common to assume that equivalent lengths of tension flanges (to resist global or element overturning) are based on likely crack patterns relating to uplift in flange walls (Yi et al., 2008). Other approaches that either model or consider different flange lengths qualitatively may result in a variety of crack patterns and corresponding sequences of actions.

C8.8.6.3 URM spandrel capacity**General**

The recommended generalised force-deformation relationship for URM spandrels is illustrated in **Figure C8.82**. The recommended generalised force-deformation relationship is based on experimental work undertaken by Beyer and Dazio (2012a and 2012b), Knox (2012), Graziotti et al. (2012), and Graziotti et al. (2014) and as recommended by Cattari et al. (2014).

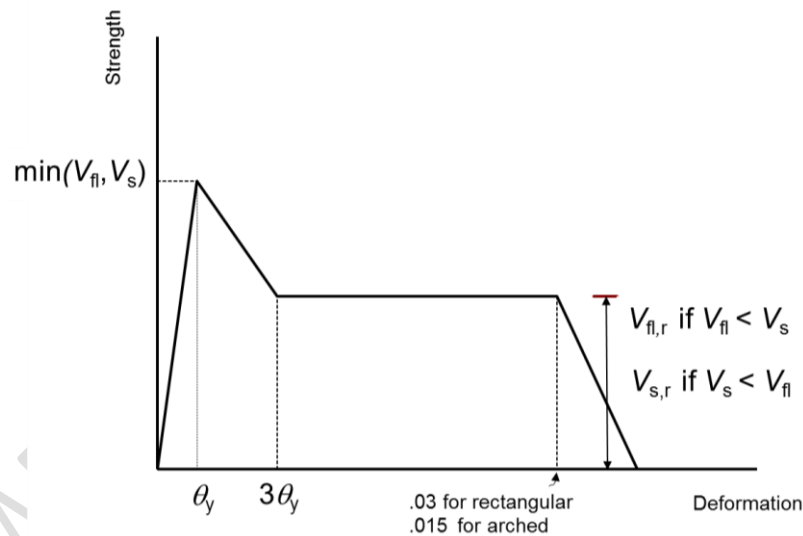


Figure C8.82: Generalised force-deformation relationship for unreinforced masonry spandrels

The probable in-plane shear capacity of a URM spandrel should not be taken greater than that implied by the probable spandrel flexural strength.

θ is the chord rotation of the spandrel, relative to the piers.

Note:

It is considered prudent to limit the deformation capacity of a spandrel panel to a panel drift of $3\theta_y$ (Beyer and Mangalathu, 2014) if its capacity is to be relied on as part of the seismic resisting system. Panel chord rotation capacities beyond 0.02 or 0.01 for rectangular and arched spandrels respectively, for **spandrel** panels that are not assumed to

be part of the lateral seismic resisting system, are not recommended as the performance of the spandrel (i.e. its ability to remain in place) could become unreliable at rotations beyond these limits. These greater limits can also be used for all spandrel elements when cyclic stiffness and strength degradation are included in the analysis method used. Such an analysis will automatically include redistribution of the lateral loads between elements when this is necessary. Therefore, the need to distinguish, in advance, between elements of the lateral and non-lateral load resisting systems is not required.

Two generic types of spandrel have been identified: rectangular and those with shallow arches. Recommendations for the various capacity parameters for these two cases are given in the following sections.

Investigations are continuing on appropriate parameters for deep arched spandrels. In the interim, until more specific guidance is available, it is recommended that deep arched spandrels are considered as equivalent rectangular spandrels with a depth that extends to one third of the depth of the arch below the arch apex.

The geometrical definitions used in the following sections are shown on **Figure C8.83**.

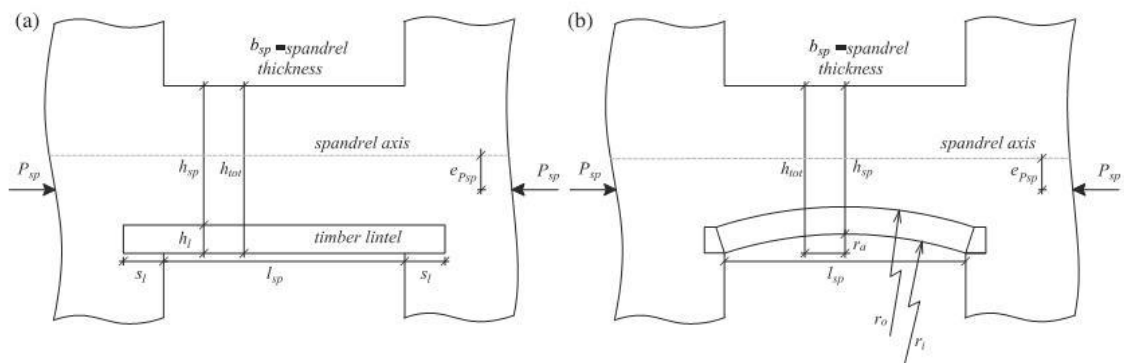


Figure C8.83: Geometry of spandrels with (a) timber lintel and (b) shallow masonry arch (Beyer, 2012)

Rectangular spandrels

The expected in-plane strength of URM spandrels with and without timber lintels can be determined following the procedures detailed below.

Note:

There is limited experimental information on the performance of URM spandrels with lintels made from materials other than timber. However, URM spandrels with steel lintels are expected to perform in a similar manner to those with timber lintels.

When reinforced concrete lintels are present the capacity of the spandrel can be calculated neglecting the contribution of the URM.

Shear due to flexural behaviour

The shear developed in a rectangular URM spandrel limited by the probable flexural strength of a spandrel, V_{fl} , can be estimated using Equation C8.33 (Beyer, 2012). Timber lintels do

not make a significant contribution to the probable flexural capacity of the spandrels so can be ignored.

$$V_{fl} = (f_{t,eff} + p_{sp}) \frac{h_{sp}^2 b_{sp}}{3l_{sp}} \quad \dots C8.33$$

where:

$$\begin{aligned} f_{t,eff} &= \text{equivalent probable tensile strength of masonry spandrel} \\ p_{sp} &= \text{axial stress in the spandrel} \\ h_{sp} &= \text{height of spandrel excluding depth of timber lintel if present} \\ b_{sp} &= \text{width of spandrel} \\ l_{sp} &= \text{clear length of spandrel between adjacent wall piers.} \end{aligned}$$

Unless the spandrel is prestressed or provided with continuous bond beam above the opening, the axial stress in the spandrel can be assumed to be negligible when determining the peak flexural capacity.

The equivalent probable tensile strength of a masonry spandrel, $f_{t,eff}$, can be estimated using Equation C8.34:

$$f_{t,eff} = \alpha_s \left(c + 0.5 \mu_f p_p \right) + \frac{c}{2 \mu_f} \quad \dots C8.34$$

where:

$$\begin{aligned} p_p &= \text{mean axial stress due to superimposed and dead load in the adjacent wall piers} \\ \mu_f &= \text{masonry coefficient of friction} \\ c &= \text{masonry bed-joint cohesion} \\ \alpha_s &= \text{bond pattern factor taken as the ratio of horizontal crack length vs sum of the vertical crack length.} \end{aligned}$$

For spandrels constructed using 230 mm x 110 mm x 70 mm bricks α_s can be estimated as follows:

$$\begin{aligned} \text{Running bond: } \alpha_s &= 1.4 \\ \text{Common bond: } \alpha_s &= 1.2 \\ \text{English bond: } \alpha_s &= 0.7 \\ \text{Stack bond: } \alpha_s &= 0.0. \end{aligned}$$

Shear due to residual flexural behaviour

The shear developed in a rectangular URM spandrel due to the probable residual flexural strength of the spandrel, $V_{fl,r}$, can be estimated using Equation C8.35 (Beyer, 2012). Timber lintels do not often make a significant contribution to the residual flexural capacity of URM spandrels so they can be ignored.

$$V_{fl,r} = \frac{p_{sp} h_{sp}^2 b_{sp}}{l_{sp}} \left(1 - \frac{p_{sp}}{0.85 f_{hm}} \right) \quad \dots C8.35$$

where:

$$p_{sp} = \text{axial stress in the spandrel}$$

f_{hm} = compression strength of the masonry in the horizontal direction ($0.5f'_m$).

Axial stresses are generated in spandrel elements due to the restraint of geometric elongation. Results from experimental research indicate that negligible geometric elongation can be expected when peak spandrel strengths are developed (Beyer, 2012; Graziotti et al., 2012), as this is at relatively small spandrel rotations. As a result, there is little geometric elongation. Significant geometric elongation can occur once peak spandrel strengths have been exceeded, and significant spandrel cracking occurs within the spandrel, as higher rotations are sustained in the element. An upper bound estimate of the axial stress in a restrained spandrel, p_{sp} , can be determined using Equation C8.36 (Beyer, 2014):

$$p_{sp} = (1 + \beta_s)f_{dt} \frac{l_{sp}}{2 \times \sqrt{l_{sp}^2 + h_{sp}^2}} \quad \dots C8.36$$

where:

f_{dt} = masonry probable diagonal tension strength
 β_s = spandrel aspect ratio (l_{sp}/h_{sp}).

In Equation C8.36 the limiting axial stress generated in a spandrel associated with diagonal tension failure of the spandrel is calculated. The equation assumes the spandrel has sufficient axial restraint to resist the axial forces generated by geometric elongation.

In most typical situations the engineer can assume that spandrels comprising the interior bays of multi-bay pierced URM walls will have sufficient axial restraint such that diagonal tension failure of the spandrels could occur.

Spandrels comprising the outer bays of multi-bay pierced URM walls typically have significantly lower levels of axial restraint. In this case the axial restraint may be insufficient to develop a diagonal tension failure in the spandrels. Sources of axial restraint that may be available include horizontal post-tensioning, diaphragm tie elements with sufficient anchorage into the outer pier, or substantial outer piers with sufficient strength and stiffness to resist the generated axial forces. For the latter to be effective the pier would need to have enough capacity to resist the applied loads as a cantilever.

It is anticipated that there will be negligible axial restraint in the outer bays of many typical unstrengthened URM buildings. In this case the engineer can assume the axial stress in the spandrel is nil when calculating the residual flexural strength.

Probable shear strength

The probable shear strength of a rectangular URM spandrel, V_s , can be estimated using either Equation C8.37 (Beyer, 2012) or Equation C8.38 (Turnsek and Čačovič, 1970) as outlined below. Timber lintels do not make a significant contribution to the peak shear capacity of URM spandrels so can be ignored.

$$V_s = \frac{2}{3}(c + \mu_f p_{sp})h_{sp}b_{sp} \quad \dots C8.37$$

$$V_s = f_{dt}\beta_{sp} \left(\sqrt{1 + \frac{p_{sp}}{f_{dt}}} \right) h_{sp}b_{sp} \quad \dots C8.38$$

where:

$$\begin{aligned} f_{dt} &= \text{probable masonry diagonal tension strength} \\ \beta_{sp} &= \text{factor to correct the nonlinear stress distribution in the spandrel from Table C8.14.} \end{aligned}$$

Table C8.14: Shear stress factor, β_{sp} , for Equation C8.30

Criterion	β_{sp}
Slender spandrels, where $l_{sp}/h_{sp} > 1.5$	0.67
Squat spandrels, where $l_{sp}/h_{sp} < 1.0$	1.00
Note: Linear interpolation is permitted for intermediate values of l_{sp}/h_{sp}	

Unless the spandrel is prestressed the engineer can assume the axial stress in the spandrel is negligible when determining the shear capacity. Equation C8.37 is the shear strength associated with the formation of cracks through head and bed joints over almost the entire height of the spandrel: use this equation when the mortar is weaker than the brick. If the mortar is stronger than the brick and fracture of the bricks is likely to occur, use Equation C8.38.

Residual shear strength

Once shear cracking has occurred the URM spandrel can no longer transfer in-plane shear demands. When present, timber lintels acting as beams (simply supported at one end and fixed at the other) can transfer the vertical component of the spandrel load, F , to the adjacent pier (refer to Figure C8.84).

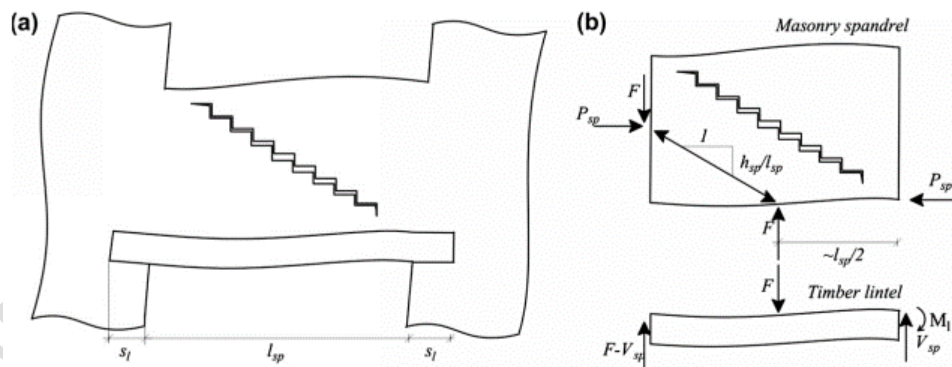


Figure C8.84: Shear mechanism of URM spandrels with timber lintels (Beyer, 2012)

Residual shear strength of cracked rectangular URM spandrels with timber lintels can be estimated as the minimum of Equation C8.39 or the capacity of the timber lintel to resist the applied load (Beyer, 2012). When no timber lintel is present the residual shear capacity of URM spandrels is negligible and can be assumed to be nil.

$$V_{s,r} = \frac{11}{16} p_{sp} \frac{h_{sp}^2 b_{sp}}{l_{sp}} \quad \dots \text{C8.39}$$

The applied load, F , to be resisted by the timber lintel can be calculated as:

$$F = p_{sp} \frac{h_{sp}^2 b_{sp}}{l_{sp}} \quad \dots C8.40$$

Spandrel axial stresses, p_{sp} , can be calculated in accordance with the procedures outlined above. Confirm the ability of the timber lintel to sustain the applied load.

Spandrels with a shallow arch

Shear due to flexural behaviour

The shear developed in an URM spandrel due to the probable flexural capacity of a spandrel with a shallow arch, V_{fl} , can be estimated using Equation C8.41 (Beyer 2012):

$$V_{fl} = h_{sp} b_{sp} \left(f_{t,eff} \frac{h_{sp}}{3l_{sp}} + p_{sp} \tan \alpha_a \right) \quad \dots C8.41$$

where α_a is the arch half angle of embrace computed as:

$$\alpha_a = \tan^{-1} \left(\frac{l_{sp}}{2(r_i - r_a)} \right) \quad \dots C8.42$$

where dimensions r_i , r_a and l_{sp} are defined in Figure C8.85. The arch is considered shallow if the half angle of embrace, α_a , satisfies Equation C8.45 where r_o is also defined in Figure C8.83.

$$\cos \alpha_a \geq \frac{r_i}{r_o} \quad \dots C8.43$$

Unless the spandrel is prestressed the engineer can assume the axial stress in the spandrel is negligible when determining the peak flexural capacity.

Shear due to residual flexural behaviour

The shear developed in an URM spandrel due to the residual flexural capacity, $V_{fl,r}$, of a spandrel with a shallow arch can be estimated using Equation C8.44 (Beyer 2012) and by referring to Figure C8.83.

$$V_{fl,r} = \frac{p_{sp} h_{sp} h_{tot} b_{sp}}{l_{sp}} \left(1 - \frac{p_{sp}}{0.85 f_{hm}} \right) \quad \dots C8.44$$

where the dimension h_{tot} is defined in Figure C8.83. Spandrel axial stresses, p_{sp} , can be calculated with the procedures set out in the previous section.

shear stresses analogous to the behaviour occurring in reinforced concrete beam-column joints.

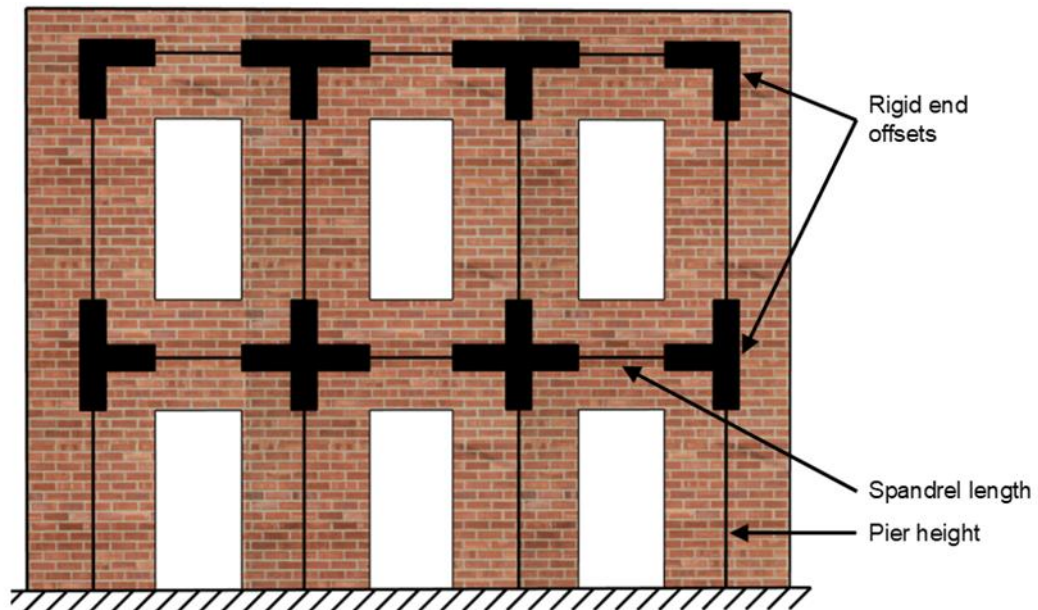


Figure C8.86: Primary geometry for the equivalent frame model

For 1-storey and 2-storey buildings where the spandrel depth h_{sp} is comparable to or greater than the spandrel length l_{sp} the in-plane analysis of penetrated URM walls can be carried out using the simplified “pier only” model shown in Figure C8.87 (Tomazevic, 1999). This simplified analysis procedure assumes that the spandrels are infinitely stiff and strong, and therefore that the response of the piers will govern the seismic response of the building. This simplified procedure may lead to non-conservative assessments for those structures which contain weak spandrels, or for structures assessed on the assumption that piers of dissimilar width will rock simultaneously with shears calculated pro rata based on the rocking resistance.

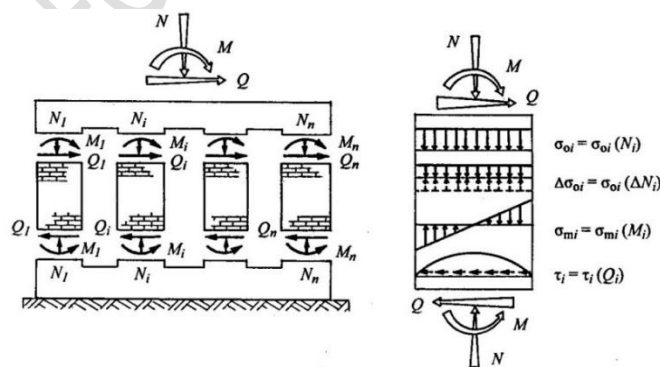


Figure C8.87: Forces and stresses in in-plane loaded piers when applying the simplified “pier only” assumption (Tomazevic, 1999)

For URM walls with openings of differing sizes and relatively weaker piers compared to stronger spandrels, Dolce (1989) has recommended that the effective height of each rocking pier is represented as the height over which the pier is considered to deform when accounting for the influence of the surrounding spandrels. The angles to the piers generally depends on masonry unit bed and head joint dimensions and the formation of stair-step cracking along

mortar joints. If the diaphragms are rigid or reinforced concrete bands are provided then the effective height of the piers may be limited to the bottom of the diaphragm or the concrete band, as appropriate.

The recommended procedure to establish the pier effective height is illustrated in Figure C8.88 and computationally reported in Equation C8.48. This procedure assumes a maximum inclination of 30° for the projection of lines between the two corners of adjacent openings, corresponding to the typical angle of shear cracks.

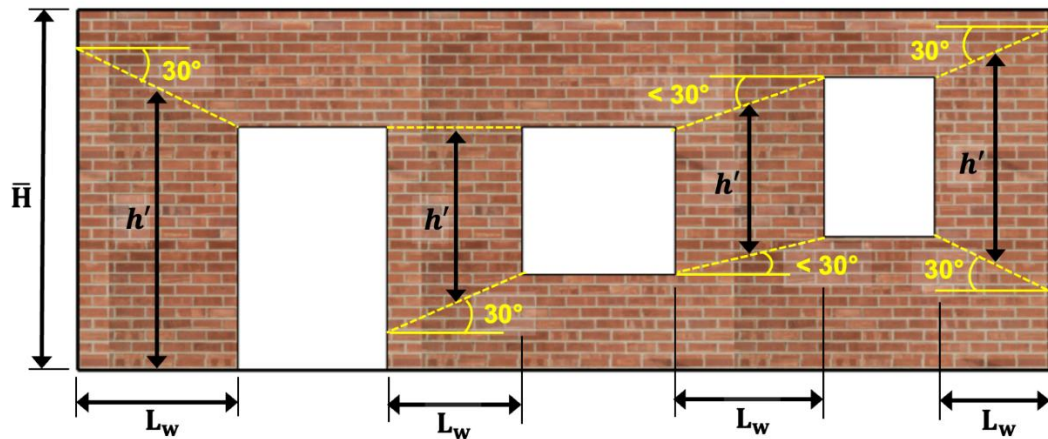


Figure C8.88: Pier effective height as proposed by Dolce (1989)

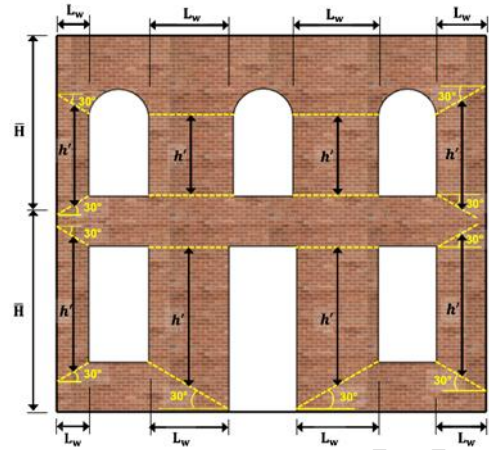
$$h_{eff} = h' + D \frac{(\bar{H} - h')}{3h'} \quad \dots C8.48$$

Note that for non-symmetrical walls it will be necessary to develop two equivalent frame models for the two directions of loading.

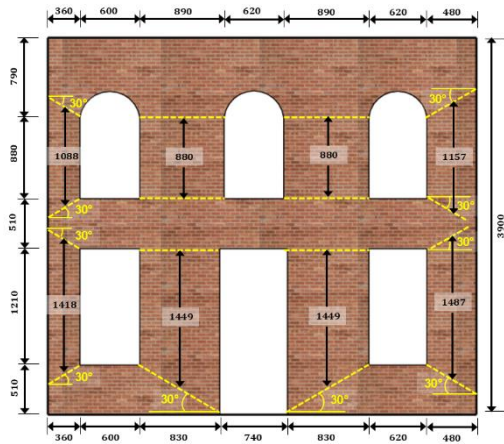
Knox (2012) undertook experimental validation using the equivalent frame approach. Application of the procedure shown in Figure C8.88 and computationally reported in Equation C8.48 is illustrated in Figure C8.89. See also Knox et al. 2018.



(a) Lab experimental set-up



(b) Symbol definitions (see Equation C8.48)



(c) Dimensions

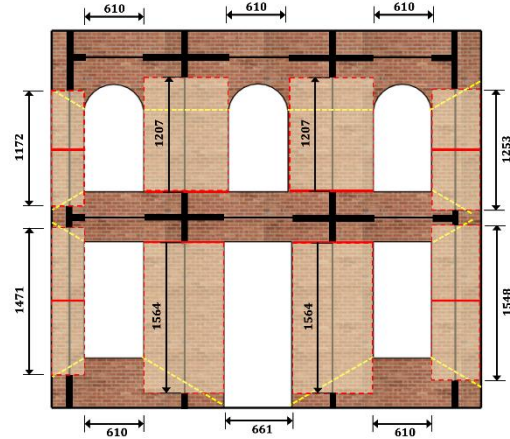

 (d) Effective pier heights, h_{eff}

Figure C8.89: Knox (2012) equivalent frame model using the Dolce (1989) procedure

To investigate whether perforated wall behaviour is governed by spandrel capacity or by pier capacity a sway potential index, S_i , can be defined for each spandrel-pier joint by comparing the demand:capacity ratios for the piers and spandrels at each joint:

$$S_i = \frac{\frac{\Sigma V_{u,Pier}^*}{\Sigma V_{n,Pier}}}{\frac{\Sigma V_{u,Spandrel}^*}{\Sigma V_{n,Spandrel}}} \quad \dots C8.49$$

where:

$\Sigma V_{u,Pier}^*$ = sum of the 100%NBS shear force demands on the piers above and below the joint calculated using $K_R = 1.0$

$\Sigma V_{n,Pier}$ = sum of the pier capacities above and below the joint

$\Sigma V_{u,Spandrel}^*$ = sum of the 100%NBS shear force demands on the spandrels to the left and right of the joint calculated using $K_R = 1.0$

$\Sigma V_{n,Spandrel}$ = sum of the spandrel capacities to the left and right of the joint.

When $S_i > 1.0$ a weak pier–strong spandrel mechanism may be expected to form, and when $S_i < 1.0$ a strong pier–weak spandrel mechanism may be expected to form.

Linear and nonlinear equivalent frame models can be used to analyse the in-plane response of perforated URM walls (Magenes, 2006). Nonlinear analysis of URM piers and spandrels can be carried out using 2D plane stress elements or solid 3D elements. This method has the advantage that the stresses and strains developed in the URM piers and spandrels can be assessed directly and deformation compatibility is maintained. Compression-only gap elements can be included in the analysis model to account for pier rocking (Knox, 2012).

The capacity of a penetrated wall element at a particular level can also be determined from the capacity (strength and deformation) of the individual wall/pier elements assuming that displacement compatibility must be maintained along the element and using the force deformation relationships defined above for the governing mode of behaviour of each element. This procedure can be extended to multiple levels if required, and the capacity of the whole wall determined if the engineer has some knowledge of the lateral load distribution with height. This procedure can be considered a variant of the Simple Lateral Mechanism Analysis (SLaMA) approach described elsewhere in these guidelines.

Commercial software has been developed for the in-plane analysis of perforated masonry frames. One example is shown in Figure C8.90.

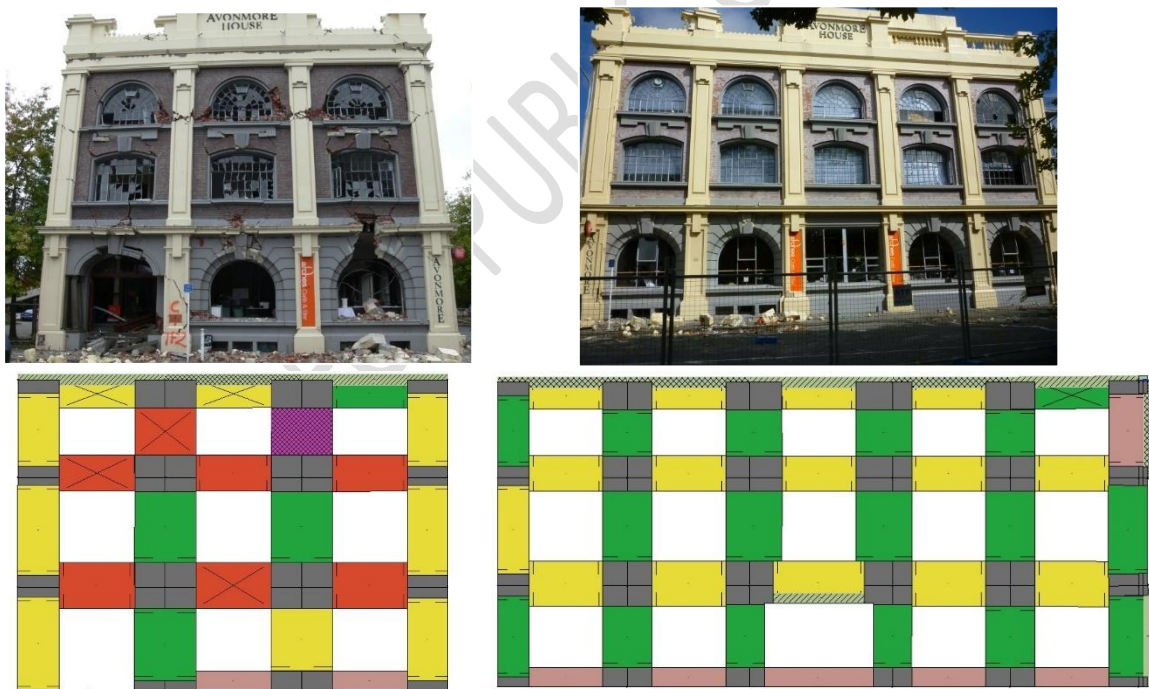


Figure C8.90: Equivalent frame software output (Marino et al. 2019)

C8.8.7 Other items of a secondary nature

Items of a secondary nature such as canopies and architectural features should be assessed for parts and components loads.

C8.9 Assessment of Global Capacity

C8.9.1 General

The global capacity of the building is the strength and deformation capacity of the building taken as a whole, ignoring the performance of secondary elements. For this purpose face-loaded masonry walls are considered to be secondary elements unless the wall is providing primary support to the building or building part; e.g. by cantilever action of the wall. Diaphragms distributing lateral shears between lateral load resisting elements (as opposed to providing support to face-loaded walls) are considered to be primary structure and therefore the capacity of these load paths through diaphragms and through connections from walls to diaphragms needs to be considered when assessing the global capacity.

The global capacity of the building is likely to be significantly influenced by the relative in-plane stiffness of the diaphragms compared with the in-plane lateral stiffness of the masonry walls. Timber and cross-braced steel diaphragms will typically be “flexible” in this sense and this allows simplifications to be made in the assessment of global capacity, as outlined below. Assuming high diaphragm stiffness where this is not assured can lead to erroneous assessment results; e.g. non-conservative assessments of diaphragm accelerations and inaccurate estimates of load distribution between lateral load resisting elements (Oliver, 2010). Flexible diaphragms can be explicitly modelled in 3D analysis models using linear or nonlinear 2D plane stress or shell elements, but care is required and the additional complexity will rarely be warranted for basic buildings. Well-proportioned concrete floor and roof slabs in small buildings may be assumed to be rigid.

Consideration of the nonlinear capacity of masonry members/elements is encouraged as it often leads to a higher global capacity than if the member/element capacities are limited to yield (elastic) levels. Consideration of nonlinear behaviour requires a displacement-based assessment approach. In many situations this is reasonably easy to implement and is recommended for the greater understanding of building seismic behaviour that it often provides.

When more than one lateral load mechanism is present, or when there are elements with varying strengths and stiffness, a displacement-based approach is considered essential to ensure displacement compatibility is achieved and the global capacity is not overstated. This is often the case for masonry buildings, particularly those that have been previously retrofitted with flexible and assumed ductile (low strength) systems.

When assessing the global capacity it will be necessary to complete an analysis of the building structure to assess the relationship between the individual member/element capacities and the global demands. Simple hand methods of analysis are encouraged in preference to overly sophisticated methods which may imply unrealistic transfers in shear between members/elements that will be difficult to achieve in practice and may go unrecognised in the assessment. When sophisticated analyses are used, it is recommended that simpler methods are also used to provide order of magnitude verification.

The objective of global capacity assessment is to find the highest globally applied load/displacement that is consistent with reaching the strength/deformation capacity in the most critical member/element. The recommended approach for URM buildings is described in **Figure C8.91**. The global strength capacity can be referred to in terms of base shear

capacity. The deformation capacity will be the lateral displacement at h_{eff} for the building consistent with the base shear capacity accounting for nonlinear behaviour as appropriate.

This section provides guidance on the assessment of the global capacity for both basic and complex buildings. It also provides guidance on methods of analysis and modelling parameters.

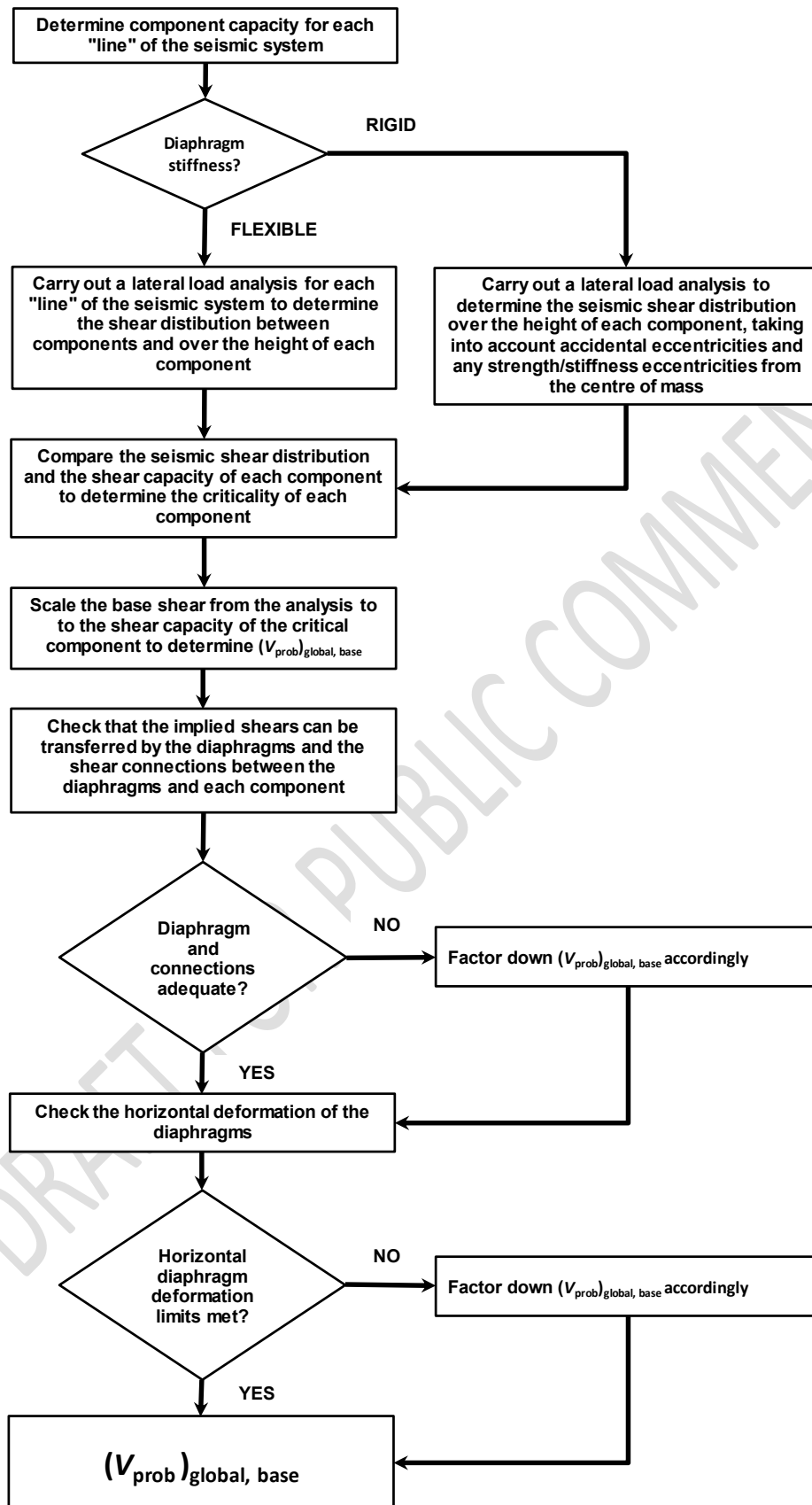


Figure C8.91: Global capacity assessment approach for URM buildings

C8.9.2 Global capacity of basic buildings

Determining the global capacity of basic URM buildings can be a simple exercise. Consider, for example, the single storey buildings shown in Figure C8.92. If the roof diaphragm is flexible the global capacity in each direction will be the lowest element capacity on any system line in that direction when there are only two system lines. When there are more than two system lines then the global capacity in a direction will be the capacity of the line in that direction which has the lowest value of $V_{\text{prob}}/\text{tributary mass}$, where V_{prob} in this context is the sum of the element probable capacities along the particular line of the seismic system.

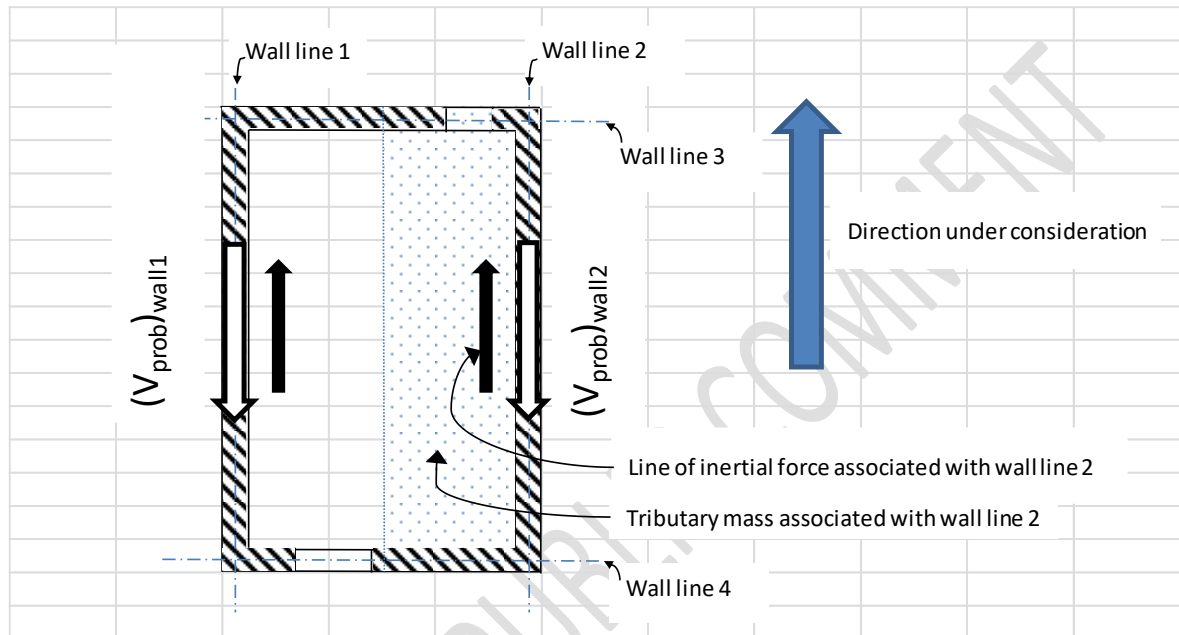


Figure C8.92: Relationship between demand and capacity for a basic building with a flexible diaphragm

For such buildings there would be little to gain from consideration of the nonlinear behaviour of the elements when determining the global capacity. However, an understanding of the nonlinear capability, without jeopardising the vertical load carrying capacity, will provide confidence that the building has resilience. If the demand is to be calculated in accordance with Section C8.10.2.2, nonlinear behaviour is assumed if K_R is greater than 1.

Some small buildings with flexible diaphragms will not have identifiable or effective lateral load paths to provide lateral resistance to all parts of the building. An example of this is the open front commercial building where the sole means of lateral support might be cantilever action of the ends of the side walls, the capacity of which will be highly dependent on the restraint available from the wall foundation, and likely to be negligible.

Basic buildings of two or three storeys with flexible diaphragms can be considered in a similar fashion, after first completing a simple analysis to determine the variation in shear over the height of each line of the seismic system. The global capacity of such buildings will be limited to the capacity of the line where $(V_{\text{prob}})_{\text{line},i}/\beta_i$ is the lowest. $(V_{\text{prob}})_{\text{line},i}$ is the sum of the element capacities along a line of the seismic system at level i and β_i is the ratio of the applied shear at level i to the shear at the base of the line under consideration. For most basic buildings β_i will be the same for all lines of the seismic system.

The presence of rigid diaphragms in basic buildings introduces an additional level of complexity into the building analysis. However, this analysis can still be kept quite simple for many buildings.

For buildings with rigid diaphragms it will be necessary to consider the effect of the demand and resistance eccentricities (accidental displacement of the seismic floor mass and the location of the centre of stiffness or strength as appropriate). Refer to **Figure C8.93**. If the lines of the seismic system in the direction being considered have some nonlinear capability it is considered acceptable to resist the torque resulting from the eccentricities solely by the couple available from the lines of the seismic system perpendicular to the direction of loading. This will lead to a higher global capacity in many buildings than would otherwise be the case. If this approach is to be followed it would be more appropriate to consider the centre of strength rather than the centre of stiffness when evaluating the eccentricities.

NZS 1170.5:2004 requires that buildings not incorporating capacity design are subjected to a lateral action set comprising 100% of the specified earthquake actions in one direction plus 30% of the specified earthquake actions in the orthogonal direction. The 30% actions perpendicular to the direction under consideration are not shown in **Figure C8.93** for clarity and, suitably distributed, would need to be added to the shears to be checked for the perpendicular walls. These are unlikely to be critical for basic buildings. If the diaphragm is flexible, concurrency of the lateral actions should be ignored.

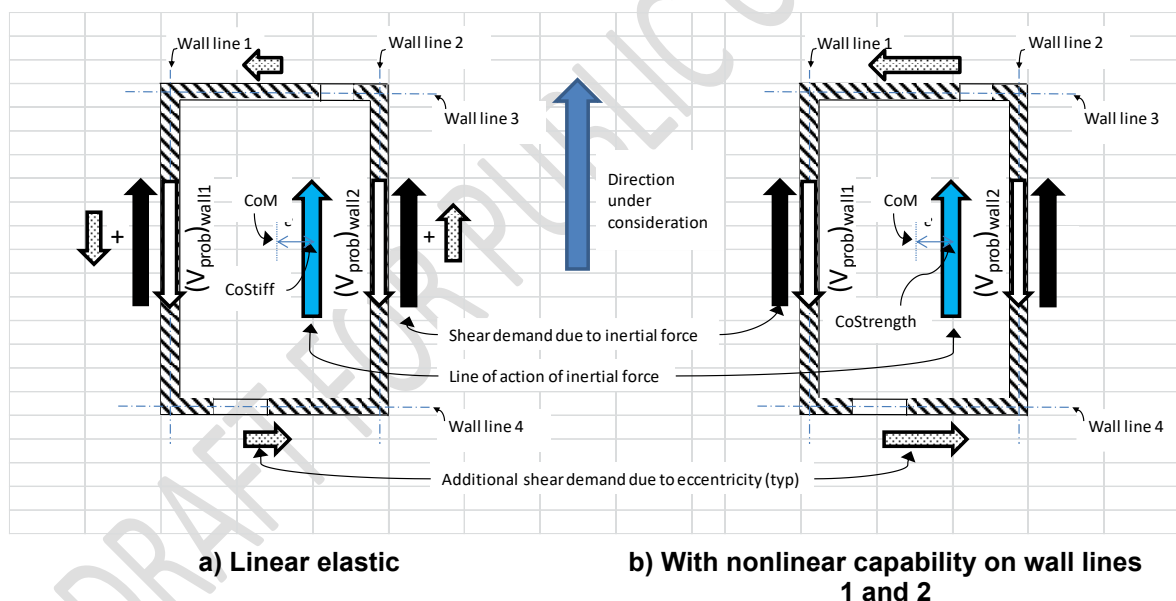


Figure C8.93: Relationship between demand and capacity for a basic building with rigid diaphragms

In the above discussion it has been assumed that the diaphragms are stiff enough to provide the required support to the face-loaded walls orientated perpendicular to the direction of loading. Diaphragms are considered as primary structural elements for the transfer of these actions and their ability to do so may affect the global capacity of the building in that component direction. Limits have been suggested in Section C8.8.3.2 for the maximum diaphragm deflections to ensure adequate wall support. These limits are likely to be exceeded in flexible diaphragms, even in small basic buildings, and should be checked. If the limits are exceeded, the global capacity of the building in that direction will need to be reduced accordingly.

C8.9.3 Global capacity of complex buildings

Many complex URM buildings will be able to be assessed adapting the recommendations outlined above for basic buildings. However, the assessment of complex buildings will often require a first-principles approach and a good understanding of the past performance of such buildings.

The overall objective discussed in Section C8.9.1 remains. However, the more complex the building the more likely it will be necessary to utilise more complicated analysis techniques simply to keep track of element actions and applied inertial forces. It is recommended that simple techniques be used in all cases to identify the primary load paths and to verify the order of magnitude of the outputs.

Use of linear-elastic analysis techniques and limiting member/element capacities to elastic behaviour may significantly underestimate the global capacity of complex buildings. However, nonlinear considerations can completely alter the mechanisms that can occur.

Aspects that are likely to require specific consideration in the assessment of complex buildings include:

- foundation stiffness
- diaphragm stiffness
- nonlinear behaviour of multi-storey, penetrated walls and development of sway mechanisms
- potential soft storeys
- non-horizontal diaphragms.

C8.9.4 Global analysis

C8.9.4.1 Selection of analysis methods

Four analysis methods are generally considered:

- equivalent static analysis (linear static)
- modal response analysis (linear dynamic)
- nonlinear pushover (nonlinear static)
- nonlinear time history (nonlinear dynamic).

Linear analysis techniques supplemented with simple nonlinear techniques (e.g. adapted SLAMA) are likely to be appropriate for all but the most complex of New Zealand's URM buildings.

Nonlinear analysis techniques are appropriate for buildings which contain irregularities and when higher levels of nonlinear behaviour are anticipated. If nonlinear pushover analysis procedures are used, include appropriate allowances in the analysis for anticipated cyclic strength and stiffness degradation.

Nonlinear time history analyses can be used to analyse most URM buildings. They are able to account explicitly for cyclic strength and stiffness degradation. These analyses are complex. They should not be undertaken lightly and then only by those that have experience in the processes involved. A full appreciation of the reliability of the input parameters and

the likely sensitivity of the outputs to these is required. Refer to relevant references for nonlinear acceptance criteria.

Note:

Nonlinear modelling of URM walls is feasible, but experience to date suggests that analytical results will not always provide reliable estimates of performance because of the variability in actual material strength and condition. Any analytical modelling should include several analyses to test sensitivity to material variation, modelling method and earthquake motion.

Special care is required with the application of damping, especially when considering a mix of low and high period modes. The resulting force reduction from damping for the mode considered should be investigated by a special study for finite element analysis. For assessing URM buildings, Caughey damping rather than Raleigh damping should be considered.

C8.9.4.2 Mathematical modelling

Mathematical models used for linear analysis techniques should include the elastic, uncracked in-plane stiffness of the primary lateral load resisting elements. Consider both shear and flexural deformations.

If using nonlinear analysis techniques, the mathematical model should directly incorporate the nonlinear load-deformation characteristics of individual in-plane elements (i.e. backbone curves). Include cyclic degradation of strength and stiffness in the member modelling when appropriate. Recommended nonlinear analysis parameters for non-brittle URM failure modes are given in Section C8.8.6.2.

C8.9.4.3 Fundamental period

The mass of URM buildings is normally dominated by the mass of the masonry. However, stiffness will depend on the relative flexibility of the walls, the floor diaphragms and the ground (foundation rotation). While the period of these structures can be quite difficult to calculate with precision and there are several modes of vibration to consider, it will often fall within the plateau section of the spectra, so precision is not required. For larger buildings (tall or long), especially those with long flexible diaphragms, special consideration of these effects may be required.

In the case of large buildings, it may not be sufficient to consider all parts of the building loaded at the same time and having the same time period. Commonly used methods include sub-structuring: i.e. subdividing the structure into sections, each including its elements and all mass tributary to it. Each section is then analysed separately and checked for compatibility with neighbouring sections along the margins between the sections. These sections should typically be no more than one third of the building width or more than 30 m.

Note:

The effective period of individual sections of URM buildings will often still be short and, if this is the case, this final step will not be required.

C8.9.4.4 Seismic mass

URM buildings are essentially systems with mass distributed over the height, with barely 10-20% of the seismic mass contributed by floors and roof. This is especially the case for buildings with timber floors and lightweight roofs. In this context, the concept of a lumped mass system is problematic. However, unless a more sophisticated analysis has been undertaken to capture the effect of distributed mass systems, an assessment based on masses lumped at diaphragm levels is acceptable as loads from the face-loaded walls would be transferred to the in-plane walls through the diaphragm.

However, for shear checks at the base of the in-plane walls and piers of any storey, the seismic demand should include accumulated floor level forces from the upper storeys and the seismic force due to the total mass of the in-plane wall above the level being considered. This is in contrast to assessments of concrete construction, where the mass of the lower half of the bottom storey is ignored when estimating the active mass for the base shear.

C8.9.4.5 Stiffness of URM walls and wall piers subject to in-plane actions

The stiffness of in-plane URM walls subjected to seismic loads should be determined considering flexural, shear and axial deformations. The masonry should be considered to be a homogeneous material for stiffness computations with an expected elastic modulus in compression, E_m , as discussed in earlier sections.

For elastic analysis, the stiffness of an in-plane URM wall and pier should be considered to be linear and proportional with the geometrical properties of the un-cracked section, excluding any wythe that does not meet the criteria given in Section C8.2.4.3.

Laboratory tests of solid shear walls have shown that behaviour can be depicted at low force levels using conventional principles of mechanics for homogeneous materials. In such cases, the lateral in-plane stiffness of a solid cantilevered wall, k , can be calculated using Equation C8.50:

$$k = \frac{1}{\frac{h_{\text{eff}}^3}{3E_m I_g} + \frac{h_{\text{eff}}}{A_{n,\text{wall}} G_m}} \quad \dots \text{C8.50}$$

where:

h_{eff}	=	wall height, mm
$A_{n,\text{wall}}$	=	net plan area of masonry wall, mm ²
I_g	=	moment of inertia for the gross section representing uncracked behaviour, mm ⁴
E_m	=	masonry elastic modulus, MPa
G_m	=	masonry shear modulus, MPa.

The lateral in-plane stiffness of a pier between openings with full restraint against rotation at its top and bottom can be calculated using Equation C8.51:

$$k = \frac{1}{\frac{h_{\text{eff}}^3}{12E_m I_g} + \frac{h_{\text{eff}}}{A_{n,\text{wall}} G_m}} \quad \dots \text{C8.51}$$

Note that a completely fixed condition is often not present in actual buildings. Equation C8.51 could be used to estimate spandrel stiffness.

C8.10 Assessment of Earthquake Force and Displacement Demands

C8.10.1 General

This section sets out the procedures for estimating both force and displacement demands on URM buildings and their parts.

Section C3 describes how the earthquake demands are to be assessed.

For the purposes of defining seismic demands, the structural system which carries seismic load and provides lateral resistance to the global building should be considered the primary seismic resisting system (primary structure). The members/elements which do not participate in the overall lateral resistance of the structure and which rely on the primary structure for strength and/or stability should be assumed to be parts and components. Parts and components need to be assessed for any imposed deformations from the primary seismic resisting system.

Therefore all in-plane walls and diaphragms are classified as primary lateral structure. Everything else, such as face-loaded walls and parapets, and ornamentation, are considered to be secondary structure, and where appropriate, critical non-structural items.

C8.10.2 Primary lateral structure

C8.10.2.1 General

Determine the horizontal demands on the primary lateral structure, in accordance with Section C3 taking $\mu = 1$, $S_p = 1$ and $\xi_{sys} = 15\%$. Although μ is set at 1 it is intended that the benefits of any nonlinear deformations from the assessment of the capacity are also taken.

Note:

The use of 15% damping accounts for a number of factors including low likelihood of resonance between elements in a building or the building as a whole, and additional damping from flexible diaphragms, radiation damping and localised damage. Where these phenomena are not present in a mechanism, lower levels of damping may need to be considered. For example, the monument shown in Table C8.1 (“monumental - single form”), when the base width is small compared with the height, is likely to exhibit clear single-degree-of-freedom rocking with minimal interference by other mechanisms and so lower levels of damping values, even less than 5%, may need to be considered.

It should be noted that if building response is likely to be governed by diagonal tension failure, damping should be limited to 5%, unless capacity of those wall or pier is ignored from total capacity, but consequences of loss of gravity load support from these walls/piers does not cause instability to any of the structure above.

When required, a triangular distribution of earthquake load demands over the height of the structure may be assumed, without allowance for additional demand at the top of the structure.

Note:

The additional force required to be distributed to the top of the structure using the equivalent static horizontal force distribution determined from NZS 1170.5:2004 is considered to be too conservative for stiff URM buildings where higher mode effects are likely to be insignificant.

C8.10.2.2 Basic buildings

For basic buildings, as defined in Section C8.2.2, a force-based assessment of in-plane demands for walls/piers and spandrels, for each line of resistance, may be determined using a horizontal demand seismic coefficient, $C(T_1)$, given by Equation C8.52 where a load reduction factor, K_R , has been used in lieu of the ratio of the structural performance factor and structural ductility factor given in NZS 1170.5:2004.

$$C(T_1) = C_h(T_1) Z R_u N(T_1, D) / K_R \quad \dots \text{C8.52}$$

where:

$C_h(T_1)$ = the spectral shape factor determined from Clause 3.1.2, NZS 1170.5:2004 for the first mode period of the walls/piers making up the line of resistance, T_1 , g .

Lines of resistance in basic buildings will typically have a short period, within the plateau region of the spectral shape factor plot, which means the calculation of the period can often be avoided.

Z = the hazard factor determined from Clause 3.1.4, NZS 1170.5:2004

R_u = the return period factor, R_u determined from Clause 3.1.5, NZS 1170.5:2004

$N(T_1, D)$ = the near fault factor determined from Clause 3.1.6, NZS 1170.5:2004

K_R = the seismic force reduction factor determined from Table C8.15 for each line of resistance.

Note:

The horizontal design coefficient for basic buildings from Equation C8.53 is based on the damping allowance of 5% defined by NZS 1170.5:2004 rather than the general allowance of 15% given in Section C8.10.2.1. This is because the performance enhancement effects that justify the use of the higher damping in the general case are allowed for separately and explicitly in the K_R factor.

As a defined characteristic of basic buildings is flexible diaphragms each line of resistance can be individually assessed, ignoring (where reasonable) the stiffness or failure modes of an adjacent line.

Table C8.15: Recommended force reduction factors for linear static method

Seismic performance/controlling parameters	Force reduction factor, K_R	Notes
Pier rocking, bed-joint sliding, stair-step failure modes	3	Failure dominated by strong brick-weak mortar
Pier toe failure modes	1.5	
Pier diagonal tension failure modes (dominated by brick splitting)	1.0	Failure dominated by weak brick-strong mortar
Spandrel failure modes	1.0	The spandrels need not be assessed as outlined below.

Note:

The concept of a ductility factor (deflection at ultimate load divided by the elastic deflection) can be meaningless for most URM buildings. The introduction of K_R primarily reflects an increase in the damping available and therefore reduced elastic response rather than ductile capability assessed by traditional means. Therefore the displacements calculated from the application of $C(T_1)$ are the expected displacements and should not be further modified by K_R .

These force reduction factors apply in addition to relief from period shift (if any).

Redistribution of seismic demands between individual elements of up to 50% within a line of resistance is permitted when $K_R = 3.0$ applies, provided that the effects of redistribution are accounted for in the analysis.

Engineering judgement should be used when an element's mechanisms are close in capacity as to the consequence of the assessment being inaccurate: if diagonal tension failure were to occur and cause either a significant reduction in capacity for the building, or cause a loss of gravity support to an area of the building, the more conservative $K_R = 1.0$ should be adopted. The designer must keep in mind the highly variable nature of the material and the approximations made in the estimates of material strengths.

When there are mixed behaviour modes among the walls/piers in a line of resistance, the engineer must take the mechanism with the lowest K_R factor to define the K_R factor for that line as a whole. Alternatively, the capacity of any piers for which K_R is less than the value that has been adopted for the line of resistance can be ignored; but only if the consequences of loss of gravity load support from these walls/piers does not cause instability to any of the structure above.

If there are mixed failure modes among the walls and piers in a line of resistance, the displacement compatibility between these piers and walls should be evaluated.

For the case of perforated walls when a strong pier – weak spandrel mechanism governs the wall behaviour $K_R = 1.0$ shall be adopted for the wall line as a whole and the capacity of the line of resistance is governed by the spandrel capacity. Alternatively, the capacities of the spandrels can be ignored and the higher K_R factors detailed in Table C8.15 used for the remaining (taller) simple rocking pier members provided the consequences of loss/collapse of the ignored spandrels are considered. When a weak pier-strong spandrel mechanism governs, a “pier only” analysis can be used and the higher than unity K_R factor given in Table C8.15 can be adopted.

C8.10.3 Secondary and critical non-structural items

Refer to Section 8 of NZS 1170.5:2004 for determination of seismic demands on secondary and critical non-structural items.

For face-loaded walls, assessed using the forced-based or displacement-based method in Section C8.8.5, the demands are included within the method. Note that for the displacement-based approach, the Part Spectral Shape Coefficient, $C_i(T_p)$, defined in NZS 1170.5:2004 has been replaced with a formulation that better converts into a displacement spectrum for this purpose.

C8.10.4 Vertical demands

Vertical ground motions in close proximity to earthquake sources can be substantial. However, opinion is divided on how significant vertical accelerations are on the performance of URM buildings.

While vertical ground accelerations could potentially reduce the gravity and compression forces in the walls, reducing their stability and reducing the pull-out strength of ties installed to restrain them back to the diaphragms, there is evidence to suggest that there is typically a time delay between the maximum vertical accelerations and the maximum horizontal accelerations, meaning that they are unlikely act together at full intensity.

In advance of further investigations on this subject, it is considered reasonable to ignore vertical accelerations when assessing the stability of masonry walls and the capacity of embedded anchors.

When vertical accelerations are considered the demands may be determined from NZS 1170.5:2004.

C8.10.5 Flexible diaphragms

C8.10.5.1 General

Masonry walls loaded in-plane are typically relatively rigid structural elements. Consequently, the dominant mode of response for buildings containing flexible diaphragms is likely to be the response of the diaphragms themselves, due to inertial forces from diaphragm self-weight and the connected URM boundary walls responding out-of-plane.

Note:

Flexible diaphragms in the context of URM buildings and these guidelines are those constructed of timber or which are steel braced.

Concrete diaphragms can be assumed to be rigid. A concrete diaphragm with large penetrations could be relatively flexible compared with the supporting walls. ASCE 41-13 (2014) provides a procedure for checking the relative stiffness should this be of concern.

Seismic demands on flexible diaphragms in URM buildings which are braced by URM walls should, therefore, be based on the period of the diaphragm and a horizontal seismic coefficient assuming that the diaphragm is supported at ground level (i.e. no amplification

to reflect its height in the building). The seismic coefficient to be used is therefore $C(T)$ from NZS 1170.5:2004, where T is the first horizontal mode period of the diaphragm. If the diaphragm is able to behave in a ductile fashion (e.g. steel bracing with connection capacities exceeding the overstrength capacity of the brace) μ of up to 3 may be assumed. Otherwise, μ should be taken as 1. The value of S_p should be in accordance with the ductile capability of the diaphragm.

If the diaphragm is braced by flexible lateral load resisting elements (i.e. non-URM or short URM walls), the seismic demands can be determined using a seismic coefficient equal to F_i/m_i , with a lower limit of $C(0)$ where F_i is the equivalent static horizontal force determined from NZS 1170.5:2004 at the level of the diaphragm (assuming 5% damping) and m_i is the seismic mass at that level. This is the pseudo-Equivalent Static Analysis (pESA) method outlined in Section C2.

C8.10.5.2 Timber diaphragms

The diaphragm in-plane mid-span lateral displacement demand, Δ_d , is given by Equation C8.53.

$$\Delta_d \text{ (m)} = \frac{3}{16} \frac{C(T_d)W_{\text{trib}}L}{BG'_{d,\text{eff}}} \quad \dots\text{C8.53}$$

where:

- $C(T_d)$ = seismic coefficient at required height for period, T_d , determined in accordance with Section C8.10.5.1
- W_{trib} = uniformly distributed tributary weight, kN
- L = span of diaphragm, m
- B = depth of diaphragm, m
- $G'_{d,\text{eff}}$ = effective shear stiffness of diaphragm, refer to Equation C8.55, kN/m
- T_d = lateral first mode period of the diaphragm determined in accordance with Equation C8.55, sec.

The period, T_d , of a timber diaphragm, based on the deformation profile of a shear beam excited in an approximately parabolic distribution, is given by Equation C8.54 (Wilson et al., 2013c).

$$T_d \text{ (sec)} = 0.7 \times \sqrt{\frac{W_{\text{trib}}L}{G'_{d,\text{eff}}B}} \quad \dots\text{C8.54}$$

where:

- W_{trib} = total tributary weight acting on the diaphragm, being the sum of the weight of the tributary face-loaded walls both half-storey below and above the diaphragm being considered (i.e. the product of the tributary height, thickness and density of the out-of-plane URM walls tributary to the diaphragm accounting for wall penetrations) and diaphragm self-weight plus live load ($\psi_E \times Q_i$ as per NZS 1170.5:2004 Section 4.2).

Other terms are as defined for Equation C8.53.

0.7 has units of $1/\sqrt{g}$.

C8.10.6 Rigid diaphragms

Rigid diaphragms are primary structure and the demands are determined in accordance with NZS 1170.5:2004 as outlined in Section C8.10.2. If required, floor acceleration demands should be assessed as indicated in Section C8.10.5.1 however, damping should be limited to 5% for flexible diaphragms supported by flexible lateral load resisting systems.

C8.10.7 Connections providing support to face-loaded walls

The demands on connections providing support to face-loaded masonry walls shall be calculated in accordance with Steps 12, 13 and 14 in Section C8.8.5.2.

Assume that the demand is uniformly distributed across all anchorages located at the specific wall-diaphragm interface. Repeat the exercise for the orthogonal loading direction, reversing loading regimes for a given anchorage.

C8.10.8 Connections transferring diaphragm shear loads

Wall-diaphragm connections required to transfer shears from diaphragms to walls (loaded in-plane) should be considered to be primary structure and therefore the demands are evaluated in accordance with Section C8.10.2. The demand may be assumed to be uniformly distributed along the wall to diaphragm connection.

Unless capacity design principles are applied, the demands should be assessed assuming $\mu = S_p = 1$.

C8.11 Assessment of %NBS

The assessment of the %NBS earthquake rating for the building should be in accordance with Section C1.

C8.12 Improving Seismic Performance of URM Buildings

The overarching problem is that New Zealand's URM building stock is simply not designed for earthquake loads and lacks a basic degree of connection between structural elements to allow all parts of the building to act together (Goodwin et al., 2011).

The basic approach to improving the seismic performance of URM buildings is to:

- secure all unrestrained parts that represent falling hazards to the public (e.g. chimneys, parapets and ornaments)
- improve the wall-diaphragm connections or provide alternative load paths; improve the diaphragm; and improve the performance of the face-loaded walls (gables, facades and other walls) by improving the configuration of the building and in-plane walls
- strengthen specific structural elements, and
- consider adding new structural components to provide extra support for the building.

When developing strengthening options, note that differing levels of seismic hazard will mean that a solution advised in a high seismic area could be too conservative in a low seismic area. Also note that even though a building may have more than 34% *NBS* seismic capacity, if that is limited by a brittle mode of failure and/or the failure mode could trigger a sequence of failure of other elements, the risk of failure of the limiting element should be carefully assessed and mitigated.

C8.13 References

ABK Consultants (1981). A Joint Venture, Methodology for mitigation of seismic hazards in existing unreinforced masonry buildings: wall testing, out-of-plane, El Segundo, Calif., ABK-TR-04, 1981.

Almesfer, N., Dizhur, D., Lumantarna, R. and Ingham, J.M. (2014). *Material properties of existing unreinforced clay brick masonry buildings in New Zealand*, Bulletin of the New Zealand Society for Earthquake Engineering, Vol. 47, No. 2, 75-96, June 2014.

Anthoine, A. (1995). Derivation of the in-plane elastic characteristics of masonry through homogenization theory, International Journal of Solids and Structures, Vol. 32, 137-163.

AS 3700:2011. Masonry structures, Standard Australia, Sydney, Australia.

ASCE 41-13 (2014). *Seismic evaluation of existing buildings*, American Society of Civil Engineers, and Structural Engineering Institute, Reston, Virginia, USA.

ASCE 41-23 (2023). *Seismic evaluation and retrofit of existing buildings*. American Society of Civil Engineers, and Structural Engineering Institute, Reston, Virginia, USA.

ASTM (2003). *Standard test methods for strength of anchors in concrete and masonry elements*, E 488-96. ASTM International, Pennsylvania, USA.

ASTM (2003a). *Standard test methods for sampling and testing brick and structural clay tile*, C 67-03a. ASTM International, Pennsylvania, USA.

ASTM (2003b). *Standard test methods for in situ measurement of masonry mortar joint shear strength index*, C 1531-03. ASTM International, Pennsylvania, USA.

ASTM (2003c). *Standard test method for compressive strength of masonry prisms*, C 1314-03b. ASTM International, Pennsylvania, United States.

ASTM (2004). *Standard test method for in situ measurement of masonry deformability properties using the flatjack method*, C 1197-04, ASTM International, Pennsylvania, United States.

ASTM (2008). *Standard test method for compressive strength of hydraulic cement mortars (using 2-in. or [50 mm] cube specimens)*, C 109/C 109M-08, ASTM International, Pennsylvania, United States.

Beyer, K. (2012). *Peak and residual strengths of brick masonry spandrels*, Engineering Structures, Vol. 41, 533-547, August 2012.

Beyer, K. (2014). Personal communication, July 2014.

Beyer, K. and Dazio, A. (2012a). *Quasi-static monotonic and cyclic tests on composite spandrels*, Earthquake Spectra, Vol. 28, No. 3, 885-906.

Beyer, K. and Dazio, A. (2012b). *Quasi-static cyclic tests on masonry spandrels*, Earthquake Spectra, Vol. 28, No.3, 907-929.

Beyer, K. and Mangalathu, S. (2014). *Numerical study on the force-deformation behaviour of masonry spandrels with arches*, Journal of Earthquake Engineering, Vol. 18, No. 2, 169-186.

Blaikie, E.L. (1999). *Methodology for the assessment of face-loaded unreinforced masonry walls under seismic loading*, Opus International Consultants, Wellington, NZ.

Blaikie, E.L. (2001). *Methodology for the assessment of face-loaded unreinforced masonry walls under seismic loading*, EQC funded research by Opus International Consultants, under Project 99/422.

Blaikie, E.L. (2002). *Methodology for assessing the seismic performance of unreinforced masonry single storey walls, parapets and free standing walls*, Opus International Consultants, Wellington, NZ.

Blaikie, E.L. and Spurr, D.D. (1993). *Earthquake vulnerability of existing unreinforced masonry buildings*, EQC.

- Bothara, J.K. and Hiçyılmaz, K. (2008). *General observations of the building behaviour during the 8th October 2005 Pakistan earthquake*, Bulletin of the New Zealand Society for Earthquake Engineering, Vol. 41, No. 4.
- Bothara, J.K., Dhakal, R.P. and Mander, J.B. (2010). *Seismic performance of an unreinforced masonry building: An experimental investigation*, Earthquake Engineering and Structural Dynamics, Vol. 39, Issue 1, pages 45–68, January 2010.
- Bruneau, M. and Paquette, J. (2004). *Testing of full-scale single storey unreinforced masonry building subjected to simulated earthquake excitations*, SÍSMICA 2004 - 6^o Congresso Nacional de Sismologia e Engenharia Sísmica.
- BS EN 1052-3:2002, BSI (2002). *Methods of test for masonry. Determination of initial shear strength*. British Standards Institution, United Kingdom.
- Campbell, J., Dizhur, D., Hodgson, M., Fergusson, G. and Ingham, J.M. (2012). *Test results for extracted wall-diaphragm anchors from Christchurch unreinforced masonry buildings*, Journal of the Structural Engineering Society New Zealand (SESOC), Vol. 25, Issue 1, 57-67.
- Cassol, D., Ingham, J., Dizhur, D., & Giongo, I. (2025a). *Analytical formulation describing the behaviour of URM walls seismically strengthened using timber strong-backs*. Engineering Structures, Vol. 324, 119343.
- Cassol, D., Ingham, J., & Giongo, I. (2025b). *Seismic out-of-plane repair and strengthening of masonry infill walls using timber strong-backs*. Structures, Vol. 71, 107990.
- Cassol, D., Giongo, I., Ingham, J., & Dizhur, D. (2021). *Seismic out-of-plane retrofit of URM walls using timber strong-backs*. Construction and Building Materials, Vol. 269, 121237.
- Cattari, S., Beyer, K. and Lagomarsino, S. (2014). Personal communication, November 2014.
- Cole, G.L., Dhakal, R.P. and Turner, F.M. (2012). *Building pounding damage observed in the 2011 Christchurch earthquake*. Earthquake Engineering and Structural Dynamics, Vol. 41, 893-913.
- Costley, A.C. and Abrams, S.P. (1996). *Dynamic response of unreinforced masonry buildings with flexible diaphragm*, Technical Report NCEER-96-0001, State University of New York at Buffalo, Buffalo, U.S.A.
- Derakhshan, H., Dizhur, D.Y., Griffith, M.C. and Ingham, J.M. (2014a). *Seismic assessment of out-of-plane loaded unreinforced masonry walls in multi-storey buildings*, Bulletin of the New Zealand Society for Earthquake Engineering, Vol. 47, No. 2, 119-138. June 2014.
- Derakhshan, H., Dizhur, D.Y., Griffith, M.C. and Ingham, J.M. (2014b). *In-situ out-of-plane testing of as-built and retrofitted unreinforced masonry walls*, ASCE Journal of Structural Engineering, 140, 6, 04014022. [http://dx.doi.org/10.1061/\(ASCE\)ST.1943-541X.0000960](http://dx.doi.org/10.1061/(ASCE)ST.1943-541X.0000960).
- Derakhshan, H., Griffith, M.C. and Ingham, J.M. (2013a). *Out-of-plane behaviour of one-way spanning URM walls*, ASCE Journal of Engineering Mechanics, 139, 4, 409-417. [http://dx.doi.org/10.1061/\(ASCE\)EM.1943-7889.0000347](http://dx.doi.org/10.1061/(ASCE)EM.1943-7889.0000347).
- Derakhshan, H., Griffith, M.C. and Ingham, J.M. (2013b). *Airbag testing of unreinforced masonry walls subjected to one-way bending*, Engineering Structures, 57, 12, 512-522. <http://dx.doi.org/10.1016/j.engstruct.2013.10.006>.
- Dizhur, D., Campbell, J., Schultz, A. and Ingham, J.M. (2013). *Observations from the 2010/2011 Canterbury earthquakes and subsequent experimental pull-out test program of wall-to-diaphragm adhesive anchor connections*, Journal of the Structural Engineering Society of New Zealand, 26(1), April, 11-20.
- Dizhur, D., Ingham, J.M., Moon, L., Griffith, M., Schultz, A., Senaldi, I., Magenes, G., Dickie, J., Lissel, S., Centeno, J., Ventura, C., Leiti, J. and Lourenco, P. (2011). *Performance of masonry buildings and churches in the 22 February 2011 Christchurch earthquake*, Bulletin of the New Zealand Society for Earthquake Engineering, 44, 4, Dec., 279-297.
- Dolce, M. (1989). *Models for in-plane loading of masonry walls*, Corso sul consolidamento degli edifici in muratura in zona sismica, Ordine degli Ingegneri, Potenza (in Italian).
- Drysdale, R.G. and Essawy, A.S. (1988). *Out-of-plane bending of concrete block walls*, Journal of Structural Engineering, ASCE, Vol. 114, No. 1, 121-133, Jan. 1988.
- Fattal, S.G. and Gattaneo, L.E. (1976). *Structural performance of masonry walls under compression and flexure*, National Bureau of Standards, Washington, DC.
- FEMA 306 (1998). *Evaluation of earthquake damaged concrete and masonry wall buildings*, Federal Emergency Management Agency, FEMA Report 306, Washington, DC.
- FEMA 454 (2006). *Risk management series: Designing for earthquakes - a manual for architects*, Federal Emergency Management Agency, FEMA Report 454, Washington, DC.
- FEMA P-750 (2009). : *NEHRP recommended seismic provisions for new buildings and other structures*, Federal Emergency Management Agency, FEMA Report P-750, Washington, DC.

- Foss, M. (2001). *Diagonal tension in unreinforced masonry assemblages*, MAEC ST-11: Large Scale Test of Low Rise Building System, Georgia Institute of Technology.
- Franklin, S., Lynch, J. and Abrams, D.P. (2001). *Performance of rehabilitated URM shear walls: Flexural behaviour of piers*, Department of Civil Engineering, University of Illinois at Urbana-Champaign Urbana, Illinois.
- Galvez, F., Abeling, S. R., Ip, K., Giovinnazzi, S., Dizhur, D., & Ingham, J. M. (2018, February). *Using the Macroelement Method to Seismically Assess Complex URM Buildings*. 10th Australian Masonry Conference.
- Galvez, F., Sorrentino, L., Dizhur, D., Ingham, J. M. (2022). *Seismic rocking simulation of unreinforced masonry parapets and façades using the discrete element method*. Earthquake Engineering and Structural Dynamics, Vol. 51, 1840–1856.
- Giaireton, M., Dizhur, D., da Porto, F., and Ingham, J. (2016). *Construction details and observed earthquake performance of Unreinforced Clay Brick Masonry Cavity-walls*. Structures Vol. 6, 159-169.
- Giongo, I., Dizhur, D.Y., Tomasi, R. and Ingham, J.M. (2013). *In-plane assessment of existing timber diaphragms in URM buildings via quasi-static and dynamic in-situ tests*, Advanced Materials Research, 778, 495-502. <http://dx.doi.org/10.4028/www.scientific.net/AMR.778.495>.
- Giongo, I., Wilson, A., Dizhur, D.Y., Derakhshan, H., Tomasi, R., Griffith, M.C., Quenneville, P. and Ingham, J. (2014). *Detailed seismic assessment and improvement procedure for vintage flexible timber diaphragms*, Bulletin of the New Zealand Society for Earthquake Engineering, Vol. 47, No. 2, 97-118, June 2014.
- Goodwin, C., Tonks, G. and Ingham, J. (2011). *Retrofit techniques for seismic improvement of URM buildings*, Journal of the Structural Engineering Society New Zealand Inc., Vol. 24 No. 1, 30-45.
- Graziotti, F., Magenes, G. and Penna, A. (2012). *Experimental behaviour of stone masonry spandrels*, Proceedings of the 15th World Conference for Earthquake Engineering, Lisbon, Portugal, Paper No. 3261.
- Graziotti, F., Penna, A. and Magenes, G. (2014). *Influence of timber lintels on the cyclic behaviour of stone masonry spandrels*, 2014 International Masonry Conference, Guimarães, Portugal.
- Gregorczyk, P. and Lourenço, P. (2000). *A review on flat-jack testing*, Universidade do Minho, Departamento de Engenharia Civil Azurém, P – 4800-058 Guimarães, Portugal.
- Griffith, M.C., Vaculik, J., Lam, N.T.K., Wilson, J. and Lumantarna, E. (2007). *Cyclic testing of unreinforced masonry walls in two-way bending*. Earthquake Engineering and Structural Dynamics, 36(6), 801-821.
- Haseltine, B.A., West, H.W.H. and Tutt, J.N. (1977). *Design of walls to resist lateral loads*, The Structural Engineers, Vol. 55, No. 10, 422-30.
- Hendry, A.W. (1973). *The lateral strength of unreinforced brickwork*, Structural Engineers, Vol. 52, No. 2, 43-50.
- Hendry, A.W. (1981). *Structural brickwork*, Macmillian Press, Hong Kong.
- ICBO (2000). *Guidelines for seismic evaluation and rehabilitation of tilt-up buildings and other rigid wall/flexible diaphragm structures*, International Conference of Building Officials.
- Ingham, J.M. and Griffith, M.C. (2011). *The performance of unreinforced masonry buildings in the 2010/2011 Canterbury earthquake swarm*, Report to the Royal Commission of Inquiry into Building Failure Caused by the Canterbury Earthquake. <http://canterbury.royalcommission.govt.nz/documents-by-key/20110920.46>.
- Ismail, N. (2012). *Selected strengthening techniques for the seismic retrofit of unreinforced masonry buildings*, a thesis submitted in partial fulfilment of the requirements for the Degree of Doctor of Philosophy, University of Auckland.
- Kariotis, J.C. (1986). Rule of General Application – Basic Theory, *Earthquake hazard mitigation of unreinforced pre-1933 masonry buildings*, Structural Engineers Association of Southern California, Los Angeles, California.
- Kasai, K., & Maison, B. F. (1997). *Building pounding damage during the 1989 Loma Prieta earthquake*. Engineering structures, Vol. 19, No. 3, 195-207.
- Kitching, N. (1999). *The small scaling modelling of masonry*, Masonry Research, Civil Engineering Division, Cardiff School of Engineering.
- Knox, C.L. (2012). *Assessment of perforated unreinforced masonry walls responding in-plane*, Doctoral dissertation, The University of Auckland, Auckland, NZ, January, 547p. <https://researchspace.auckland.ac.nz/handle/2292/19422>.
- Knox, C. L., Dizhur, D. and Ingham, J. M. (2018). *Two-story perforated URM wall subjected to cyclic in-plane loading*. Journal of Structural Engineering. Vol. 144, No. 5, 04018037.
- La Mendola, L., Papia, M., & Zingone, G. (1995). *Stability of masonry walls subjected to seismic transverse forces*. Journal of Structural Engineering, Vol. 121, No. 11, 1581-1587.

Lam, N.T.K., J.L. Wilson and Hutchinson, G.L. (1995). *Seismic resistance of unreinforced masonry cantilever walls in low seismicity areas*. Bulletin of the New Zealand National Society for Earthquake Engineering 28 (3):179-195.

Lagomarsino, S., & Cattari, S. (2015). *PERPETUATE guidelines for seismic performance-based assessment of cultural heritage masonry structures*. Bulletin of Earthquake Engineering, Vol. 13, 13-47.

Lawrence, S.J. and Marshall, R.J. (1996). *Virtual work approach to design of masonry walls under lateral loading*, Technical Report DRM429, CSIRO Division of Building, Construction and Engineering, Sydney.

Lowndes, W.S. (1994). *Stone masonry*, (3rd ed, p.69), International Textbook Company.

Lumantarna, R., Biggs, D.T. and Ingham, J.M. (2014a). *Compressive, flexural bond and shear bond strengths of in-situ New Zealand unreinforced clay brick masonry constructed using lime mortar between the 1880s and 1940s*, ASCE Journal of Materials in Civil Engineering, 26, 4, 559-566. [http://dx.doi.org/10.1061/\(ASCE\)MT.1943-5533.0000685](http://dx.doi.org/10.1061/(ASCE)MT.1943-5533.0000685).

Lumantarna, R., Biggs, D.T. and Ingham, J.M. (2014b). *Uniaxial compressive strength and stiffness of field extracted and laboratory constructed masonry prisms*, ASCE Journal of Materials in Civil Engineering, 26, 4, 567-575. [http://dx.doi.org/10.1061/\(ASCE\)MT.1943-5533.0000731](http://dx.doi.org/10.1061/(ASCE)MT.1943-5533.0000731).

Magenes, G. (2006). *Masonry building design in seismic areas: Recent experiences and prospects from a European standpoint*, Keynote 9, 1st European Conference on Earthquake Engineering and Engineering Seismology, 3-8 September 2006, Geneva, Switzerland, CDROM.

Magenes, G. and Calvi, G.M. (1995). *Shaking table tests on brick masonry walls*, Proceedings of the 10th European Conference on Earthquake Engineering, Vienna, Austria, Vol. 3, 2419–2424.

Magenes, G. and Calvi, G.M. (1997). *In-plane seismic response of brick masonry walls*, Earthquake Engineering and Structural Dynamics, 26, 1,091-1,112.

Maison, B.F. and Kasai, K. (1992). *Dynamics of pounding when two buildings collide*. Earthquake Engineering and Structural Dynamics, Vol. 21, 771-786.

Marino, S., Cattari, S., Lagomarsino, S., Dizhur, D., & Ingham, J. M. (2019). *Post-earthquake damage simulation of two colonial unreinforced clay brick masonry buildings using the equivalent frame approach*. Structures Vol. 19, 212-226.

Mendola, L.L., Papia, M. and Zingone, G. (1995). *Stability of masonry walls subjected to seismic transverse forces*, Journal of Structural Engineering, New York: ACSE. Vol. 121, No. 11, 1581-1587.

Ministry of Business, Innovation and Employment: Determination 2012/043: *Whether the special provisions for dangerous, earthquake-prone, and insanitary buildings in Subpart 6 of the Building Act that refer to a building can also be applied to part of a building*, www.dbh.govt.nz/UserFiles/File/Building/Determinations/2012/2012-043.pdf.

Moon, F.L. (2004). *Seismic strengthening of low-rise unreinforced masonry structures with flexible diaphragms*, PhD Dissertation, Georgia Institute of Technology, Atlanta, GA.

Moon, F.L., Yi, T., Leon, R.T. and Kahn, L.F. (2006). *Recommendations for seismic evaluation and retrofit of low-rise URM structures*, Journal of Structural Engineering, 132(5), 663-672.

Moon, L., Dizhur, D., Griffith, M. and Ingham, J. (2011). *Performance of unreinforced clay brick masonry buildings during the 22nd February 2011 Christchurch earthquake*, SESOC, Vol. 24 No. 2.

Nederlands Normalisatie Instituut, (2020). "NPR9998:2020: Assessment of structural safety of buildings in case of erection, reconstruction and disapproval – Induced earthquakes – Basis of design, actions and resistances," Netherlands Standardization Institute (NEN), Delft, The Netherlands.

Neill, S.J., Beer, A.S. and Amende, D. (2014). *The Church of Jesus Christ of Latter-Day Saints, New Zealand*, Proceedings of the New Zealand Society for Earthquake Engineering Conference, Auckland, 21-23 March 2014.

Newmark, N.M. (1965). *Effects of earthquakes on dams and embankments*, Geotechnique 15, 139-159.

Noland, J.L., Atkinson, R.H. and Schuller M.P. (1991). *A review of the flat jack method for non-destructive evaluation of civil structures and materials*, The National Science Foundation. Grant No. MSM 9005818.

NZS 1170.5:2004. *Structural design actions, Part 5: Earthquake actions – New Zealand*, Standards New Zealand, Wellington, NZ.

NZSEE (1995). *Draft guidelines for assessing and strengthening earthquake risk buildings*, New Zealand Society for Earthquake Engineering (NZSEE), Wellington, NZ.

NZSEE (2006). *Assessment and improvement of the structural performance of buildings in earthquakes. Incl. Corrigenda 1, 2, 3 and 4*, New Zealand Society for Earthquake Engineering (NZSEE), Wellington, NZ.

- NZSS 1900.8:1965 (1965). *Model building bylaw: Basic design loads*, New Zealand Standards Institute, Wellington, NZ.
- Oliver, S.J. (2010). *A design methodology for the assessment and retrofit of flexible diaphragms in unreinforced masonry buildings*, Journal of the Structural Engineering Society of New Zealand (SESOC), 23(1), 19-49.
- Parivallal, S., Kesavan, K., Ravisankar, K., Arun Sundram, B. and Farvaze Ahmed, A.K. (2011). *Evaluation of in-situ stress in masonry structures by flat jack technique*, Proceedings of the National Seminar & Exhibition on Non-Destructive Evaluation. NDE 2011, December 8-10, 2011 CSIR-Structural Engineering Research Centre, Chennai 600 113.
- Russell, A. (2010). *Characterisation and seismic assessment of unreinforced masonry buildings*, Doctoral dissertation, The University of Auckland, Auckland, New Zealand, 344p. <https://researchspace.auckland.ac.nz/handle/2292/6038>.
- Russell, A.P. and Ingham, J.M. (2010a). *Prevalence of New Zealand's unreinforced masonry buildings*, Bulletin of the New Zealand Society for Earthquake Engineering, Vol. 43, No. 3, 183-202.
- Russell, A.P. and Ingham, J.M. (2010b). *The influence of flanges on the in-plane performance of URM walls in New Zealand buildings*, Proceedings of the 2010 New Zealand Society for Earthquake Engineering Conference, Wellington, New Zealand, March 2010, 1-10.
- Simões, A., Gago, A., Lopes, M. and Bento, R. (2012). *Characterization of old masonry walls: Flat-jack method*, 15th World Conference on Earthquake Engineering (15WCEE) Lisbon, Portugal 24-28 September 2012.
- Sinha, B.P. (1978). *A simplified ultimate load analysis of laterally loaded model orthotropic brickwork panel of low tensile strength*, Structural Engineers, 50B(4), 81-84.
- Tena-Colunga, A. and Abrams, D. (1996). *Seismic behavior of structures with flexible diaphragms*, Journal of Structural Engineering, 122(4), 439-445.
- Tocher, H., Slavin, N., Maduh, U., & Dizhur, D. (2020). *Retrofitted URM cavity walls experimentally validated and a simplified out-of-plane assessment*. SESOC Journal, Vol. 33, No. 2, 29-42.
- Tomazevic, M. (1999). *Earthquake resistant design of masonry buildings*, ISBN 1-86094-066-8, Imperial College Press.
- Turnsek, V. and Čačovič, F. (1970). *Some experimental results on the strength of brick masonry walls*, Proceedings of the 2nd International Brick Masonry Conference, Stoke-on-Trent, 149-156.
- Vaculik, J.J. (2012). *Unreinforced masonry walls subject to out-of-plane seismic actions*, University of Adelaide, School of Civil, Environmental and Mining Engineering, April 2012.
- Valek, J. and Veiga, R. (2005). *Characterisation of mechanical properties of historic mortars - testing of irregular samples*, Ninth international conference on structural studies, repairs and maintenance of heritage architecture, Malta, 22-24 June.
- Vlachakis, G., Vlachaki, E., Lourenço, P. B. (2020). *Learning from failure: Damage and failure of masonry structures, after the 2017 Lesvos earthquake (Greece)*, Engineering Failure Analysis, Vol. 117, 104803.
- West, H.W.H., Hodkinson, H.R. and Haseltine, B.A. (1977). *The resistance of brickwork to lateral loading*, The Structural Engineer, Vol. 55, No. 10, 411-421, Oct 1977.
- Willis, C.R., Griffith, M.C. and Lawrence, S.J. (2004). *Horizontal bending of unreinforced clay brick masonry walls*, Masonry International, 17(3): 109-121.
- Wilson, A., Kelly, P.A., Quenneville, P.J.H. and Ingham, J.M. (2013b). *Nonlinear in-plane deformation mechanics of timber floor diaphragms in unreinforced masonry buildings*, ASCE Journal of Engineering Mechanics, [http://dx.doi.org/10.1061/\(ASCE\)EM.1943-7889.0000694](http://dx.doi.org/10.1061/(ASCE)EM.1943-7889.0000694).
- Wilson, A., Quenneville, P.J.H. and Ingham, J.M. (2013c). *Natural period and seismic idealization of flexible timber diaphragms*, Earthquake Spectra, Vol. 29 No. 3, 1003-1019.
- Wilson, A., Quenneville, P.J.H., Moon, F.L. and Ingham, J.M. (2013a). *Lateral performance of nail connections from century old timber floor diaphragms*, ASCE Journal of Materials in Civil Engineering, [http://dx.doi.org/10.1061/\(ASCE\)MT.1943-5533.0000792](http://dx.doi.org/10.1061/(ASCE)MT.1943-5533.0000792).
- Xu, W. and Abrams, D.P. (1992). *Evaluation of lateral strength and deflection for cracked unreinforced masonry walls*, U.S. Army Research Office, Report ADA 264-160, Triangle Park, North Carolina.
- Yi, T., Moon, F.L., Leon, R.T. and Kahn, L.F. (2008). *Flange effects on the nonlinear behavior of URM piers*, TMS Journal. November 2008.
- Yokel, F.Y. and Dikkers, R.D. (1971). *Strength of load bearing masonry walls*, Journal of the Structural Division, American Society of Civil Engineers, 120(ST 5), 1593-1609.

C8.13.1 Suggested Reading

- Benedetti, D. and Petrini, V. (1996). *Shaking table tests on masonry buildings*, Results and Comments. ISMES, Bergamo.
- Chena, S.-Y., Moona, F.L. and Yib, T. (2008). *A macroelement for the nonlinear analysis of in-plane unreinforced masonry piers*, Engineering Structures, 30 (2008) 2242–2252.
- Clifton, N.C., 2012 (1990). *New Zealand timbers; exotic and indigenous*, GB Books, Wellington, 170p.
- CRGN, 2012. Section 5: *Unreinforced masonry buildings and their performance in earthquakes*, [http://canterbury.royalcommission.govt.nz/vwlresources/final-report-docx-vol-4-s5/\\$file/vol-4-s-5.docx](http://canterbury.royalcommission.govt.nz/vwlresources/final-report-docx-vol-4-s5/$file/vol-4-s-5.docx).
- Curtin, W.G., Shaw, G., Beck, J.K., Bray, W.A. and Easterbrook, D. (1999). *Structural masonry designers' manual*, Blackwell Publishing.
- De Felice, G. and Giannini, R. (2001). *Out-of-plane seismic resistance of masonry walls*. Journal of Earthquake Engineering, 5(2), 253-271.
- Doherty, K., Griffith, M.C., Lam, N. and Wilson, J. (2002). *Displacement-based seismic analysis for out-of-plane bending of unreinforced masonry walls*, Earthquake Engineering and Structural Dynamics, 31(4), 833-850.
- FEMA 356 (2000). *Prestandard and commentary for the seismic rehabilitation of buildings*, Federal Emergency Management Agency, FEMA Report 356, Washington, DC.
- Ghobarah, A. and El Mandooh Galal, K. (2004). *Out-of-plane strengthening of unreinforced masonry walls with openings*, Journal of Composites for Construction, 8(4), 298-305.
- Griffith, M.C., Lawrence, S.J. and Willis, C.R. (2005). *Diagonal bending of unreinforced clay brick masonry*, Masonry International, 18(3): 125-138.
- Griffith, M.C., Magenes, G., Melis, G. and Picchi, L. (2003). *Evaluation of out-of-plane stability of unreinforced masonry walls subjected to seismic excitation*, Journal of Earthquake Engineering, 7(SPEC. 1), 141-169.
- Knox, C.L. (2012). *Assessment of perforated unreinforced masonry walls responding in-plane*, University of Auckland, PhD Thesis, Auckland, NZ.
- Lam, N.T.K., Griffith, M., Wilson, J. and Doherty, K. (2003). *Time-history analysis of URM walls in out-of-plane flexure*, Engineering Structures, 25(6), 743-754.
- Lumantarna, R. (2012). *Material characterisation of New Zealand's clay brick unreinforced masonry buildings*, Doctoral Dissertation, University of Auckland, Department of Civil and Environmental Engineering Identifier: <http://hdl.handle.net/2292/18879>.
- Magenes, G. and Calvi, G.M. (1992). *Cyclic behavior of brick masonry walls*, Tenth World Conference on Earthquake Engineering. 1992. 3517–22.
- Magenes, G., della Fontana, A. (1998). *Simplified nonlinear seismic analysis of masonry buildings*, Proceedings of the Fifth International Masonry Conference. British Masonry Society, London.
- Mann, W. and Müller, H. (1982). *Failure of shear-stressed masonry - an enlarged theory, tests and applications to shear walls*, Proceedings of the British Ceramic Society, No. 30.
- Naeim, F. (ed.) (2001). *The seismic design handbook*, 2nd edition, Springer.
- Najafgholipour, M.A., Maheri, M.R. and Lourenço, P.B. (2012). *Capacity interaction in brick masonry under simultaneous in-plane and out-of-plane loads*, Construction and Building Materials. 38:619–626.
- Paulay, T. and Priestley, M.J.N. (1992). *Seismic design of reinforced concrete and masonry buildings*, J. Wiley and Sons, New York.
- Priestley, M.J.N., Calvi, G.M. and Kowalsky, M.J. (2007). *Displacement-based design of structures*, IUSSS Press, Pavia, Italy.
- Simsir, C.C. (2004). *Influence of diaphragm flexibility on the out-of-plane dynamic response of unreinforced masonry walls*, PhD Thesis, University of Illinois at Urbana-Champaign, —Illinois, USA.
- STM, 2002. *Standard test method for conducting strength tests of panels for building construction (No. E72-02)*, ASTM International.
- Vaculik, J.J. (2004). *Unreinforced masonry walls subjected to out-of-plane seismic action*, a thesis submitted in partial fulfilment of the requirements for the degree of Doctor of Philosophy, The University of Adelaide, School of Civil, Environmental and Mining Engineering.
- Wilson, A. (2012). *Seismic assessment of timber floor diaphragms in unreinforced masonry buildings*, Doctoral dissertation, University of Auckland, Auckland, New Zealand, March, 568p. <https://researchspace.auckland.ac.nz/handle/2292/14696>.

Wilson, A., Quenneville, P.J.H. and Ingham, J.M. (2013). *In-plane orthotropic behaviour of timber floor diaphragms in unreinforced masonry buildings*, ASCE Journal of Structural Engineering, [http://dx.doi.org/10.1061/\(ASCE\)ST.1943-541X.0000819](http://dx.doi.org/10.1061/(ASCE)ST.1943-541X.0000819).

Yi, T., Moon, F.L., Leon, R.T. and Kahn, L.F. (2006). *Lateral load tests on a two-storey unreinforced masonry building*, Journal of Structural Engineering, 132_5_ 643–652.

DRAFT FOR PUBLIC COMMENT

Appendix C8A: On-site Testing

C8A.1 General Considerations

While the seismic response of URM buildings is significantly influenced by characteristics such as boundary conditions and the behaviour of inter-element connections, on-site testing of material properties improves the reliability of the seismic assessments and the numerical models that describe the seismic behaviour of URM buildings, and it may lead to less conservative retrofit designs. However, the non-homogenous nature of masonry combined with the age of URM buildings make it difficult to reliably predict the material properties of masonry walls.

It is recommended that field sampling or field testing of URM elements is conducted. Field sampling refers to the extraction of samples from an existing building for subsequent testing offsite, while field testing refers to testing for material properties in situ. The following sections describe a set of techniques that can be used to determine masonry material properties.

Before proceeding to on-site testing, it is important to sensibly understand what information will be collected from the investigation, how that would be used and what value the information will add to reliability of the assessment. Before deciding an investigation programme, sensitivity analyses should be undertaken to determine what assessment parameters are more important and likely to influence the assessment result and whether the default parameter values given are likely to be appropriate/sufficient.

Only rarely should on-site testing be considered necessary for basic buildings.

C8A.2 Masonry Assemblage (Prism) Material Properties

If masonry assemblage (prism) samples are to be extracted for laboratory testing they should be single leaf and at least three bricks high. If they are two leaves thick or more, cut them into single leaf samples. If rendering plaster is present, remove this from both sides of the samples. Cap the prepared samples using gypsum plaster to ensure uniform stress distribution.

Test individual brick units and mortar samples as per Section C8A.3 when sampling of larger assemblages is not permitted or practical. Masonry properties can then be predicted using the obtained brick and mortar properties as set out in Section C8.7.

C8A.2.1 Masonry compressive strength

Determine masonry compressive strength in accordance with ASTM C 1314-03b (ASTM, 2003c). Figure C8A.1 shows a typical prism sample before testing. Aluminium frames are attached to the sample ends and a displacement gauge spans between the frames to measure the sample displacement.

ASTM C 1314-03b (ASTM, 2003c) also enables the engineer to determine the masonry modulus of elasticity (further detailed in Section C8A.2.2).



Figure C8A.1: Example of extracted sample with test rig attached for the prism compression test

C8A.2.2 Masonry modulus of elasticity

C8A.2.2.1 Laboratory calibrated displacement measurement

Laboratory calibrated displacement measurement devices may be attached to the masonry prisms during the compression tests detailed in Section C8A.2.1. Incorporate a minimum of two measurement devices to record displacements at opposing sample faces. Their gauge lengths should cover the distance from the middle of the top brick to the middle of the bottom brick. Use the recorded measurement to derive the masonry stress-strain relationship and subsequently the masonry modulus of elasticity, E_m . The stress and strain values considered in the calculation of E_m are those between 0.05 and 0.70 times the masonry compressive strength (f'_m).

C8A.2.2.2 In situ deformability test incorporating flat jacks

Flat jack testing is a versatile and effective technique that provides useful information on the mechanical properties of historical constructions. In situ measurements of masonry modulus of elasticity should be performed in accordance with the ASTM C 1197-04 (ASTM, 2004) in situ deformability test.

Note:

Extensive studies have been conducted to confirm the reliability of this test, including the work by Noland et al. (1991), Gregorczyk and Lourenço (2000); Parivallal et al. (2011); and Simões et al. (2012).

The in situ deformability test is moderately destructive as it requires the removal of horizontal mortar joints (bed-joint) for the insertion of the two flat jacks (refer to Figure C8A.2(a)). The horizontal slots are separated by at least five courses of brickwork, but the separation distance should not exceed 1.5 times the flat jack length. A pressure controlled hydraulic pump is used to inflate the flat jacks, applying vertical confinement pressure to the masonry between the two jacks. To monitor displacement, typically three measurement devices are attached between the two flat jacks (refer to Figure C8A.2(b)). These flat jacks need to be calibrated, following ASTM C 1197-04 (ASTM, 2004).



(a) Cutting mortar bed-joints and insertion of flat jacks into clay brick masonry



(b) In situ deformability test set-up under preparation in clay brick masonry

Figure C8A.2: In situ deformability test preparation (EQ STRUC Ltd)

C8A.2.3 Masonry flexural bond strength

Extract masonry prisms two bricks high and a single brick wide, and subject these to the flexural bond test of AS 3700-2001 (Australian Standards, 2001). Remove any rendering plaster from the sides of the sample before performing this test. Cut any samples that are two leaves thick or more into single leaf masonry prism samples. Alternatively, the engineer may conduct the flexural bond test in situ if this is more practical.

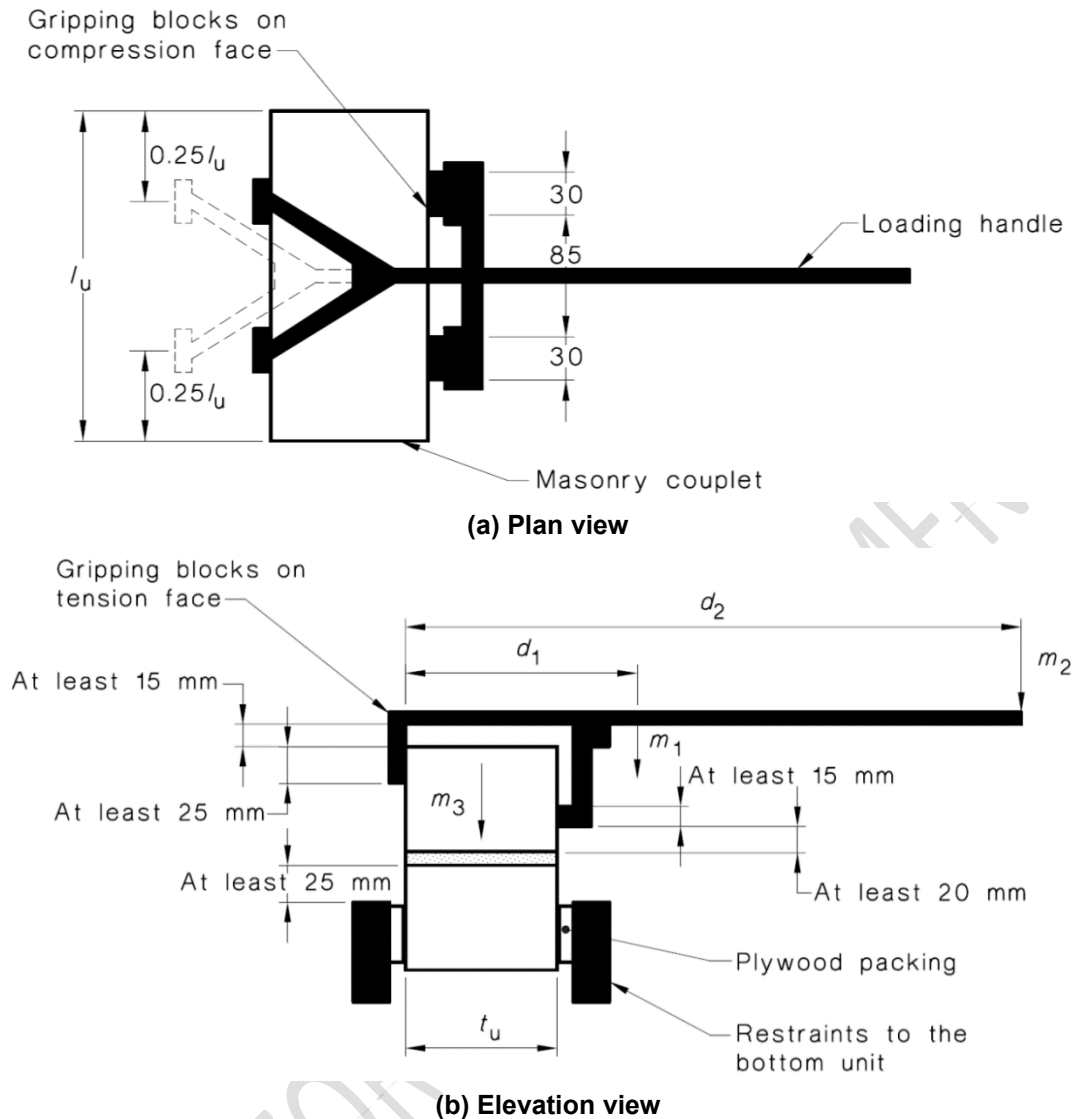


Figure C8A.3: Flexural bond test set-up (AS 3700-2001)

C8A.2.4 Masonry bed-joint shear strength

Conduct the ASTM C 1531-03 (ASTM, 2003b) in situ bed-joint shear test to determine masonry bed-joint properties. This type of test is moderately destructive as it requires the removal of at least one brick on one side of the test specimen to allow for insertion of a hydraulic jack, as well as the removal of a vertical mortar joint on the opposite side to allow horizontal bed-joint movement to occur. The hydraulic jack is then loaded, using a pressure controlled hydraulic pump, until visible bed-joint sliding failure occurred. The bed-joint shear strength can then be derived from the peak pressure records.

Alternatively, extract three brick high masonry prisms for laboratory testing following the triplet shear test BS EN 1052-3 (BSI, 2002). This test should be conducted while applying axial compression loads of approximately 0.2 MPa, 0.4 MPa and 0.6 MPa. At least three masonry prism samples should be tested at each level of axial compression. Remove any rendering plaster from both sides of the sample before testing. Cut any masonry samples that are two leaves thick or more into single leaf samples. Bed-joint shear tests performed in the laboratory and in situ are shown in Figure C8A.4.



(a) Laboratory shear triplet test



(b) In situ shear test without flat jacks (EQ STRUC Ltd)

Figure C8A.4: In situ and laboratory bed- joint shear test

The in-situ bed-joint shear test is limited to tests of the masonry face leaf. When the masonry unit is pushed in a direction parallel to the bed joint, shear resistance is provided across not only the bed-joint shear planes but also the collar joint shear plane. Because seismic shear is not transferred across the collar joint in a multi-leaf masonry wall, the estimated shear resistance of the collar joint must be deducted from the test values. This reduction is achieved by including a 0.75 reduction factor in Equation C8.33, which is the ratio of the areas of the top and bottom bed joints to the sum of the areas of the bed and collar joints for a typical clay masonry unit.

The term P in Equation C8.33 represents the axial overburden acting on the bed joints. This value multiplied by the bed-joint coefficient of friction, (μ_f), allows estimation of the frictional component contributing to the recorded bed-joint stress. Due to the typically large variation of results obtained from individual bed-joint shear strength tests, the equation conservatively assumes $\mu_f = 1.0$ for the purposes of determining cohesion, c . Therefore, for simplicity, the μ_f term has been omitted from the equation.

C8A.3 Constituent Material Properties

C8A.3.1 Brick compressive strength

Extract individual brick units for the ASTM C 67-03a (ASTM, 2003a) half brick compression test. Cut these brick units into halves and cap them using gypsum plaster before compression testing (refer to Figure C8A.5). Note that it is possible to obtain half brick units from the residual samples of the Modulus of Rupture test described in Section C8A.3.2.



Figure C8A.5: Brick and mortar sample and compression test set-up (EQ STRUC Ltd)

C8A.3.2 Brick modulus of rupture

Extract individual brick units from the building and subject these to the Modulus of Rupture (MoR) test ASTM C 67-03a (ASTM, 2003a). The tested brick specimens from the MoR test may be subjected to the half brick compression test ASTM C 67-03a (ASTM, 2003a) in order to obtain a direct relationship between the brick MoR and compressive strength, f'_b . Previous experimental investigation has confirmed that the brick unit MoR can be approximated to equal $0.12f'_b$.

C8A.3.3 Mortar compressive strength

Extract irregular mortar samples for laboratory testing. As it is common for URM walls to have eroded mortar joints that were later repaired using stronger mortar, take care when selecting the location for mortar sample extraction to ensure that these samples are representative.

The method to determine mortar compressive strength is detailed in ASTM C 109-08 (ASTM, 2008). This method involves testing 50 mm cube mortar samples, which generally are not attainable in existing buildings as most mortar joints are only 10 to 18 mm thick. Therefore, cut the irregular mortar samples into approximately cubical sizes with two parallel sides (top and bottom). The height of the mortar samples should exceed 15 mm in order to satisfactorily maintain the proportion between sample size and the maximum aggregate size. Cap the prepared samples using gypsum plaster to ensure a uniform stress distribution and testing in compression (Valek and Veiga, 2005). Refer to Figure C8A.6 for examples.

Measure the height to minimum lateral dimension (h/t) ratio of the mortar samples and use this **ratio** to determine the mortar compressive strength correction factors. Divide the compression test result by the corresponding correction factors in Equation C8A.1. The average corrected strength is equal to the average mortar compressive strength, f'_j .

$$f'_j = \alpha_{tl} \alpha_{ht} f'_{ji} \quad \dots \text{C8A.1}$$

where:

$$\begin{aligned}
 f'_j &= \text{probable mortar compressive strength} \\
 \alpha_{tl} &= t/l \text{ ratio correction factor} \\
 \alpha_{ht} &= h/t \text{ ratio correction factor} \\
 f'_{ji} &= \text{measured irregular mortar compressive strength.}
 \end{aligned}$$

Equation C8A.1 normalises the measured compressive strength of irregular mortar samples to the compressive strength of a 50 mm cube mortar. Factors α_{tl} and α_{ht} are calculated as per Equation C8A.2 and Equation C8A.3 (where $M.F$ should be calculated as per Equation C8A.4) respectively. Factor α_{tl} is required in order to normalise the sample t/l ratio to 1.0, while factor α_{ht} is required in order to normalise the sample h/t ratio to 1.0, corresponding to a cubic mortar sample that is comparable to a 50 mm cube. These factors were derived based on the study detailed in Lumantarna (2012).

$$\alpha_{tl} = 0.42 \frac{t}{l} + 0.58 \quad \dots \text{C8A.2}$$

$$\alpha_{ht} = \frac{1}{M.F} \quad \dots \text{C8A.3}$$

$$M.F = 2.4 \left(\frac{h}{t} \right)^2 - 5.7 \left(\frac{h}{t} \right) + 4.3 \quad \dots \text{C8A.4}$$

When conducting tests on laboratory manufactured samples make 50 mm mortar cubes, leave these to cure under room temperature ($\pm 20^\circ \text{C}$) for 28 days, and test them in compression following the mortar cube compression test ASTM C 109-08 (ASTM, 2008).



(a) Example of typical extracted mortar samples



(b) Example of typical mortar sample preparations



(c) Example of typical test set-up

Figure C8A.6: Determination of mortar compression strength (EQ STRUC Ltd)

C8A.4 Proof Testing of Anchor Connections

An epoxied or grouted anchorage system is a typical method of connecting the floor and roof diaphragms of the building to masonry walls. Reliable anchor pull-out and shear strength is important for assessment or design of anchors and the specification of anchor spacing. Standard installation procedures of embedded anchors involve drilling the masonry wall, cleaning the drilled hole, and epoxying or grouting threaded steel bars to the specified embedment depth, typically 50 mm less than the wall thickness. Two-part epoxy or high strength grouts are typically used with surface preparation conducted in accordance with the manufacturer's specifications.

On-site quality control and proof testing should be undertaken on at least 15% of all installed adhesive anchors, of which 5% should be tested prior to the installation of more than 20% of all anchors. Testing is required to confirm workmanship (particularly the mixing of epoxy and cleaning of holes) and anchor capacity against load requirements. If more than 10% of the tested anchors fail below a test load of 75% of the nominated probable capacity, discount the failed anchors from the total number of anchors tested as part of the quality assurance test. Test additional anchors to meet the 15% threshold requirements. Failures that cannot be attributed to workmanship issues are likely to be indicative of an overestimation of the available capacity and a reassessment of the available probable capacity is likely to be required.

C8A.4.1 Anchors loaded in tension

Once the adhesive is cured (typically over 24 hours), the steel anchors can be loaded in tension using a hydraulic jack until ultimate carrying capacity is reached (ASTM, 2003) or when the load exceeds two times the specified load. The typical test set-up is shown in Figure C8A.7. A 600 mm clear span of reaction frame allows testing of up to 300 mm embedment depth without exerting any confining pressures onto the test area, as the reaction frame supports are outside the general zone of influence. On completing the test, the anchor stud is typically cut flush with the wall surface.



(a) Typical anchor pull test set-up



(b) Close up of the typical test set-up with an alternative test frame

Figure C8A.7: Typical anchor pull-out test set-up (EQ STRUC Ltd)

C8A.4.2 Anchors loaded in shear

The test set-up that could be adopted for in situ testing of anchors loaded in shear is shown in Figure C8A.8. Monotonic shear loading can be applied by using a single acting hydraulic actuator, with the external diameter of the actuator selected to be as small as possible. The bracket arrangements should minimise the tension loads in the anchors. The aim is to determine the shear capacity in the absence of tension.



(a) Typical anchor shear tests set-up
(push cycle)



(b) Typical anchor shear tests set-up
(pull cycle)

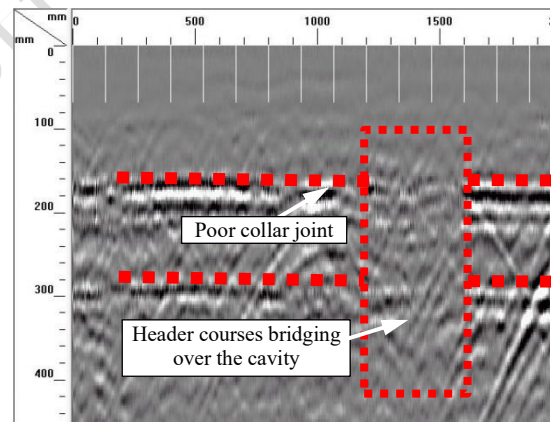
Figure C8A.8: Shear tests set-up used (EQ STRUC Ltd)

C8A.5 Investigation of Collar Joints and Wall Cavities

Investigation of collar joints quality and wall cavities can be undertaken using a Ground Penetrating Radar (GPR) structural scanner (refer to Figure C8A.9(a)). The scanner is capable of accurately determining the member thickness, metallic objects, voids and other information. An example of the information provided by GPR scanning is presented in Figure C8A.9(b).



(a) GPR scanner



(b) Typical results output

Figure C8A.9: Example of non-invasive scanning using Ground Penetrating Radar (GPR) scanner technology (EQ STRUC Ltd)

C8A.6 Cavity Tie Examination

The main focus of the cavity tie examination is to identify the condition and frequency of the cavity ties embedded between the leaves of the cavity URM walls. A borescope inspection camera can be used to inspect the air cavity through a void left from a removed brick or an air vent (refer to Figure C8A.10).



(a) Borescope inspection camera



(b) Typical example of cavity observations

Figure C8A.10: Borescope inspection camera (EQ STRUC Ltd)

Appendix C8B: Derivation of Instability Deflection and Fundamental Period for Face-Loaded Masonry Walls

C8B.1 General Considerations and Approximations

There are many variations that need to be taken into account when considering a general formulation for URM walls that might fail out-of-plane. These include the following:

- Walls will not usually be of a constant thickness in a building, or even within a storey.
- Walls will have embellishments, appendages and ornamentation that may lead to eccentricity of masses with respect to supports.
- Walls may have openings for windows or doors.
- Support conditions will vary.
- Existing buildings may be rather flexible, leading to possibly large inter-storey displacements that may adversely affect the performance of face-loaded walls.

The following approximations can be used to simplify the analysis while still accounting for some key factors.

- 1 Deformations due to distortions (straining) in the wall can be ignored. Assume deflections to be entirely due to rigid body motion.

Note:

This is equivalent to saying that the change in potential energy from a disturbance of the wall from its initial position is mostly due to the movement of the masses of the elements comprising the wall and the movements of the masses tributary to the wall. Strain energy contributes less to the change in potential energy.

- 2 Assume that potential rocking occurs at the support lines (e.g. at roof or floor levels) and, for walls that are supported at the top and bottom of a storey, at the mid height. The mid height rocking position divides the wall into two parts of equal height: a bottom part (subscript *b*) and a top part (subscript *t*). The masses of each part are not necessarily equal.

Note:

It is implicit within this assumption and (1) above that the two parts of the wall remain undistorted when the wall deflects. For walls constructed of softer mortars or walls with little vertical pre-stress from storeys above, this is not actually what occurs: the wall takes up a curved shape, particularly in the upper part. Nevertheless, errors occurring from the use of the stated assumptions have been found to be small and the engineer will still obtain acceptably accurate results.

- 3 Assume the thickness to be small relative to the height of the wall. Assume the slope, A , of both halves of the wall to be small; in the sense that $\cos(A) \approx 1$ and $\sin(A) \approx A$.

Note:

The approximations for slope are likely to be sufficiently accurate for reasonably thin walls. For thick walls where the height to thickness ratio is smaller, the formulations in this appendix are likely to provide less accurate results and force-based approaches provide an alternative.

- 4 Inter-storey slopes due to deflection of the building are assumed to be small.

Note:

Approximate corrections for this effect are noted in the method.

- 5 In dynamic analyses, the moment of inertia is assumed constant and equal to that applying when the wall is in its undisturbed position, whatever the axes of rotation.

Note:

The moment of inertia is dependent on the axes of rotation. During excitation, these axes continually change position. Assuming that the inertia is constant is reasonable within the context of the other approximations employed.

- 6 Damping is assumed as the default value in NZS 1170.5:2004, which is 5% of critical.

Note:

For the aspect ratio of walls of interest, additional effective damping due to loss of energy on impact is small. Furthermore, it has been found that the surfaces at rocking (or hinge) lines tend to fold onto each other rather than experience the full impact that is theoretically possible, reducing the amount of equivalent damping that might be expected. However, for in-plane analysis of buildings constructed largely of URM, adopting a damping ratio that is significantly greater than 5% is appropriate.

- 7 Assume that all walls in storeys above and below the wall under study move “in phase” with the subject wall.

Note:

Analytical studies have found this **assumption** to be the case. One reason for this **behaviour** is that the effective stiffness of a wall as it moves close to its limit deflection (e.g. as measured by its period) becomes very low, affecting its resistance to further deflection caused by accelerations transmitted to the walls through the supports. This assumption means that upper walls, for example, will tend to restrain the subject wall by exerting restraining moments.

C8B.2 Vertically Spanning Walls

C8B.2.1 General formulation

Figure C8B.1 and Figure C8B.2 show the configuration of a URM wall within a storey at two stages of deflection due to rocking. The URM wall is intended to be quite general, hence why the geometry in Figure C8B.1 appears distorted. Simplifications to the general solutions for walls that are simpler (e.g. of uniform thickness) are made in a later section.

Figure C8B.1 shows the configuration at incipient rocking. Figure C8B.2 shows the configuration after significant rocking has occurred, with the wall having rotated through an angle A and with mid height deflection, Δ , where $\Delta = Ah/2$.

In Figure C8B.1 the dimensions e_b and e_t relate to the mass centroids of the upper and lower segments of the vertically spanning wall. The dimension e_p relates to the position of the line of action of weights from upper storeys (walls, floors and roofs) relative to the centroid of the upper segment of the wall. The arrows on the associated dimensioning lines indicate the positive direction of these dimensions for the assumed direction of motion (angle A at the bottom of the wall is positive in the anticlockwise sense). Under some circumstances the signs of the eccentricities may be negative; for example for e_p when an upper storey wall is much thinner than the upper storey wall represented here, particularly where the thickness steps on one face. When the lines of axial force from diaphragm and walls from above are different, the resultant force should be calculated.

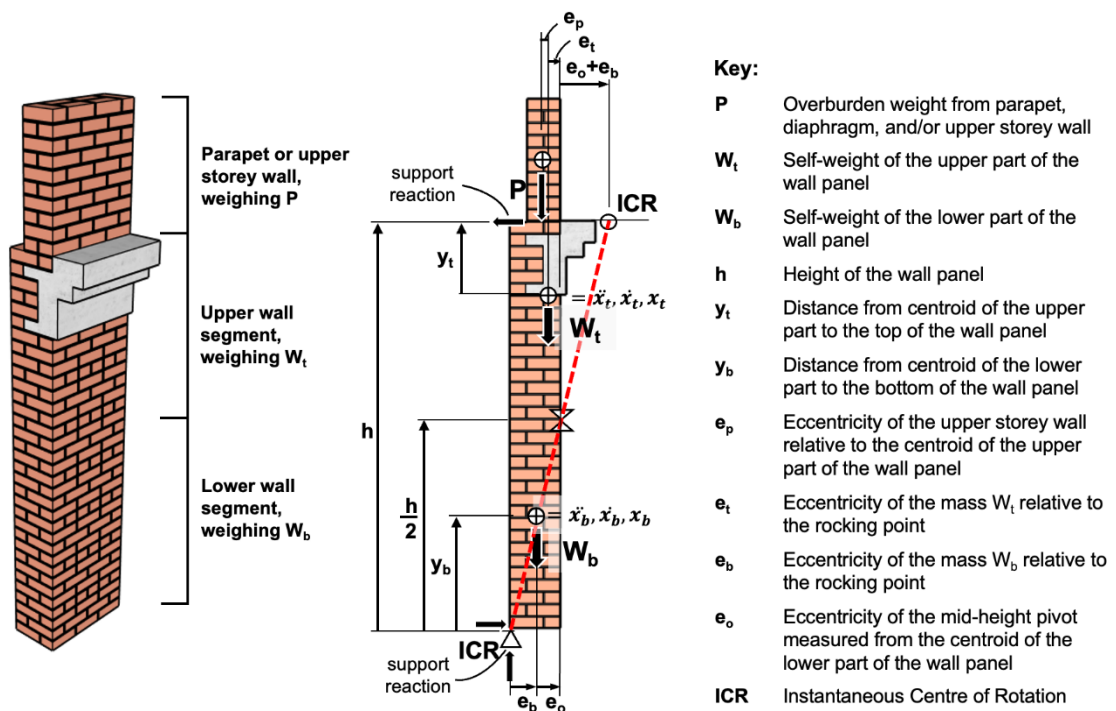


Figure C8B.1: Configuration at incipient rocking

Note that in Figure C8B.1 the lower wall segment is shown rotating about the lower left corner. This position is assumed to be fixed horizontally and vertically. As rocking of the lower wall segment commences in an anticlockwise direction the upper right corner of the lower wall segment will displace both horizontally and vertically (see Figure C8B.2). The

base of the upper wall segment is assumed to rock while staying connected to the upper right corner of the lower wall segment, such that the base rocking position of the upper segment is itself in motion as rocking occurs. Just as the lower wall segment is assumed to rock anticlockwise about the lower left corner of the lower segment, the upper wall segment is rocking in a clockwise direction about a position referred to as the Instantaneous Centre of Rotation (ICR), recognising that this position is in motion. The instantaneous centres of rotation (ICR) are marked on these figures and these positions are useful in deriving virtual work expressions.

C8B.2.2 Limiting deflection for static instability

The equation of equilibrium can be written directly by referring to Figure C8B.2 and using virtual work expressions. For static conditions this expression is:

$$W_b(e_b - Ay_b) + W_t(e_o + e_b + e_t - A(h - y_t)) + P(e_o + e_b + e_t + e_p - Ah) - \Psi(W_b y_b + W_t y_t) = 0 \quad \dots \text{C8B.1}$$

The final term Ψ represents the effect of any inter-storey drift. In the derivation presented, the total deformation has been assumed to be that resulting from the summation of the rocking wall and the inter-storey drift.

Writing:

$$a = W_b y_b + W_t(h - y_t) + Ph \quad \dots \text{C8B.2}$$

and:

$$b = W_b e_b + W_t(e_o + e_b + e_t) + P(e_o + e_b + e_t + e_p) - \Psi(W_b y_b + W_t y_t) \quad \dots \text{C8B.3}$$

and collecting terms in A , the equation of equilibrium is rewritten as:

$$-aA + b = 0 \quad \dots \text{C8B.4}$$

from which:

$$A = \frac{b}{a} \quad \dots \text{C8B.5}$$

when the wall becomes unstable.

Note:

The parameters a and b are introduced as a mathematical shortcut to conveniently obtain a simplified expression for A , which is then used to derive Δ_i and T_p . The terms a and b can be understood as work done by forces during motion decomposed into vertical and horizontal components respectively, but they do not represent a specific physical concept.

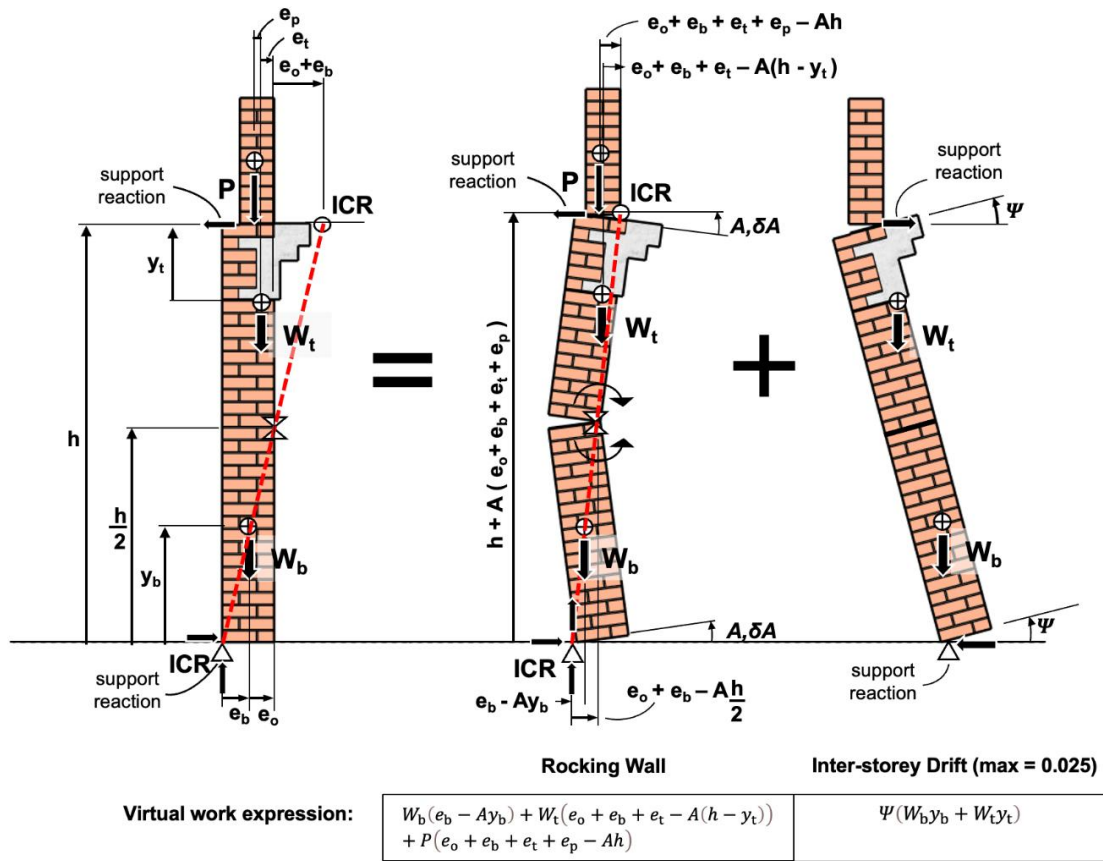


Figure C8B.2: Configuration when rotations have become significant and there is inter-storey drift

Therefore, the critical value of the deflection at mid height of the wall, at which the wall will be unstable, is referred to as the instability displacement Δ_i :

$$\Delta_i = A \frac{h}{2} = \frac{bh}{2a} \quad \dots \text{C8B.6}$$

It is assumed that Δ_m , a fraction of this deflection, is the maximum useful deflection. Experimental and analytic studies indicate that this fraction might be assumed to be about 0.6. At larger displacements than $0.6\Delta_i$, analysis reveals an undue sensitivity to earthquake spectral content and a wide scatter in results.

Note:

The value for inter-storey drift, Ψ , is often taken as 2.5%, which is the limiting value for ULS inter-storey deflection given in Cl. 7.5.1 of NZS 1170.5:2004. While it may be conservative to assume that each storey deflects by the maximum allowable amount, this assumption should be testing against knowledge that the engineer may have obtained through analysis or observation regarding the likely drift response affecting the floors supporting the wall section under consideration. For example, in buildings having highly perforated lower floors and stiff upper floors, an assumption of 2.5% inter-storey drift may be inappropriate for the upper levels. The influence of the assumed value of Ψ can be tested using a sensitivity study.

The value e_p , as shown in Figure C8B.1 and Figure C8B.2, relates to the eccentricity of the imposed loads. As presented in the standard formulation, when applying this value there is no differentiation between top loads from parapets, upper levels, etc and from roof or wall loads and it is assumed that the top load acts at the top of the upper wall segment. Some options for engineers include:

- in most cases, the level-above wall loads and/or parapet top loads will dominate the floor/roof loads. Taking e_p relative to the parapet/wall above is an acceptable simplification where these loads are clearly larger than the floor/roof loads.
- where parapet/wall top loads are of similar magnitude to floor/roof top loads, and the effort is required by the project at hand, two separate e_p values can be used to represent the different top loads. This procedure would require some modifications to the formulation of the instability deflection calculation.

C8B.2.3 Equation of motion for free vibration

When conditions are not static, the virtual work expression on the left side in Equation C8B.4 above is unchanged but the zero on the right side of the equation is replaced by mass x acceleration, in accordance with Newton's law. This gives:

$$-aA + b = -J\ddot{A} \quad \dots\text{C8B.7}$$

This expression uses the usual notation for acceleration (a double dot to denote the second derivative with respect to time; in this case indicating angular acceleration), and J as the rotational inertia.

The rotational inertia can be written directly from Figure C8B.1 and Figure C8B.2, noting that the centroids undergo accelerations vertically and horizontally as well as rotationally, and these accelerations relate to the angular acceleration in the same way as the displacements relate to the angular displacement. While the rotational inertia is dependent on the displacements, the effects of this variation are ignored. Therefore, the rotational inertia is taken as that when no displacement has occurred. This gives the following expression for rotational inertia:

$$J = J_{bo} + J_{to} + \frac{1}{g} \left\{ W_b [e_b^2 + y_b^2] + W_t [(e_o + e_b + e_t)^2 + y_t^2] + P [(e_o + e_b + e_t + e_p)^2] \right\} + J_{anc} \quad \dots\text{C8B.8}$$

where J_{bo} and J_{to} are the mass moments of inertia of the bottom and top parts of the wall respectively about their centroids, and J_{anc} is the inertia of any ancillary masses, such as veneers, that are not integral with the wall but contribute to its inertia.

For a wall with unit length, held at the top and bottom, and with a rocking crack at mid height, with a density of ρ per unit volume, the mass moment of inertia about the horizontal axis through the centroid is given by:

$$I_{xx}(\text{kgm}^2) = \frac{1}{12} \rho t_{\text{Gross}} \left(\frac{h}{2} \right)^3 \quad \dots\text{C8B.9}$$

The corresponding mass moment of inertia about the vertical axis through the centroid is:

$$I_{yy} \text{ (kgm}^2\text{)} = \frac{1}{12} \rho \left(\frac{h}{2} \right) t_{\text{Gross}}^3 \quad \dots\text{C8B.10}$$

The **rotational mass** moment of inertia through the centroid is the sum of these, or:

$$\begin{aligned} J_{\text{bo}} \text{ (kgm}^2\text{)} &= J_{\text{to}} = I_{xx} + I_{yy} = \rho t_{\text{Gross}} \left(\frac{h}{2} \right) \left[t_{\text{Gross}}^2 + \left(\frac{h}{2} \right)^2 \right] / 12 \\ &= \frac{m}{2} \frac{[t_{\text{Gross}}^2 + (h/2)^2]}{12} = \frac{W}{2g} \frac{[t_{\text{Gross}}^2 + (h/2)^2]}{12} \quad \dots\text{C8B.11} \end{aligned}$$

where m is the mass (kg), W (N) is the weight of the whole wall and g is the acceleration of gravity.

Note that in Equation C8B.11 the expressions in square brackets are the squares of the radii from the instantaneous centres of rotation to the mass centroids, where the locations of the instantaneous centres of rotation are those when there is no displacement. Some CAD programs have functions that will assist in determining the inertia about an arbitrary point (or locus), such as about the ICR shown in Figure C8B.2.

Collecting terms and normalising Equation C8B.7 so that the coefficient of the acceleration term is unity gives the following differential equation of free vibration:

$$\ddot{A} - \frac{a}{J} A = -\frac{b}{J} \quad \dots\text{C8B.12}$$

C8B.2.4 Period of free vibration

To find the solution to the differential equation of free vibration, Equation C8B.12 is rewritten as:

$$\ddot{A} - \kappa^2 A = -\frac{b}{J} \quad \dots\text{C8B.13}$$

from which:

$$\kappa^2 = \frac{a}{J} \quad \dots\text{C8B.14}$$

To solve the differential equation of free vibration Equation C8B.13 is separated into its homogeneous and particular parts. The homogeneous equation of free vibration is derived from Equation C8B.13 by eliminating the external excitation $(-b/J)$, to describe the natural response of the moving body without external force and written as:

$$\ddot{A}_h - \kappa^2 A_h = 0 \quad \dots\text{C8B.15}$$

And the general solution to this homogeneous equation can be written as:

$$A_h = C_1 \sinh(\kappa \tau) + C_2 \cosh(\kappa \tau) \quad \dots\text{C8B.16}$$

Note:

The general solution to the homogeneous equation in Equation C8B.15 can be expressed using the hyperbolic functions because the second derivative of the hyperbolic sine (\sinh) and the hyperbolic cosine (\cosh) are equal to the functions themselves: $\frac{d^2 \sinh(\tau)}{d\tau^2} = \sinh(\tau)$ and $\frac{d^2 \cosh(\tau)}{d\tau^2} = \cosh(\tau)$. Thus, the solutions for a differential equation can be written as $\frac{d^2 \sinh(\tau)}{d\tau^2} - \sinh(\tau) = 0$ and $\frac{d^2 \cosh(\tau)}{d\tau^2} - \cosh(\tau) = 0$.

The particular equation is derived from Equation C8B.13 by considering the steady-state behaviour of the moving body. Assuming the angular displacement A remains constant over time in the steady-state behaviour, the angular acceleration becomes zero. Then, Equation C8B.13 is written by substituting A equals constant A_p as:

$$0 - \kappa^2 A_p = -\frac{b}{J} \quad \dots \text{C8B.17}$$

And the solution to the above equation can be written by substituting $\kappa^2 (= a/J)$ as:

$$A_p = \frac{b}{a} \quad \dots \text{C8B.18}$$

The general solution of the equation for free vibration is the sum of the solutions of the homogeneous and particular equations:

$$A = A_h + A_p = C_1 \sinh\left(\sqrt{\frac{a}{J}}\tau\right) + C_2 \cosh\left(\sqrt{\frac{a}{J}}\tau\right) + \frac{b}{a} \quad \dots \text{C8B.19}$$

and:

$$\dot{A} = \frac{dA}{d\tau} = C_1 \sqrt{\frac{a}{J}} \cosh\left(\sqrt{\frac{a}{J}}\tau\right) + C_2 \sqrt{\frac{a}{J}} \sinh\left(\sqrt{\frac{a}{J}}\tau\right) \quad \dots \text{C8B.20}$$

By taking the condition that the rotational velocity is zero when time $\tau = 0$, constant C_1 becomes:

$$C_1 = \frac{-C_2 \sinh(0)}{\cosh(0)} = 0 \quad \dots \text{C8B.21}$$

And by taking time, τ , as zero when the wall has its maximum rotation, $A (= 2\Delta/h)$, the constant C_2 is:

$$C_2 = \frac{2\Delta}{h} - \frac{b}{a} \quad \dots \text{C8B.22}$$

Then, the solution becomes:

$$A = \left(\frac{2\Delta}{h} - \frac{b}{a}\right) \cosh\left(\sqrt{\frac{a}{J}}\tau\right) + \frac{b}{a} \quad \dots \text{C8B.23}$$

Taking the period of the “part”, T_p , as four times the duration for the wall to rotate from its position at maximum deflection to return to vertical. The wall reaches its vertical position, $A = 0$, when the time $\tau = \tau_v$. Solving $A(\tau_v) = 0$ from Equation C8B.23 gives:

$$\tau_v = \sqrt{\frac{J}{a}} \cosh^{-1} \left(\frac{b/a}{b/a - 2\Delta/h} \right) \quad \dots \text{C8B.24}$$

Then the period is given by:

$$T_p = 4 \sqrt{\frac{J}{a}} \cosh^{-1} \left(\frac{b/a}{b/a - 2\Delta/h} \right) \quad \dots \text{C8B.25}$$

Note:

The total period of one complete cycle consists of movement from maximum positive deflection to vertical, vertical to maximum negative deflection, maximum negative deflection to vertical, and vertical to maximum positive deflection. Hence, $T_p = 4\tau_v$.

The **period of the rocking part** can be simplified further by substituting the term for Δ_i found from the static analysis and putting the value of Δ used for the calculation of period as Δ_t to give:

$$T_p = 4 \sqrt{\frac{J}{a}} \cosh^{-1} \left(\frac{1}{1 - \Delta_t/\Delta_i} \right) \quad \dots \text{C8B.26}$$

By accepting that the deflection ratio of interest is 0.6 (i.e. $\Delta_m/\Delta_i = 0.6$), this **then** becomes:

$$T_p = 6.27 \sqrt{\frac{J}{a}} \quad \dots \text{C8B.27}$$

as in the 2006 guidelines. However, research (Derakhshan et al. (2014a)) indicates that the resulting period and responding displacement demand is too large if a spectrum derived from linear elastic assumptions is used. Rather, this research suggests that an effective period calculated from an assumed displacement of 60% of the assumed displacement capacity should be used. Therefore, the period is based on $\Delta_t = 0.36\Delta_i$ so that:

$$T_p = 4.07 \sqrt{\frac{J}{a}} \quad \dots \text{C8B.28}$$

C8B.2.5 Maximum acceleration for vertically spanning walls

The acceleration required to start rocking of the wall occurs when the wall is in its initial (undisturbed) state. This **requirement** can be determined from the virtual work equations by assuming that $A = 0$. Accordingly:

$$\ddot{A}_{\max} = \frac{b}{J} \quad \dots \text{C8B.29}$$

However, a more cautious appraisal assumes that the acceleration is influenced primarily by the instantaneous acceleration of the supports, transmitted to the wall masses, without relief by wall rocking. Accordingly:

$$C_m = \frac{b}{(W_b y_b + W_t y_t)} \quad \dots \text{C8B.30}$$

where C_m is the acceleration *coefficient* to just initiate rocking.

C8B.2.6 Participation factor for vertically spanning walls

The conventional equation of motion derivation for forced vibration assumes a lumped mass (lollipop) model whereas a rocking URM wall has distributed mass based upon its geometry. This difference between lumped mass and distributed mass is accounted for using the participation factor, denoted as γ . The participation factor is applied to the rotational mass moment of inertia J such that γJ for the distributed mass is equated to the rotational mass moment of inertia of an equivalent lumped mass represented as my^2 where y is the distance from the point of rotation to the location of the centroidal lumped mass. Because virtual work is deployed elsewhere in the overall procedure the mass m is replaced by W/g . Furthermore, the derivation must be extrapolated from the centroidal height to the height y of the location of the critical displacement $h/2$ to obtain midheight deflection Δ_i , as indicated by Equation C8B.6. The participation factor is then given as:

$$\gamma = \frac{(W_b y_b + W_t y_t)h}{2gJ} \quad \dots \text{C8B.31}$$

Note that the above discussion specifically refers to vertically spanning walls as shown in Figure C8B.1 and Figure C8B.2, but that the generalised procedure to establish the participation factor for a rocking masonry cantilever is shown in Figure C8B.4.

C8B.2.7 Simplifications for regular vertically spanning walls

Simplifications can be made where the thickness of a wall within a storey is constant, there are no openings, and there are no ancillary masses. Further approximations can then be applied:

- The weight of each part (top and bottom) is half the total weight, W .
- $y_b = y_t = h/4$

The moment of inertia of the whole wall is further approximated by assuming that all e are very small relative to the height (or, for the same result, by ignoring the shift of the ICR from the mid-line of the wall), giving $J = Wh^2/12g$. Alternatively, use the simplified expressions for J given in Table C8B.1.

C8B.2.8 Approximate displacements for static instability of regular vertically spanning walls

Table C8B.1 gives values for a and b and the resulting midheight deflection to cause static instability when e_b and/or e_p are either zero or half of the effective thickness of the wall, t . In this table e_o and e_t are both assumed equal to half the effective wall thickness. While these values of the eccentricities are reasonably common, they are not the only values that will occur in practice.

The effective thickness may be assumed as follows:

$$t = \left(0.975 - 0.025 \frac{P}{W}\right) t_{\text{nom}} \quad \dots \text{C8B.32}$$

where t_{nom} is the nominal thickness of the wall.

Experiments show that this is a reasonable approximation, even for walls with soft mortar. In that case there is greater damping and that reduces response, which compensates for errors in the expression for effective thickness.

C8B.2.9 Approximate expression for period of vibration of regular vertically spanning walls

Noting that:

$$a = \left(\frac{W}{2} + P\right)h \quad \dots\text{C8B.33}$$

and using the approximation for J relevant to a wall with large aspect ratio, the expression for the period is given by:

$$T_p = 4.07 \sqrt{\frac{2Wh}{12g(W+2P)}} \quad \dots\text{C8B.34}$$

where it should be noted that the period is independent of the restraint conditions at the top and bottom of the wall (i.e. independent of both e_b and e_p).

If the height is expressed in metres then this expression simplifies to:

$$T_p = \sqrt{\frac{0.28h}{(1+2P/W)}} \quad \dots\text{C8B.35}$$

with typical values of approximately 0.5–1.0 seconds. It should be appreciated that periods may be rather long for tall walls with little overburden.

This approximation errs on the low side, which leads to an underestimate of displacement demand and therefore to slightly incautious results. The fuller formulation is therefore preferred.

C8B.2.10 Participation factor of regular vertically spanning walls

Suitable approximations can be made for the participation factor presented in Equation C8B.31 by adopting the simplifications presented above: $y_b = y_t = h/4$ and $J = Wh^2/12g$ to obtain a maximum value of $\gamma = 1.5$. Alternatively, the numerator can be simplified as provided in the following expression, and the simplified value of J shown in Table C8B.1 can be used.

C8B.2.11 Maximum acceleration of regular vertically spanning walls

By making the same simplifications as above, the maximum acceleration required to commence rocking is given by:

$$\ddot{A}_{\max} = \frac{b}{J} = \frac{12gb}{Wh^2} \quad \dots\text{C8B.36}$$

Or, more cautiously, the acceleration coefficient, C_m , is given in Table C8B.1 for the common cases regularly encountered.

C8B.2.12 Adjustments required for vertically spanning walls when inter-storey displacement is large

Using the common limit on Ψ of 0.025, and substituting for $W_b = W_t = W/2$ and $y_b = y_t = h/4$, δb is found to be $Wh/160$. Taking $h/t = 25$, in the absence of any surcharge, the percentage reduction in the instability deflection for each case shown in Table C8B.1 is 31% for Cases 0 and 2, and 16% for Cases 1 and 3. These are not insignificant, and these affects should be assessed especially in buildings with flexible principal framing such as steel moment resisting frames.

Table C8B.1: Static instability deflection for uniform walls, various boundary conditions

Boundary condition number	0	1	2	3
e_p	0	0	$t/2$	$t/2$
e_b	0	$t/2$	0	$t/2$
b	$(W/2 + P)t$	$(W + 3P/2)t$	$(W/2 + 3P/2)t$	$(W + 2P)t$
a	$(W/2 + P)h$	$(W/2 + P)h$	$(W/2 + P)h$	$(W/2 + P)h$
$\Delta_i = bh/(2a)$	$t/2$	$\frac{(2W + 3P)t}{(2W + 4P)}$	$\frac{(W + 3P)t}{(2W + 4P)}$	t
J	$\left\{ \left(\frac{W}{12} \right) [h^2 + 7t^2] + Pt^2 \right\} / g$	$\left\{ \left(\frac{W}{12} \right) [h^2 + 16t^2] + 9Pt^2/4 \right\} / g$	$\left\{ \left(\frac{W}{12} \right) [h^2 + 7t^2] + 9Pt^2/4 \right\} / g$	$\left\{ \left(\frac{W}{12} \right) [h^2 + 16t^2] + 4Pt^2 \right\} / g$
C_m	$(2 + 4P/W)t/h$	$(4 + 6P/W)t/h$	$(2 + 6P/W)t/h$	$4(1 + 2P/W)t/h$

Note:

1. The boundary conditions of the piers shown above are for clockwise potential rocking.
2. The top eccentricity, e_t , is not related to a boundary condition, so is not included in the table. The top eccentricity, e_t , is the horizontal distance from the central pivot point to the centre of mass of the top block which is not related to a boundary condition.
3. The eccentricities shown in the sketches are for the positive sense. Where the top eccentricity is in the other sense e_p should be entered as a negative number.

C8B.3 Vertical Cantilevers

C8B.3.1 General formulation

Figure C8B.3 shows a general arrangement of a cantilever. The wall illustrated has an overburden load at the top, but this load will commonly be zero, as for a parapet. Where a load does exist it is important to realise that the mass associated with that load can move horizontally. As a result the inertia of the wall is affected by the overburden to a greater extent than if the wall was supported horizontally at the top. If the top load is supported on

the wall in such a way that its point of application can change, as is the case **when the loading occurs due to the presence of** a continuous beam or slab that crosses the wall, **then** there will be an eccentricity of the point of application of P .

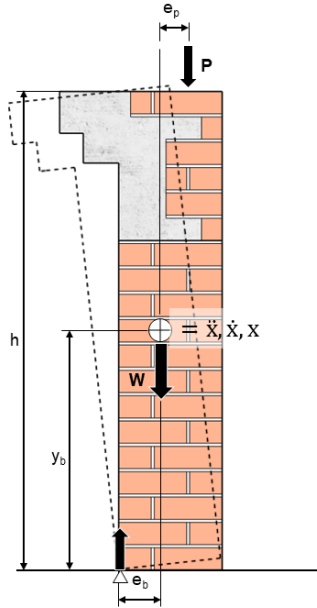


Figure C8B.3: Single cantilever wall

Sometimes several walls will be linked, **such as occurs** when a series of face-loaded walls provide the lateral resistance to a single storey building. This case can be solved by methods derived from the general formulation, but express formulations for **this scenario** are not provided here.

For the single **cantilever** wall illustrated in **Figure C8B.3** it is assumed that P is applied eccentric to the centre of the wall at the top and that **the** point of application remains constant. It is straightforward to obtain the following parameters:

$$a = Wy_b + Ph \quad \dots\text{C8B.37}$$

$$b = We_b + P(e_b + e_p) \quad \dots\text{C8B.38}$$

$$J = \frac{W}{12g}(h^2 + t_{\text{nom}}^2) + \frac{W}{g}(y_b^2 + e_b^2) + \frac{P}{g}[h^2 + (e_b + e_p)^2] \quad \dots\text{C8B.39}$$

Note that in these equations e_p is taken as positive in the sense shown in **Figure C8B.3**.

In the above expressions the properties of centroids can be employed for more complex configurations of rocking parapets:

$$W_{\text{Tot}}y_b = W_1\bar{y}_{b1} + W_2\bar{y}_{b2} + W_3\bar{y}_{b3}$$

$$W_{\text{Tot}}e_b = W_1\bar{e}_{b1} + W_2\bar{e}_{b2} + W_3\bar{e}_{b3}$$

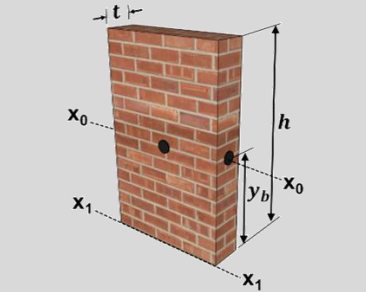
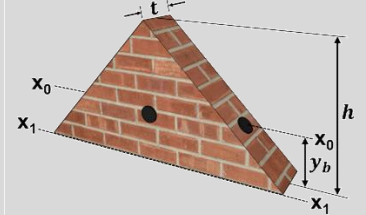
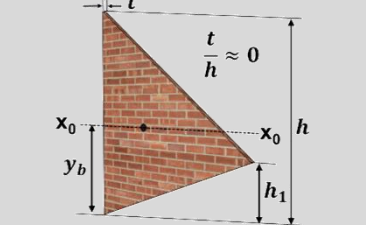
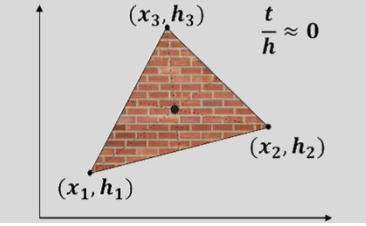
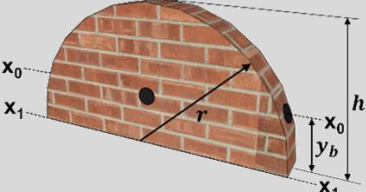
Similarly, the above expressions can be used to account for windows and other wall penetrations by treating such opening as ‘negative area’:

$$W_{\text{Tot}}y_b = W_1\bar{y}_{b1} + (-W_2)\bar{y}_{b2} + (-W_3)\bar{y}_{b3}$$

$$W_{\text{Tot}}e_b = W_1\bar{e}_{b1} + (-W_2)\bar{e}_{b2} + (-W_3)\bar{e}_{b3}$$

Note also that the first term in Equation C8B.39 applies specifically to a rectangular block rotating about its centroid, whereas the second and third terms are generic applications of the parallel axes theorem. Table C8B.2 can be used to find the properties of shapes other than rectangles.

Table C8B.2: Properties of regular shapes

Shape	y_b	J_{00}	J_{11}
	$\frac{h}{2}$	$\frac{W}{12g}(h^2 + t^2)$	$\frac{W}{3g}(h^2 + t^2)$
	$\frac{h}{3}$	$\frac{W}{36g}(2h^2 + 3t^2)$	$\frac{W}{12g}(2h^2 + 3t^2)$
	$\frac{(h + h_1)}{3}$	$\frac{W}{18g}(h^2 - h \cdot h_1 + h_1^2)$	$\frac{W}{6g}(h^2 + h \cdot h_1 + h_1^2)$
	$\frac{h_1 + h_2 + h_3}{3}$		
	$\frac{4r}{3\pi}$	$\left(\frac{1}{4} - \frac{16}{9\pi^2}\right) \frac{W}{g}(r^2 + t^2)$	$\frac{W}{4g}(r^2 + t^2)$

C8B.3.2 Limiting deflection of cantilever for static instability

When the wall shown in Figure C8B.3 just becomes unstable, the relationship for A remains the same as before but the critical deflection at the top of the vertical cantilever is Ah . Thus, the limiting deflection is given by:

$$\Delta_i = Ah = \frac{bh}{a} = \frac{[We_b + P(e_b + e_p)]h}{Wy_b + Ph} \quad \dots \text{C8B.40}$$

For the case where $P = 0$ and $y_b = h/2$ this relationship reduces to $\Delta_i = 2e_b = t$.

C8B.3.3 Period of vibration of cantilever

If $\Delta_t = 0.36\Delta_i$ as for the simple case, then the general expression for period would remain valid. However, cantilevers are much more susceptible to instability under real earthquake stimulation than vertically spanning walls that are supported both top and bottom. Therefore, the maximum useable displacement for calculation of capacity, Δ_m , is reduced from $0.6\Delta_i$ to $0.3\Delta_i$ and the displacement for calculation of period changes from $0.6\Delta_m$ to $0.8\Delta_m = 0.24\Delta_i$ so that:

$$T_p = 3.1 \sqrt{\frac{I}{a}} \quad \dots \text{C8B.41}$$

where $P = 0$, $e_b = t/2$, $y_b = h/2$. Approximating $t = t_{\text{nom}}$ and expressing h in metres, the period of vibration is given by:

$$T_p = 3.1 \sqrt{\frac{2h}{3g} \left[1 + \left(\frac{t}{h} \right)^2 \right]} = \sqrt{0.65h \left[1 + \left(\frac{t}{h} \right)^2 \right]} \approx 0.81\sqrt{h} \quad \dots \text{C8B.42}$$

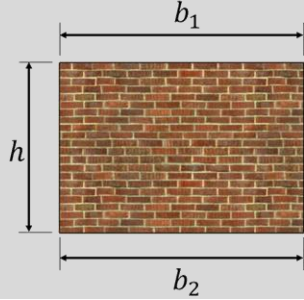
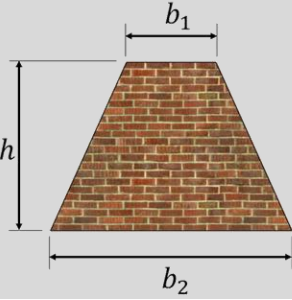
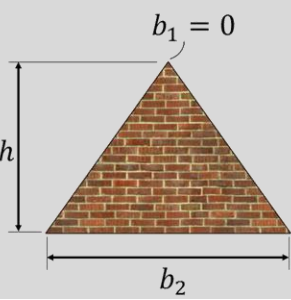
Note that P , whether eccentric or not, will not affect the static instability displacement, and therefore neither the displacement demand (by affecting the period) nor the displacement capacity. Typical values for the period of a rocking rectangular cantilever range between 0.8 seconds and 1.5 seconds dependent on height, with typically wall thicknesses having limited influence on period.

The above expression can be generalised for a rocking trapezoidal cantilever. Defining the base length dimension as b_2 and the top length dimension as b_1 , the Equation C8B.42 becomes:

$$T_p = 3.1 \sqrt{\frac{\left(1 + \frac{b_1}{b_2}\right)^2}{\left(1 + 2\frac{b_1}{b_2}\right)^2} \frac{h}{g} \left[1 + \left(\frac{t}{h} \right)^2 \right]} \quad \dots \text{C8B.43}$$

The outputs from Equation C8B.43 for several specific configurations are reported in Table C8B.2.

Table C8B.2: Period and Participation Factor for generalised rocking cantilever ($P = 0$, $t \ll h$)

$\frac{b_1}{b_2}$	1	0.5	0
Shape			
T_p	$0.81\sqrt{h}$	$0.74\sqrt{h}$	$0.70\sqrt{h}$
γ	1.5	1.6	2

Note:

The above relationships apply when $P = 0$ and $t \ll h$. For cases where these simplifications do not apply it is required to evaluation Equation C8B.41 using the correct values for J and a .

C8B.3.4 Participation factor for cantilever

The purpose of the participation factor is to:

1. Translate the rotational inertia of a distributed mass (J) to that of an equivalent lumped mass (My_b^2) for application into the dynamic equation of motion that is used to obtain displacement demand by double integration of the acceleration demand.
2. To linearly extrapolate the lateral displacement calculated at the height of the centroid (y_b) to obtain the displacement at the critical location, which is at the top of a rocking cantilever or at the mid-height for a vertically spanning wall.

Additionally, because most aspects of the methodology use weights rather than masses, the mass is substituted for (W/g). Therefore the general form of the expression for the participation factor is given by:

$$\gamma = \left(\frac{My_b^2}{J} \right) \times \left(\frac{h}{y_b} \right) = \frac{Wy_b h}{gJ} \quad \dots \text{C8B.44}$$

All versions of the participation factor reported herein are an adaption of this general logic for the specific application under consideration.

The expression for the participation factor for a regular vertical cantilever is comparable to the expression for the vertical bending scenario, with the terms $\left[\left(\frac{W}{g} \right) \left(\frac{h}{2} \right)^2 \left(\frac{1}{J} \right) \right]$ accounting for the ratio of the rotational mass moment of a lumped mass model and a distributed mass, and the displacement at the height of the lumped mass being extrapolated to the top of the cantilever via a factor of 2 (for a uniform rectangular cantilever $\frac{h}{y_b} = 2$), such that $\gamma = Wh^2/(2gJ)$. This expression may be simplified for uniform walls with $P = 0$ (no added

load at the top) by inserting the specific expression for a **rocking rectangular cantilever** of $J = \frac{W}{3g}(h^2 + t^2)$. This **simplification** gives:

$$\gamma = \frac{3}{2(1+(t/h)^2)} \quad \dots\text{C8B.45}$$

Note that for non-rectangular geometries as may be encountered for parapets and cantilevered gable walls (see Figure C8B.4) the above expression can be further extended. Assuming $P = 0$ and $(t/h) \approx 0$, the participation factor for a trapezoidal parapet having a base length dimension of b_2 and a top length dimension of b_1 can be shown to be:

$$\gamma = 2 \frac{\left(1+2\left(\frac{b_1}{b_2}\right)\right)}{\left(1+3\left(\frac{b_1}{b_2}\right)\right)} \quad \dots\text{C8B.46}$$

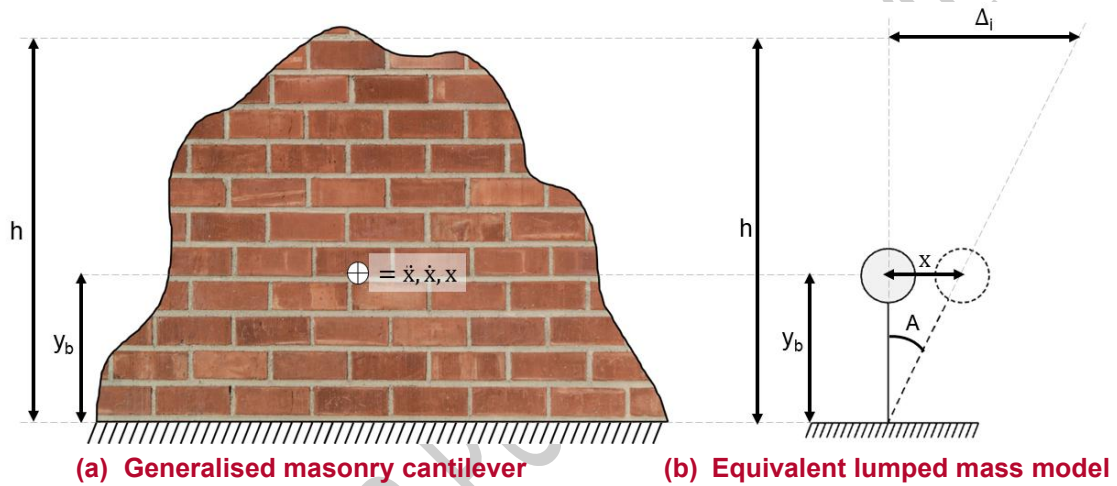


Figure C8B.4: Single cantilever

For a rectangular cantilever $b_1 = b_2$ (■) and Equation C8B.46 gives $\gamma = 1.5$ as reported previously. For a triangular cantilever $b_1 = 0$ (▲) and Equation C8B.46 gives $\gamma = 2$. For $b_1 = 0.5b_2$ Equation C8B.46 gives $\gamma = 1.6$.

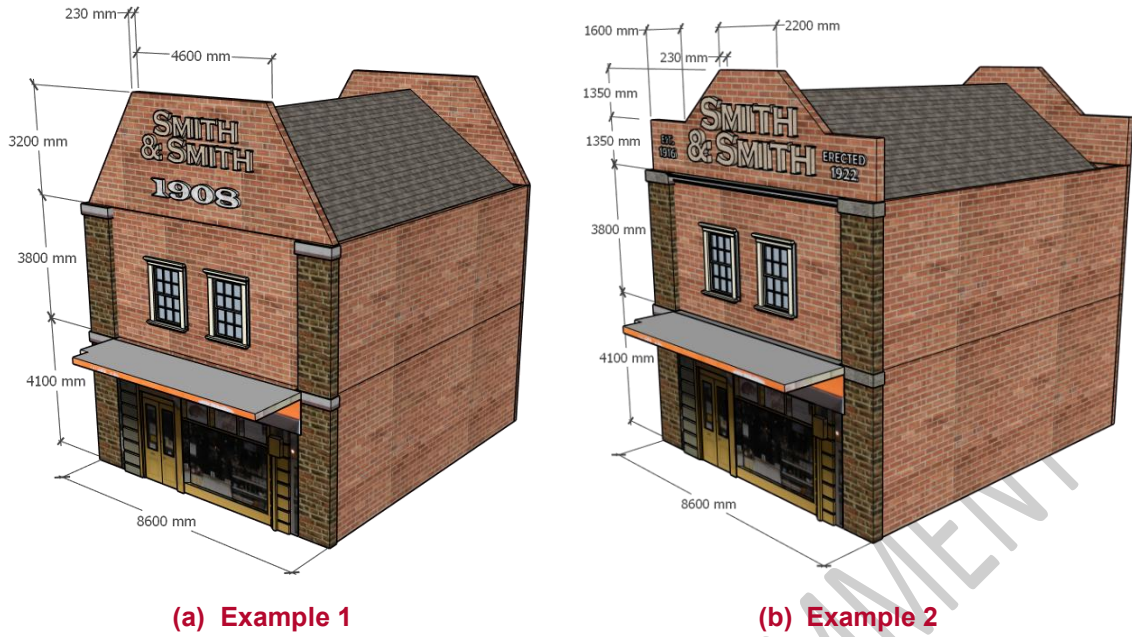
C8B.3.5 Maximum acceleration of cantilever

Using the same simplifications as described above, the maximum acceleration necessary to commence rocking is given by:

$$C = \frac{t}{h} \quad \dots\text{C8B.47}$$

C8B.3.6 Pediment cantilever worked example 1

Consider the building shown in Figure C8B.5a. Assume the building is located in Cromwell and is situated on shallow soil.



(a) Example 1

(b) Example 2

Figure C8B.5: Pediment cantilever worked examples

Step 1 and 2: Establish loading.

From Table C8.6, unit weight of masonry is 18 kN/m^3 .

Separate the pediment into a rectangular section and a triangular section:

$$W_{Rect} = 18 \times 4.6 \times 3.2 \times 0.23 = 60.9 \text{ kN}$$

$$W_{Tri} = 18 \times \frac{1}{2} \times (8.6 - 4.6) \times 3.2 \times 0.23 = 26.5 \text{ kN}$$

No axial load acting on pediment:

$$P = 0$$

Step 3: Establish the effective thickness.

See Equation C8B.32:

$$t = \left(0.975 - 0.025 \frac{P}{W} \right) t_{nom} = 0.975 \times 0.230 = 0.224 \text{ m}$$

Step 4: Establish boundary conditions.

$$e_{b,Rect} = e_{b,Tri} = t/2 = 0.224/2 = 0.112 \text{ m}$$

$$y_{b,Rect} = h/2 = 3.2/2 = 1.6 \text{ m}$$

$$y_{b,Tri} = h/3 = 3.2/3 = 1.067 \text{ m}$$

Step 5: Establish the instability displacement.

From Equation C8B.37 with $P = 0$:

$$a = W_{Rect} y_{b,Rect} + W_{Tri} y_{b,Tri} = 60.9 \times 1.6 + 26.5 \times 1.067 = 125.7 \text{ kNm}$$

From Equation C8B.38 with $P = 0$:

$$b = W_{Rect} e_{b,Rect} + W_{Tri} e_{b,Tri} = (60.9 + 26.5) \times 0.112 = 9.79 \text{ kNm}$$

From Equation C8B.40:

$$\Delta_i = Ah = \frac{bh}{a} = \frac{9.79 \times 3.2}{125.7} = 0.249 \text{ m}$$

Step 6: Determine the maximum usable deflection at the top of the parapet:

$$\Delta_m = 0.3\Delta_i = 0.3 \times 0.249 = 0.075 \text{ m}$$

Step 7: Evaluate the period:

From C8B.3.4 with $P = 0$:

$$\begin{aligned} J &= J_{Rect} + J_{Tri} = \frac{W_{Rect}}{3g}(h^2 + t^2) + \frac{W_{Tri}}{12g}(2h^2 + 3t^2) \\ &= \frac{60.9}{3 \times 9.81} \times (3.2^2 + 0.112^2) + \frac{26.5}{12 \times 9.81} \times (2 \times 3.2^2 + 3 \times 0.112^2) \\ &= 21.22 + 4.62 = 25.84 \text{ kNms}^2 \end{aligned}$$

From Equation C8B.41:

$$T_p = 3.1 \sqrt{\frac{J}{a}} = 3.1 \sqrt{\frac{25.84}{125.7}} = 1.41 \text{ seconds}$$

Step 8: Calculate the design response coefficient for the part.

From Equation C8.16 and the note to Step 8 in the general procedure in section C8.8.5.2:

$$C_i(T_p) = 2.0 \left(\frac{0.5}{T_p} \right)^{0.75} = 2.0 \left(\frac{0.5}{1.41} \right)^{0.75} = 0.92$$

From NZS 1170.5 Table 3.1 footnote for parts:

$$C_h(0) = 1.33$$

From NZS 1170.5 Table 3.3 for Cromwell: $Z = 0.24$.

From NZS 1170.5 Table 3.7: Because parts are calculated for $T = 0$ (and because actual periods are generally less than 1.5 seconds), $N(T=0, D) = 1$.

From NZS 1170.5 Table 3.5 for 1/500 annual probability of exceedance: $R_U = 1$.

From NZS 1170.5 Equation 3.1(1):

$$C(0) = C_h(0) \cdot Z \cdot R \cdot N(T, D) = 1.33 \times 0.24 \times 1 \times 1 = 0.32$$

See section C8C.3 for clarification of height h_i to be used for the floor height coefficient:

$$h_i = \text{height to base of cantilever} = 4.1 + 3.8 = 7.9 \text{ m}$$

From NZS 1170.5 Equation 8.3:

$$C_{Hi} = \left(1 + \frac{h_i}{6} \right) = \left(1 + \frac{7.9}{6} \right) = 2.32$$

From NZS 117.5 Equation 8.2(1):

$$C_p(T_p) = C(0) \cdot C_{Hi} \cdot C_i(T_p) = 0.32 \times 2.32 \times 0.92 = 0.68$$

Step 9: Calculate the Participation Factor.

From section C8B.3.4:

$$\gamma = \frac{(W_{Rect}y_{b,Rect} + W_{Tri}y_{b,Tri})h}{gJ} = \frac{(60.9 \times 1.6 + 26.5 \times 1.067) \times 3.2}{9.81 \times 25.83} = 1.59$$

See also Table C8B.2 where a value of $\gamma = 1.6$ is reported.

Step 10: Calculate the displacement demand D_{ph} .

From NZS 1170.5 Table 8.1 for Category P.1 where the part represents a hazard to human life outside the structure, $R_p = 1$.

From Equation C8.18:

$$D_{ph} = \gamma(T_p/2\pi)^2 C_p(T_p) \cdot R_p \cdot g = 1.59 \left(\frac{1.41}{2\pi} \right)^2 \times 0.68 \times 1 \times 9.81 = 0.534 \text{ m}$$

Step 11: Calculate %NBS:

From Equation C8.20 but adapted for a vertical cantilever as per step 6 of section C8.8.5.3:

$$\%NBS = 100 \times \Delta_m / D_{ph} = 30(\Delta_i / D_{ph}) = 100 \times \frac{0.075}{0.534} = 14\% \approx 15\%$$

Pediment is earthquake prone.

C8B.3.7 Pediment cantilever worked example 2

Consider the building shown in Figure C8B.5b. Assume the building is located in Taihape and is situated on shallow soil.

Step 1 and 2: Establish loading.

From Table C8.6, unit weight of masonry is 18 kN/m^3 .

Separate the pediment into two rectangular sections (tall and short) and a triangular section:

$$W_{Rect,Tall} = 18 \times 2.2 \times (1.35 + 1.35) \times 0.23 = 24.6 \text{ kN}$$

$$W_{Rect,Short} = 18 \times (1.6 + 1.6) \times 1.35 \times 0.23 = 17.9 \text{ kN}$$

$$W_{Tri} = 18 \times \frac{1}{2} \times (8.6 - 2 \times 1.6 - 2.2) \times 2.7 \times 0.23 = 17.9 \text{ kN}$$

No axial load acting on pediment:

$$P = 0$$

Step 3: Establish the effective thickness.

See Equation C8B.32:

$$t = \left(0.975 - 0.025 \frac{P}{W} \right) t_{nom} = 0.975 \times 0.230 = 0.224 \text{ m}$$

Step 4: Establish boundary conditions.

$$e_{b,Rect} = e_{b,Tri} = t/2 = 0.224/2 = 0.112 \text{ m}$$

$$y_{b,Rect,Tall} = h/2 = 2.70/2 = 1.35 \text{ m}$$

$$y_{b,Rect,Short} = h/2 = 1.35/2 = 0.68 \text{ m}$$

$$y_{b,Tri} = h/3 = 2.70/3 = 0.90 \text{ m}$$

Step 5: Establish the instability displacement.

From Equation C8B.37 with $P = 0$:

$$\begin{aligned} a &= W_{Rect,Tall} y_{b,Rect,Tall} + W_{Rect,Short} y_{b,Rect,Short} + W_{Tri} y_{b,Tri} \\ &= 24.6 \times 1.35 + 17.9 \times 0.68 + 17.9 \times 0.90 = 61.49 \text{ kNm} \end{aligned}$$

From Equation C8B.38 with $P = 0$:

$$\begin{aligned} b &= W_{Rect,Tall} e_{b,Rect,Tall} + W_{Rect,Short} e_{b,Rect,Short} + W_{Tri} e_{b,Tri} \\ &= (24.6 + 17.9 + 17.9) \times 0.112 = 6.76 \text{ kNm} \end{aligned}$$

From Equation C8B.40:

$$\Delta_i = Ah = \frac{bh}{a} = \frac{6.76 \times 2.7}{61.49} = 0.297 \text{ m}$$

Step 6: Determine the maximum usable deflection at the top of the parapet:

$$\Delta_m = 0.3\Delta_i = 0.3 \times 0.297 = 0.089 \text{ m}$$

Step 7: Evaluate the period:

From C8B.3.4 with $P = 0$:

$$\text{Recall } J_{Rect} = \frac{W_{Rect}}{3g} (h^2 + t^2) \text{ and } = \frac{W_{Tri}}{12g} (2h^2 + 3t^2)$$

$$\begin{aligned} J &= J_{Rect,Tall} + J_{Rect,Short} + J_{Tri} \\ &= \frac{24.6}{3 \times 9.81} \times (2.7^2 + 0.112^2) + \frac{17.9}{3 \times 9.81} \times (1.35^2 + 0.112^2) \\ &\quad + \frac{17.9}{12 \times 9.81} \times (2 \times 2.7^2 + 3 \times 0.112^2) = 6.104 + 1.116 + 2.223 \\ &= 9.44 \text{ kNms}^2 \end{aligned}$$

From Equation C8B.41:

$$T_p = 3.1 \sqrt{\frac{J}{a}} = 3.1 \sqrt{\frac{9.44}{61.49}} = 1.21 \text{ seconds}$$

Step 8: Calculate the design response coefficient for the part.

From Equation C8.16 and the note to Step 8 in the general procedure in section C8.8.5.2:

$$C_i(T_p) = 2.0 \left(\frac{0.5}{T_p} \right)^{0.75} = 2.0 \left(\frac{0.5}{1.21} \right)^{0.75} = 1.03$$

From NZS 1170.5 Table 3.1 footnote for parts:

$$C_h(0) = 1.33$$

From NZS 1170.5 Table 3.3 for Taihape: $Z = 0.33$.

From NZS 1170.5 Table 3.7: Because parts are calculated for $T = 0$ (and because actual periods are generally less than 1.5 seconds), $N(T=0,D) = 1$.

From NZS 1170.5 Table 3.5 for 1/500 annual probability of exceedance: $R_U = 1$.

From NZS 1170.5 Equation 3.1(1):

$$C(0) = C_h(0) \cdot Z \cdot R \cdot N(T, D) = 1.33 \times 0.33 \times 1 \times 1 = 0.44$$

See section C8C.3 for clarification of height h_i to be used for the floor height coefficient:

$$h_i = \text{height to base of cantilever} = 4.1 + 3.8 = 7.9 \text{ m}$$

From NZS 1170.5 Equation 8.3:

$$C_{Hi} = \left(1 + \frac{h_i}{6}\right) = \left(1 + \frac{7.9}{6}\right) = 2.32$$

From NZS 117.5 Equation 8.2(1):

$$C_p(T_p) = C(0) \cdot C_{Hi} \cdot C_i(T_p) = 0.44 \times 2.32 \times 1.03 = 1.05$$

Step 9: Calculate the Participation Factor.

From section C8B.3.4:

$$\begin{aligned} \gamma &= \frac{(W_{Rect,Tall} y_{b,Rect,Tall} + W_{Rect,Short} y_{b,Rect,Short} + W_{Tri} y_{b,Tri}) h}{gJ} \\ &= \frac{(24.6 \times 1.35 + 17.9 \times 0.68 + 17.9 \times 0.90) \times 2.7}{9.81 \times 9.44} = 1.79 \end{aligned}$$

Step 10: Calculate the displacement demand D_{ph} .

From NZS 1170.5 Table 8.1 for Category P.1 where the part represents a hazard to human life outside the structure, $R_p = 1$.

From Equation C8.18:

$$D_{ph} = \gamma (T_p / 2\pi)^2 C_p(T_p) \cdot R_p \cdot g = 1.79 \left(\frac{1.21}{2\pi}\right)^2 \times 1.05 \times 1 \times 9.81 = 0.684 \text{ m}$$

Step 11: Calculate %NBS:

From Equation C8.20 but adapted for a vertical cantilever as per step 6 of section C8.8.5.3:

$$\%NBS = 100 \times \Delta_m / D_{ph} = 30 (\Delta_i / D_{ph}) = 100 \times \frac{0.089}{0.684} = 13\% \approx 15\%$$

Pediment is earthquake prone.

C8B.4 Gable Walls

See section C8.8.5.4 for a description of the different failure modes that occur for masonry gables, including supporting photographs of post-earthquake damage.

Note:

Where a roof or ceiling connection is based on bearing only (ie friction) then it should be assumed that the potential for vertical acceleration makes such a connection unreliable and that such a connection should be discounted.

Note:

As reported in Table C8B.2, the value of the Participation Factor for a triangular element as per gable failure mechanism cases 1, 2 and 3 has a maximum of $\gamma = 2$ for $t \ll h$ and $P = 0$.

Note:

According to Galvez et al. (2022), when assessing the vulnerability of a façade that is rocking against return walls, the capacity can be considered equal to that of an equivalent two-sided free standing rocking block, without considering the effect of impact between the rocking wall and the transverse structure.

C8B.4.1 Vertical cantilever gables

Section C8B.3 for vertical cantilevers may be applied for gables also, by applying the following adaptations and with the configuration shown in Figure C8B.6:

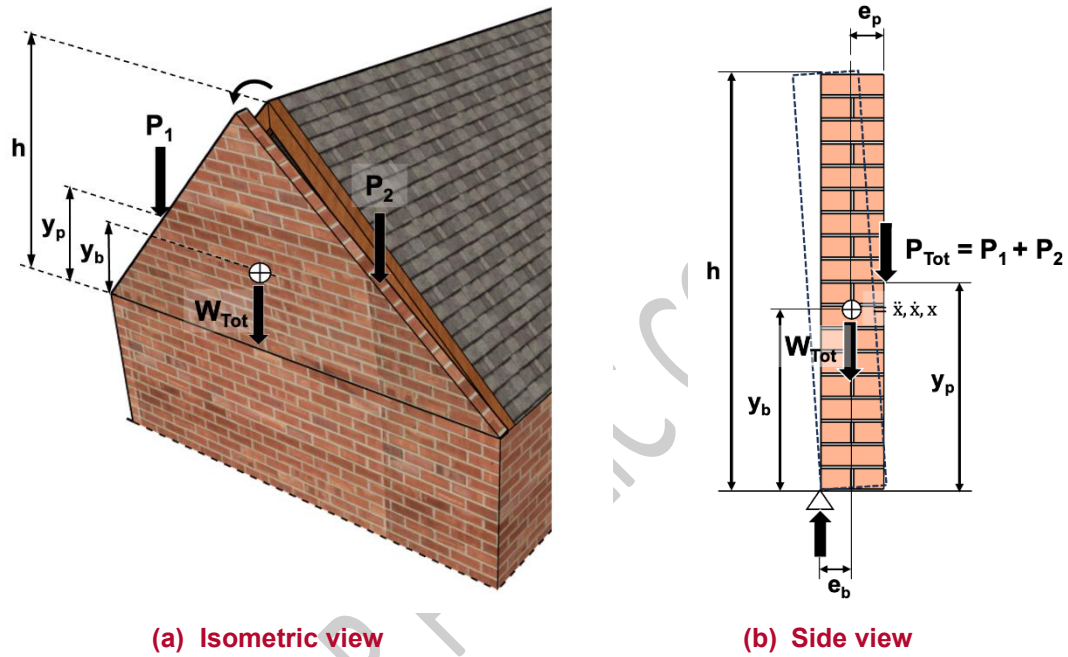


Figure C8B.6: Vertical cantilever gable configuration (see also Figure C8.72)

$$a = W_{Tot}y_b + P_{Tot}y_p \quad \dots\text{C8B.48}$$

$$b = W_{Tot}e_b + P_{Tot}(e_b + e_p) \quad \dots\text{C8B.49}$$

$$J = \frac{W_{Tot}}{18g} h^2 + \frac{W_{Tot}}{g} (y_b^2 + e_b^2) + \frac{P_{Tot}}{g} [y_p^2 + (e_b + e_p)^2] \quad \dots\text{C8B.50}$$

$$\gamma = \frac{W_{Tot}h^2}{3gJ} \quad \dots\text{C8B.51}$$

For regular triangular gables with $y_b = h/3$ and $y_p = h/2$, Equation C8B.48 simplifies to:

$$a = \frac{h}{6} (2W_{Tot} + 3P_{Tot}) \quad \dots\text{C8B.52}$$

For the case when P_{Tot} can travel with the rotating gable, $e_p = 0$ and $e_b = t/2$ and Equation C8B.49 simplifies to:

$$b = \frac{t}{2} (W_{Tot} + P_{Tot}) \quad \dots C8B.53$$

For the case when P_{Tot} is restrained from travelling with the rotating gable, $e_p = t/2$ and $e_b = t/2$ and Equation C8B.49 simplifies to:

$$b = \frac{t}{2} (W_{Tot} + 2P_{Tot}) \quad \dots C8B.54$$

Note:

Figure C8B.6 shows an isosceles gable configuration (see also Figure C8.72). However, the formulation applies for all triangular gables independent of their specific geometry.

In the above equations W_{Tot} and P_{Tot} are total weights for the entire gable and for the full roof, not weights per unit length.

C8B.4.1.1 Vertical cantilever gable worked example

Consider the façade gable wall shown in Figure C8B.7a. Assume that the roof provides no restraint to the gable but that reliable anchorage exists at the ceiling height (base of gable). Note that the wall has thickenings at the two edges that terminate at the height of the base of the gable. There are no changes in thickness up the height of the gable, nor any openings, buttresses, or lintels that might suggest that partial gable failure may occur. Therefore the gable is expected to fail as a triangular cantilever rocking about its base.

The building is located in Masterton and is situated on shallow soil.

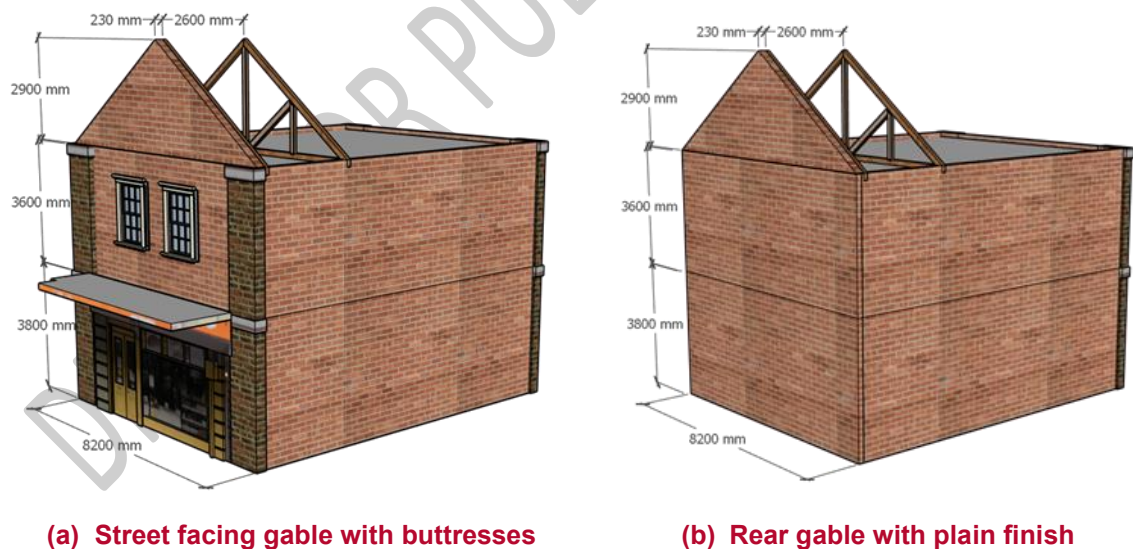


Figure C8B.7: Gable wall used for worked example

The calculations follow the procedure explained in section C8.8.5.3.

Step 1 and 2: Establish loading.

From Table C8.6, unit weight of masonry is 18 kN/m^3 .

Assume roof load is 1 kPa .

$$W_{Tot} = 18 \times \left(\frac{1}{2} \times 8.2 \times 2.9\right) \times 0.23 = 49.2 \text{ kN}$$

$$\text{Roof pitch} = \tan^{-1} \left(\frac{2.9}{8.2/2} \right) = 35.3^\circ$$

$$P_{Tot} = 1.0 \times \left(\frac{8.2}{\cos(35.3^\circ)} \right) \times \left(\frac{2.6}{2} \right) = 13.1 \text{ kN}$$

Step 3: Establish the effective thickness.

$$t = \left(0.975 - 0.025 \frac{P}{W} \right) t_{nom} = \left(0.975 - 0.025 \times \frac{13.1}{49.2} \right) \times 0.230 = 0.223 \text{ m}$$

Step 4: Establish boundary conditions.

Assume that the roof is restrained from rotating with the gable. Therefore:

$$e_p = t/2 = 0.223/2 = 0.111 \text{ m}$$

$$e_b = t/2 = 0.223/2 = 0.111 \text{ m}$$

$$y_b = h/3 = 2.9/3 = 0.967 \text{ m}$$

$$y_p = h/2 = 2.9/2 = 1.45 \text{ m.}$$

Step 5: Establish the instability displacement. Recall for this case that $P \neq 0$ and we are considering rocking of the entire triangular gable rather than a uniform 1 m strip, so simplifications given for rocking parapets do not apply.

From Equation C8B.52:

$$a = \frac{h}{6} (2W_{Tot} + 3P_{Tot}) = \frac{2.9}{6} (2 \times 49.2 + 3 \times 13.1) = 66.6 \text{ kNm}$$

The roof load is assessed to not travel with the parapet as rocking occurs. Therefore, from Equation C8B.54:

$$b = \frac{t}{2} (W_{Tot} + 2P_{Tot}) = \frac{0.23}{2} (49.2 + 2 \times 13.1) = 8.67 \text{ kNm}$$

From Equation C8B.40:

$$\Delta_i = Ah = \frac{bh}{a} = \frac{[We_b + P(e_b + e_p)]h}{Wy_b + Ph} = \frac{8.67 \times 2.9}{66.6} = 0.378 \text{ m}$$

Step 6: Determine the maximum usable deflection at the top of the gable:

$$\Delta_m = 0.3\Delta_i = 0.3 \times 0.378 = 0.113 \text{ m}$$

Step 7: Evaluate the period:

From Equation C8B.50:

$$\begin{aligned}
J &= \frac{W_{Tot}}{18g} h^2 + \frac{W_{Tot}}{g} (y_b^2 + e_b^2) + \frac{P_{Tot}}{g} [y_p^2 + (e_b + e_p)^2] \\
&= \frac{49.2}{18 \times 9.81} 2.9^2 + \frac{49.2}{9.81} (0.967^2 + 0.111^2) \\
&\quad + \frac{13.1}{9.81} [1.45^2 + (0.111 + 0.111)^2] = 2.343 + 4.752 + 2.874 \\
&= 9.97 \text{ kNms}^2
\end{aligned}$$

From Equation C8B.41:

$$T_p = 3.1 \sqrt{\frac{J}{a}} = 3.1 \sqrt{\frac{9.97}{66.6}} = 1.20 \text{ seconds}$$

Step 8: Calculate the design response coefficient for the part.

From Equation C8.16 and the note to Step 8 in the general procedure in section C8.8.5.2:

$$C_i(T_p) = 2.0 \left(\frac{0.5}{T_p} \right)^{0.75} = 2.0 \left(\frac{0.5}{1.20} \right)^{0.75} = 1.04$$

From NZS 1170.5 Table 3.1 footnote for parts:

$$C_h(0) = 1.33$$

From NZS 1170.5 Table 3.3 for Masterton: $Z = 0.42$ and $D = 6-10$ km.

From NZS 1170.5 Table 3.7: Because parts are calculated for $T = 0$ (and because actual periods are generally less than 1.5 seconds), $N(T=0, D=6-10) = 1$.

From NZS 1170.5 Table 3.5 for 1/500 annual probability of exceedance: $R_U = 1$.

From NZS 1170.5 Equation 3.1(1):

$$C(0) = C_h(0) \cdot Z \cdot R \cdot N(T, D) = 1.33 \times 0.42 \times 1 \times 1 = 0.56$$

See section C8C.3 for clarification of height h_i to be used for the floor height coefficient:

$$h_i = \text{height to base of cantilever} = 3.8 + 3.6 = 7.4 \text{ m}$$

From NZS 1170.5 Equation 8.3:

$$C_{Hi} = \left(1 + \frac{h_i}{6} \right) = \left(1 + \frac{7.4}{6} \right) = 2.23$$

From NZS 1170.5 Equation 8.2(1):

$$C_p(T_p) = C(0) \cdot C_{Hi} \cdot C_i(T_p) = 0.56 \times 2.23 \times 1.04 = 1.30$$

Step 9: Calculate the Participation Factor.

From Equation C8B.51:

$$\gamma = \frac{W_{Tot} h^2}{3gJ} = \frac{49.2 \times 2.9^2}{3 \times 9.81 \times 9.97} = 1.41$$

Step 10: Calculate the displacement demand D_{ph} .

From NZS 1170.5 Table 8.1 for Category P.1 where the part represents a hazard to human life outside the structure, $R_p = 1$.

From Equation C8.18:

$$D_{ph} = \gamma(T_p/2\pi)^2 C_p(T_p) \cdot R_p \cdot g = 1.41 \left(\frac{1.20}{2\pi} \right)^2 \times 1.30 \times 1 \times 9.81 = 0.656 \text{ m}$$

Step 11: Calculate %NBS:

From Equation C8.20 but adapted for a vertical cantilever as per step 6 of section C8.8.5.3:

$$\%NBS = 100 \times \Delta_m / D_{ph} = 30(\Delta_i / D_{ph}) = 100 \times \frac{0.113}{0.656} = 17\% \approx 20\%$$

The unsecured gable wall is earthquake prone.

C8B.4.1.2 Return wall separation cantilever worked example

Consider the façade gable wall shown in Figure C8B.8. Assume that the roof provides no restraint to the gable but that reliable anchorage exists at the mid-height floor (base of second storey). The wall is to be assessed for return wall separation with the entire top storey and gable acting as a cantilever.

The building is located in Motueka and is situated on shallow soil. The rafter spacing is 2.8 m.

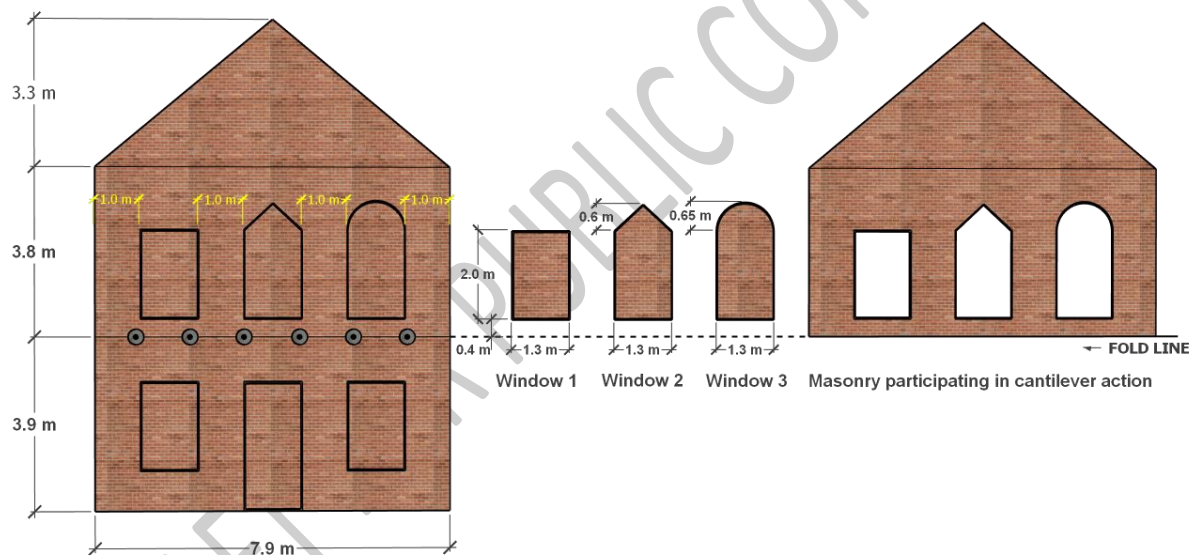


Figure C8B.8: Gable wall used for worked example

Note:

In Figure C8B.8 above superposition is used to begin by considering the rotational mass moment of inertia of the upper storey wall and gable without windows (image on left), then separately accounting for the rotational mass moment of inertia of the windows (images in centre), and subtracting the second value from the first to obtain the true rotational mass moment of inertia of the penetrated wall (image on right). The calculations below show that the windows contributed less than 6% to the calculated value of the final rotational mass moment of inertia. For the calculation of the rocking period, accounting for the influence of the windows affected the answer by 2%.

The calculations follow the procedure explained in section C8.8.5.3.

Step 1 and 2: Establish loading.

From Table C8.6, unit weight of masonry is 18 kN/m^3 .

Assume roof load is 1 kPa .

$$W_{Gable} = 18 \times \left(\frac{1}{2} \times 7.9 \times 3.3 \right) \times 0.23 = 54.0 \text{ kN}$$

$$W_{Upper\ storey} = 18 \times (7.9 \times 3.8) \times 0.23 = 124.3 \text{ kN}$$

$$W_{Window\ 1} = 18 \times (1.3 \times 2.0) \times 0.23 = 10.8 \text{ kN}$$

$$W_{Window\ 2} = 18 \times \left(1.3 \times 2.0 + \frac{1}{2} \times 1.3 \times 0.6 \right) \times 0.23 = 10.8 + 1.6 = 12.4 \text{ kN}$$

$$W_{Window\ 3} = 18 \times \left(1.3 \times 2.0 + \frac{\pi \times 0.65^2}{2} \right) \times 0.23 = 10.8 + 2.7 = 13.5 \text{ kN}$$

$$W_{Tot} = 54.0 + 124.3 - (10.8 + 12.4 + 13.5) = 141.6 \text{ kN}$$

$$Roof\ pitch = \tan^{-1} \left(\frac{3.3}{7.9/2} \right) = 39.9^\circ$$

$$P_{Tot} = 1.0 \times \left(\frac{7.9}{\cos(39.9^\circ)} \right) \times \left(\frac{2.8}{2} \right) = 14.4 \text{ kN}$$

Step 3: Establish the effective thickness.

$$t = \left(0.975 - 0.025 \frac{P}{W} \right) t_{nom} = \left(0.975 - 0.025 \times \frac{14.4}{141.6} \right) \times 0.230 = 0.224 \text{ m}$$

Step 4: Establish boundary conditions.

Assume that the roof is restrained from rotating with the gable. Therefore:

$$e_p = t/2 = 0.224/2 = 0.112 \text{ m}$$

$$e_b = t/2 = 0.224/2 = 0.112 \text{ m}$$

$$y_{b,gable} = 3.8 + \frac{3.3}{3} = 4.90 \text{ m}$$

$$y_{b,upper\ storey} = \frac{3.8}{2} = 1.90 \text{ m}$$

$$y_{b>window\ 1} = 0.4 + \frac{2.0}{2} = 1.4 \text{ m}$$

$$y_{b>window\ 2} = \frac{\left(1.3 \times 2.0 \times 1.4 + \frac{1}{2} \times 1.3 \times 0.6 \times \left(2.4 + \frac{0.6}{3} \right) \right)}{\left(1.3 \times 2.0 + \frac{1}{2} \times 1.3 \times 0.6 \right)} = \frac{3.64 + 1.014}{2.99} = 1.56 \text{ m}$$

$$y_{b,window\ 3} = \frac{\left(1.3 \times 2.0 \times 1.4 + \frac{\pi}{2} \times 0.65^2 \times \left(2.4 + \frac{4 \times 0.65}{3\pi}\right)\right)}{\left(1.3 \times 2.0 + \frac{\pi}{2} \times 0.65^2\right)} = \frac{3.64 + 1.776}{3.264} = 1.66\ m$$

Step 5: Establish the instability displacement. Recall for this case that $P \neq 0$ and we are considering rocking of the entire triangular gable rather than a uniform 1 m strip, so simplifications given for rocking parapets do not apply.

From Equation C8B.37 and the explanation that follows after Equation C8B.37:

$$a = \{54.0 \times 4.90 + 124.3 \times 1.90 - 10.8 \times 1.4 - 12.4 \times 1.56 - 13.5 \times 1.66\} + 14.4 \times (3.8 + 3.3) = 443.9 + 102.2 = 546.1\ kNm$$

The roof load is assessed to not travel with the parapet as rocking occurs. Therefore, from Equation C8B.38:

$$b = W_{Tot}e_b + P_{Tot}(e_b + e_p) = 141.6 \times 0.112 + 14.4 \times (0.112 + 0.112) = 30.5\ kNm$$

From Equation C8B.40:

$$\Delta_i = Ah = \frac{bh}{a} = \frac{30.5 \times (3.8 + 3.6)}{546.1} = 0.413\ m$$

Step 6: Determine the maximum usable deflection at the top of the gable:

$$\Delta_m = 0.3\Delta_i = 0.3 \times 0.413 = 0.124\ m$$

Step 7: Evaluate the period:

From Equation C8B.39 and Table C8B.2, applying parallel axes theorem and assuming $t/h \approx 0$:

$$J_{Gable} = \frac{54.0}{36 \times 9.81} \times 2 \times 3.3^2 + \frac{54.0}{9.81} \times \left(3.8 + \frac{3.3}{3}\right)^2 = 3.3 + 132.2 = 135.5\ kNms^2$$

$$J_{Upper\ storey} = \frac{124.3}{3 \times 9.81} \times 3.8^2 = 61.0\ kNms^2$$

$$J_{Window\ 1} = \frac{10.8}{12 \times 9.81} \times 2.0^2 + \frac{10.8}{9.81} \times 1.4^2 = 0.4 + 2.2 = 2.6\ kNms^2$$

$$J_{Window\ 2} = \frac{10.8}{12 \times 9.81} \times 2.0^2 + \frac{10.8}{9.81} \times 1.4^2 + \frac{1.6}{36 \times 9.81} \times 0.6^2 + \frac{1.6}{9.81} \times \left(2.4 + \frac{0.6}{3}\right)^2 = 0.4 + 2.2 + 0 + 1.1 = 3.7\ kNms^2$$

$$J_{Window\ 3} = \frac{10.8}{12 \times 9.81} \times 2.0^2 + \frac{10.8}{9.81} \times 1.4^2 + \frac{2.7}{4 \times 9.81} \times (0.65^2 + 0.224^2) + \frac{2.7}{9.81} \times (2.4 + 0.28)^2 = 0.4 + 2.2 + 0 + 2.0 = 4.6\ kNms^2$$

$$J_P = \frac{14.4}{9.81} (7.1^2 + (0.112 + 0.112)^2) = 3.7\ kNms^2$$

$$J_{Tot} = 135.5 + 61.0 - 2.6 - 3.7 - 4.6 + 3.7 = 189.3\ kNms^2$$

Note:

From observation it is obvious that neither the windows nor the roof load significantly influenced J . The data is presented here for demonstration purposes.

From Equation C8B.41:

$$T_p = 3.1 \sqrt{\frac{J}{a}} = 3.1 \sqrt{\frac{189.3}{546.1}} = 1.83 \text{ seconds}$$

Step 8: Calculate the design response coefficient for the part.

From Equation C8.16 and the note to Step 8 in the general procedure in section C8.8.5.2:

$$C_i(T_p) = \frac{1.32}{T_p} = \frac{1.32}{1.83} = 0.72$$

From NZS 1170.5 Table 3.1 footnote for parts:

$$C_h(0) = 1.33$$

From NZS 1170.5 Table 3.3 for Motueka: $Z = 0.26$.

From NZS 1170.5 Table 3.7: No known faults nearby $N(T=0, D) = 1$.

From NZS 1170.5 Table 3.5 for 1/500 annual probability of exceedance: $R_U = 1$.

From NZS 1170.5 Equation 3.1(1):

$$C(0) = C_h(0) \cdot Z \cdot R \cdot N(T, D) = 1.33 \times 0.26 \times 1 \times 1 = 0.35$$

See section C8C.3 for clarification of height h_i to be used for the floor height coefficient:

$$h_i = \text{height to base of cantilever} = 3.9 \text{ m}$$

From NZS 1170.5 Equation 8.3:

$$C_{Hi} = \left(1 + \frac{h_i}{6}\right) = \left(1 + \frac{3.9}{6}\right) = 1.65$$

From NZS 117.5 Equation 8.2(1):

$$C_p(T_p) = C(0) \cdot C_{Hi} \cdot C_i(T_p) = 0.35 \times 1.65 \times 0.72 = 0.42$$

Step 9: Calculate the Participation Factor.

Use general relationship and establish centroid height of actual shape:

$$y_b = \frac{54.0 \times 4.90 + 124.3 \times 1.90 - 10.8 \times 1.4 - 12.4 \times 1.56 - 13.5 \times 1.66}{54.0 + 124.3 - 10.8 - 12.4 - 13.5} = \frac{443.9}{141.6} = 3.13 \text{ m}$$

From Equation C8B.51:

$$\gamma = \frac{W_{Tot} y_b h}{gJ} = \frac{141.6 \times 3.13 \times 7.1}{9.81 \times 189.3} = 1.69$$

Step 10: Calculate the displacement demand D_{ph} .

From NZS 1170.5 Table 8.1 for Category P.1 where the part represents a hazard to human life outside the structure, $R_p = 1$.

From Equation C8.18:

$$D_{ph} = \gamma(T_p/2\pi)^2 C_p(T_p) \cdot R_p \cdot g = 1.69 \left(\frac{1.83}{2\pi} \right)^2 \times 0.42 \times 1 \times 9.81 = 0.591 \text{ m}$$

Step 11: Calculate %NBS:

From Equation C8.20 but adapted for a vertical cantilever as per step 6 of section C8.8.5.3:

$$\%NBS = 100 \times \Delta_m / D_{ph} = 30(\Delta_i / D_{ph}) = 100 \times \frac{0.124}{0.591} = 21.0 \approx 20\%$$

The unsecured upper storey wall is earthquake prone.

C8B.4.2 Vertically spanning gables

C8B.4.2.1 Symmetrical (isosceles) gable configuration

Figure C8B.9 shows the configuration for a full isosceles-triangular gable (Figure C8B.9a) and for a half-gable with a free vertical edge (Figure C8B.9a). The following mass moment of inertia can be derived for both cases, formed similarly as for vertically spanning walls. The combined mass moment of inertia is calculated by summing the mass moment of inertia of the top and bottom triangles shown in Figure C8B.9b, each calculated about their own centroids. The roof load P_1 is the total load acting on the right-angle triangle shown. The parallel axis theorem is then applied to find the mass moment of inertia about the centre of rotation at the edge of the wall:

$$J = J_{bo} + J_{to} + \frac{1}{g} \{ W_b (e_b^2 + y_b^2) + W_t [(e_o + e_t + e_b)^2 + y_t^2] + P_1 (e_o + e_t + e_b + e_p)^2 \} \quad \dots \text{C8B.55}$$

where J_{bo} and J_{to} are the mass moment of inertia of a triangle about their centroids and $P_{Tot,h}$ is the total roof weight acting on the half triangle.

$$J_{bo} = J_{to} = \frac{W_b}{18g} \cdot (h/2)^2 = \frac{W_t}{18g} \cdot (h/2)^2 \quad \dots \text{C8B.56}$$

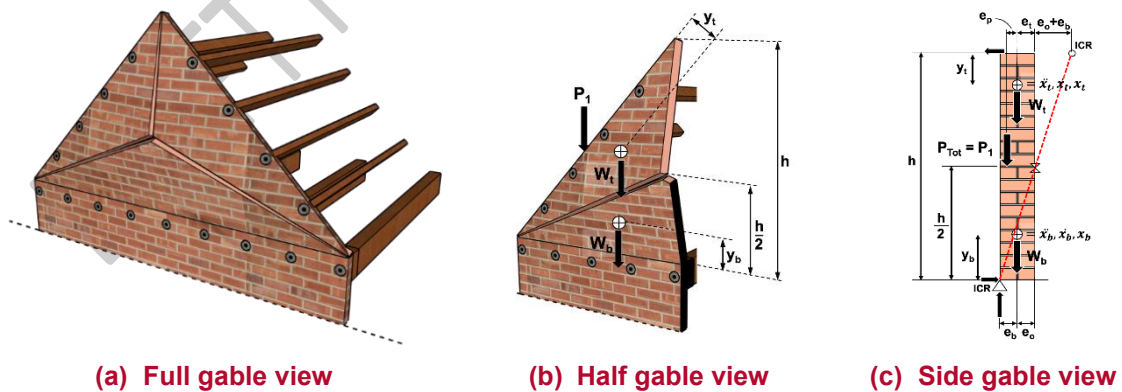


Figure C8B.9: Vertically spanning gable (see Figure C8.72 for definition of P_1)

Note:

In the above equations W_t , W_b and P_1 are total weights, not weights per unit length. Also note that the participation factor now has a maximum value of 2.0 ($t \ll h, P = 0$).

Note:

The failure mechanism shown in Figure C8B.9 can also be applied to a sawtooth right-angle gable when the vertical face is mostly composed of windows and hence no restraint is provided to the vertical edge (see Figure C8.74b).

Virtual work has been used to calculate C_m , resulting in:

$$C_m = \frac{W_b e_b + W_t(e_o + e_t + e_b) + P_1(e_o + e_t + e_b + e_p)}{W_b y_b + W_t y_t} = \frac{b}{W_b y_b + W_t y_t} \quad \dots \text{C8B.57}$$

and the expression for the participation factor results in:





$$\gamma = \frac{(W_t + W_b)h^2}{12gJ} \quad \dots \text{C8B.58}$$

Simplifications can be made where the thickness of the gable is constant and there are no openings. Further approximations can then be applied:

- The weight of each triangular part (top and bottom triangles) is half the total weight of the half gable, W .
- $e_o = e_t = t/2$
- $y_b = y_t = h/6$

The term b is the same as for vertically spanning walls because it is influenced only by the horizontal distance of the masses to the ICR. However, a is different than for the case of rectangular vertically spanning walls and therefore Δ_i changes. Simplified expressions for regular walls are presented in Table C8B.3.

Table C8B.3: Static instability deflection for uniform gables – various boundary conditions

Boundary condition number	0	1	2	3
				
e_p	0	0	$t/2$	$t/2$
e_b	0	$t/2$	0	$t/2$
b	$(W/2 + P)t$	$(W + 3P/2)t$	$(W/2 + 3P/2)t$	$(W + 2P)t$
a	$\frac{h(2W + 3P)}{6}$	$\frac{h(2W + 3P)}{6}$	$\frac{h(2W + 3P)}{6}$	$\frac{h(2W + 3P)}{6}$
$\Delta_i = bh/(2a)$	$\frac{3t(W/2 + P)}{2W + 3P}$	$\frac{3t(W + 3P/2)}{2W + 3P}$	$\frac{3t(W/2 + 3P/2)}{2W + 3P}$	$\frac{3t(W + 2P)}{2W + 3P}$
J	$\frac{W}{24g} (h^2 + 12t^2) + \frac{Pt^2}{g}$	$\frac{W}{24g} (h^2 + 30t^2) + \frac{9Pt^2}{4g}$	$\frac{W}{24g} (h^2 + 27t^2) + \frac{9Pt^2}{4g}$	$\frac{W}{24g} (h^2 + 30t^2) + \frac{4Pt^2}{g}$
C_m	$\frac{t}{h} (3 + 6 \frac{P}{W})$	$\frac{t}{h} (6 + 9 \frac{P}{W})$	$\frac{t}{h} (3 + 9 \frac{P}{W})$	$\frac{t}{h} (6 + 12 \frac{P}{W})$

Note:

1. W refers to the total weight of a half gable. Referring to Figure C8B.9, $W = W_t + W_b$. P refers to the total roof load on a half gable. Referring to Figure C8B.9, $P = P_t$.
2. The boundary conditions of the gables shown above are for clockwise potential rocking.
3. The top eccentricity, e_t , is not related to a boundary condition, so is not included in the table. The top eccentricity, e_t , is the horizontal distance from the central pivot point to the centre of mass of the top block which is not related to a boundary condition.
4. The eccentricities shown in the sketches are for the positive sense. Where the top eccentricity is in the other sense e_p should be entered as a negative number.

C8B.4.2.2 Vertical spanning symmetrical (isosceles) gable worked example

Assume the same gable as shown in Figure C8B.7a but with the anchorage conditions shown in Figure C8B.9a.

Step 1 and 2: Establish loading.

From C8B.4.2.2 we have $W_{Tot} = 49.2$ kN and $P_{Tot} = 13.1$ kN. By observation (see Figure C8B.9a):

$$W_b = W_t = \frac{W_{Tot}}{4} = \frac{49.2}{4} = 12.3 \text{ kN}$$

$$W_{half \text{ gable}} = \frac{W_{Tot}}{2} = 24.6 \text{ kN}$$

$$P_1 = \frac{P_{Tot}}{2} = \frac{13.1}{2} = 6.6 \text{ kN}$$

Step 3: Establish the effective thickness.

See Equation C8B.32:

$$t = \left(0.975 - 0.025 \frac{P}{W}\right) t_{\text{nom}} = \left(0.975 - 0.025 \times \frac{6.6}{24.6}\right) \times 0.230 = 0.223 \text{ m}$$

Step 4: Establish boundary conditions.

Assume condition 3 boundary conditions (see Table C8B.3). Therefore:

$$e_b = t/2 = 0.223/2 = 0.111 \text{ m}$$

$$e_o = e_t = t/2 = 0.111 \text{ m}$$

$$y_b = y_t = h/6 = 2.9/6 = 0.483 \text{ m}$$

Step 5: Establish the instability displacement.

From Table C8B.3, condition 3:

$$a = \frac{h(2W + 3P)}{6} = \frac{2.9 \times (2 \times 24.6 + 3 \times 6.6)}{6} = 33.35 \text{ kNm}$$

$$b = (W + 2P)t = (24.6 + 2 \times 6.6) \times 0.223 = 8.43 \text{ kNm}$$

Step 6: Determine the maximum usable deflection for vertically spanning gable:

$$\Delta_m = 0.6\Delta_i = 0.6 \times 0.367 = 0.220 \text{ m}$$

Step 7: Evaluate the period:

From Equation C8B.56:

$$J_{bo} = J_{to} = W_b \cdot \frac{(h/2)^2}{18g} = W_t \cdot \frac{(h/2)^2}{18g} = 12.3 \times \frac{(2.9/2)^2}{18 \times 9.81} = 0.146 \text{ kNms}^2$$

From Equation C8B.55:

$$\begin{aligned} J &= J_{bo} + J_{to} + \frac{1}{g} \{W_b (e_b^2 + y_b^2) + W_t [(e_o + e_t + e_b)^2 + y_t^2] + P_1 (e_o + e_t + e_b + e_p)^2\} \\ &= 0.146 + 0.146 + \frac{1}{9.81} \{12.3 (0.111^2 + 0.483^2) \\ &\quad + 12.3 [(0.111 + 0.111 + 0.111)^2 + 0.483^2] \\ &\quad + 6.6 (0.111 + 0.111 + 0.111 + 0.111)^2\} \\ &= 0.292 + \frac{1}{9.81} \{3.021 + 4.233 + 1.301\} = 1.164 \text{ kNms}^2 \end{aligned}$$

From Equation C8B.28:

$$T_p = 4.07 \sqrt{\frac{J}{a}} = 4.07 \sqrt{\frac{1.164}{33.35}} = 0.76 \text{ seconds}$$

Step 8: Calculate the design response coefficient for the part.

From Equation C8.16 and the note to Step 8 in the general procedure in section C8.8.5.2:

$$C_i(T_p) = 2.0 \left(\frac{0.5}{T_p}\right)^{0.75} = 2.0 \left(\frac{0.5}{0.76}\right)^{0.75} = 1.46$$

As for the earlier example in section C8B.4.1.1:

$$C(0) = C_h(0).Z.R.N(T,D) = 1.33 \times 0.42 \times 1 \times 1 = 0.56$$

See section C8C.3 or note to step 8 for clarification of height h_i to be used for the floor height coefficient. For walls spanning vertically and held at the top, h_i should be taken as the average of the heights of the points of support.

$$h_i = \text{height to middle of gable} = 3.8 + 3.6 + \frac{2.9}{2} = 8.85 \text{ m}$$

From NZS 1170.5 Equation 8.3:

$$C_{Hi} = \left(1 + \frac{h_i}{6}\right) = \left(1 + \frac{8.85}{6}\right) = 2.48$$

From NZS 117.5 Equation 8.2(1):

$$C_p(T_p) = C(0) \cdot C_{Hi} \cdot C_i(T_p) = 0.56 \times 2.48 \times 1.46 = 2.03$$

Step 9: Calculate the Participation Factor.

From Equation C8B.58:

$$\gamma = \frac{(W_t + W_b)h^2}{12gJ} = \frac{(12.3 + 12.3) \times 2.9^2}{12 \times 9.81 \times 1.164} = 1.51$$

Step 10: Calculate the displacement demand D_{ph} .

As for the earlier example in section C8B.4.1.1, $R_P = 1$.

From Equation C8.18:

$$D_{ph} = \gamma(T_p/2\pi)^2 C_p(T_p) \cdot R_p \cdot g = 1.51 \times \left(\frac{0.76}{2\pi}\right)^2 \times 2.03 \times 1 \times 9.81 = 0.440 \text{ m}$$

From Equation C8.20:

$$\%NBS = 100 \times \Delta_m / D_{ph} = 60(\Delta_i / D_{ph}) = 100 \times \frac{0.220}{0.440} = 50\%$$

The secured gable wall is not earthquake prone.

C8B.4.2.3 Non-symmetrical (scalene) gable configuration

Figure C8B. shows the configuration for any scalene shaped gable. The following mass moment of inertia is calculated by summing the mass moment of inertia of the three triangles formed after cracking the gable with crack following the bisectors of the corners, each sub-triangle calculated about their own centroids. The parallel axis theorem is then applied to find the mass moment of inertia about the centre of rotation at the edge of the wall.

$$J = J_a + J_b + J_c + \frac{1}{g} \{ W_b (e_b^2 + y_b^2) + W_a [(e_o + e_t + e_b)^2 + y_a^2] + W_c [(e_o + e_t + e_b)^2 + y_c^2] + P(e_o + e_t + e_b + e_p)^2 \} \quad \dots \text{C8.55}$$

where J_a , J_b and J_c are the mass moment of inertia of the sub-triangles about their centroids, and $y_a = y_b = y_c = h_s/3$, where h_s is the height of the three triangles, and is calculated as $h_s = \frac{hb}{a+b+c}$.

$$J_a = W_a \cdot h_s^2 / 18g \quad \dots C8.56$$

$$J_b = W_b \cdot h_s^2 / 18g \quad \dots C8.57$$

$$J_c = W_c \cdot h_s^2 / 18g \quad \dots C8.58$$

where the weight of each sub-triangle can be calculated through the area as $A = (a, b \text{ or } c) \cdot h_s / 2$.

Resulting in

$$J = \frac{W_{Tot} h^2}{18g} + \frac{W_b}{g} (e_b^2 + \frac{h_s^2}{9}) + \frac{(W_a + W_c)}{g} \left[(e_o + e_t + e_b)^2 + \frac{h_s^2}{9} \right] + \frac{P}{g} (e_o + e_t + e_b + e_p)^2 \quad \dots C8.59$$

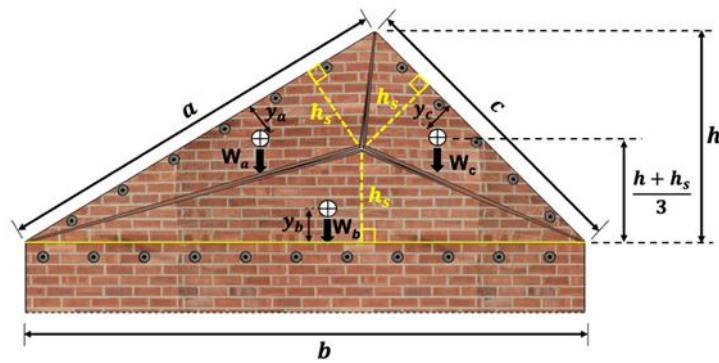


Figure C8B.10: Vertically spanning non-symmetrical (scalene) gable configurations

The values of a and b can be calculated from the equation of equilibrium immediately before collapse.

$$W_b \left(e_b - A \frac{h_s}{3} \right) + (W_a + W_c) \left(e_o + e_t + e_b - A \left(\frac{h+h_s}{3} \right) \right) + P \left(e_o + e_t + e_b + e_p - A \frac{h}{2} \right) \quad \dots C8.60$$

Results in:

$$a = W_b \frac{h_s}{3} + (W_a + W_c) \frac{h+h_s}{3} + P \frac{h}{2} \quad \dots C8.61$$

$$b = W_b e_b + (W_a + W_c) (e_o + e_t + e_b) + P_{Tot} (e_o + e_t + e_b + e_p) \quad \dots C8.62$$

the expression for the participation factor results in:

$$\gamma = \frac{W_{Tot} h_s^2}{3gJ} \quad \dots C8.63$$

With the period being:

$$T_p = 4.07 \sqrt{\frac{I}{a}} \quad \dots \text{C8.64}$$

C8B.4.2.4 Secured sawtooth gable worked example

With respect to Figure C8B.10 assume the following:

The building is located in Palmerston North and situated on soft soil.

The height to the base of the gable is 6.8 m.

The gable length $b = 5.8$ m

The left gable angle is 35° and the right gable angle is 75° .

The nominal gable thickness is 0.23 m

Top gable angle is $(180^\circ - 35^\circ - 75^\circ) = 70^\circ$

From the sine rule:

$$\begin{aligned} a &= 5.8 \times \frac{\sin(75^\circ)}{\sin(70^\circ)} = 5.962 \text{ m} \\ c &= 5.8 \times \frac{\sin(35^\circ)}{\sin(70^\circ)} = 3.540 \text{ m} \\ h &= 3.540 \times \sin(70^\circ) = 3.327 \text{ m} \\ h_s &= \frac{hb}{a + b + c} = \frac{3.327 \times 5.800}{5.962 + 5.800 + 3.540} = \frac{19.297}{15.302} = 1.261 \text{ m} \end{aligned}$$

Step 1 and 2: Establish loading.

$$\begin{aligned} W_a &= 18 \times \frac{1}{2} \times 5.962 \times 1.261 \times 0.23 = 15.56 \text{ kN} \\ W_b &= 18 \times \frac{1}{2} \times 5.8 \times 1.261 \times 0.23 = 15.14 \text{ kN} \\ W_c &= 18 \times \frac{1}{2} \times 3.540 \times 1.261 \times 0.23 = 9.24 \text{ kN} \\ W_{Tot} &= 15.56 + 15.14 + 9.24 = 39.9 \text{ kN} \end{aligned}$$

Assume roof load of 1 kPa.

$$P = 1.0 \times (a + c) = 1.0 \times (6.0 + 3.5) = 9.5 \text{ kN}$$

Step 3: Establish the effective thickness.

See Equation C8B.32:

$$t = \left(0.975 - 0.025 \frac{P}{W}\right) t_{nom} = \left(0.975 - 0.025 \times \frac{9.5}{39.9}\right) \times 0.230 = 0.223 \text{ m}$$

Step 4: Establish boundary conditions.

Assume condition 3 boundary conditions (see Table C8B.3). Therefore:

$$e_p = t/2 = 0.223/2 = 0.111 \text{ m}$$

$$e_b = t/2 = 0.223/2 = 0.111 \text{ m}$$

$$e_o = e_t = t/2 = 0.111 \text{ m}$$

$$y_b = y_t = h/6 = 2.9/6 = 0.483 \text{ m}$$

Step 5: Establish the instability displacement.

From Equation C8.61:

$$\begin{aligned} a &= W_b \frac{h_s}{3} + (W_a + W_c) \frac{h + h_s}{3} + P \frac{h}{2} \\ &= 15.14 \times \frac{1.261}{3} + (15.56 + 9.24) \times \frac{3.327 + 1.261}{3} + 9.5 \times \frac{3.327}{2} \\ &= 6.36 + 37.93 + 15.80 = 60.1 \text{ kNm} \end{aligned}$$

From Equation C8.62:

$$\begin{aligned} b &= W_b e_b + (W_a + W_c)(e_o + e_t + e_b) + P_{Tot}(e_o + e_t + e_b + e_p) \\ &= 15.14 \times 0.111 + (15.56 + 9.24) \times (0.111 + 0.111 + 0.111) \\ &\quad + 9.5 \times (0.111 + 0.111 + 0.111 + 0.111) = 1.68 + 8.26 + 4.22 \\ &= 14.2 \text{ kNm} \end{aligned}$$

$$\Delta_i = Ah = \frac{bh}{a} = \frac{14.2 \times 3.327}{60.1} = 0.786 \text{ m}$$

Step 6: Determine the maximum usable deflection at the top of the gable:

$$\Delta_m = 0.6\Delta_i = 0.6 \times 0.786 = 0.472 \text{ m}$$

Step 7: Evaluate the period:

From Equation C8B.69:

$$\begin{aligned} J &= \frac{W_{Tot} h^2}{18g} + \frac{W_b}{g} \left(e_b^2 + \frac{h_s^2}{9} \right) + \frac{(W_a + W_c)}{g} \left[(e_o + e_t + e_b)^2 + \frac{h_s^2}{9} \right] \\ &\quad + \frac{P}{g} (e_o + e_t + e_b + e_p)^2 \\ &= \frac{39.9 \times 3.33^2}{18 \times 9.81} + \frac{15.14}{9.81} \left(0.111^2 + \frac{1.26^2}{9} \right) \\ &\quad + \frac{(15.56 + 9.24)}{9.81} \left[(0.111 + 0.111 + 0.111)^2 + \frac{1.26^2}{9} \right] \\ &\quad + \frac{9.5}{9.81} (0.111 + 0.111 + 0.111 + 0.111)^2 = 2.51 + 0.29 + 0.73 + 0.19 \\ &= 3.69 \text{ kNms}^2 \end{aligned}$$

From Equation C8.64:

$$T_p = 4.07 \sqrt{\frac{J}{a}} = 4.07 \sqrt{\frac{3.69}{60.1}} = 1.01 \text{ seconds}$$

Step 8: Calculate the design response coefficient for the part.

From Equation C8.16 and the note to Step 8 in the general procedure in section C8.8.5.2:

$$C_i(T_p) = 2.0 \left(\frac{0.5}{T_p} \right)^{0.75} = 2.0 \left(\frac{0.5}{1.01} \right)^{0.75} = 1.18$$

The building is located in Palmerston North, $Z = 0.38$ and $N(T,D) = 0$.

From section C8B.4.1.1:

$$C(0) = C_h(0).Z.R.N(T,D) = 1.33 \times 0.38 \times 1 \times 1 = 0.51$$

See section C8C.3 or note to step 8 for clarification of height h_i to be used for the floor height coefficient.

$$h_i = \text{height to middle of gable} = 6.8 + 1.261 = 8.06 \text{ m}$$

From NZS 1170.5 Equation 8.3:

$$C_{Hi} = \left(1 + \frac{h_i}{6}\right) = \left(1 + \frac{8.06}{6}\right) = 2.34$$

From NZS 117.5 Equation 8.2(1):

$$C_p(T_p) = C(0).C_{Hi}.C_i(T_p) = 0.51 \times 2.34 \times 1.18 = 1.41$$

Step 9: Calculate the Participation Factor.

From Equation C8.63:

$$\gamma = \frac{W_{Tot}h_s^2}{3gJ} = \frac{39.9 \times 1.26^2}{3 \times 9.81 \times 3.69} = 0.58$$

Step 10: Calculate the displacement demand D_{ph} .

As for the earlier example in section C8B.4.1.1, $R_P = 1$.

From Equation C8.18:

$$D_{ph} = \gamma(T_p/2\pi)^2 C_p(T_p).R_P.g = 0.58 \times \left(\frac{1.01}{2\pi}\right)^2 \times 1.41 \times 1 \times 9.81 = 0.207 \text{ m}$$

From Equation C8.20:

$$\%NBS = 100 \times \Delta_m/D_{ph} = 60(\Delta_i/D_{ph}) = 100 \times \frac{0.472}{0.207} > 100\%$$

The secured sawtooth gable is not earthquake prone.

C8B.4.3 Vertical-horizontal spanning gables

In Figure C8B.11a the collapse configuration is shown for an isosceles (symmetrical) gable spanning vertically and horizontally with a free top.

Note:

This procedure is only valid for gables having a symmetrical isosceles configuration. The procedure depends on mirror-image symmetry.

Note:

In the presented procedure it is assumed that $t \ll h$ and therefore the wall thickness has been omitted from the calculations of rotational mass moment of inertia (ie $h^2 \approx (h^2 + t^2)$). Thickness is accounted for when calculating weight (W) and when determining the boundary conditions.

The procedure used to establish the crack pattern and failure mechanism for a vertical-horizontal spanning gable is explained in the following steps:

Note:

The procedure explained below can be completed using CAD software, which is expected to make the process much easier to complete when compared to the use of trigonometric procedures.

Step A: Identify the inclined ‘Base Diagonal Line’ (BDL) shown in green in Figure C8B.11 using the masonry bond pattern angle $\alpha_{bond} = \text{atan}\left(2 \frac{h+t}{l+t}\right)$, where h and l are the height and length of the brick, with t being the mortar joint thickness. Note that the length of the Base Diagonal Line (\overline{BDL}) is half the total length of the line, hence why the lower half of the line is shown dashed in Figure C8B.11.

Note:

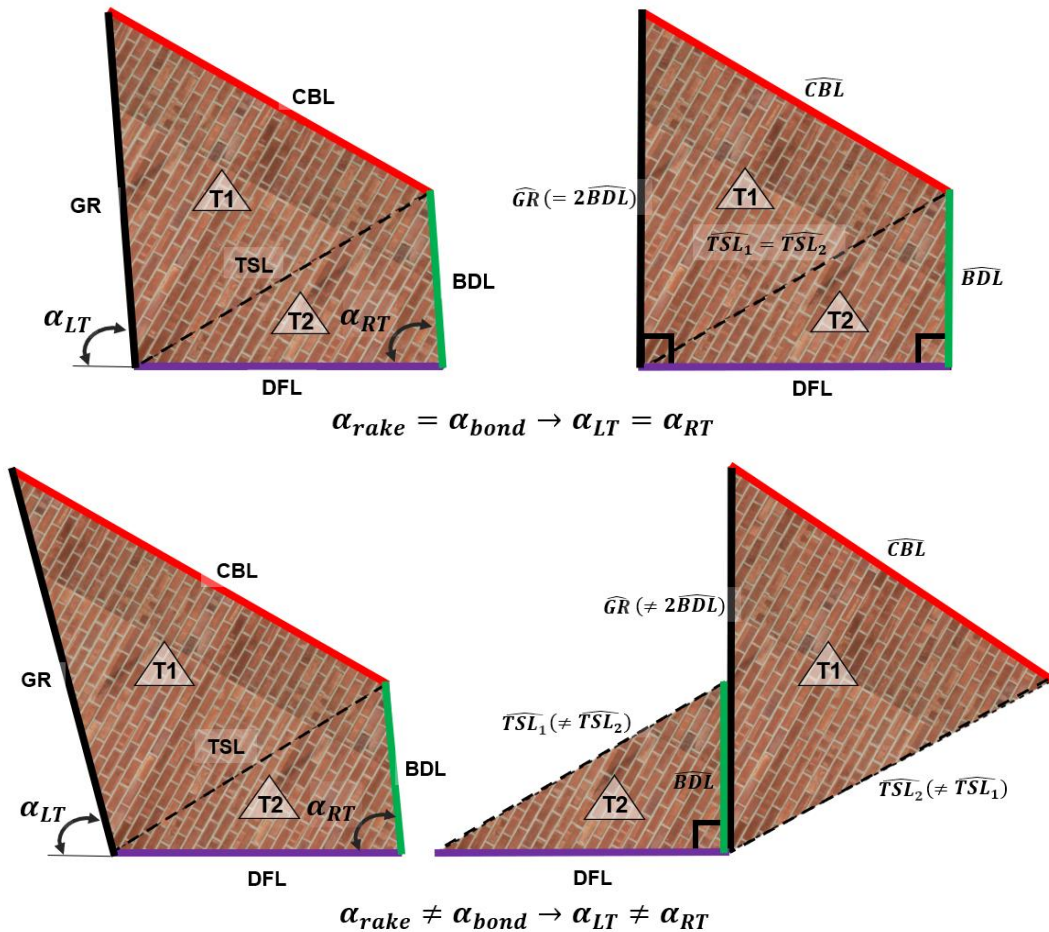
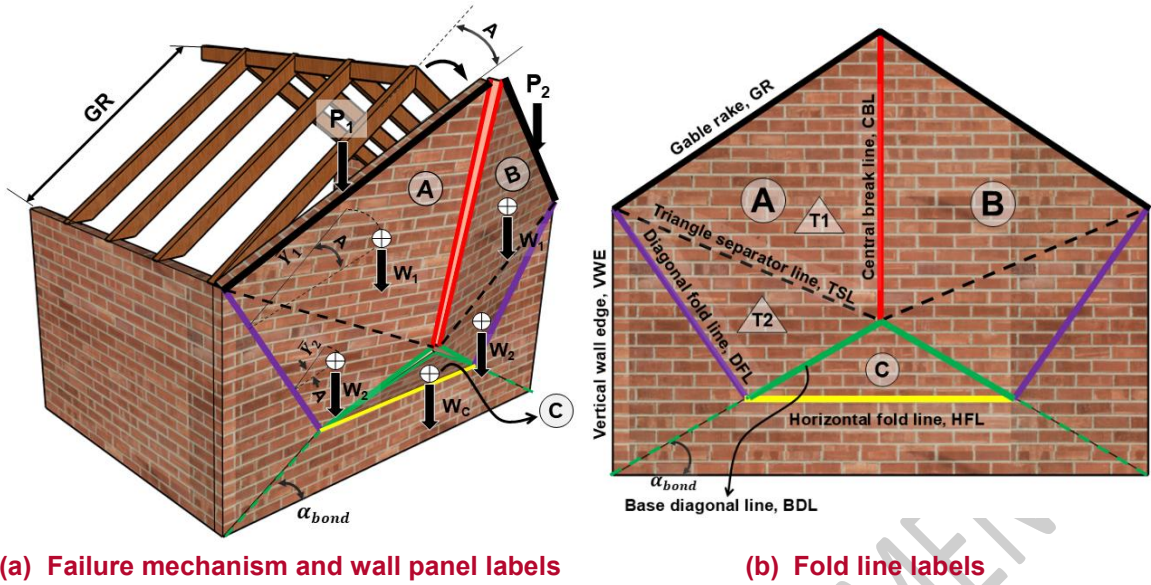
The typical geometry of a brick is illustrated in Figure C8.7. For $h = 70$ mm, $t = 10$ mm, and $l = 230$ mm the masonry bond pattern angle is $\alpha_{bond} = \text{atan}\left(2 \frac{70+10}{230+10}\right) = \text{atan}(0.666) = 33.7^\circ$.

Note:

Typical values of the bond angle α_{bond} are very similar to typical angles of the gable rake with respect to the horizontal, α_{rake} . This observation can be used to develop a simplified approximate solution as described below.

Where deemed acceptable, the adoption of $\alpha_{bond} \cong \alpha_{rake}$ results in the calculations being substantially easier to complete. The simplification is illustrated in Figure C8B.11, where:

1. The length of the green base diagonal line can be equated to half the length of the black gable rake: $\overline{BDL} = \frac{\overline{GR}}{2}$.
2. The left transpose angle will equal the right transpose angle. Therefore $\widehat{BDL} = \frac{\widehat{GR}}{2}$.
3. The centroidal height of T1 will equal the transposed height BDL: $h_1 = \overline{BDL}$.
4. The area of T1 will equal twice the area of T2. Therefore the weight of T1 will be twice the weight of T2: $W_A = W_B = 3W_1$ and $W_{Tot} = 6W_1 + W_C$.
5. $h_1 = \overline{BDL}$ and $h_2 = \frac{\overline{BDL}}{3}$. Therefore $h_A = \frac{7}{6}\overline{BDL}$. Also $h_p = h_1 = \overline{BDL}$.



(c) Wall panel (left) and equivalent transformed right-angle wall panel (right)

Figure C8B.11: Case 3 gable configuration (isosceles configuration shown, P and W symmetrically distributed, $W_{Tot} = 2 \times (W_1 + W_2) + W_C$, $P_{Tot} = P_1 + P_2$). See also Figure C8B.8

Step B: Define the rotating ‘Diagonal Fold Line, DFL’ shown in purple in Figure C8B.11a,b by drawing a line from the top corner of the gable to the centre of the green BDL line.

- Step C: Draw a vertical ‘Central Break Line’ (CBL) from the intersection of the two Base Diagonal Lines to the apex as shown by the red line in Figure C8B.11a,b.
- Step D: Where the purple DFL line intersects with the green line, draw a ‘Horizontal Fold Line’ (HFL) as shown in yellow in Figure C8B.11a,b.
- Step E: Determine the weight W_C and the height to centroid h_C of Triangle C.
- Step F: Establish the length of the gable rake (GR).
- Step G: Identify dimensions of Panel A. Note that these are the ‘true dimensions’ before the shape is transposed as explained below.
- Step H: Find the angles that line GR and line BDL make with respect to line DFL. See Figure C8B.11c for clarification. The left angle is referred to as the ‘Left Transpose Angle’ (α_{LT}) and the right angle is referred to as the ‘Right Transpose Angle’ (α_{RT}).
- Step I: Establish the height to the overburden axial load, assumed to act mid-way along line GR.

Note:

Panel A (and its mirrored counterpart, Panel B) can be subdivided into two triangular segments, referred to as Triangle 1 and Triangle 2, for simplified calculation of their properties.

- Step J: Transpose Triangle 1 and Triangle 2 to equivalent right-angle triangles. Established the transposed height of Triangle 1 (\widehat{GR}) and the transposed height of Triangle 2 (\widehat{BDL}). Establish panel weight and the location of panel centroids.
- Step K: Establish the width of the transposed Triangle 1 (b_{TI}).
- Step L: Determine the height to the centroid of Panel A.
- Step M: Establish the maximum usable deflection.

The values of a and b can be calculated from the equation of equilibrium immediately before collapse. W_A is multiplied by 2 to account for symmetry in the system, given that $W_A = W_B$. To express the rotation of panel C in terms of the angular rotation A of panel A, the height of the centroid of panel C is projected in \widehat{BDL} .

$$W_A = W_B = W_1 + W_2$$

$$2W_A(e_b - \Delta_{WA}) + P_{Tot}(e_b + e_p - \Delta_P) + W_C(e_b - \Delta_{WC}) = 0$$

$$2W_A(e_b - h_A A) + P_{Tot}(e_b + e_p - h_P A) + W_C(e_b - h_C A) = 0$$

Substituting for known dimensions:

$$h_A = \text{Centre of gravity of panel A} = \frac{A_1 \bar{Y}_1 + A_2 \bar{Y}_2}{A_1 + A_2} \quad h_p = \frac{\widehat{GR}}{2}$$

The formulas for a and b result as follows:

$$a = 2W_A h_A + P_{Tot} h_p + W_C h_C = 2W_A \left(\frac{A_1 \bar{Y}_1 + A_2 \bar{Y}_2}{A_1 + A_2} \right) + P \cdot \frac{\widehat{GR}}{2} + W_C \frac{\widehat{BDL}}{3} \quad \dots \text{C8B.59}$$

$$b = 2W_A e_b + P_{Tot} (e_b + e_p) + W_C e_b \quad \dots \text{C8B.60}$$

Given that the instability displacement is taken at the apex of the gable, h is equal to R :

$$\Delta_i = \frac{b}{a} \widehat{GR} \quad \dots \text{C8B.61}$$

Step N: Calculate the rotational mass moment of inertia.

$$J_A = J_B = J_1 + J_2 + \frac{W_1}{g} (\bar{Y}_1^2 + e_b^2) + \frac{W_2}{g} (\bar{Y}_2^2 + e_b^2) + \frac{P}{g} \left(\left(\frac{\widehat{GR}}{2} \right)^2 + e_p^2 \right) \quad \dots \text{C8B.62}$$

Substituting J_1 and J_2 :

$$J_A = J_B = \frac{W_1}{18g} (\widehat{GR}^2 - \widehat{GR} \cdot \widehat{BDL} + \widehat{BDL}^2) + \frac{W_2}{18g} \widehat{BDL}^2 + \frac{W_1}{g} \left(\frac{2(\widehat{GR} + \widehat{BDL})^2}{18} + e_b^2 \right) + \frac{W_2}{g} \left(\frac{2\widehat{BDL}^2}{18} + e_b^2 \right) + \frac{P}{g} \left(\frac{\widehat{GR}^2}{4} + e_p^2 \right) \quad \dots \text{C8B.63}$$

Normalising by a factor of $\frac{1}{6g}$:

$$J_A = J_B = \frac{1}{6g} [W_1 (\widehat{GR}^2 + \widehat{GR} \cdot \widehat{BDL} + \widehat{BDL}^2 + 6e_b^2) + W_2 (\widehat{BDL}^2 + 6e_b^2)] + \frac{P}{g} \left(\frac{\widehat{GR}^2}{4} + e_p^2 \right) \quad \dots \text{C8B.64}$$

The rotational mass moment of inertia of the bottom Triangle C (see Figure C8B.12) is equal to J_C derived below, where h_c is the height of Triangle C and y_c is the height of the centroid of Triangle C, which is $y_c = h_c/3$. Therefore, it can be reduced to:

$$J_C = \frac{W_C}{18g} h_c^2 + \frac{W_C}{g} (e_b^2 + y_c^2) = \frac{W_C}{g} \left(\frac{h_c^2}{6} + e_b^2 \right) \quad \dots \text{C8B.65}$$

The rotational mass moment of inertia of the total wall is given by the summation of the three wall panels:

$$J_G = J_A + J_B + J_C$$

$$J_G = \frac{1}{3g} [W_1 (\widehat{GR}^2 - \widehat{GR} \cdot \widehat{BDL} + \widehat{BDL}^2 + 6e_b^2) + W_2 (\widehat{BDL}^2 + 6e_b^2) + W_C \left(\frac{h_c^2}{2} + 3e_b^2 \right)] + \frac{P}{g} \left(\frac{\widehat{GR}^2}{4} + e_p^2 \right) \quad \dots \text{C8B.66}$$

Note:

In the above equations P is total weight, not weight per unit length, W_C is the total weight of the triangular panel PC, W_1 is the weight of Triangle T1 and W_2 is the weight of Triangle T2. It is assumed that contributions from horizontal arching of the wall are ignored, and that each wall panel has its own instantaneous centre of rotation at its rotating edge.

Step O: Establish the rocking period of the part:

$$T_p = 3.1 \sqrt{\frac{J_G}{a}} \quad \dots \text{C8B.67}$$

Step P: Establish the participation factor.

The expression for the participation factor results in:

$$\gamma = \frac{(2W_A h_A + W_C h_C) \bar{G} R}{g J_G} \quad \dots \text{C8B.68}$$

Note:

Because Panel A and Panel B have different heights to the base of cantilever compared to panel C a weighted mean approach can be adopted. For typical geometries the value will likely be similar to the mid-height value for Panel A and Panel B.

Note:

It is recognised that the method may generate unusual results for gable walls that are particularly slender. In such a case it is encouraged that thought be given to a modified failure mechanism as shown in Figure C8B.12a. No research findings are available at the current time to provide greater guidance.

Note:

The procedure presented here can be applied to non-gable non-symmetrical side walls as shown in Figure C8B.12b but no research findings are available at the current time to provide greater guidance.

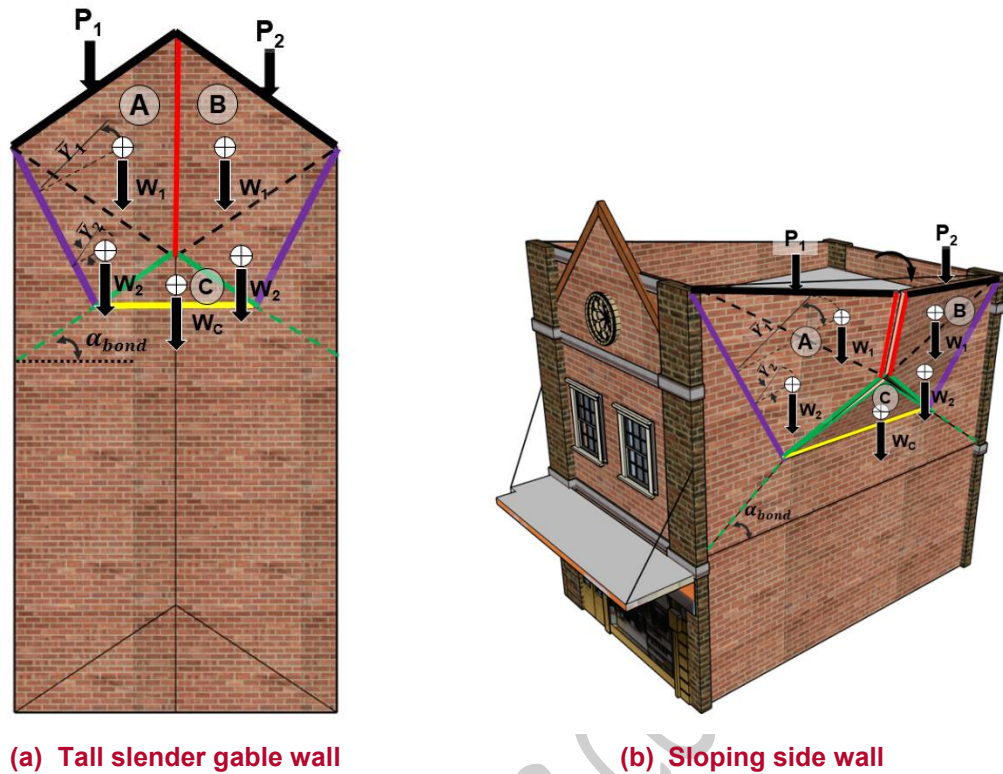


Figure C8B.12: Possible alternative applications for the vertical-horizontal spanning method. No specific guidance available at the current time

C8B.4.3.1 Vertical-horizontal spanning gable worked example

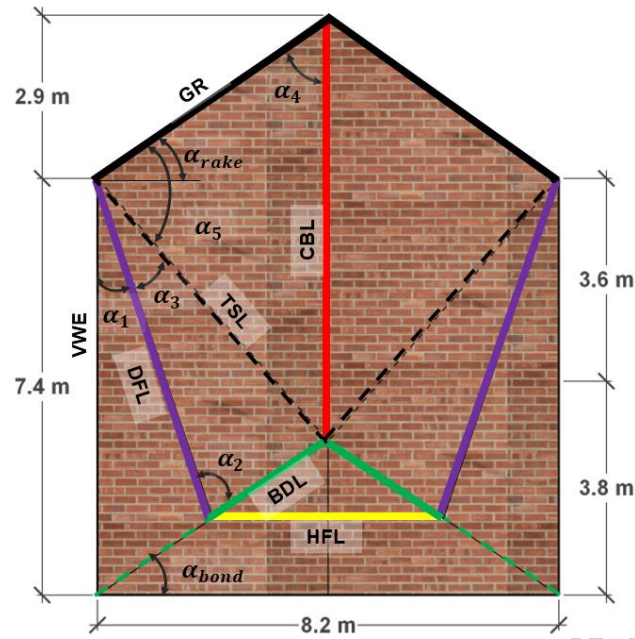
Consider the rear gable with plain finish shown in Figure C8B.7. The building is located in Masterton and is situated on shallow soil.

Establish the the masonry bond pattern angle: $\alpha_{bond} = \text{atan}\left(2 \frac{70+10}{230+10}\right) = 33.7^\circ$.

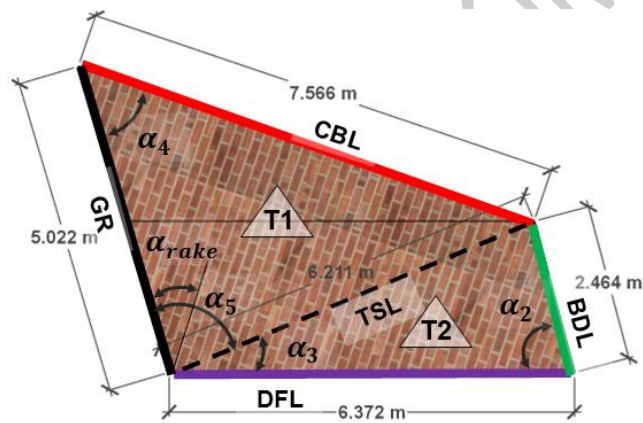
Establish the gable rake angle: $\alpha_{rake} = \text{atan}\left(\frac{2900}{0.5 \times 8200}\right) = 35.3^\circ$

Note:

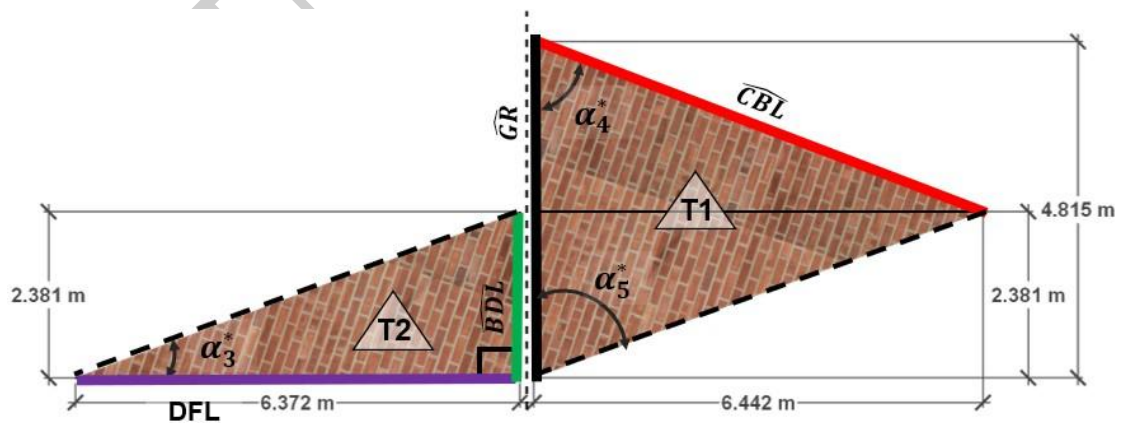
Consult Figure C8B.13a in conjunction with the calculations presented below.



(a) Primary fold lines



(b) Dimensions of Panel A (T1 and T2)



(c) Dimensions of transposed Panel A (T1 and T2)

Figure C8B.13: Mirrored gable collapse mechanism and Panel A details

Step A: Find the length of the base diagonal length \overline{BDL} .

Note that the length of the base diagonal line (\overline{BDL}) is associated with a quarter of the wall length of 8.2 m.

$$\overline{BDL} = \frac{L_g}{4 \cos(\alpha_{bond})} = \frac{8.2}{4 \cos(33.7^\circ)} = 2.464 \text{ m}$$

Step B: Find the length of the diagonal fold line (\overline{DFL}).

Applying the cosine rule and defining the wall height as the wall vertical edge WVE:

$$\begin{aligned}\overline{DFL}^2 &= \overline{WVE}^2 + \overline{BDL}^2 - 2 \times \overline{WVE} \times \overline{BDL} \cos(90^\circ - 33.7^\circ) \\ \overline{DFL} &= \sqrt{7.4^2 + 2.464^2 - 2 \times 7.4 \times 2.464 \times \cos(56.3^\circ)} = 6.372 \text{ m}\end{aligned}$$

Establish the angle between the diagonal fold line (\overline{DFL}) and the vertical edge \overline{WVE} :

Using the cosine rule:

$$\begin{aligned}\overline{BDL}^2 &= \overline{DFL}^2 + \overline{WVE}^2 - 2 \times \overline{DFL} \times \overline{WVE} \cos(\alpha_1) \\ 2.464^2 &= 6.372^2 + 7.4^2 - 2 \times 6.372 \times 7.40 \cos(\alpha_1) \\ \alpha_1 &= \cos^{-1}\left(\frac{89.29}{94.306}\right) = 18.8^\circ\end{aligned}$$

Or:

$$\begin{aligned}\overline{DFL} \sin(\alpha_1) &= \overline{BDL} \cos(\alpha_{bond}) \\ \alpha_1 &= \sin^{-1}\left(\frac{2.050}{6.372}\right) = 18.8^\circ\end{aligned}$$

Step C: Find the length of the central break line (\overline{CBL}).

Height to the base of the central break line is $0.5L_g \tan(33.7^\circ) = 2.734 \text{ m}$

$$\overline{CBL} = 7.4 + 2.9 - 2.734 = 7.566 \text{ m}$$

Step D: Find the length of the horizontal fold line (\overline{HFL}).

$$\overline{HFL} = \frac{L_g}{2} = \frac{8.2}{2} = 4.1 \text{ mm}$$

Step E: Establish properties for Triangle C:

$$W_c = 18 \times 0.5 \times 4.1 \times 2.464 \times \sin(\alpha_{bond}) \times 0.23 = 11.6 \text{ kN}$$

$$h_c = \frac{1}{3} \times 2.464 \times \sin(\alpha_{bond}) = 0.456 \text{ m}$$

Step F: Find the length of the gable rake (\overline{GR}).

The gable length (also wall length) is $L_g = 8200 \text{ mm}$ and the gable height is $h_g = 2900 \text{ mm}$.

$$\overline{GR} = \sqrt{0.25L_g^2 + h_g^2} = \sqrt{0.25 \times 8.2^2 + 2.9^2} = 5.022 \text{ m}$$

Alternatively:

$$\overline{GR} = \frac{h_g}{\sin(\alpha_{rake})} = \frac{2.9}{\sin(35.3^\circ)} = 5.022 \text{ m}$$

Step G: Identify true dimensions of Panel A as shown in Figure C8B.13b.

Divide Panel A into Triangle T1 and Triangle T2.

Step H: Find the transpose angles α_{LT} and α_{RT} .

Using the summation of angles in triangles and information already acquired, the ‘Right Transpose Angle’ (α_{RT}) is:

$$\alpha_{RT} = \alpha_2 = (90^\circ - \alpha_{bond}) - \alpha_1 = (90^\circ - 33.7^\circ) + 18.8^\circ = 75.1^\circ$$

Applying the cosine rule to define the length of the triangular separator line TSL:

$$\overline{TSL}^2 = \overline{DFL}^2 + \overline{BDL}^2 - 2 \times \overline{DFL} \times \overline{BDL} \cos(\alpha_3)$$

$$\overline{TSL} = \sqrt{6.372^2 + 2.464^2 - 2 \times 6.372 \times 2.464 \times \cos(75.1^\circ)} = 6.211 \text{ mm}$$

Using the sine rule, the angle between the triangular separator line TSL and the diagonal fold line DFL is:

$$\alpha_3 = \sin^{-1} \left(\frac{\overline{BDL}}{\overline{TSL}} \sin(\alpha_2) \right) = \sin^{-1} \left(\frac{2.464}{6.211} \sin(75.1^\circ) \right) = 22.5^\circ$$

The angle between the gable rake GR and the central break line CBL is:

$$\alpha_4 = 90^\circ - \alpha_{rake} = 54.7^\circ$$

or

$$\alpha_4 = \cos^{-1} \left(\frac{\overline{CBL}^2 + \overline{GR}^2 - \overline{TSL}^2}{2 \times \overline{CBL} \times \overline{GR}} \right) = \cos^{-1} \left(\frac{7.566^2 + 5.022^2 - 6.211^2}{2 \times 7.566 \times 5.022} \right) = 54.7^\circ$$

Using the sine rule, the angle between the gable rake GR and the triangular separator line TSL is:

$$\alpha_5 = \sin^{-1} \left(\frac{\overline{CBL}}{\overline{TSL}} \sin(\alpha_4) \right) = \sin^{-1} \left(\frac{7.566}{6.211} \sin(54.7^\circ) \right) = 83.8^\circ$$

Using the information already acquired, ‘Left Transpose Angle’ (α_{LT}) is:

$$\alpha_{LT} = 180^\circ - (\alpha_3 + \alpha_5) = 180^\circ - 22.5^\circ - 83.8^\circ = 73.7^\circ$$

Note:

In Figure C8B.13b the left transpose angle ($\alpha_{LT} = 73.7^\circ$) appears similar to the right transpose angle ($\alpha_{LR} = 75.1^\circ$). This observation occurs because the masonry bond pattern angle of $\alpha_{bond} = 33.7^\circ$ is similar to the gable rake angle of $\alpha_{rake} = 35.3^\circ$. For different gable angles the variation in angles will be more obvious.

This observation is the basis of the approximate method discussed below.

Step I: Height to axial load P :

$$h_P = 0.5 \times \overline{GR} \times \sin(\alpha_{LT}) = 0.5 \times 5.022 \sin(73.5^\circ) = 2.408 \text{ m}$$

Step J: Transpose Panel A to have vertical (right angle) dimensions and establish the panel weight and the location of the panel centroid.

Triangle T2

Maintaining the same area for Triangle T2 and using α_{RT} to transpose the base diagonal line \overline{BDL} to have a vertical (right angle) dimension:

$$\widehat{BDL} = \overline{BDL} \times \sin(\alpha_{RT}) = 2.464 \times \sin(75.1^\circ) = 2.381 \text{ m}$$

$$W_2 = 18 \times \frac{1}{2} \times \overline{DFL} \times \widehat{BDL} \times 0.23 = 18 \times 0.5 \times 6.372 \times 2.381 \times 0.23 = 31.4 \text{ kN}$$

$$\overline{Y}_2 = \frac{1}{3} \times 2.381 = 0.794 \text{ m}$$

Triangle T1

The area of triangle T1 is:

$$A_{T1} = 0.5 \times \overline{GR} \times \overline{CBL} \sin(\alpha_4) = 0.5 \times 5.022 \times 7.566 \sin(54.7^\circ) = 15.51 \text{ m}^2$$

Maintaining the same area for Triangle T1 and using α_{LT} to transpose the gable rake \widehat{GR} to have vertical (right angle) dimension:

$$\widehat{GR} = \overline{GR} \times \sin(\alpha_{LT}) = 5.022 \times \sin(73.5^\circ) = 4.815 \text{ m}$$

$$W_1 = 18 \times 15.51 \times 0.23 = 64.2 \text{ kN}$$

$$\overline{Y}_1 = \frac{1}{3} (4.815 + 2.381) = 2.399 \text{ m}$$

Step K: The length of line perpendicular to the transposed gable rake \widehat{GR} , b_{T1} , is:

$$b_{T1} = \frac{2 \times \text{Area}_{T1}}{\widehat{GR}} = \frac{2 \times 15.51}{4.815} = 6.442 \text{ m}$$

Step L: Evaluation the height to the centroid of Panel A:

$$W_A = W_B = 64.2 + 31.4 = 95.6 \text{ kN}$$

$$W_{Tot} = 2 \times (64.2 + 31.4) + 11.6 = 202.8 \text{ kN}$$

$$P_{Tot} = 13.1 \text{ kN (see previous worked example)}$$

$$h_A = \frac{W_1 \overline{Y}_1 + W_2 \overline{Y}_2}{W_1 + W_2} = \frac{64.2 \times 2.399 + 31.4 \times 0.794}{64.2 + 31.4} = 1.872 \text{ m}$$

Step M: Calculate the maximum usable deflection:

Establish the effective thickness.

$$t = \left(0.975 - 0.025 \frac{P}{W}\right) t_{nom} = \left(0.975 - 0.025 \times \frac{13.1}{202.8}\right) \times 0.230 = 0.224 \text{ m}$$

Establish boundary conditions. Assume that the roof is restrained from rotating with the gable. Therefore:

$$e_p = t/2 = 0.224/2 = 0.112 \text{ m}$$

$$e_b = t/2 = 0.224/2 = 0.112 \text{ m}$$

Establish the instability displacement.

From Equation C8B.59:

$$\begin{aligned} a &= 2W_A h_A + P_{Tot} h_P + W_C h_C \\ &= 2 \times (64.2 + 31.4) \times 1.872 + 13.1 \times 2.408 + 11.6 \times 0.456 \\ &= 394.8 \text{ kNm} \end{aligned}$$

From Equation C8B.60:

$$\begin{aligned} b &= 2W_A e_b + P_{Tot}(e_b + e_p) + W_C e_b \\ &= 2 \times (64.2 + 31.4) \times 0.112 + 13.1 \times (0.112 + 0.112) + 11.6 \times 0.112 \\ &= 25.6 \text{ kNm} \end{aligned}$$

Given that the instability displacement is taken at the apex of the gable, h is equal to R :

$$\Delta_i = \frac{b}{a} \widehat{GR} = \frac{25.6}{394.8} \times 4.815 = 0.312 \text{ m}$$

Determine the maximum usable deflection:

$$\Delta_m = 0.3\Delta_i = 0.3 \times 0.312 = 0.094 \text{ m}$$

Step N: Calculate the rotational mass moment of inertia.

$$\begin{aligned} J_G &= \frac{1}{3g} \left[W_1 (\widehat{GR}^2 + \widehat{GR} \cdot \widehat{BDL} + \widehat{BDL}^2 + 6e_b^2) + W_2 (\widehat{BDL}^2 + 6e_b^2) \right. \\ &\quad \left. + W_C \left(\frac{h_c^2}{2} + 3e_b^2 \right) \right] + \frac{P}{g} \left(\frac{\widehat{GR}^2}{4} + e_p^2 \right) \\ &= \frac{1}{3g} \left[64.2 \times (4.815^2 + 4.815 \times 2.381 + 2.381^2 + 6 \times 0.112^2) \right. \\ &\quad \left. + 31.4 \times (2.381^2 + 6 \times 0.112^2) + 11.6 \left(\frac{0.456^2}{2} + 3 \times 0.112^2 \right) \right] \\ &\quad + \frac{13.1}{g} \left(\frac{4.815^2}{4} + 0.112^2 \right) \\ &= \frac{1}{3g} [64.2 \times 40.4 + 31.4 \times 5.74 + 11.6 \times 0.14] + \frac{13.1 \times 5.8}{g} \\ &= \frac{2773.9 + 1.6}{3 \times 9.81} + \frac{13.1 \times 5.8}{9.81} = 102.1 \text{ kNm} \end{aligned}$$

Step O: Evaluate the period:

$$T_p = 3.1 \sqrt{\frac{J_G}{a}} = 3.1 \sqrt{\frac{102.1}{394.8}} = 1.58 \text{ seconds}$$

Step P: Determine the participation factor:

$$\gamma = \frac{(2W_A h_A + W_C h_C) \widehat{GR}}{g J_G} = \frac{(2 \times 95.6 \times 1.872 + 11.6 \times 0.456) \times 4.815}{9.81 \times 102.1} = \frac{1748.9}{1001.6} = 1.75$$

Calculate the design response coefficient for the part.

From Equation C8.16 and the note to Step 8 in the general procedure in section C8.8.5.2:

$$C_i(T_p) = \frac{1.32}{T_p} = \frac{1.32}{1.58} = 0.84$$

From NZS 1170.5 Table 3.1 footnote for parts:

$$C_h(0) = 1.33$$

From NZS 1170.5 Table 3.3 for Masterton: $Z = 0.42$.

From NZS 1170.5 Table 3.7: $N(T=0, D=6-10) = 1$.

From NZS 1170.5 Table 3.5 for 1/500 annual probability of exceedance: $R_U = 1$.

From NZS 1170.5 Equation 3.1(1):

$$C(0) = C_h(0) \cdot Z \cdot R \cdot N(T, D) = 1.33 \times 0.42 \times 1 \times 1 = 0.56$$

Weighted mean height to base of cantilevers:

$$h_{iA} = 7.4 - \frac{1}{2} \times \overline{DFL} \cos \alpha_1 = 7.4 - 0.5 \times 6.372 \times \cos 18.8^\circ = 4.384 \text{ m}$$

$$h_{iC} = \overline{BDL} \sin \alpha_{bond} = 2.464 \times \sin 33.7^\circ = 1.367 \text{ m}$$

$$h_i = \frac{2 \times 95.6 \times 4.384 + 11.6 \times 1.367}{2 \times 95.6 + 11.6} = 4.212 \text{ m}$$

From NZS 1170.5 Equation 8.3:

$$C_{Hi} = \left(1 + \frac{h_i}{6}\right) = \left(1 + \frac{4.212}{6}\right) = 1.70$$

From NZS 117.5 Equation 8.2(1):

$$C_p(T_p) = C(0) \cdot C_{Hi} \cdot C_i(T_p) = 0.56 \times 1.70 \times 0.84 = 0.80$$

Calculate the displacement demand D_{ph} .

From NZS 1170.5 Table 8.1 for Category P.1 where the part represents a hazard to human life outside the structure, $R_p = 1$.

From Equation C8.18:

$$D_{ph} = \gamma(T_p/2\pi)^2 C_p(T_p) \cdot R_p \cdot g = 1.75 \left(\frac{1.58}{2\pi}\right)^2 \times 0.80 \times 1 \times 9.81 = 0.868 \text{ m}$$

Step 11: Calculate %NBS:

From Equation C8.20 but adapted for a vertical cantilever as per step 6 of section C8.8.5.3:

$$\%NBS = 100 \times \Delta_m / D_{ph} = 30(\Delta_i / D_{ph}) = 100 \times \frac{0.094}{0.868} = 10.8 \approx 10\%$$

The unsecured gable wall is earthquake prone.

C8B.5 Cavity Walls

This section provides a procedure for assessing cavity walls and accompanying guidance to determine an improved capacity when additional cavity ties are to be installed.

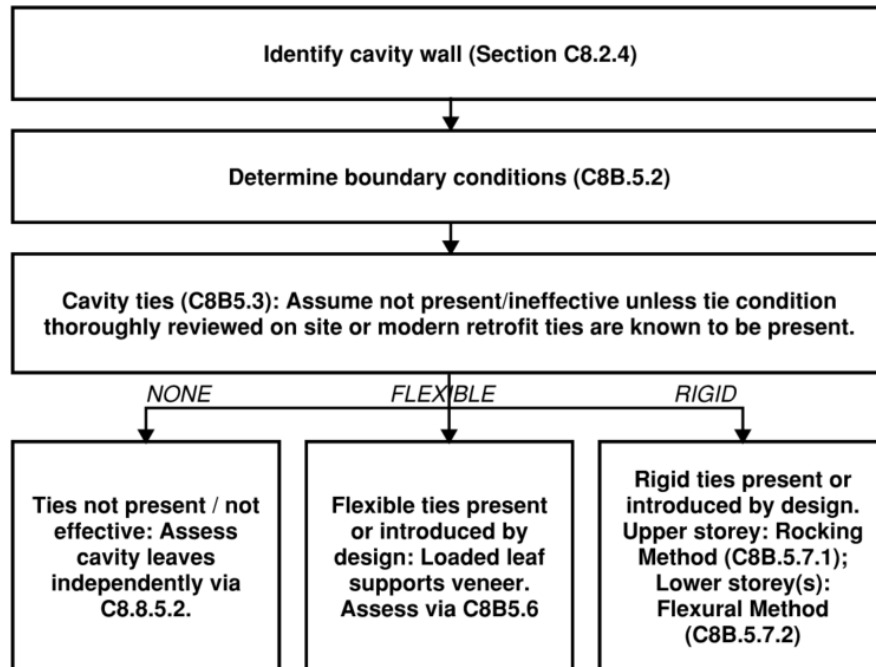


Figure C8B.14: Assessment procedure for cavity walls

C8B.5.1 Identification of cavity walls

Refer to the guidance in Section C8.2.4.3.

C8B.5.2 Cavity wall boundary conditions

Using existing building drawings and/or site investigation, identify the boundary conditions for both leaves of the cavity wall. Items requiring consideration include:

- Distribution of roof/floor roof loading: Often surcharge loading may be to the internal leaf of the cavity wall only, especially from internal suspended floors.
- Distribution of parapet loading (where present): Parapet loading may be unevenly distributed to cavity wall leaves. If a bond beam supporting a parapet is present and supported on both leaves then the load may be assumed to be shared evenly between the leaves, although the bond beam shape and position may affect the e_p value and hence the Boundary Condition chosen from Table C8.12.
- Existing tie condition: Refer to Section C8.2.4.2 and C8B.5.3.
- Return wall configuration: Return walls may be connected to internal leaves ONLY and therefore the horizontal span of the exterior leaf may differ from that of the internal leaf.
- Pier/buttress/pilaster configuration: Piers may support only the outer leaf although in some cases the cavity will stop and start at piers.

- Connection of outer leaf to roof/floor levels: It is possible that the outer leaf of the cavity has little or no practical connection to the structure at roof and/or floor levels in the as-built state. If this is the case then the outer leaf may have a vertical span that is significantly greater than the span of the inner leaf. In the most extreme case, if the outer leaf is not connected at the roof level (or is insufficiently well-connected) then the outer leaf may effectively be cantilevering from the foundation.

C8B.5.3 Cavity tie types and definitions

For the purposes of this Appendix the following tie types are proposed:

- No tie / ineffective ties. Although walls were usually provided with ties when constructed, the default assumption should be that these ties are inadequate to transfer forces between leaves, or are degraded in condition such that they are ineffective. Refer C8B.5.4.
- Flexible ties. These ties are either as-built ties which have been thoroughly site-verified for presence, spacing and condition, or modern ties which have been introduced (or are proposed to be introduced). These ties are assessed for their ability to drag loads from the veneer into the loaded leaf. Flexible ties have no/little shear and moment capacity. Refer C8B.5.6.
- Rigid shear-transferring ties. These ties will be modern in origin. These ties are assessed for their ability to constrain leaves to act compositely as a single wall section, requiring review of their shear and moment capacity. Refer C8B.5.7.

C8B.5.4 Assessment of cavity wall in as-built state

If cavity ties are proven to be (or assumed to be) ineffective then the leaves of the cavity wall should be assessed separately, using the procedure contained in C8.8.5.2. Take into account different top loads P and Boundary Conditions as per Table C8.12.

Note:

It is anticipated that many cavity walls may have inadequate capacity in the as-built state, especially single-wythe outer leaves (veneers). Many seismic improvement schemes will include the introduction of supplementary cavity ties. These ties change the response of the cavity wall system. Some guidance on assessment of the modified system is provided in C8B.5.6 and C8B.5.7 to assist with designing tie systems that achieve a required performance level, and/or with determination of the capacity of earlier seismic upgrade schemes which employed supplementary cavity ties.

C8B.5.5 Connection of cavity wall at roof/floor level

For C8B.5.6 and C8B.5.7 both leaves of the cavity wall should be connected to the roof/floor level, such that they are constrained to have the same height, h . Connections may be designed using demand from C8.8.5.2 Steps 12-14.

C8B.5.6 Assessment of cavity walls with flexible ties

For cavity walls with supplementary flexible cavity ties introduced, or for cavity walls where the existing ties have been shown to be present and in good condition, the following assessment may be used.

- Step 1:** Determine which is the “loaded leaf” and which is the “veneer”. The loaded leaf should be chosen as the leaf with the most capacity (usually the thicker leaf, or the leaf with the greatest top load). In most cases the inner leaf will be the loaded leaf.
- Step 2:** Show by calculation that the ties have adequate capacity to drag the full seismic weight of the veneer leaf into the loaded leaf by checking the tributary weight on ties against the axial capacity of the tie and its anchorage. New or modern supplementary flexible ties should have tested anchorage (withdrawal) capacities provided by the manufacturer. As-built ties may require testing to determine a capacity, (noting that such testing would be intrusive in nature and would require multiple locations to be tested).

Note:

Calculation showing adequate tie axial/withdrawal capacity per Step 2 is required for ties to be considered “flexible” and use the remainder of the procedure in this subsection. Alternatively assess leaves separately per C8B.5.4.

Once the two leaves are shown to be adequately connected, the cavity wall may be assessed as a single unit.

The following procedure is suggested for evaluating the score for a cavity wall **with flexible ties**. It is assumed that there is a common height, h , and that the total load applied to the top of the combined panel, P , is appropriately allocated into each wythe.

- Step 3:** Separately for each wythe work out J , a and b , as per Table C8.12.
- Step 4:** Find the combined J , a and b by adding the individual values for each wythe determined from Step 1.
- Step 5:** Using the combined a and b to find the static instability displacement $\Delta_i = (b/a) \times (h/2)$. The maximum usable deflection is $0.6 \Delta_i$. The displacement used for the calculation of period is $\Delta_t = 0.36 \Delta_i$.
For the determination of Δ_m , note that the maximum usable deflection is not to exceed $0.6 \times \frac{t}{2}$, where t is the thickness of the loaded leaf.
- Step 6:** Find the participation factor γ . This is $Wh^2/8gJ$, but with W being the combined weight of both wythes and J being the **rotational mass** moment of inertia for the combined system as derived in Step 4.
- Step 7:** Use J and Δ_t to derive the period, T_p , and the displacement demand, D_{ph} , using the appropriate equations from Section C8.8.5.

Step 8: Use the demand D_{ph} determine from Step 7 and the reliable capacity Δ_m determined from Step 5 to determine the score as:

$$\%NBS = 100 \Delta_m / D_{ph} = 60 \Delta_i / D_{ph}. \quad \dots C8B.69$$

with a limit to Δ_m of $0.6 \times \frac{t}{2}$ as per Step 5.

C8B.5.7 Assessment of cavity walls with rigid shear-transferring ties

For cavity walls with supplementary rigid shear-transferring cavity ties introduced the following assessment methods may be used.

Note:

The assessment method considers two possible states: C8B.5.8 (Rocking Method) and C8B.5.9 (Flexural Method).

The Rocking Method is intended for use in upper-storey walls, where the magnitude of the top load limits the flexural capacity of the masonry. The Rocking Method assumes that the ties have adequate capacity to lift and support the inner and outer masonry leaves, alternately, during rocking cycles. This assumption is tested by calculation. Note that in practice this method decouples tie design from geographic seismic demand as the tie demand is proportional to the lifted wall weight, not the seismic load. The method is unlikely to be suited to the assessment of lower-storey walls because the lifted weights will likely be too high and the full composite rocking mechanism may be less likely to form.

The use of the Rocking Method is based on full-scale specimen shake-table testing at the University of Auckland (Tocher et al., 2020) which demonstrated that rigid ties were able to lift cavity leaves. The testing was carried out for single-single and single-double wall specimens, and may be unsuitable for extension to other wall types (eg double-double or single-triple).

It is anticipated that the Rocking Method should increase the calculated capacity of cavity walls by 2-4 times the sum of their individually-calculated capacities when assessed as separate inner and outer wall elements. The Flexural Method is intended for application to lower storey-walls. This method checks the combined capacity of the tied cavity wall as a composite section, with the tied wall essentially acting as a Vierendeel truss. The capacity of the composite section is limited by the ability of the masonry and the ties to resist local flexure.

This method has not been physically verified and engineers should use their judgement in applying it to building assessments.

It is anticipated that the Flexural Method should increase the capacity of cavity walls by approximately twice when compared to the sum of the calculated capacities as separate inner and outer wall elements.

C8B.5.8 Rocking Method for assessment of cavity walls with rigid shear-transferring ties

Refer to Figure C8B.15C8B.15(a) and Figure C8B.15(b).

- Step 1: Calculate the top load P , including roof or floor loads, and the weight of the top and bottom portions of the inner and outer leaves of the cavity wall $W_{t,1}$, $W_{t,2}$, $W_{b,1}$ and $W_{b,2}$. For determination of the size of the upper and lower portions the wall can be assumed to crack at midheight.
- Step 2: Determine the critical case, which is either when the wall rocks inward or outward. The critical case occurs when the ties in the lower portion of the wall lift the most weight.
- Step 3: Check the upper tie spacings. The tie spacing can be determined by comparing the sum of the shear capacities of the ties with the sum of the weight transferred by the ties, eg:

$$\sum v_{t,i} \geq \max(W_{t,1}, W_{t,2}) + P \quad \dots \text{C8B.70}$$

The flexural capacity of the ties cantilevering across the cavity gap should also be checked.

Note:

The calculation considers vertical spacings. Horizontal spacings should be adjusted to achieve an appropriate tributary weight. Vertical position of tie installation should be maintained through the wall section (ties should not be staggered).

Cavity gaps are commonly 1½” or 2” (38 mm or 50 mm) but should be determined from site measurement of wall thickness.

- Step 4: Check the lower tie spacings. The tie spacing can be determined as per Step 3 including the weight of the lower portion of the wall:

$$\sum v_{b,i} \geq W_{t,1} + W_{t,2} + \max(W_{b,1}, W_{b,2}) + P \quad \dots \text{C8B.71}$$

The flexural capacity of the ties cantilevering across the cavity gap should also be checked and may be critical for the spacing design.

Note:

The checks in Step 3 and Step 4 should show a different spacing for ties in the upper and lower portion of the wall. Engineers may wish to assign a single spacing to ensure that construction work is carried out correctly, and because the actual crack height may differ from the predicted height. Tie spacings should consider the size of the masonry module as ties should generally not be placed into mortar.

Calculation showing adequate tie shear/moment capacity per Step 3 and 4 is required for ties to be considered “rigid” and use the remainder of the procedure in this subsection. Alternatively consider applying the Flexible Tie method in given in C8B.5.6.

- Step 5: Analyse the wall using the method given in Section C8.8.5.2. For the purposes of assessment in Step 5, assume that the cavity wall is a single wall with a solid section equal to its gross thickness (including the cavity).
The displacement limit Δ_m should be taken as $\Delta_m = 0.6 \times \Delta_i$, where Δ_i is calculated using the gross thickness of the wall.

Note:

A cavity wall has lower mass than a solid wall due to the presence of the cavity. The reduction in mass due to the cavity decreases the restoring force and also decreases the demand. The reduction in demand from reduced weight is linear. However, the reduction in restoring force occurs more slowly, as cavity walls have most of their weight at the edges, where the weight is most effective in producing restoring force. The “missing weight” at the cavity, in the middle of the wall, does not provide much of the restoring force. Due to this beneficial relationship between demand and capacity, and provided that the rigid behaviour of the ties has been established, it is appropriate to assess rigidly-tied cavity walls as solid walls. Differences in the wall period for solid vs cavity walls (due to changes in the rotational inertia) are not significant for common wall configurations.

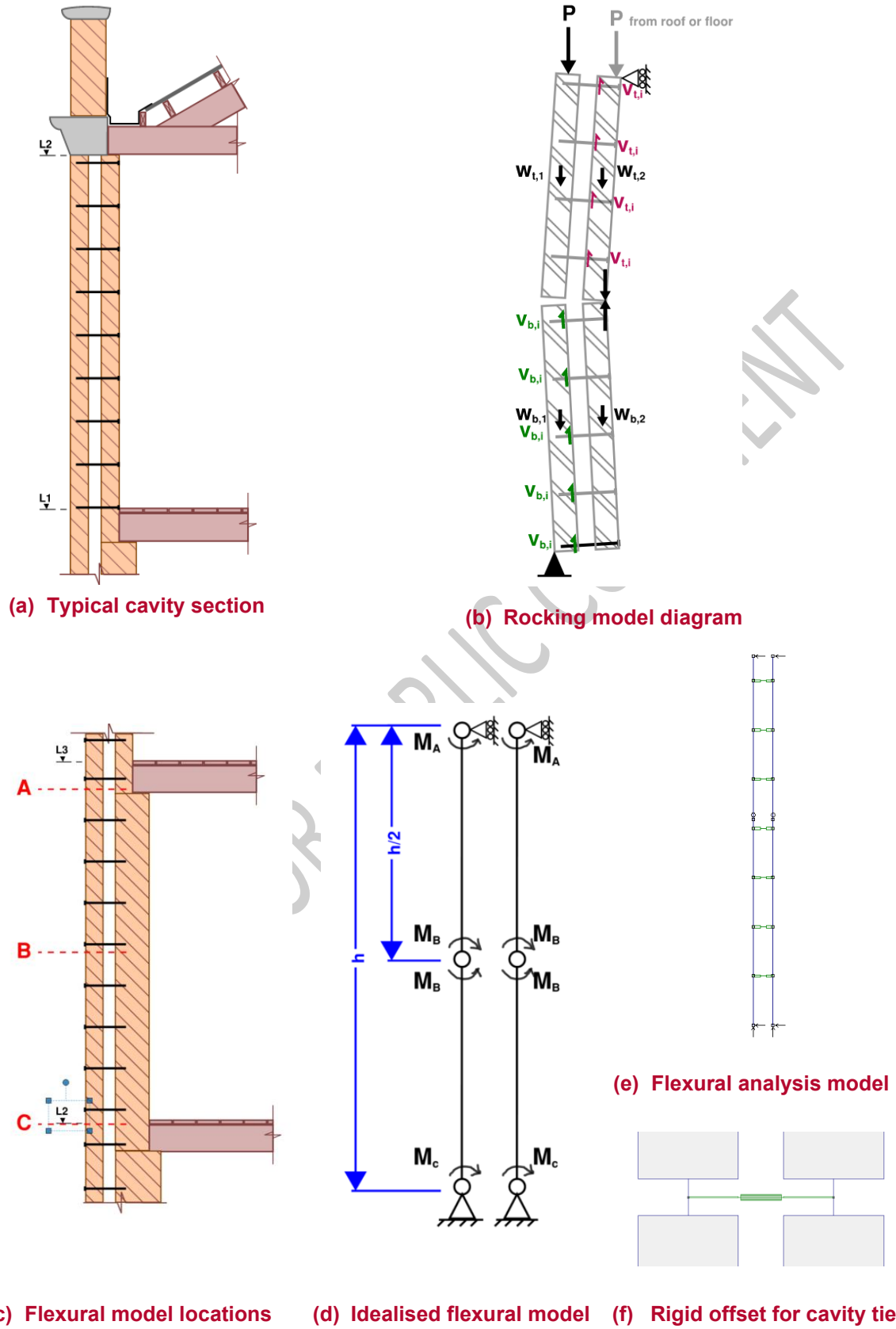


Figure C8B.15: Rocking cavity wall model and Flexural cavity wall model

C8B.5.9 Flexural Method for Assessment of cavity walls with rigid shear-transferring ties

Refer to Figure C8B.15(c-f):

- Step 1: Calculate the moment capacity of the leaves at the top (M_A) and bottom (M_C) of the cavity wall section. The method given in C8.8.5.2 and the relationship $M = \frac{t_{nom}^2}{6} (f'_t + \frac{P}{A_n})$ (see Equation C8.9) may be used for determination of the moment capacity.
- Step 2: Assume that the wall cracks at mid-height, $\frac{h}{2}$.
- Step 3: Calculate moment capacity at the crack height, M_B .
- Step 4: Generate structural analysis model as shown in Figure C8B.15(d). Provide rotational release and calculated moments at A, B and C. Provide tie elements using a rigid offset to ensure that the ties span only the cavity width.

Note:

The analysis model should be loaded using Parts loading from Chapter 8 of NZS 1170.5:2004. The use of $\mu_p = 1.25$ to account for energy dissipation due to wall cracking, tie deflection and partial rocking effects may be considered appropriate.

The substitution of $C_{hc}(T_p)$ given in Step 8 of Section C8.8.5.2 does not apply.

The period should be assumed to be less than 0.7 seconds unless specifically calculated, noting that the flexural wall period is likely to be shorter than the rocking period.

- Step 5: Using the analysis model, review the masonry sections and the ties for flexural capacity. Masonry flexural capacity can be calculated per Step 1 above; tie flexural capacity should be calculated or be provided by the tie supplier.

Note:

Calculation showing adequate tie shear/moment capacity per Step 5 is required for ties to be considered “rigid” and use the remainder of the procedure in this subsection. Alternatively consider applying the Flexible Tie method in given in C8B.5.6

- Step 6: Displacement limit at the wall hinge should be taken as $\Delta_m = \frac{t}{2}$, where t is the thickness of the most slender leaf.

Note:

The factor of 0.6 on wall displacements applies to a rocking response and is considered overly conservative for use in the context of C8B.5.9.

Temperature effects and rigid ties:

Engineers may wish to consider the potential for long term effects on masonry condition due to thermal cycling for cavity walls connected with rigid ties.

C8B.5.10 Flexural method worked examples

Rocking Method

Note that this worked example is for a single wythe – single wythe case. A double wythe – single wythe case at similar capacity width struggles to provide sufficient tie capacity to transfer force across the lower portion of the cavity wall.

Example Parameters

Single wythe – single wythe standard thickness brick (refer §C8.2.4) with 38 mm (1.5”) cavity spanning 3 m (~10ft) from Level 1 to Roof located in Timaru ($Z = 0.15$), soil class C. The roof load is only transferred to the inner wythe, and there is no bond beam nor parapet. Height to Level 1 is 4 m.

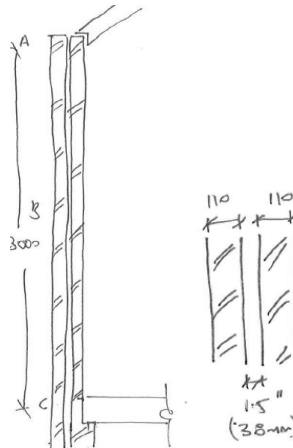


Figure C8B.16: Cavity wall details used for Rocking Method example

- Step 1: Assume crack height at $0.5h$
- Step 2: Determine the critical case → wall rocking inwards, as this has more load to initially transfer to the ‘bearing’ surface on the outer wythe.

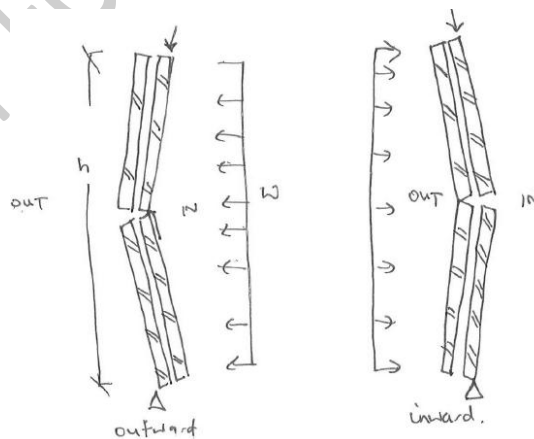


Figure C8B.17: Rocking cavity wall used for example

- Step 3: Determine number of upper ties required.

$$V^* = W_{upper\ inner} + P_{imposed}$$

$$V^* = 18 \times 0.11 \times 0.5 \times 3\text{ m} + 2\text{ m of roof @ } 0.6\text{ kPa}$$

$$V^* = 4.2 \text{ kN/m width}$$

Find tie capacity, from supplier literature eg:

$$V_n = 1.5 \text{ kN}$$

Therefore:

$$n_{reqd} = 2.8 \text{ ties over } 1500 \text{ mm height, per metre width of wall}$$

Say 3 ties ie 500 mm ctrs.

Check flexural capacity of ties. Ideally flexural capacity of tie is provided by supplier/manufacturer. In lieu of information, assume $f_y = 1000 \text{ MPa}$ and estimate from tie shank area.

Assumed double bending:

$$M^* = \frac{0.5V^* \times \text{cavity width}}{n_{ties}}$$

$$M^* = \frac{0.5 \times 4.2 \times 0.038}{3} = 0.0266 \text{ kNm/m}$$

$$M_n = \phi f_y Z = 0.9 \times 1000 \times \frac{\pi d^3}{32} = 0.9 \times 1000 \times \frac{\pi 6^3}{32} \times 10^{-6} = 0.0191 \text{ kNm/m}$$

Therefore provide ties at closer than 1 m ctrs horizontally and/or decrease vertical spacing.

Say 450 × 600 mm ctrs

Step 4: Determine number of lower ties required. These ties are transferring all of the upper weight of the wall, and the outer lower wythe, back to the inner wythe, where it is bearing.

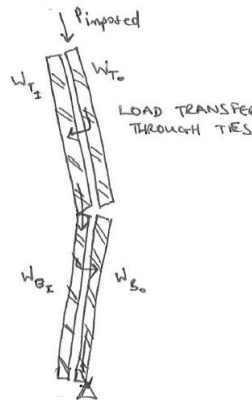


Figure C8B.18: Load transfer through ties in rocking cavity wall used for example

$$V^* = W_{upper \text{ inner}} + W_{upper \text{ outer}} + P_{imposed} + W_{lower \text{ outer}}$$

$$V^* = 2.97 + 2.97 + 1.2 + 18 \times 0.11 \times 0.5 \times 3 \text{ kN(/m width)}$$

$$V^* = 10.1 \text{ kN (/m)}$$

$$n_{reqd} = 6.7 \text{ ties over } 1500 \text{ mm height, per metre width of wall}$$

$$n_{reqd} = 4.0 \text{ ties over } 1500 \text{ mm height, if ties at } 600 \text{ mm ctrs horizontally}$$

$$n_{reqd} = 2.7 \text{ ties over } 1500 \text{ mm height, if ties at } 400 \text{ mm ctrs horizontally}$$

Check flexural capacity of ties, assumed ties at 400 mm ctrs horizontally, 500 mm ctrs vertically

$$M^* = \frac{0.5 \times 10.1 \times 0.038 \times 0.4}{4 \text{ ties}} = 0.019 \frac{\text{kNm}}{400} \text{ mm ctrs}$$

Say 400 × 400 mm ctrs

Step 5: This then allows composite action and C8.8.5.2 can be used as usual, with a couple of changes. Assuming $t_{gross} = 110 + 110 + 38 = 258$ mm solid wall and rocking at $h/2$.

$h = 3$ m, $W_t = W_b = 18 \times 0.258 \times 3/2 = 7.0$ kN/m, $P = 1.2$ kN/m as above.

Refer to Table C8.12 for ‘a’ and ‘b’ depending on boundary conditions. In our case assume case 3, as this is the closest to expected rocking behaviour (ie bearing on bottom corner of the wall)

$$e_t = e_o = e_b = \frac{t_{gross}}{2} = 29 \text{ mm} \quad e_p = 55 \text{ mm (eccentricity assumed half of inner leaf)}$$

$$y_b = y_t = \frac{h}{4} = 0.75 \text{ m}$$

We have not ascertained in-plane displacement of the perpendicular walls, so assume:

$$\psi = 2.5\% = 0.025$$

$\Delta_m = 0.6 \times \frac{t_{gross}}{2} = 77$ mm (note that if you are using a spreadsheet which automatically calculates Δ_m as per C8.8.5.2, you will need to alter.)

$$a = 25.3 \text{ kNm}, b = 3.9 \text{ kNm}, J_{bo} = J_{to} = 137 \text{ kgm}^2, J = 1214 \text{ kgm}^2$$

$$T = 4.07 \times \sqrt{\frac{J}{a}} = 0.89 \text{ sec}$$

$$C_h(0) = 1.33, Z = 0.15, R = 1, N_{(T,D)} = 1$$

$$h_i = \text{mid-point of } L_1 \text{ \& Roof} = 5.5 \text{ m} \rightarrow C_{hi} = 1.92, C_{hc}(T_p) = 1.3 \text{ and } C_p(T_p) = 0.5$$

$$\gamma = 1.32, D_{ph} = 128 \text{ mm} \rightarrow 60\% \text{NBS.}$$

Flexural Method

Similar to above, consider the wall from G-L₁ with double wythe internally and single wythe externally. Assume Level 1 joists are parallel to wall, ie no appreciable Level 1 floor load.

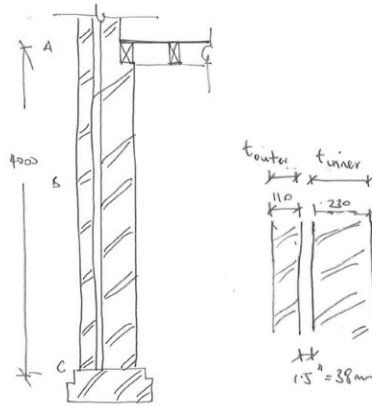


Figure C8B.19: Cavity wall details used for Flexural method example

Step 1: Calculate capacity of brick alone, considering axial load

$$\begin{aligned}
 A_{inner} &= \text{no self weight} + \text{proportion of roof} + \text{wall above (inner)} \\
 &= \text{say 2 m of roof} + 3 \text{ m wall} \\
 &= 1.5 \text{ kN/m} + 18 \times 0.11 \times 3 \text{ m} \\
 &= 7.44 \text{ kN/m}
 \end{aligned}$$

$$\begin{aligned}
 A_{outer} &= \text{Wall above (outer)} \\
 &= 5.94 \text{ kN/m}
 \end{aligned}$$

$$\begin{aligned}
 B_{inner} &= 7.44 \text{ kN/m} + 18 \times 0.23 \times 0.5 \times 4 \text{ m (assuming hinge at midspan)} \\
 &= 15.72 \text{ kN/m}
 \end{aligned}$$

$$\begin{aligned}
 B_{outer} &= 5.94 \text{ kN/m} + 18 \times 0.11 \times 0.5 \times 4 \text{ m} \\
 &= 9.9 \text{ kN/m}
 \end{aligned}$$

Assume $f'_t = 0$

$$M_{n \text{ inner}} = \frac{220^2}{6} \left(\frac{P^*}{1000 \times 220} \right)$$

$$M_{n \text{ outer}} = \frac{100^2}{6} \left(\frac{P^*}{1000 \times 100} \right)$$

$$M_{A, \text{inner}} = 0.273 \text{ kNm/m}, \quad M_{A, \text{outer}} = 0.099 \text{ kNm/m}$$

$$M_{B, \text{inner}} = 0.576 \text{ kNm/m}, \quad M_{B, \text{outer}} = 0.165 \text{ kNm/m}$$

Step 2: Create model of wall, choosing a starting layout of ties,

$$E_{\text{uncracked brick}} = 300 f'_m = 4.2 \text{ GPa}$$

$$E_{\text{steel}} = 200 \text{ GPa}$$

Start with ties at 600 mm ctrs, but model eqv 1 m of wall \rightarrow represent stiffness of 6 mm shank at 600 mm ctrs

$$I_{\text{tie}} = \frac{1000}{600} \times \frac{\pi 6^4}{64}$$

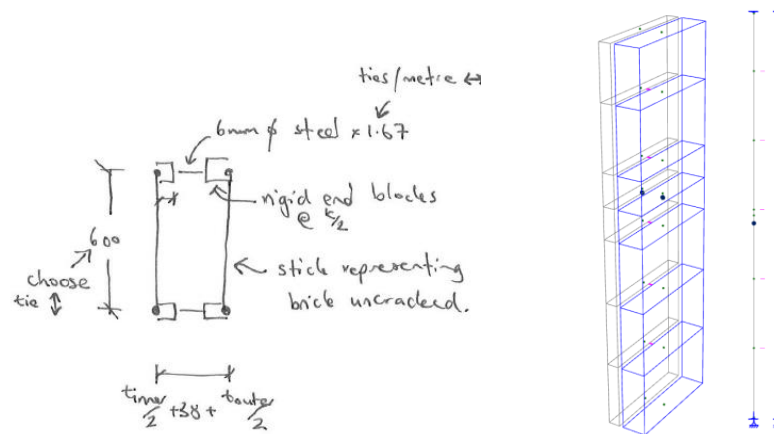


Figure C8B.20: Cavity wall tie details used for Flexural method example

Step 3: Ascertain imposed load on the wall

Assume average of parts load at Level 1 ($H = 4$ m) and Ground (PGA)

Assuming $T \leq 0.75$ s ie $C_i(T_p) = 2$

Assume $\mu = 1.25$ ie $C_{ph} = 0.85$

Level 1 = $0.567g$

Ground = $Z \times C_h(0) = 0.2g \rightarrow 0.38g$

Split load between two wythes, ie apply load to both wythes of wall.



Figure C8B.21: Cavity wall cross-section details used for Flexural method example

Step 4: Compare moment demand on wythes with capacity calculated in step 1. This comparison provides %NBS provided (a) flexural capacity of ties is sufficient and (b) step 5 is satisfied.

Step 5L: Check wall deflection ok.



C8B.6 Horizontally Spanning Walls

- Assessment of wall sections at circulation voids (lifts, stairs, risers etc), where there is no support for walls at floor levels.
- Assessment of wall sections spanning horizontally between piers, pilasters, or buttresses (although in cases where windows are present between piers, engineers will need to use judgement in applying the method).
- Assessment of wall sections spanning horizontally between vertical strongbacks. These strongbacks may be part of an **existing** seismic improvement scheme within a building that is being re-assessed, or they may be part of a retrofit programme.

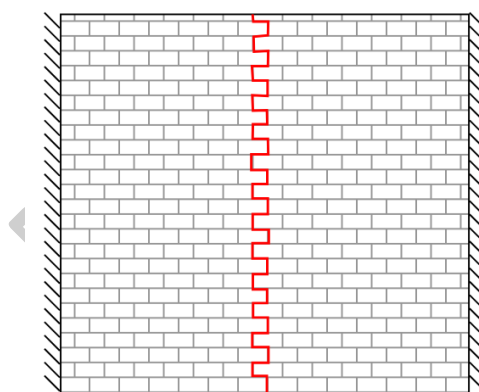
Horizontally spanning walls (and other possible wall span configurations) are treated in some detail in NPR 9998 2020 (Nederlands Normalisatie Instituut, 2020) using a force-

based approach. The NPR is available in English and free from the Royal Netherlands Standardization Institute (NEN). It is noted that the force-based approach and values for masonry capacity given in the NPR should not be adopted unmodified into the New Zealand context, as local values for parameters such as masonry materiality and assumed pre-cracked state may differ from the assumptions used in the NPR.

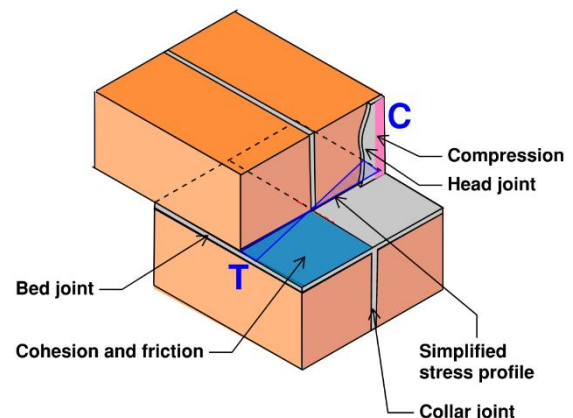
C8B.6.1 Flexural response assumptions

The procedure and examples presented in this section make the following assumptions:

- Wall panel flexure occurs along a vertical line at the midpoint between points of support. The line of flexure is stepped (bricks stronger than mortar). The physical area considered consists of the horizontal and vertical interfaces within the line of flexure, at each course.
- Wall panel flexural capacity is due to the combination of cohesion between courses of masonry and friction due to top load. These mechanisms provide resistance to rotation of the brick at the interfaces along the line of flexure.
- The calculated resistance to rotation is derived by analogy to the flexural tension capacity in a reinforced section. The horizontal moment capacity of the wall section derives from the lever arm between a compression surface on the head joint (on the compression side of the wall section), and the resistance to rotation and sliding in the bed joint on the “tension” side of the wall section (refer Figure C8B.24).
- For a one-wythe wall, the cohesion can be idealised as acting in two orthogonal directions on the plane of rotation (plane of rotation shown in blue in Figure C8B.24). For thicker walls this assumption may be valid but is more complex to demonstrate.
- Header courses are assumed to be non-effective. This assumption (disregarding the contribution from a percentage of courses) also accounts for pre-existing cracking to be present in some courses.
- Collar joints are assumed adequate to allow multiple wythes to act compositely in flexure.



(a) Assumed line of flexure with vertical support shown dashed



(b) Horizontal flexural model at the assumed line of flexure, showing single interface

Figure C8B.24: Flexural response assumptions for horizontally spanning walls

Note:

The method and assumptions presented in this section are generally consistent with approaches given in NPR 9998:2020 Appendix H (Nederlands Normalisatie Instituut, 2020).

C8B.6.2 Flexural response calculation

This section presents a potential horizontal flexural response calculation methodology, consistent with the assumptions in Section C8B.6.1.

- Step 1: Determine the appropriate cohesion c and friction coefficient μ_f values for the wall section under analysis.
- Step 2: Calculate the compressive stress at mid-height of the wall section. The mid-height is used to give an average compressive stress.
- Step 3: Define the peak stress capacity: the sum of the cohesion and compressive (frictional) stresses over a bed joint at the wall mid-height. Due to the assumption of a stepped line of flexure, the interface area under analysis is the bed-joint under half of a brick unit (refer Figure C8B.24a). Note that the friction contribution is small compared to cohesion.
- Step 4: Assume that a compressive stress develops in the head joint with the same peak magnitude as the cohesion + compressive stress. The sum of the cohesion + compression stress should generally be lower than the mortar compressive stress f'_j . This assumption of a symmetrical stress profile allows for the calculation of a “tension” force from the capacity of the cohesion + friction at the interface.
- Step 5: Calculate a moment capacity for the single interface at mid-height, using the tension force acting over an assumed lever arm. The lever arm assumed is 2/3 of the wall thickness, allowing for mortar recesses.
- Step 6: Determine how many courses are to be disregarded due to the presence of headers or cracks. An assumption of 20% is considered a reasonable starting point.
- Step 7: Multiply the interface capacity by the number of remaining courses to obtain the wall section flexural capacity.
- Step 8: Determine the load on the wall using Parts & Components per NZS 1170.5:2004 Chapter 8. The wall mid-height should be taken as the height of attachment h_i . The wall period should be assumed to be less than 0.7 seconds unless there is good reason to assume that its flexural response (not rocking response) has a longer period.

Step 9: Determine the allowable horizontal span. It is suggested that $M^* = \frac{wL^2}{10}$ could be used to account for the semi-fixed end condition of the horizontally-spanning wall sections, where sections are supported at both edges.

C8B.6.3 Tables of horizontal span values

The following tables provide some values for allowable horizontal spans between points of support for certain wall types in specific situations (as outlined in the tables). The assumptions underlying the calculated values are as follows. Assumptions per C8B.6.1 have also been applied. Calculation process per C8B.6.2.

Soil Class C.

IL2.

Parts load h_i (taken at midheight of wall) for 100%ULS demand.

$N(T,D) = 1$.

Design working life = 50 years.

Wall period = 0.7s.

$\mu = 1$.

$R_p = 1$.

Mortar = Soft per Table C8.4. (Cohesion = 0.3MPa, $\mu_f = 0.3$).

10mm mortar recess each face of wall.

Every 5th course assumed headers, only four of five courses contribute to flexural capacity.

$\gamma = 18\text{kN/m}^3$ (unit weight of masonry) per Table C8.6.

Reduction factor for cohesion + friction = 0.7 per the bed-joint sliding shear capacity (Equation C8.31) in Section C8.8.6.2.

$f'_j = 1\text{ MPa}$.

Assumed wall heights: Ground floor 4.2 m, L1 3.6 m, L2 3.6 m, parapet 0.6 m. Wall thickness consistent over full height.

Span capacity calculated from $M^* = \frac{wL^2}{10}$.

Single wythe walls' capacity accounts for two orthogonal directions of cohesion.

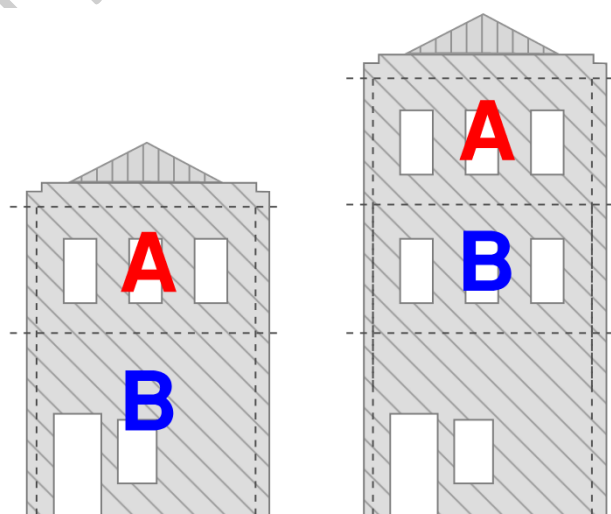


Figure C8B.25: Schematic illustration of wall levels for horizontal span tables

For one-wythe walls (110 mm):

ACCEPTABLE HORIZONTAL SPAN (m), 1-wythe (110 mm thick) Upper floor (level A)					
parapet y/n		y	y	n	n
wall position in building		Upper of 2	Upper of 3	Upper of 2	Upper of 3
total number of storeys in building		2	3	2	3
Z factor	0.15	2.0	2.0	2.0	2.0
	0.25	1.5	1.5	1.5	1.5
	0.4	1.2	1.2	1.2	1.2

ACCEPTABLE HORIZONTAL SPAN (m), 1-wythe (110 mm thick) Level below upper floor (level B)					
parapet y/n		y	y	n	n
wall position in building		Lower of 2	2 of 3	Lower of 2	2 of 3
total number of storeys in building		2	3	2	3
Z factor	0.15	2.0	2.0	2.0	2.0
	0.25	1.6	1.6	1.6	1.6
	0.4	1.2	1.2	1.2	1.2

For two-wythe walls (230 mm):

ACCEPTABLE HORIZONTAL SPAN (m), 2-wythe (230 mm thick) Upper floor (level A)					
parapet y/n		y	y	n	n
wall position in building		Upper of 2	Upper of 3	Upper of 2	Upper of 3
total number of storeys in building		2	3	2	3
Z factor	0.15	2.3	2.3	2.3	2.3
	0.25	1.8	1.8	1.8	1.8
	0.4	1.4	1.4	1.4	1.4

ACCEPTABLE HORIZONTAL SPAN (m), 2-wythe (230 mm thick) Level below upper floor (level B)					
parapet y/n		y	y	n	n
wall position in building		Lower of 2	2 of 3	Lower of 2	2 of 3
total number of storeys in building		2	3	2	3
Z factor	0.15	2.4	2.4	2.4	2.4
	0.25	1.9	1.8	1.8	1.8
	0.4	1.5	1.4	1.4	1.4

For three-wythe walls (350 mm):

ACCEPTABLE HORIZONTAL SPAN (m), 3-wythe (350 mm thick) Upper floor (level A)					
parapet y/n		y	y	n	n
wall position in building		Upper of 2	Upper of 3	Upper of 2	Upper of 3
total number of storeys in building		2	3	2	3
Z factor	0.15	3.0	3.0	3.0	3.0
	0.25	2.3	2.3	2.3	2.3
	0.4	1.8	1.8	1.8	1.8

ACCEPTABLE HORIZONTAL SPAN (m), 3-wythe (350 mm thick) Level below upper floor (level B)					
parapet y/n		y	y	n	n
wall position in building		Lower of 2	2 of 3	Lower of 2	2 of 3
total number of storeys in building		2	3	2	3
Z factor	0.15	3.1	3.1	3.1	3.0
	0.25	2.4	2.4	2.4	2.3
	0.4	1.9	1.9	1.9	1.8

C8B.6.4 Rigid strongbacks

For assessment or design of rigid strongbacks, the strongback element is designed to carry a tributary load in flexure. The horizontal span distance of masonry between strongbacks needs to be checked to demonstrate that the tributary width between strongbacks is appropriate.

Demand on the strongback should be calculated using Parts and Components. The period of the strengthened wall should be assumed to be governed by the flexural response of the strongback. It is considered probable that the period would be less than 0.7 seconds.

Care should be taken in any assumption of composite section between the strongback and the masonry, as the “composite” section would be anisotropic. For an outward-directed load, the masonry would need to take flexural tension, and this may only be possible where there is significant top load. Adequate shear flow between the strongback and the masonry would also need to be demonstrated for composite section action. Integral masonry piers could be assumed to be composite (depending on bond pattern) but would not automatically be rigid.

Rigid strongbacks should be designed for a deflection of not more than approximately a quarter of the wall useful instability displacement, eg approximately $\frac{1}{4} \times 0.6 \times \Delta_i$.

Consider the alignment of subdiaphragm ties with the strongback position.

C8B.6.5 Flexible strongbacks

Flexible strongbacks can be assessed or designed for compatibility with a partial wall rocking response. These strongbacks will likely be designed using timber sections and deform with the masonry while providing additional wall capacity.

The following steps are suggested for the assessment of existing strongbacks, and could be used in the design of flexible strongbacks.

Step 1: Determine the strongback section and spacing, or for design, devise a trial strongback and a trial spacing (eg 90x45 SG8 at 450 mm crs).

Step 2: Determine the maximum dependable flexural capacity of the strongback, M_{strong} . For a timber strongback, NZS 3603:1993 can be used to determine a flexural capacity. A strength reduction factor of 0.8 for timber is suggested in accordance with NZS 3603.

Step 3: Determine the maximum deflection of the strongback at its flexural capacity. By rearranging the expression for moment in a simple span and deflection within the span, the maximum deflection can be calculated as:

$$\Delta_{strong} = \frac{5 \times M_{strong} \times h^2}{48 \times E \times I}$$

Where h is the wall height between points of support, and the E and I values relate to the strongback alone.

Step 4: Consider the masonry wall rocking. If assessed to C8.8.5.2, it would have some instability deflection Δ_i which is almost certainly larger than Δ_{strong} for most practical configurations of wall and strongback. If there is any uncertainty the value of Δ_i can be checked against Δ_{strong} .

As explained in C8B.2.2, at Δ_i the wall has reached a point where it has no further restoring moment, allowing it to re-centre from rocking.

However, at Δ_{strong} , the wall retains some moment capacity.

Therefore calculate the moment capacity of the masonry wall when deflected to Δ_{strong} using a re-arranged form of the expression given in Equation C8B.1.

Step 5: Calculate the value of the deflected angle, A , at Δ_{strong} .

$$A = \frac{2 \times \Delta_{strong}}{h}$$

Step 6: Using the value of A , calculate the restoring moment in the wall.

$$M_{rock} = W_b(e_b - Ay_b) + W_t(e_o + e_b + e_t - A(h - y_t)) + P(e_o + e_b + e_t + e_p - Ah) - \Psi(W_b y_b + W_t y_t)$$

Refer to Equation C8B.1 for definitions of terms.

The weight terms W_b , W_t and P should be calculated in terms of the strongback spacing selected in Step 1.

Step 7: Calculate the demand on the wall. This demand should be calculated using Section 8 (Parts and Components) of NZS 1170.5:2004. The Parts demand should be used to find a bending moment for the wall section, M^* .

Step 8: Calculate:

$$\%NBS = \frac{M_{strong} + M_{rock}}{M^*}$$

Step 9: Align subdiaphragm ties with the strongback position.

Notes on the Flexible Strongback method:

The strongback and masonry are not acting compositely. In the “out-of-the-building” direction, the strongback should be tied to the masonry with ties with adequate axial capacity to transfer their tributary load. In the “into-the-building” direction, the masonry leans on the strongback through the masonry ties. In unfinished masonry walls, there is likely to be some gap between the strongback and the masonry (due to the rough/irregular surface of the wall). Unless the wall is very rough, and the gap is very large, there should be no need to prepare the strongback for bearing, and flexibility in the ties over the gap between strongback and wall may be beneficial (as below).

There is a difference between a rocking deflected shape for the masonry wall and a flexural deflected shape for the strongback. Due to the small rotations expected, this difference is not considered highly significant. However, it is worth noting that ties between the strongback and the masonry need to allow for the masonry cracking and “opening up” at the crack, while the strongback cannot extend in length at the cracked location. Under modest deflection, the crack “opens up” a small amount, which is expected to be accommodated by flexing of the ties. For larger deflections, alternative design provisions like vertical slots in the strongback could be considered.

There may be some cases and configurations where design iteration is required to ensure that the flexible strongback system does not perform worse than the rocking wall alone.

The Flexible method is checking the moment capacity available for the wall-strongback system at the point that the strongback reaches its dependable capacity. If the wall-strongback system has significantly more capacity than the demand, the strongback may take up most of the demand before wall rocking is activated, which is acceptable. If the wall-system capacity has significantly less capacity than the demand, the strongback may fail. For a timber strongback this failure may lead to a step-change from strengthened to unstrengthened capacity. It is suggested that assessments do not rely on the wall reverting to a masonry-rocking response in the case of timber strongback failure. For a well-detailed steel strongback, a flexural “failure” may be more forgiving.

Note:

New research has recently been published regarding timber strongback performance (Cassol et al. 2021; Cassol et al. 2025a; Cassol 2025b). The methods presented in Appendix C8B6.4 and Appendix C8B6.5 are intended as approximations ahead of more detailed methods becoming available for future editions of the Guidelines.

C8B.6.6 Worked examples**Horizontal bending**

Consider a 3.2 m high wall located in Whanganui ($Z = 0.25$), 230 mm thick (2 wythes), with a 600 mm high parapet of the same thickness. The parapet has a separate lateral restraint. The wall is on the upper floor of a three-storey structure with its base at 6.8m above ground.

Step 1:

Cohesion = 0.3 MPa, coefficient of friction $\mu_f = 0.3$ (from Soft mortar properties per Table C8.4).

Step 2:

Compressive stress at midheight of wall: $0.6 \text{ m parapet} + (3.2 \text{ m}/2) \times 18 \text{ kN/m}^3 = 39.6 \text{ kPa}$.
Assume no significant roof tributary load for this example.

Step 3:

Peak stress capacity from cohesion + friction.

$$\sigma = 0.7 \times (c + \mu_f \times \text{friction})$$

$$\sigma = 0.7 \times (0.3 \text{ MPa} + 0.3 \times 0.0396 \text{ MPa}) = 0.218 \text{ MPa}$$

Step 4:

Check cohesion + friction \leq probable compressive stress in mortar

$f'_j = 1 \text{ MPa}$ from Table C8.5

$0.218 \text{ MPa} \leq 1 \text{ MPa}$, OK!

Step 5:

Moment capacity. Convert cohesion + friction stress to force with triangular assumption.

$$V_s = \frac{1}{2} \times \sigma \times (t - \text{mortar recesses})/2 \times l_u/2 \text{ (where } l_u \text{ is the length of a brick} = 230 \text{ mm)}$$

$$V_s = \frac{1}{2} \times 0.218 \text{ MPa} \times (230 \text{ mm} - 2 \times 10 \text{ mm})/2 \times 230 \text{ mm}/2$$

$$V_s = 1.32 \text{ kN (per interface)}$$

Lever arm taken as $2/3 \times (t - \text{mortar recesses})$

$$\text{Lever arm} = 2/3 \times (230 \text{ mm} - 2 \times 10 \text{ mm})$$

$$\text{Lever arm} = 140 \text{ mm}$$

$$\text{Moment capacity} = V_s \times \text{Lever arm}$$

$$\text{Moment capacity} = 1.32 \text{ kN} \times 140 \text{ mm} = 0.18 \text{ kNm (per interface)}$$

Step 6:

Discount header rows etc and assume 4/5 courses are effective.

Step 7:

Wall height = 3.2 m

Height of one brick + one mortar joint = 80 mm. Therefore 40 courses in the wall height.

$$\text{Wall capacity} = 40 \text{ courses} \times (4/5) \times 0.18 \text{ kNm/course} = 5.76 \text{ kNm}$$

Step 8:

From NZS 1170.5 Ch8

Importance Level 2, Soil Class C, $Z = 0.25$, $\mu_p = 1$, $R_p = 1$, $h_i = 6.8 \text{ m} + 3.2 \text{ m}/2 = 8.4 \text{ m}$,
 $h_n = 10 \text{ m}$, $T_p = 0.4\text{s}$

$$C_{ph} = 1$$

$$C_p(T_p) = 1.60$$

$$\text{Wall weight } W_p = 18 \text{ kN/m}^3 \times 3.2 \text{ m} \times 230 \text{ mm} = 13.25 \text{ kN/m}$$

$$F_{ph} = 1.60 \times 1 \times 1 \times 13.25 \text{ kN/m} = 21.20 \text{ kN/m (for 100\%NBS)}$$

Step 9:

Allowable span. Taking $M = wL^2/10$, rearranging to find L

$$L_{\text{allow}} = \sqrt{10 \times M/w}$$

$$L_{\text{allow}} = \sqrt{10 \times 5.76 \text{ kNm} / 21.2 \text{ kN/m}} = 1.65 \text{ m}$$

If 67%NBS is the required target

$$L_{\text{allow}} = \sqrt{10 \times 5.76 \text{ kNm} / 0.67 \times 21.2 \text{ kN/m}} = 2.02 \text{ m}$$

Rigid strongback

Take the same wall in Whanganui. Demand at 67%NBS is 21.2 kN per horizontal metre of wall length. With a 2 m tributary area between strongbacks, the demand is $2 \text{ m} \times 21.2 \text{ kN/m} = 42.4 \text{ kN}$

Divide by the wall height to find the running demand on the length of the strongback.

$$w = 42.4 \text{ kN} / 3.2 \text{ m} = 13.3 \text{ kN/m.}$$

The allowable displacement is $0.25 \times 0.6 \times t/2$

$$\Delta_{\text{allow}} = 0.25 \times 0.6 \times 230 \text{ mm} = 34.5 \text{ mm}$$

Back-calculate the 2MOA of the required section for the strongback.

$$I = 5 \times w \times h^4 / 384 \times E \times \Delta_{\text{allow}}$$

$$I = 2.63 \times 10^6 \text{ mm}^4$$

Acceptable sections include:

$$100 \times 100 \times 5.0 \text{ SHS } (I = 2.66 \times 10^6 \text{ mm}^4)$$

$$127 \times 51 \times 5.0 \text{ RHS } (I = 2.89 \times 10^6 \text{ mm}^4)$$

$$100 \text{UC}14.8 \text{ } (I = 3.18 \times 10^6 \text{ mm}^4)$$

Flexible strongback

Taking the same wall in Whanganui and designing a flexible strongback solution.

Step 1:

Nominate 140x45 SG8 strongbacks at 600 mm crs.

Step 2:

Flexural capacity of strongback:

$$\phi (\text{timber}) = 0.8$$

$$k_1 = 1$$

$$k_4 = 1$$

$$k_5 = 1$$

$S_I = 3b/d$ (from Cl. 3.2.5.3 of NZS 3603:1993)

$$S_I = 3 \times 45 / 90 = 6$$

Therefore $k_8 = 1$

$$f_b = 14 \text{ MPa}$$

$$Z = bd^2/6 = 147000 \text{ mm}^3$$

$$\phi M_n = \phi \times k_1 \times k_4 \times k_5 \times k_8 \times f_b \times Z$$

$$\phi M_n = M_{strong} = 1.65 \text{ kNm}$$

Step 3:

Deflection capacity of strongback.

$$\Delta_{strong} = 5 \times M_{strong} \times h^2 / 48 E I$$

$$\Delta_{strong} = 5 \times 1.65 \text{ kNm} \times 3.2\text{m}^2 / 48 \times 8 \text{ GPa} \times 1.029 \times 10^7 \text{ mm}^4$$

$$\Delta_{strong} = 21 \text{ mm}$$

Step 4:

By inspection $\Delta_{strong} \leq \Delta_i$

Step 5:

Angle A

$$A = 2 \times \Delta_{strong} / h$$

$$A = 2 \times 21 \text{ mm} / 3200 \text{ mm}$$

$$A = 0.013 \text{ m}^2$$

Step 6:

Restoring moment.

For this example wall assumed BC1 to Table C8.12. BC1 will not always apply.

$$W_b = \gamma \times t_{gross} \times h/2 \times \text{spacing}$$

$$W_b = 18 \text{ kN/m}^3 \times 230 \text{ mm} \times 3200 \text{ mm} / 2 \times 600 \text{ mm}$$

$$W_b = 3.97 \text{ kN} = W_t$$

$$y_t = y_b = h/4 = 800 \text{ mm}$$

$$P = \gamma \times t_{gross} \times \text{height of parapet} \times \text{spacing}$$

$$P = 18 \text{ kN/m}^3 \times 230 \text{ mm} \times 600 \text{ mm} \times 600 \text{ mm}$$

$$P = 1.49 \text{ kN}$$

$$t = t_{gross} \times (0.975 - 0.025 \times (P/W))$$

$$t = 230 \text{ mm} \times ((0.975 - 0.025 \times (1.49 \text{ kN} / (3.97 \text{ kN} + 3.97 \text{ kN})))$$

$$t = 223 \text{ mm}$$

$$e_b = e_t = e_o = t/2 = 112 \text{ mm}$$

$$e_p = 0$$

$$\Psi = 0.025$$

Moment capacity M_{rock}

$$M_{rock} = W_b (e_b - A y_b) + W_t (e_o + e_b + e_t - A(h - y_t)) + P(e_o + e_b + e_t + e_p - Ah) - \Psi(W_b y_b + W_t y_t)$$

$$M_{rock} = 3.97 \text{ kN} \times (112 \text{ mm} - 0.013 \times 800 \text{ mm}) + 3.97 \text{ kN} \times (112 \text{ mm} + 112 \text{ mm} + 112 \text{ mm} - 0.013 \times (3200 \text{ mm} - 800 \text{ mm})) + 1.49 \text{ kN} \times (112 \text{ mm} + 112 \text{ mm} + 112 \text{ mm} + 0 \text{ mm} - 0.013 \times 3200 \text{ mm}) - 0.025 \times (3.97 \text{ kN} \times 800 \text{ mm} + 3.97 \text{ kN} \times 800 \text{ mm})$$

$$M_{rock} = 1.88 \text{ kNm}$$

Step 7:

Demand from NZS 1170.5 Ch8

Importance Level 2, Soil Class C, $Z = 0.25$, $\mu_p = 1$, $R_p = 1$, $h_i = 6.8 \text{ m} + 3.2 \text{ m}/2 = 8.4 \text{ m}$, $h_n = 10 \text{ m}$, $T_p = 0.4 \text{ s}$

$$C_{ph} = 1$$

$$C_p(T_p) = 1.60$$

Wall weight $W_p = 18 \text{ kN/m}^3 \times 230 \text{ mm} \times \text{spacing (600mm)} = 2.48 \text{ kN/m}$ (eg per vertical metre of wall)

$$F_{ph} = 1.60 \times 1 \times 1 \times 2.48 \text{ kN/m} = 3.97 \text{ kN/m}$$

$$M^* = F_{ph} \times h^2 / 8$$

$$M^* = 5.09 \text{ kNm}$$

Step 8:

$$\%NBS = (M_{strong} + M_{rock}) / M^*$$

$$\%NBS = (1.65 \text{ kNm} + 1.88 \text{ kNm}) / 5.09 \text{ kNm}$$

$$\%NBS = 69\%, \text{ OK for a target of } 67\% \text{ NBS.}$$

C8B.7 Boundary Conditions Worked Examples

The following section gives examples of common boundary conditions and how they should be interpreted. There is some degree of judgement in ascertaining the exact geometry and points of bearing in the wall, given detailing may not be able to be investigated fully. If in doubt, consider a number of “what if” scenarios to bound the likely range of expected performance.

C8B.7.1 Two-storey building worked example: Lower wall with upper wall and parapet above

Attributes: Floor diaphragm assumed to provide horizontal load path to bracing elements away from this cross-section: considering the wall spanning from ground up to first floor level.

Stiff ground allowing fixity of footing to be considered

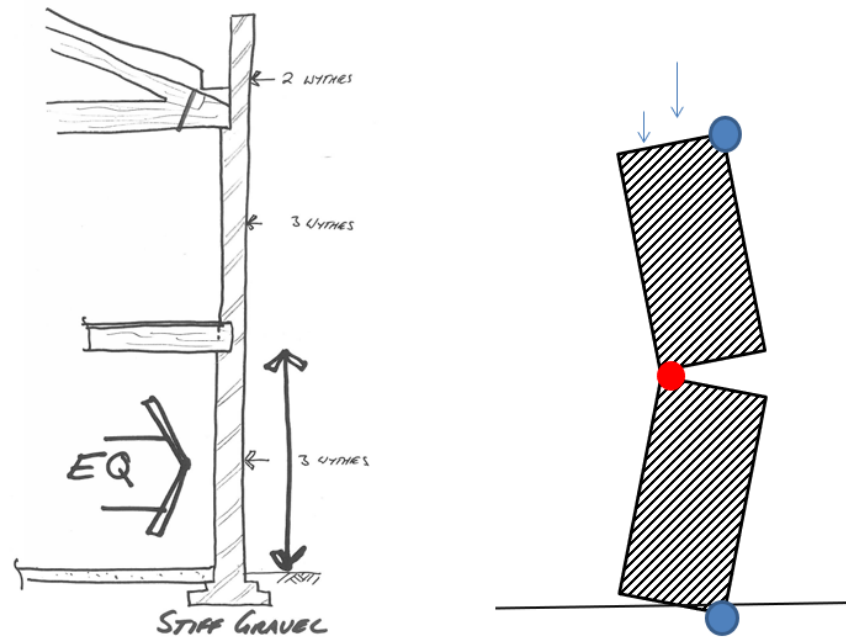


Figure C8B.26: Boundary conditions for lower wall with upper wall and parapet above, stiff ground

Analysis Considerations: Axial load position is the sum of both the parapet, roof and wall load (at its centreline without rocking) and the floor bearing load at its bearing position. The position it acts is a weighted average of the two load eccentricities (floor contribution likely small). Because the ground is stiff and the wall has a foundation, the lower rocking plane will pivot around the far (beneficial) side. The upper wall is considered to be rocking in the same direction, or at worst not rocking, meaning the upper section of the lower wall will pivot around the far (beneficial) side. Conclusion: Boundary Condition 3 of Table C8.12.

C8B.7.2 Two-storey building worked example: Lower wall with upper wall and parapet above

Attributes: Floor diaphragm assumed to provide horizontal load path to bracing elements away from this cross-section: considering the wall spanning from ground up to first floor level.

Soft ground so no fixity of footing to be considered (refer Step 4 Page C8-103).

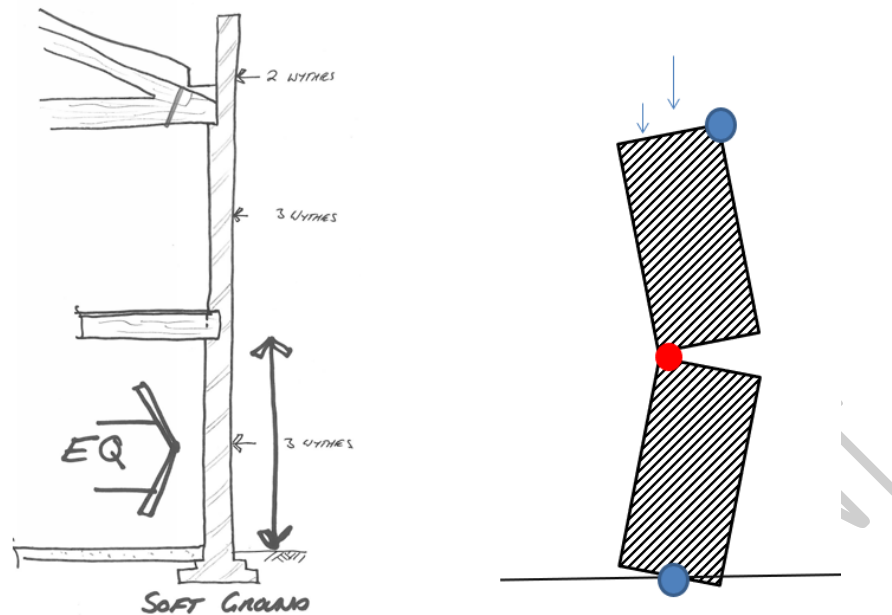


Figure C8B.27: Boundary conditions for lower wall with upper wall and parapet above, soft ground

Analysis Considerations: Upper conditions as previous example. Because the ground is soft, the lower rocking plane will pivot around the centre (neutral). Conclusion: Boundary Condition 2 Table C8.12.

C8B.7.3 Two-storey building worked example: Upper wall with parapet above

Attributes: Floor and roof diaphragms assumed to provide horizontal load path to bracing elements away from this cross-section: considering the wall spanning from the first floor up to gutter-level (some sort of transom) only.

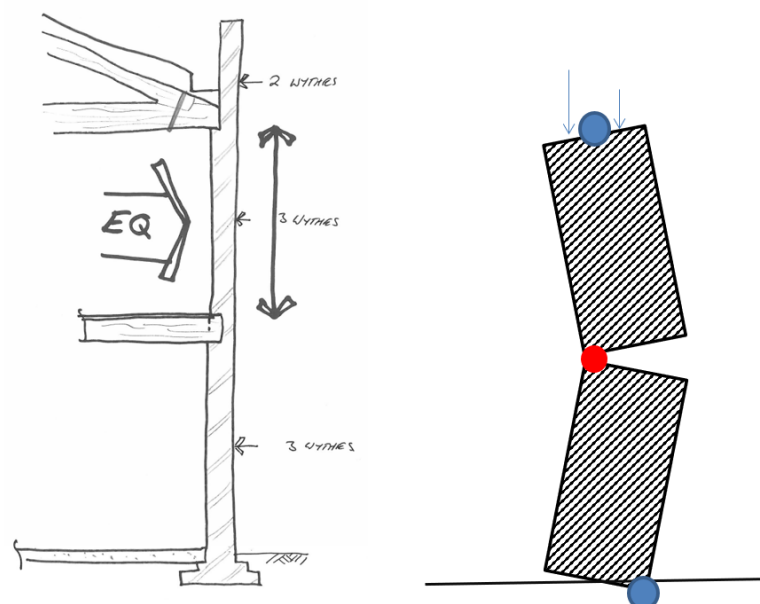


Figure C8B.28: Boundary conditions for upper wall with parapet above

Analysis Considerations: Axial load position is the sum of both the parapet load (at its centreline without rocking) and the roof truss bearing load. The position it acts is a weighted average of the two load eccentricities. The lower wall is considered to be rocking in the same direction, or at worst not rocking, meaning the lower section of the upper wall will pivot around the far (beneficial) side. Because the parapet cannot provide fixity, the upper rocking plane will be considered pivoting around the middle (neutral). Conclusion Boundary Condition 1 Table C8.12.

C8B.7.4 Two-storey building worked example: Upper cavity wall with parapet above (stiff L1 floor)

Attributes: Floor and roof diaphragms assumed to provide horizontal load path to bracing elements away from this cross-section: considering the wall spanning from the first floor up to gutter-level (some sort of transom) only. Concrete floor at level 1 and assuming no concrete above this (aside from lintels or bond-beams).

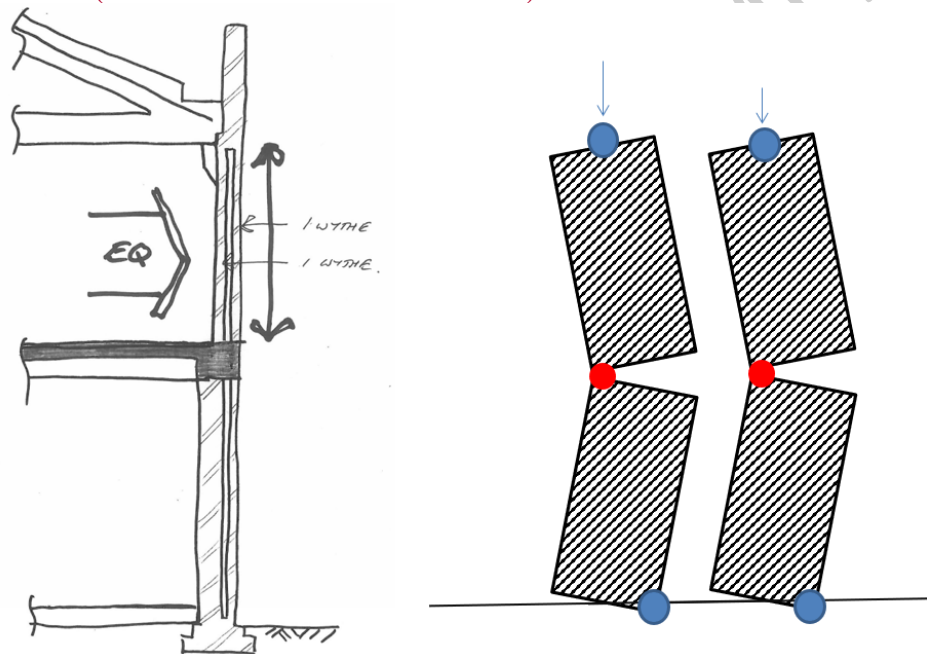


Figure C8B.29: Boundary conditions for upper cavity wall with parapet above

Analysis Considerations: Axial load is different on each leaf, and depends on relative weight of roof and parapet. Because the first floor is stiff, the lower rocking plane will pivot around the far (beneficial) side. Because the parapet cannot provide fixity, the upper rocking planes will be considered pivoting around the middle (neutral). Conclusion Boundary Condition 1 Table C8.12.

If there are no cavity ties the capacity is the lesser of the two leaves: the one with the smallest axial load.

If cavity ties are intact or new flexible ties have been added, capacity is the average of each walls' capacity: as they are joined their capacity is shared, and if they are the same thickness they have the same limiting deflection.

If new rigid ties in accordance with C8B5.7 are added, analyse as per the previous example.

C8B.7.5 Two-storey building worked example: Lower cavity wall with upper wall and parapet above

Attributes: Floor and roof diaphragms assumed to provide horizontal load path to bracing elements away from this cross-section: considering the wall spanning from t ground up to first floor level. Concrete floor at level 1. **If there are columns in the wall supporting the first floor the assessment should be carried out in accordance with Section C7 not this section.**

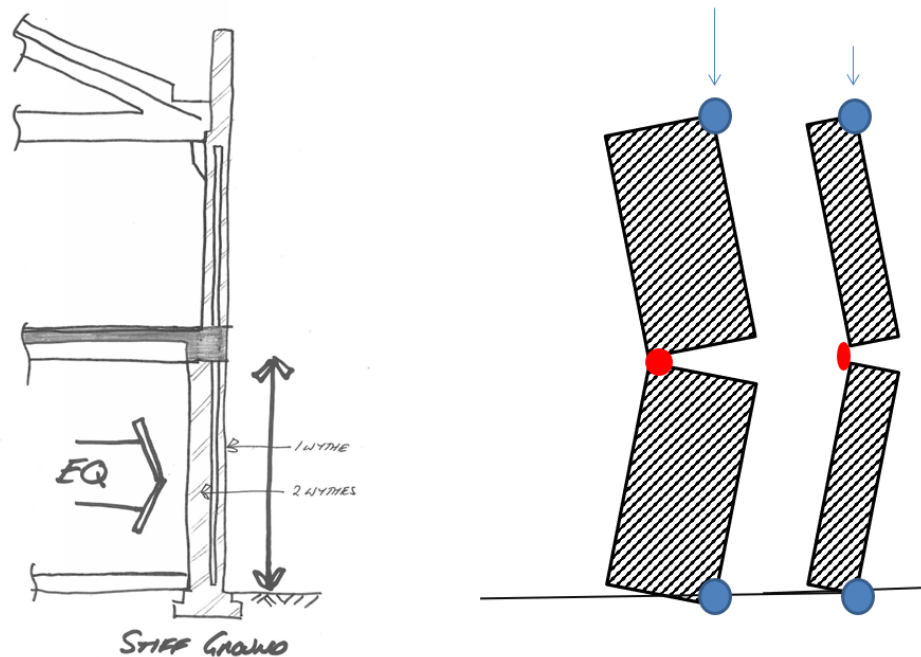


Figure C8B.30: Boundary conditions for lower cavity wall with upper wall and parapet above

Analysis Considerations: Axial load from the floor, wall above, roof and parapet is allocated to the two leaves in proportion to the area ($2/3 : 1/3$) as the floor is stiff. Because the first floor is stiff, the lower rocking plane will pivot around the far (beneficial) side. Because the ground is stiff and the wall has a foundation, the lower rocking plane will pivot around the far (beneficial) side. Conclusion Boundary Condition 3 Table C8B.1.

If there are no cavity ties the capacity is simply the (likely lesser) individual capacity of the thinner leaf.

Alternatively if cavity ties are intact or new flexible ties have been added, the total wall capacity is the half sum of the capacity of both leaves, BUT the capacity of the **thicker wall needs to be factored down to be evaluated at the permissible deflection of the thinner leaf**. Alternatively the capacity can be taken as the inner leaf (with all the axial load applied) with the outer leaf providing an additional **load** on this inner leaf. The presumption in this case is the outer leaf has some local crushing at its hinge points and therefore has no residual strength for face loads.

C8B.7.6 Two-storey building worked example: Upper cavity wall with parapet above (flexible floor)

Attributes: Floor and roof diaphragms assumed to provide horizontal load path to bracing elements away from this cross-section: considering the wall spanning from the first floor up to gutter-level (some sort of transom) only. Ties at first floor secure both the inner and the outer leaf.

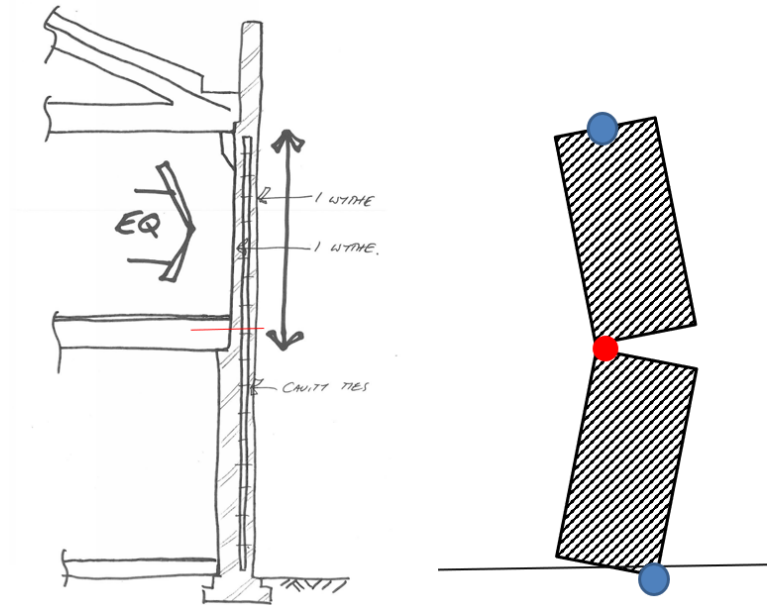


Figure C8B.31: Boundary conditions for upper cavity wall with parapet above

Analysis Considerations: Assume cavity ties are intact or new flexible ties have been added. Axial load is different on each leaf, and depends on relative weight of roof and parapet. The lower wall is considered to be rocking in the same direction, or at worst not rocking, meaning the lower section of the upper wall will pivot around the far (beneficial) side. Because the parapet cannot provide fixity, the upper rocking planes will be considered pivoting around the middle (neutral). Conclusion Boundary Condition 1 Table C8.12. Capacity is the sum of each leaf's capacity divided by two (leaves): as they are joined their capacity is shared, and if they are the same thickness they have the same limiting deflection.

If new rigid ties in accordance with C8B5.7 are added, analyse as per the earlier 2-wythe single leaf example.

C8B.7.7 Single-storey building worked example: Wall with unsecured parapet above

Attributes: Sarking diaphragm assumed to provide horizontal load path to bracing elements away from this cross-section: considering the wall spanning from the ground up to gutter-level (some sort of transom) only.

Stiff ground allowing fixity of footing to be considered

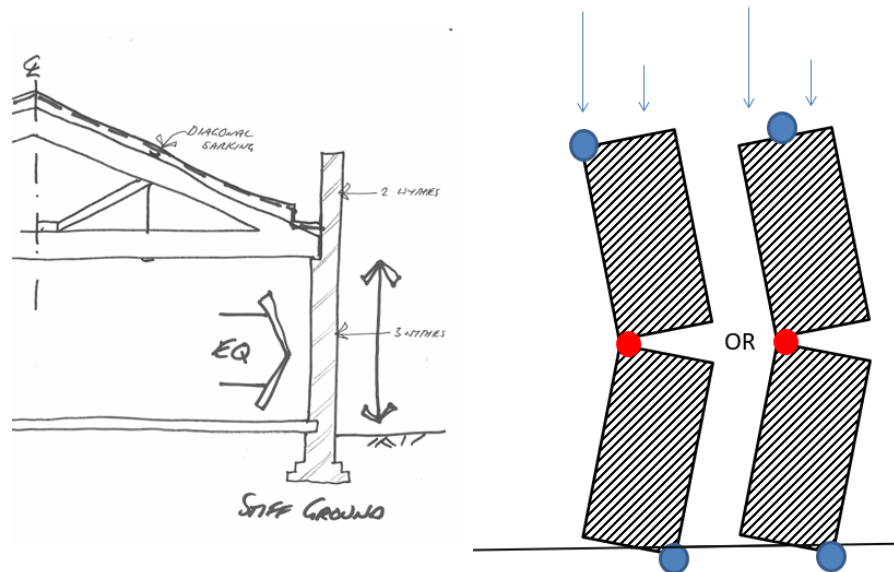


Figure C8B.32: Boundary conditions for single storey wall with unsecured parapet above

Analysis Considerations: Axial load position is the sum of both the parapet load (at its centreline without rocking) and the roof truss bearing load. The position it acts is a weighted average of the two load eccentricities. Because the ground is stiff and the wall has a foundation, the lower rocking plane will pivot around the far (beneficial) side. However if the truss load is high relative to the parapet, and being on the inside face and the parapet, the upper rocking plane could be considered pivoting around the near (adverse) side. Conclusion: Boundary Condition 1 if neutral, or not in tables if adverse condition considered.

C8B.7.8 Single-storey building worked example: Wall with secured parapet above

Attributes: Sarking diaphragm assumed to provide horizontal load path to bracing elements away from this cross-section: considering the wall spanning from the ground up to gutter-level (some sort of transom) only. Parapet braced back to trusses.

Stiff ground allowing fixity of footing to be considered

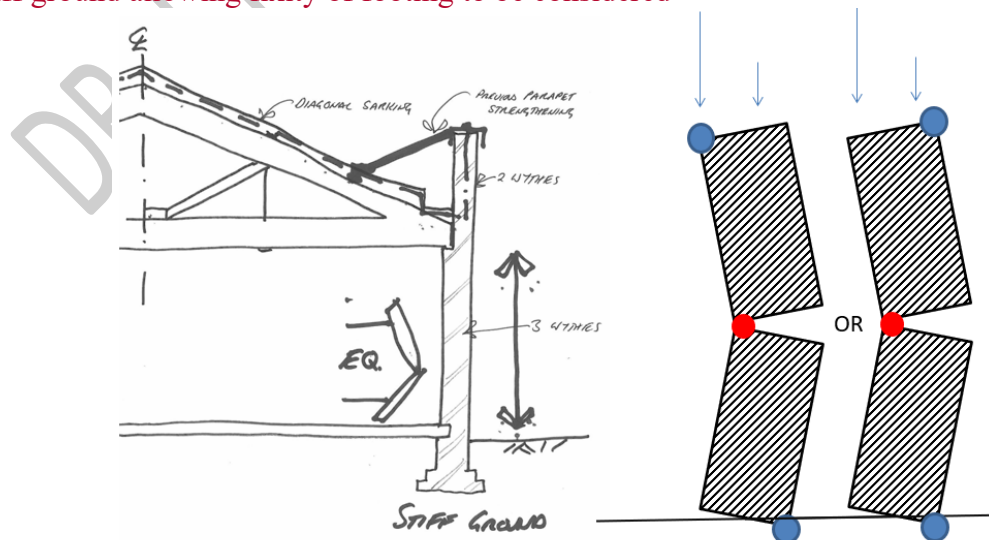


Figure C8B.33: Boundary conditions for single storey wall with secured parapet above

Analysis Considerations: Axial load position is the sum of both the parapet load (at its centreline without rocking) and the roof truss bearing load. The position it acts is a weighted average of the two load eccentricities. Because the ground is stiff and the wall has a foundation, the lower rocking plane will pivot around the far (beneficial) side. If the parapet brace and truss is stiff and its upward rake is resolved with a tie-down, the parapet can provide beneficial (far side load position) fixity to the top of the wall. Conclusion: Boundary Condition 3 Table C8.12, or not in tables if the adverse condition is considered. If the roof truss is very long/flexible (enough to oscillate the parapet itself) and/or the upward force is not resolved, consider the parapet weight either not contributing, or on the adverse side as with the example previous to this one.

C8B.8 Axial Load Position Worked Examples

C8B.8.1 Roof load on cantilever wall worked example: Stiffly tied by truss

Attributes: No sarking diaphragm so no horizontal load path to other bracing elements (e.g. end walls).

Stiff ground allowing cantilever out of the ground to be considered

Stiff truss moves walls each side of the building together

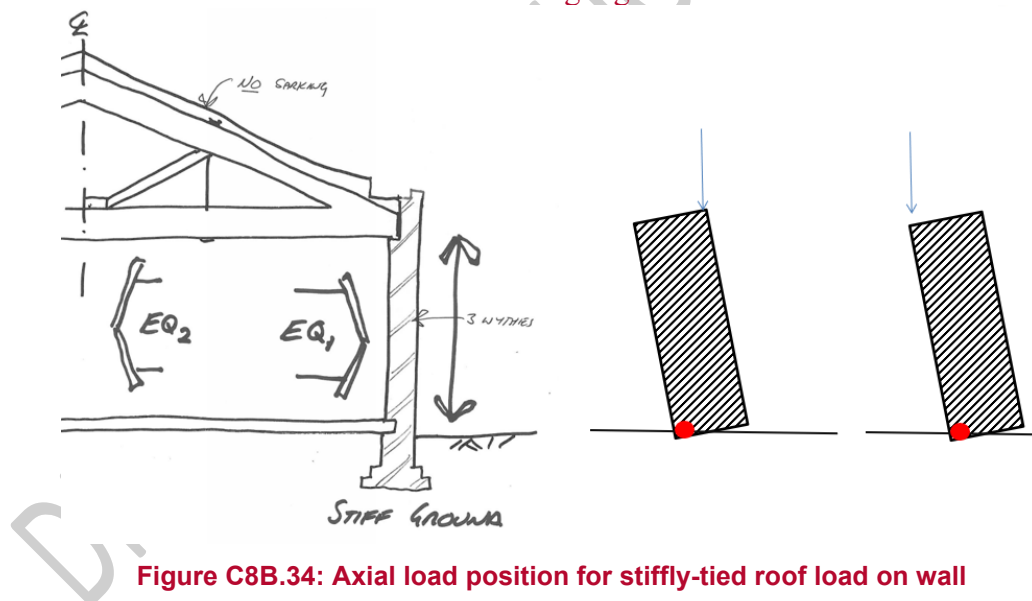


Figure C8B.34: Axial load position for stiffly-tied roof load on wall

Analysis Considerations: With no sarking forming a diaphragm, the walls each side cantilevering from the ground are envisaged to resist the lateral load. Consider both stabilising and destabilising load to occur at the same time in any one cross-section because truss stiffly connects the two walls together. Truss load assists the stability on one side but worsens it on the other.

C8B.8.2 Roof load on cantilever wall worked example: Flexibly tied

Attributes: No sarking diaphragm to provide horizontal load path to bracing elements. Stiff ground allowing cantilever out of the ground to be considered

Flexible truss means walls each side of the building may move out of phase
Building may not comply as Basic (Refer Table C8.1 and C8.9.3).

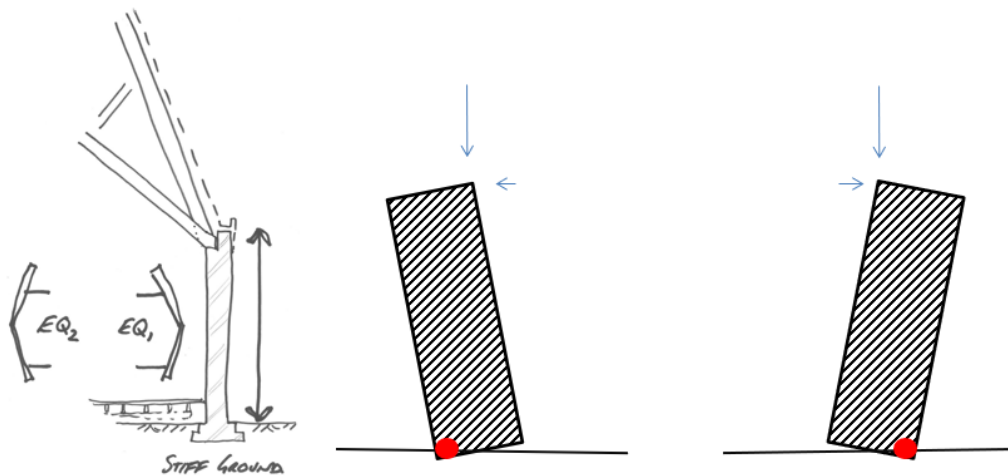


Figure C8B.35: Axial load position for flexibly-tied roof load on wall

Analysis Considerations: With no sarking forming a diaphragm, the cross-section is envisaged to resist the lateral load. If truss is sufficiently flexible, the wall with the destabilising load (therefore less capacity) would need to be considered to resist half the cross-section's seismic mass, unless a more complex analysis is carried out.

C8B.8.3 Post-tensioned parapet worked example

Attributes: Existing parapet (and wall below) fitted with unbonded post-tensioning.

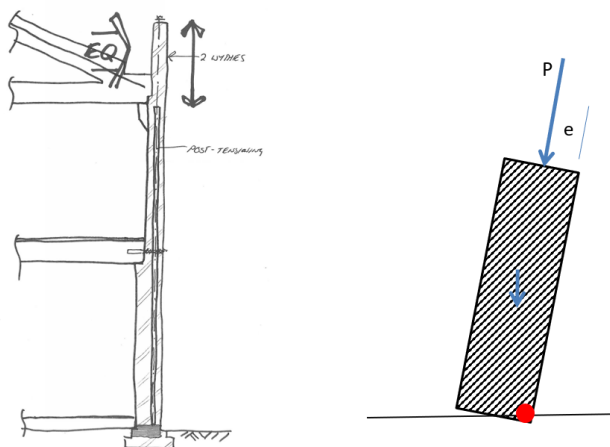


Figure C8B.36: Axial load position on post-tensioned parapet

Analysis Considerations: location of axial load key to the assessment (“e” in diagram above) whether centred on wall or not. Some interpolation of e_p between position (centre or side) required if charts are to be used. Check the post-tensioning rod has sufficient elongation capacity due to the geometric elongation from rocking. If not, a conservative analysis is to consider as if bonded (see below).

If a pair of bars are used (one each face), the position of axial load will depend on the detailing of the bridging plate at the top. A specific packer to ensure load is applied centrally

will keep applying the load in this position during rocking. However, if a flat plate is used, consider the change in force in the two rods (this will depend on their stiffness) and the bearing position on the plate with the wall in its critical displacement position.

For bonded post-tensioning or grouted in bars, assessment should be force-based, with the capacity being the ultimate capacity from the axial load acting at “e” in the diagram above, reduced by half the bearing block on the masonry.

- $M = P \times jd$

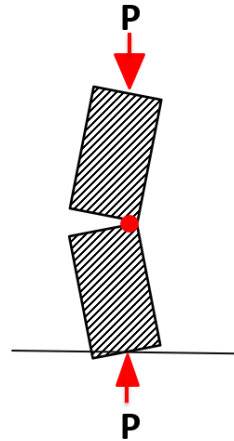


Figure C8B.37: Axial load position on a post-tensioned wall

Appendix C8C: Charts for Assessment of Out-of-Plane Masonry Walls

C8C.1 General Considerations and Approximations

This appendix presents simplified ready-to-use charts for estimation of %NBS for face-loaded URM walls with uniform thickness. The charts have been developed for walls with various slenderness ratios (wall height/thickness) vs Basic Performance Ratio (BPR). The BPR can be converted to %NBS after dividing it by the product of the appropriate spectral shape factor ($C_h(0)$), required to evaluate $C(0)$ for parts, return period factor (R), hazard factor (Z), near-fault factor ($N(T, D)$), and part risk factor (R_p) which have been assigned unit values for developing the charts. The charts are presented for various boundary conditions and ratio of load on the wall to self-weight of the wall.

Refer to Section C8.1.6 and Appendix C8B for symbols and sign conventions.

This appendix includes charts for the following cases:

- one-way vertically spanning walls laterally supported both at the bottom and the top with no inter-storey drift
- vertical cantilever walls.

The following section presents how these charts have been developed and how they should be used.

C8C.2 One-way Vertically Spanning Face-Loaded Walls

Charts for one-way vertically spanning face-loaded walls were developed using exact expressions explained in Section C8.7.5.2. Simplifications that are relevant for very small eccentricities and/or high aspect ratio were not applied in developing these charts.

The charts are presented in Figures C8C.1(a)-(f), C8C.2(a)-(f) and C8C.3(a)-(f) for 110 mm, 230 mm and 350 mm thick walls respectively assuming inter-storey drift of 0.00. The charts have been developed for $e_t = e_o = t/2$ and various values for e_p .

Follow the following steps for estimation of %NBS for a vertically spanning face-loaded wall:

- Identify thickness, t_{Gross} , and height, h , of the wall.
- Calculate slenderness ratio of the wall (h/t_{Gross}).
- Calculate the total self-weight, W , of the wall.
- Calculate vertical load, P , on the wall. This should include all the dead load and appropriate live loads on the wall from above.
- Calculate P/W .
- Calculate eccentricities (e_b and e_p). e_b could be $t/2$ or 0, whereas e_p could be $\pm t/2$ or 0. To assign appropriate values, check the base boundary condition and location of P on the wall. Calculation of effective thickness, t , is not required.
- Refer to the appropriate charts (for appropriate e_b and e_p , P/W and inter-storey drift).

- Estimate Basic Performance Ratio (BPR) from the charts.
- Refer to NZS 1170.5:2004 for $C_h(0)$ required to evaluate $C(0)$ for parts, $R, Z, N(T, D)$, C_{Hi} and R_p . For estimation of C_{Hi} , h_i is height of the mid height of the wall from the ground.
- $\%NBS = \frac{\text{Basic Performance Ratio from charts for } h/t}{C_h(0)RZN(T,D)C_{Hi}R_p}$

Example detailed calculations are provided in the next section both to illustrate how the values of BPR in the charts have been obtained and to show how BPR values can be used to calculate %NBS.

C8C.2.1 Explanatory calculations

To demonstrate the calculation of %NBS for one wall, the following three walls are analysed. Firstly, BPR is obtained for each wall from the provided charts. As an alternative and for the purpose of demonstration, the BPR is also calculated separately using the detailed procedure. Once BPR has been obtained, %NBS is calculated for one of the walls assuming several seismicity regions.

Wall	t_{Gross} (mm)	h (mm)	h/t_{Gross}	$h_b=h_t$ (mm)	$y_b=y_t$ (mm)	P/W	e_b/t	e_p/t
1	110	2750	25	1375	687.5	1	0.5	0.5
2	230	3220	14	1610	805.0	5	0.5	0
3	350	3850	11	1925	962.5	3	0.5	-0.5

Solution for BPR by using design charts in the attachments

For the given h/t_{Gross} (the 4th column) and utilising relevant charts, BPR can be obtained:

Wall	BPR
1	0.34
2	1.48
3	0.93

Alternative solution for BPR using the detailed procedure

Following **Steps 1 to 4** of detailed procedure (Section C8.8.5), the table below can be populated with basic wall properties:

Wall	t (mm)	W (kN)	W_b and W_t (kN)	P (kN)	e_b (mm)	e_p (mm)	e_o^* (mm)	e_t^* (mm)
1	104.5	5.93	2.96	5.93	52.2	52.2	52.2	52.2
2	195.5	14.52	7.26	72.62	97.8	0	97.8	97.8
3	315.0	26.42	13.21	79.28	157.5	-157.5	157.5	157.5

* Note that both e_o and e_t are assumed to be equal to $+0.5t$ for regular walls (refer Figure C8B.1)

Steps 5 and 6:

Equation C8.11, Equation C8.12, and Equation C8.13 or the simplified versions in Table C8.12 are used to calculate, respectively, instability displacement (Δ_i), b , and a . Then, maximum usable deflection, Δ_m is calculated as 0.6 times Δ_i . Note that for Wall 3, e_p is negative, and therefore, unlike for Walls 1 and 2, parameters a , b , and Δ_i cannot be calculated using Table C8.12. Results are summarised in the first 5 columns of the Table below.

1	2	3	4	5	6	7	8	9	10
Wall	b	a	Δ_i (mm)	Δ_m (mm)	J (kg.m ²)	T_p (sec)	$C_i(T_p)$	γ	BPR
1	1860	24470	104.5	62.7	416.3	0.53	1.91	1.37	0.34
2	24140	257230	151	90.6	1994	0.36	2.00	0.96	1.48
3	33300	356110	180.0	108	4493	0.46	2.00	1.11	0.93

Step 7: Rotational mass moment of inertia, J , is calculated from Table C8.12 (except when $e_p < 0$) or Equation C8.15 (also Equation C8B.8). The result is inserted into Equation C8.14 to calculate wall period, T_p . Note that Equation C8.23 should NOT be used to estimate Period unless h/t is extremely high. Further guide on calculation of J_{bo} and J_{to} that are part of J is available in Equation C8B.11.

The results for J and T_p are summarised in Columns 6 and 7 of the above Table.

Step 8: $C_i(T_p)$ are calculated using the shaded text under Step 8 in C8.8.5.2. Results are summarised in Column 8.

Step 9: Calculate participation factor, γ , is calculated using Equation C8.17 or Table C8.12 except for $e_p < 0$. Values are listed under Column 9.

Basic Performance Ratio (BPR) as defined in Appendix is calculated as:

$$BPR = (0.60)(\Delta_i) / \{g \cdot \gamma \cdot [T_p / (2\pi)]^2 \cdot C_i(T_p)\}$$

with the results listed in the last column of the above Table. It can be found that these values match the values that were obtained earlier from the design charts.

Assessment of %NBS

$$\%NBS = 100 \cdot BPR / (C_h(0) \cdot R \cdot Z \cdot N(T, D) \cdot C_{Hi} \cdot R_p)$$

For Wall 2, %NBS is calculated.

Assumptions:

- wall is situated in the top-storey of a two-storey building;
- storey heights are 4.5 m in the ground storey and 3.22 m in the upper-storey;
- Site Class: A;
- Annual Probability of Exceedance of earthquake: 1/500 ($R = 1$); and

Near-fault effects are irrelevant; $N(T,D)=1$.

The wall can be categorised as P.1 based on Table 8.1 of NZS 1170.5, and therefore, $R_p = 1$.

Height of wall attachment, $h_i = 4.5 + 3.22/2 = 6.11$ m

$C_{Hi} = 1 + 6.11/6 = 2.02$ (NZS 1170.5; Clause 8.3, Equation 8.3(1))

$C_h(0) = 1$ (bracketed value in NZS 1170.5 Table 3.1)

$\%NBS = 100 \times BPR / (C_h(0) \cdot R \cdot Z \cdot N(T,D) \cdot C_{Hi} \cdot R_p) = 148 / (2.02 \cdot Z) = 0.733/Z$

For regions with $Z = 0.15, 0.25$, and 0.40 , $\%NBS$ can be calculated as, respectively, 489%, 293%, and 183%:

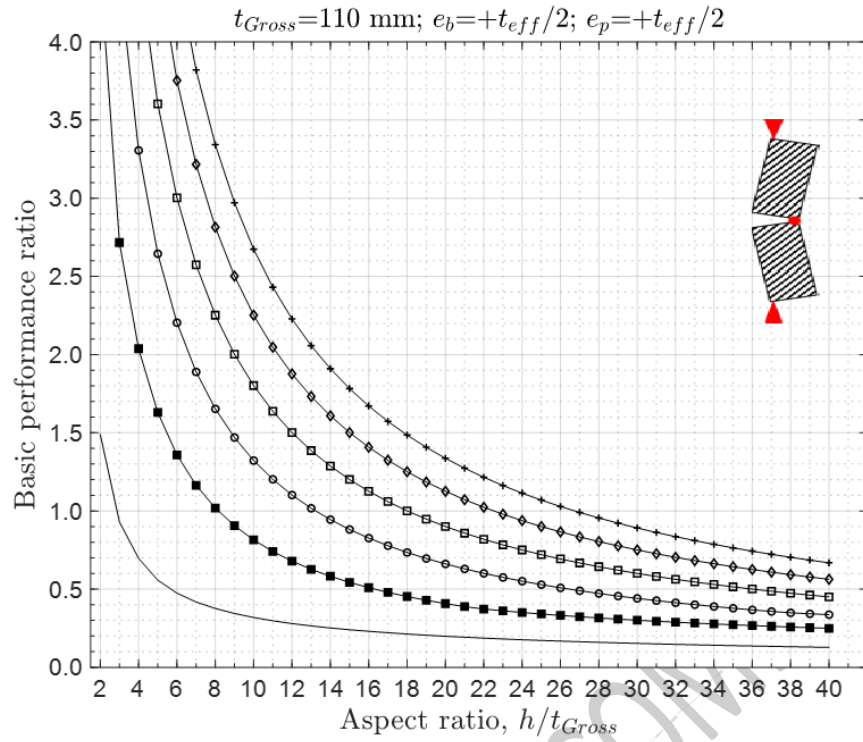
Wall	BPR	C_{Hi}	$N(T,D)$	R_p	$C_h(0)$	R	Z	$\%NBS$
2	1.48	2.02	1	1	1	1	0.15	489
2	1.48	2.02	1	1	1	1	0.25	293
2	1.48	2.02	1	1	1	1	0.40	183

C8C.3 Vertical Cantilevers

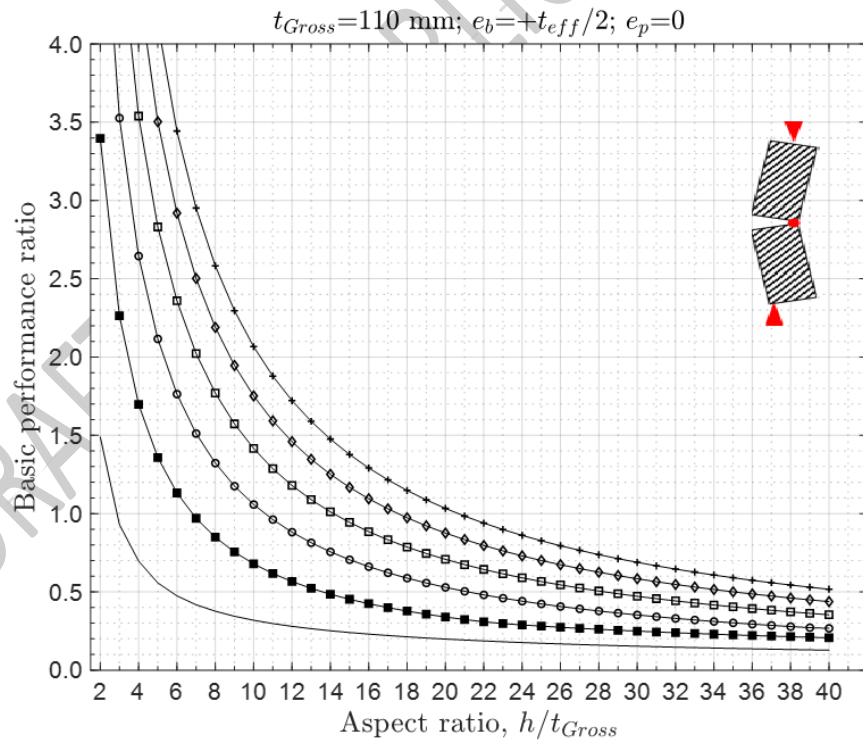
Charts for one-way cantilever walls are presented in Figures C8C.7(a)-(c), C8C.8(a)-(c) and C8C.9(a)-(c) for 110 mm, 230 mm and 350 mm thick walls respectively.

Follow the following steps for estimation of $\%NBS$ of a face-loaded cantilever wall:

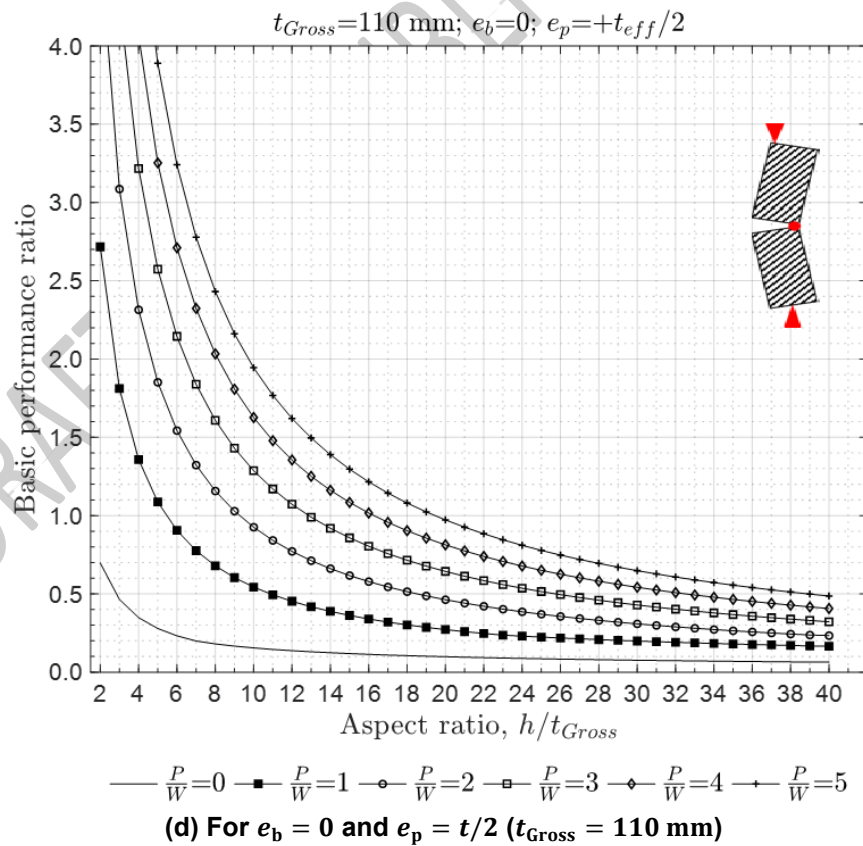
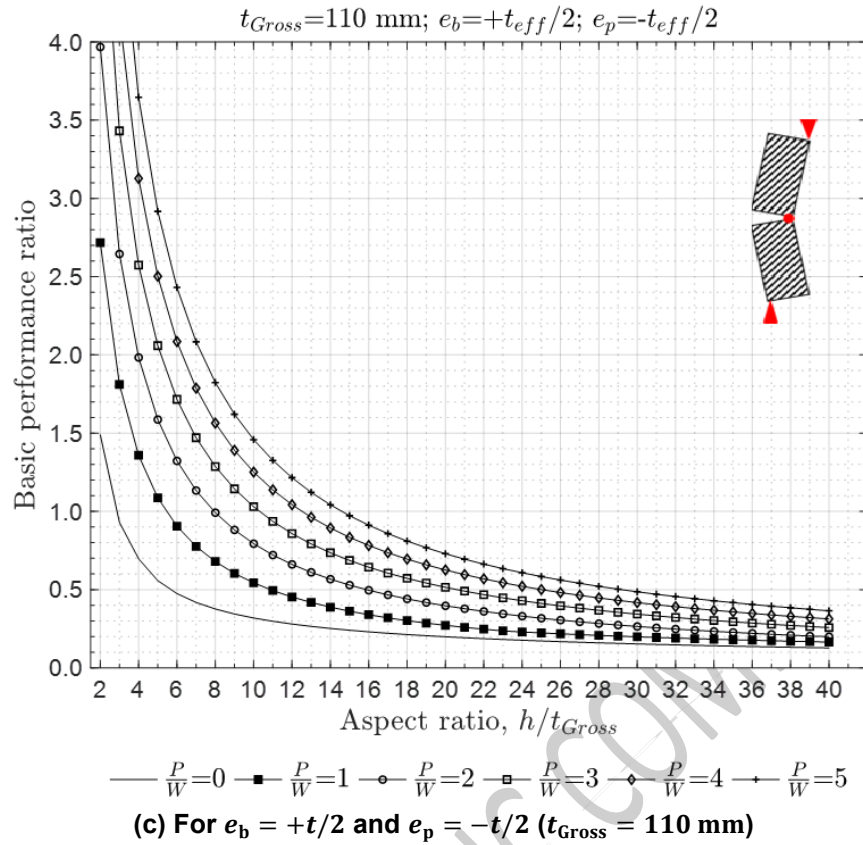
- Identify thickness, t_{Gross} , and height, h , of the wall.
- Calculate slenderness ratio of the wall (h/t_{Gross}).
- Calculate total self-weight, W , of the wall above the level of cantilevering plane.
- Calculate vertical load, P , on the wall, if any. This should include all the dead load and appropriate live loads on the wall from above.
- Calculate P/W .
- Calculate eccentricity, e_p , for loading P . e_p could be $\pm t/2$ or 0, which depends upon location of P on the wall. Calculation of effective thickness, t , is not required.
- Refer to the appropriate charts (for appropriate e_p and P/W).
- Estimate Basic Performance Ratio (BPR) from the charts. Interpolation between plots may be used as necessary.
- Refer NZS 1170.5:2004 for $C_h(0)$ required to evaluate $C(0)$ for parts, $R, Z, N(T, D)$, C_{Hi} and R_p . For estimation of C_{Hi} , h_i shall be taken as height of the base of the cantilever wall.
- $\%NBS = \frac{\text{Basic Performance Ratio from charts for } h/t}{C_h(0) R Z N(T,D) C_{Hi} R_p}$

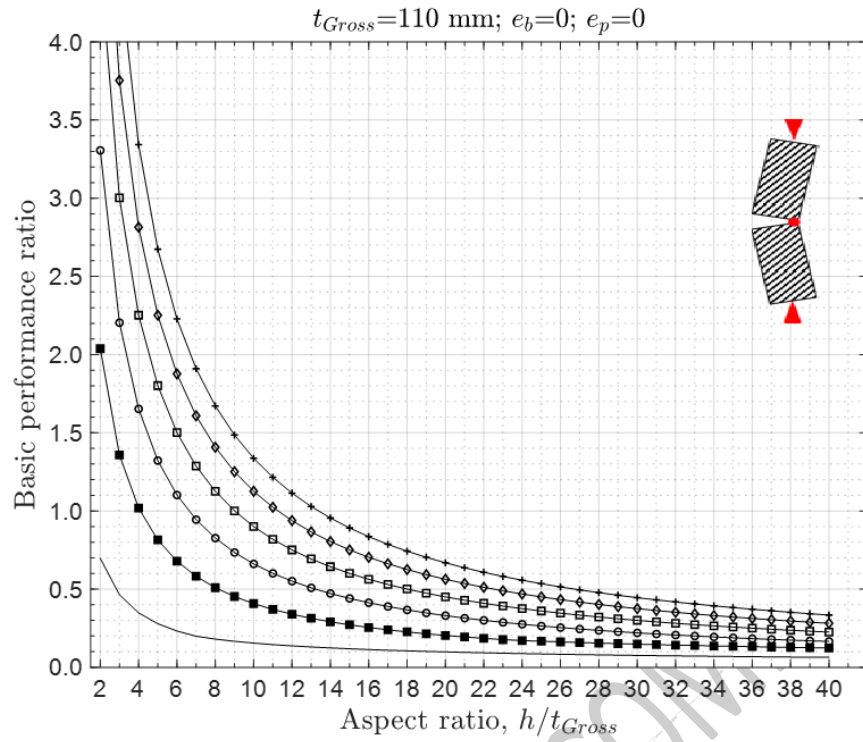


(a) For $e_b = +t/2$ and $e_p = +t/2$ ($t_{Gross} = 110 \text{ mm}$)

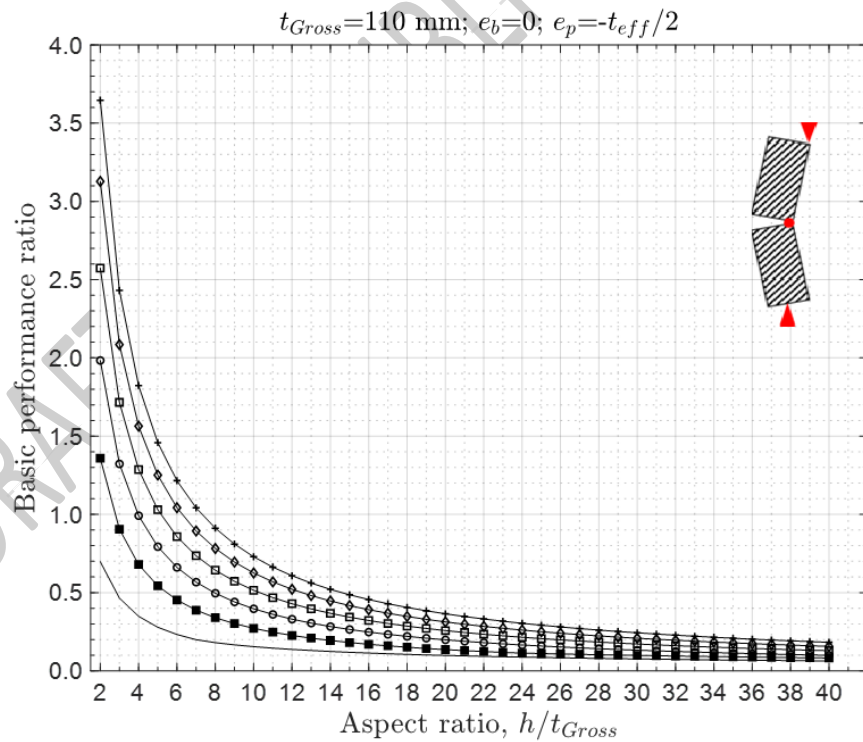


(b) For $e_b = +t/2$ and $e_p = 0$ ($t_{Gross} = 110 \text{ mm}$)



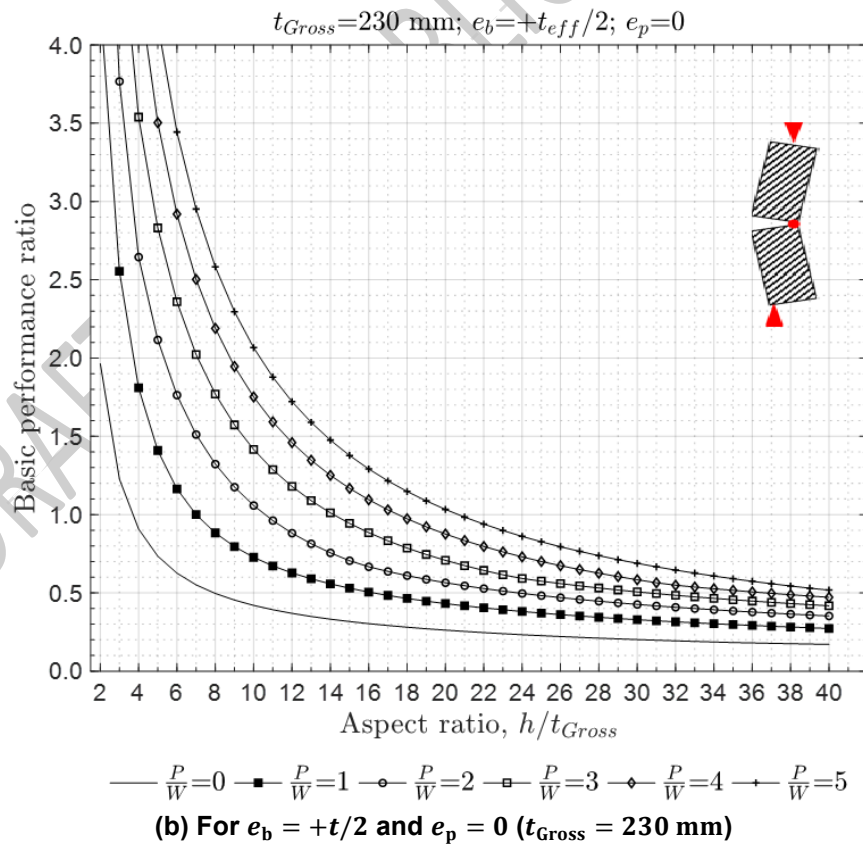
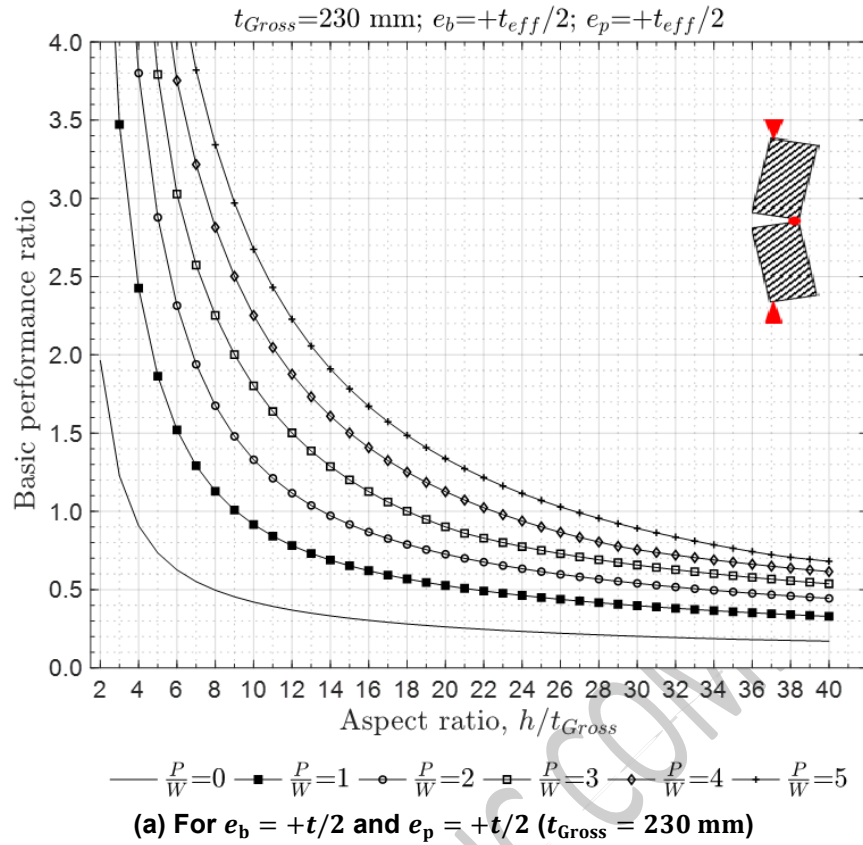


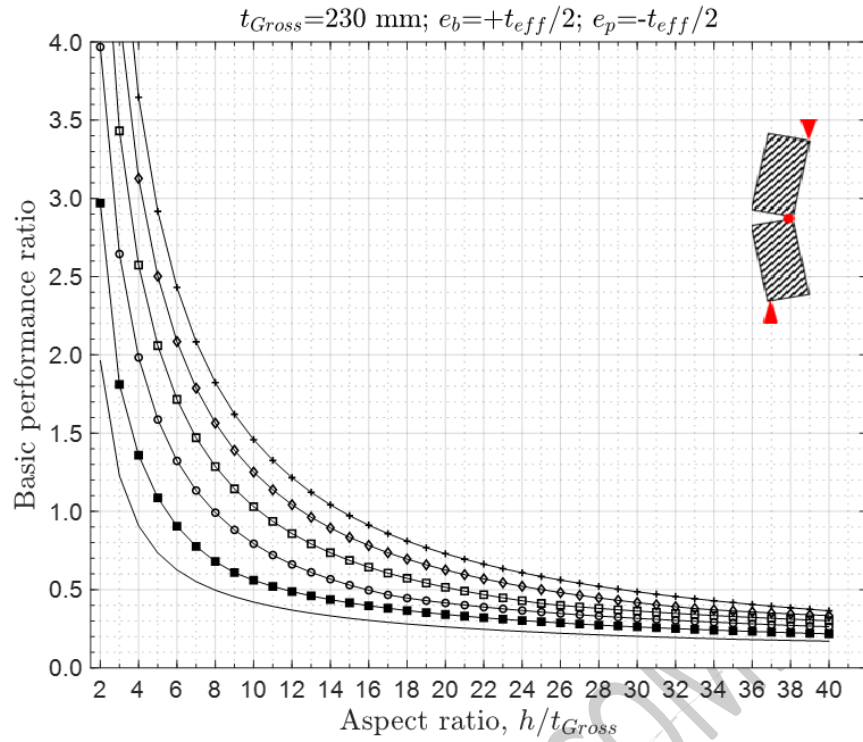
(e) For $e_b = 0$ and $e_p = 0$ ($t_{Gross} = 110 \text{ mm}$)



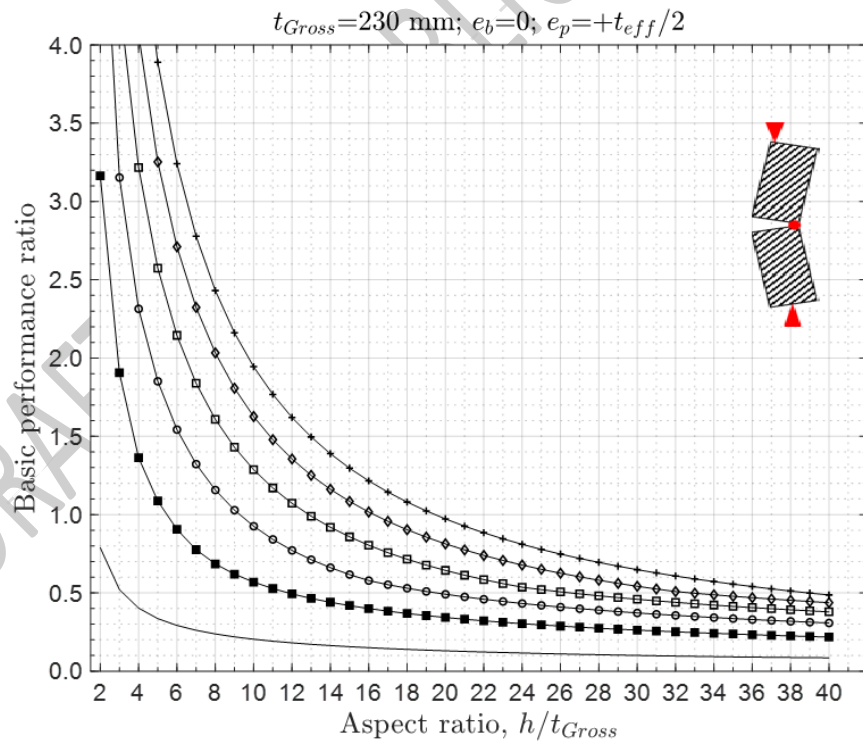
(f) For $e_b = 0$ and $e_p = -t/2$ ($t_{Gross} = 110 \text{ mm}$)

Figure C8C.1: 110 mm thick one-way vertically spanning face-loaded walls ($\Psi = 0$)





(c) For $e_b = +t/2$ and $e_p = -t/2$ ($t_{Gross} = 230 \text{ mm}$)



(d) For $e_b = 0$ and $e_p = t/2$ ($t_{Gross} = 230 \text{ mm}$)

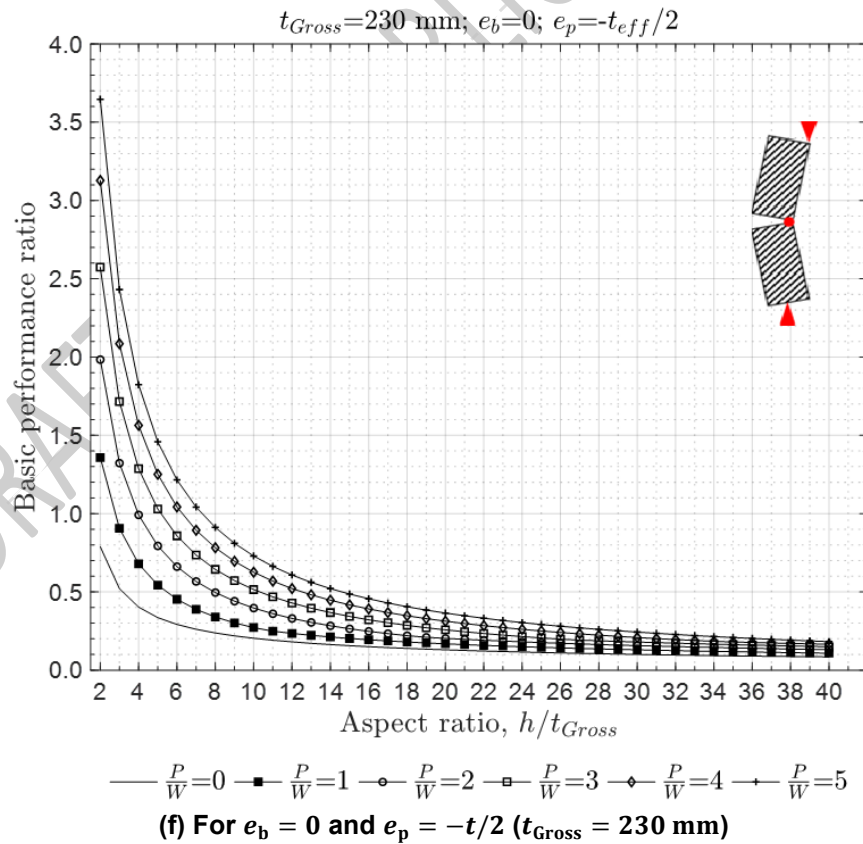
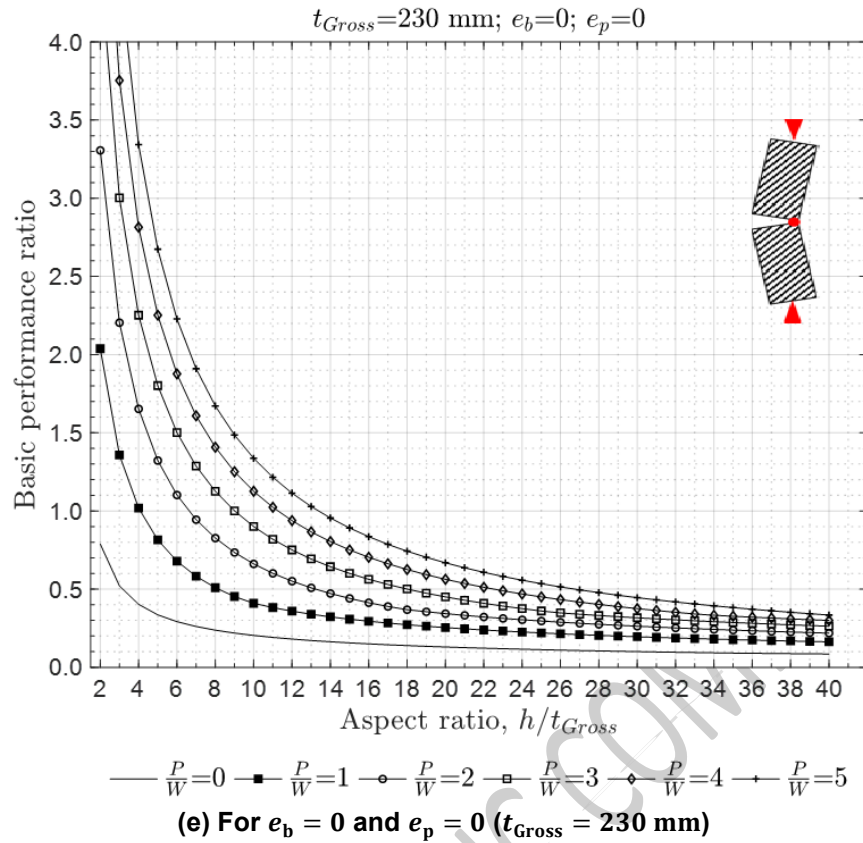
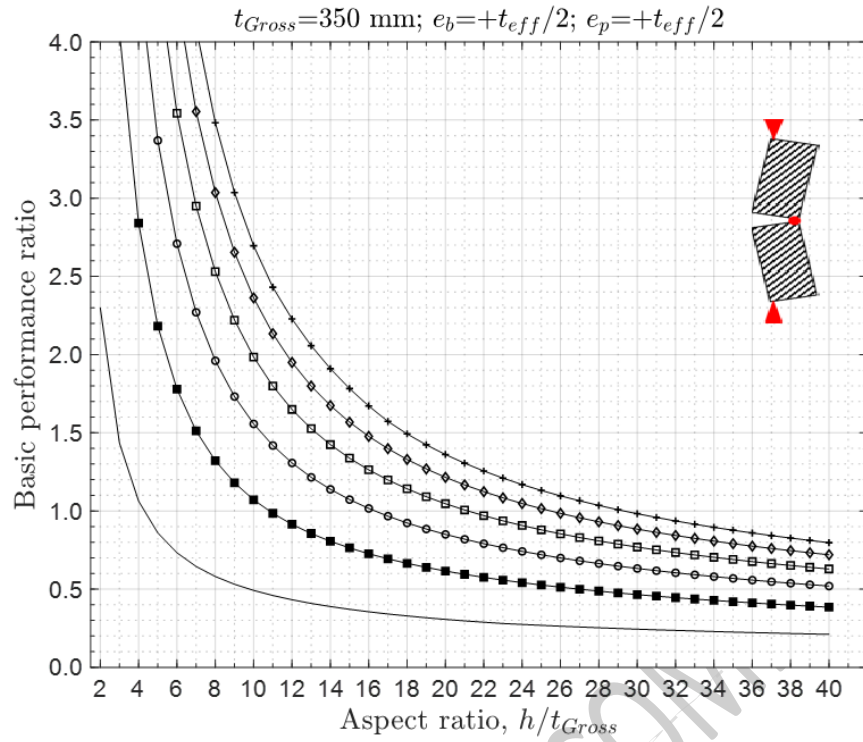
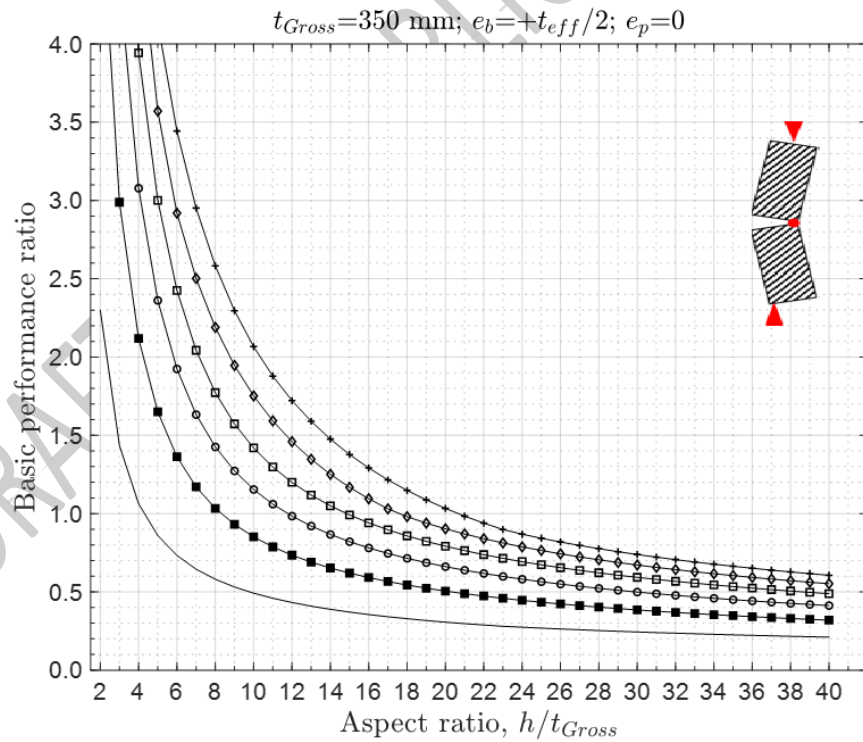


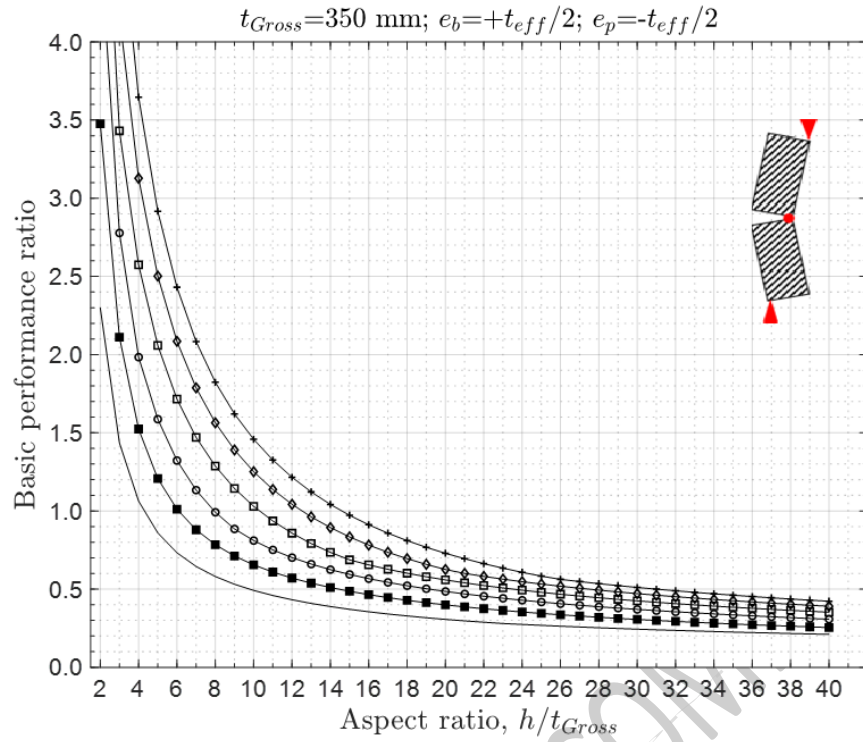
Figure C8C.2: 230 mm thick one-way vertically spanning face-loaded walls ($Y = 0$)



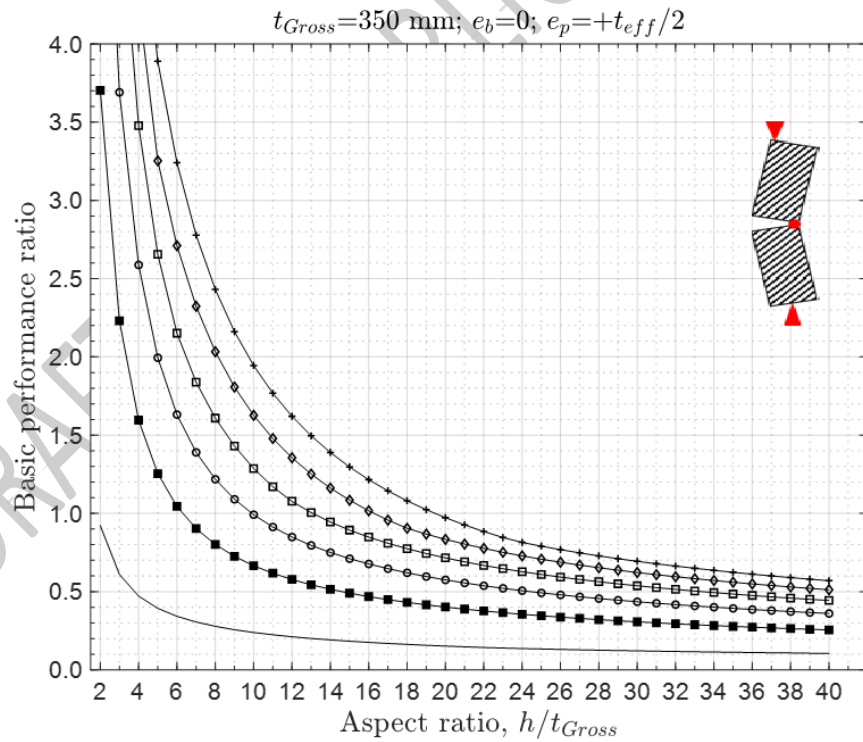
(a) For $e_b = +t/2$ and $e_p = +t/2$ ($t_{Gross} = 350 \text{ mm}$)



(b) For $e_b = +t/2$ and $e_p = 0$ ($t_{Gross} = 350 \text{ mm}$)



(c) For $e_b = +t/2$ and $e_p = -t/2$ ($t_{Gross} = 350 \text{ mm}$)



(d) For $e_b = 0$ and $e_p = t/2$ ($t_{Gross} = 350 \text{ mm}$)

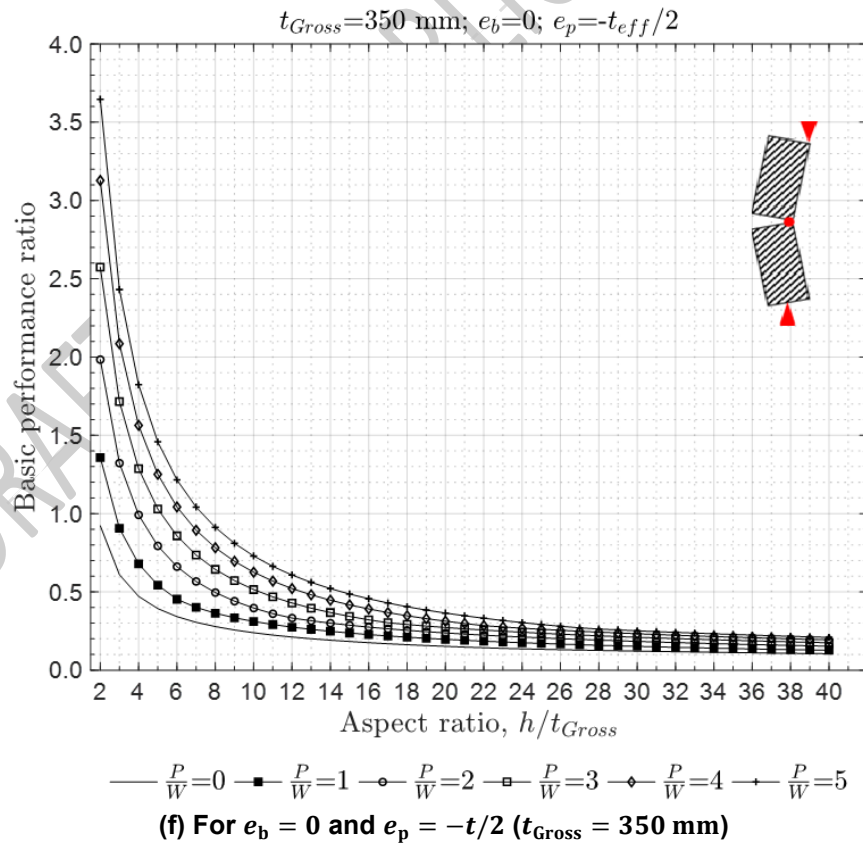
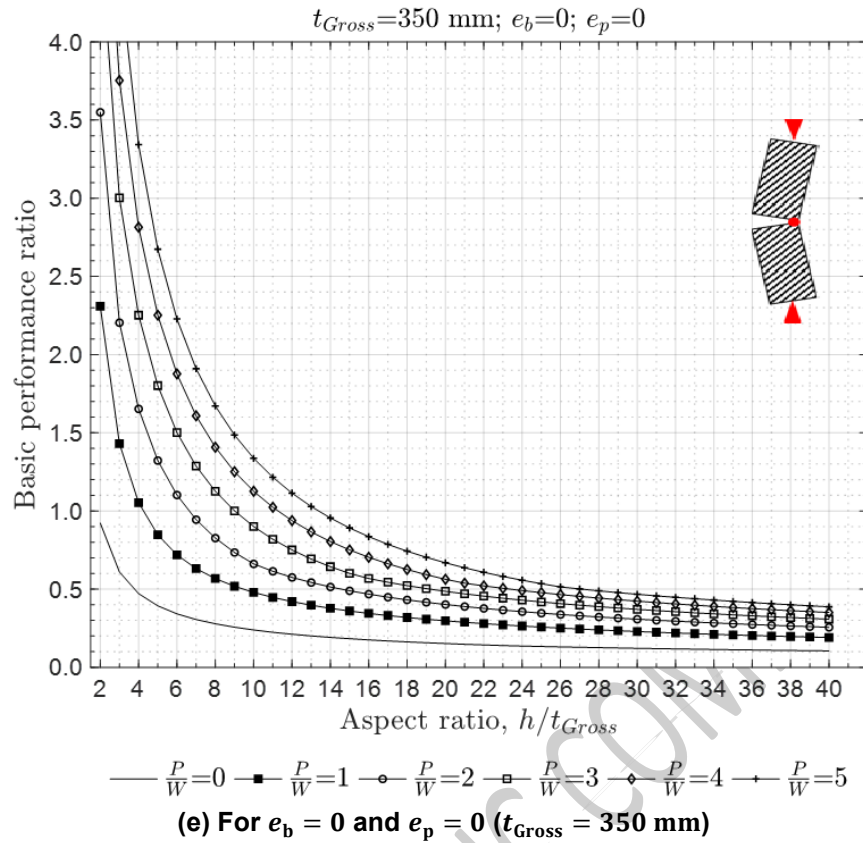
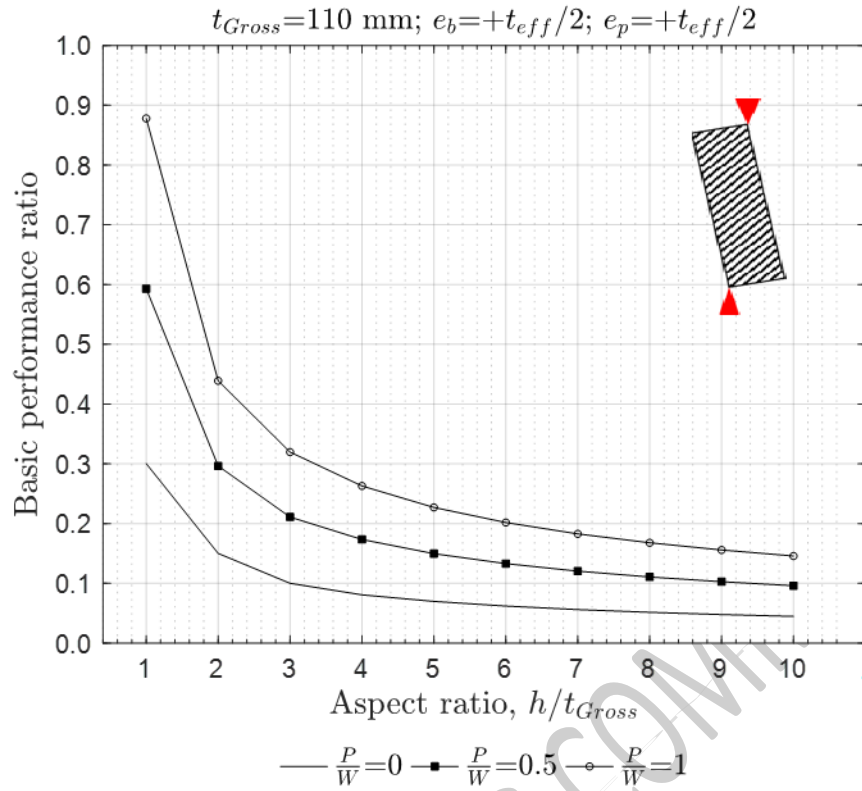
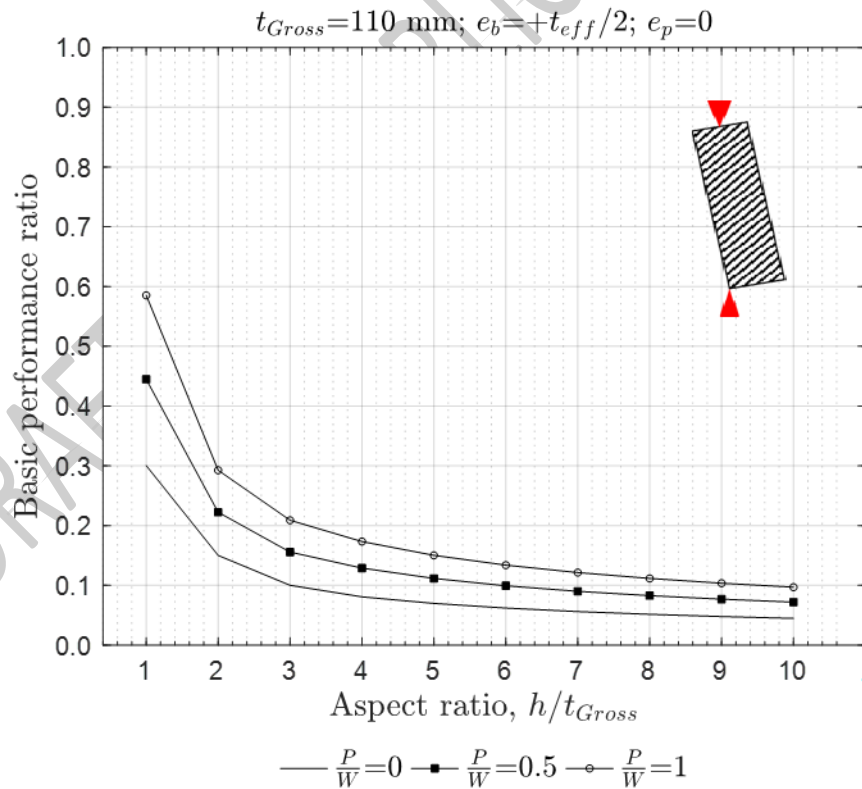


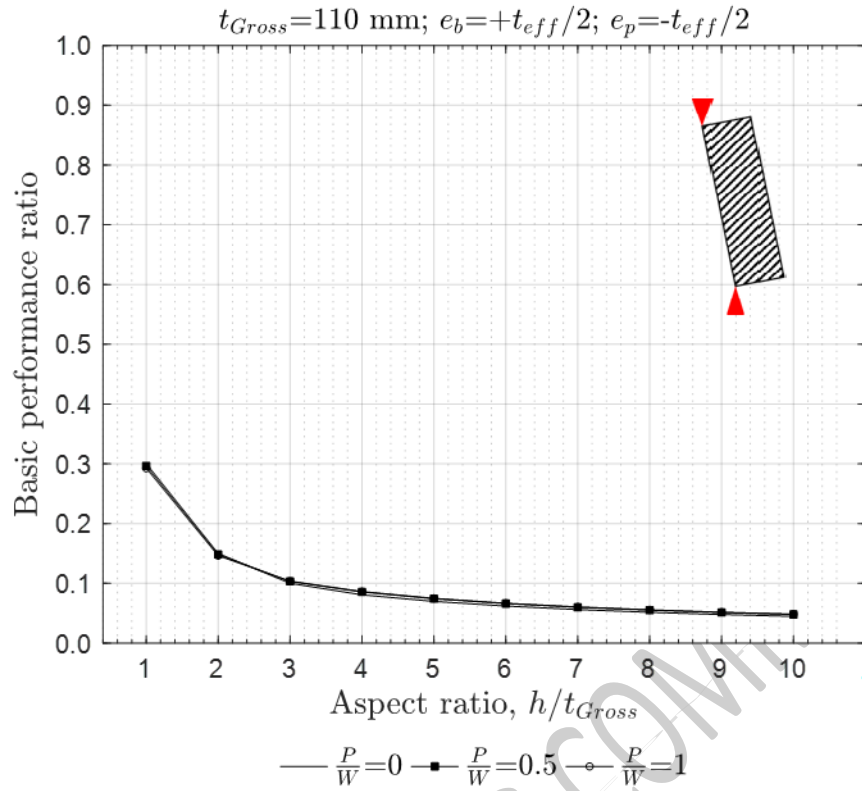
Figure C8C.3: 350 mm thick one-way vertically spanning face-loaded walls ($\Psi = 0$)



(a) For $e_b = +t/2$ and $e_p = +t/2$ ($t_{Gross} = 110 \text{ mm}$)

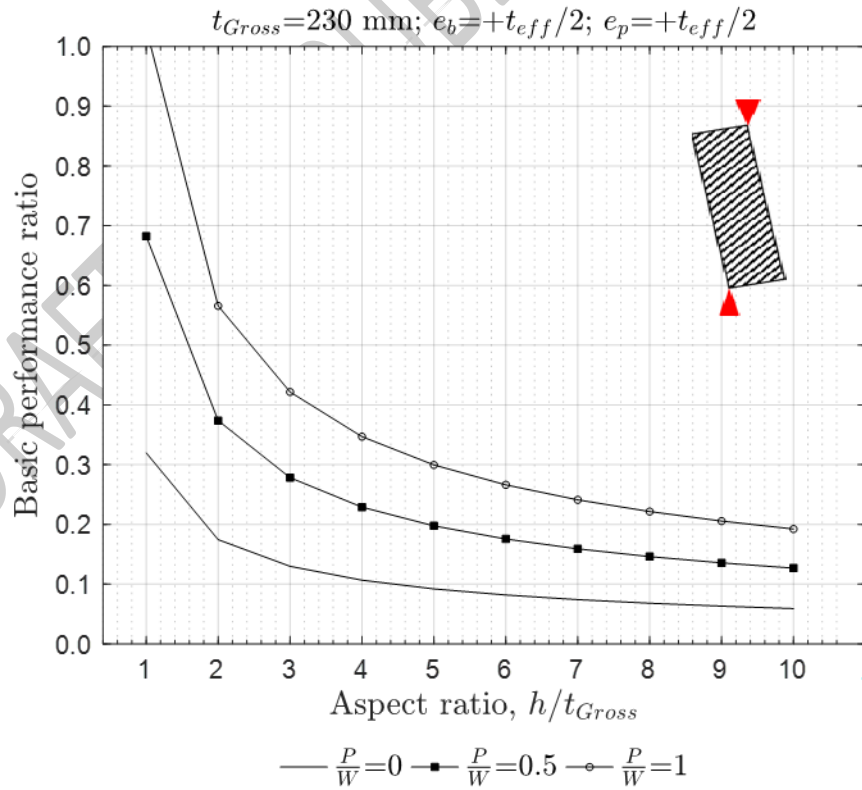


(b) For $e_b = +t/2$ and $e_p = 0$ ($t_{Gross} = 110 \text{ mm}$)

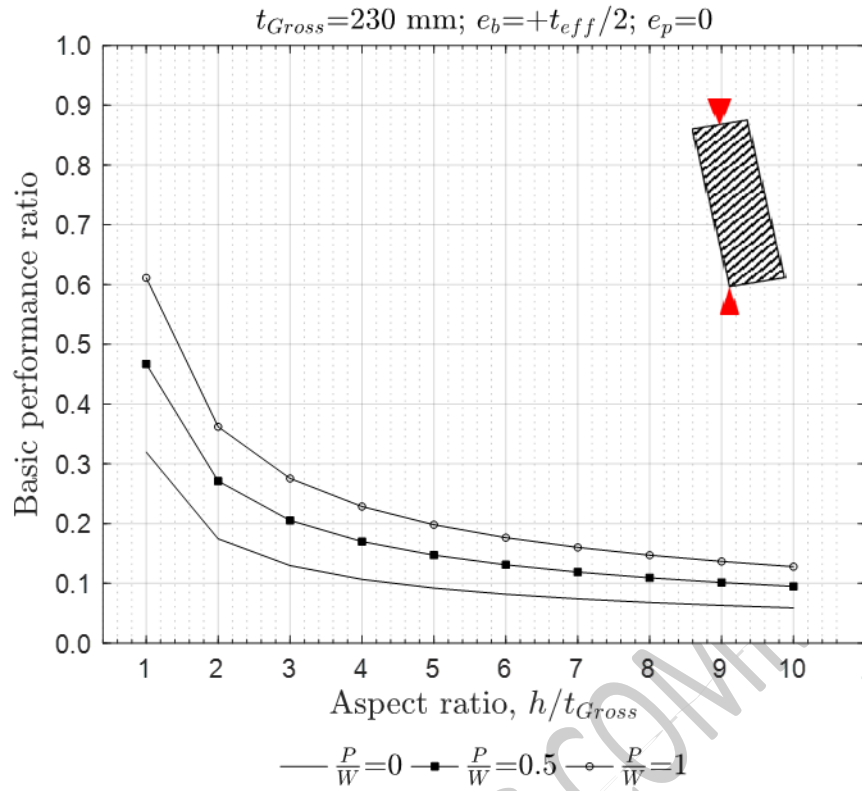


(c) For $e_b = +t/2$ and $e_p = -t/2$ ($t_{Gross} = 110 \text{ mm}$)

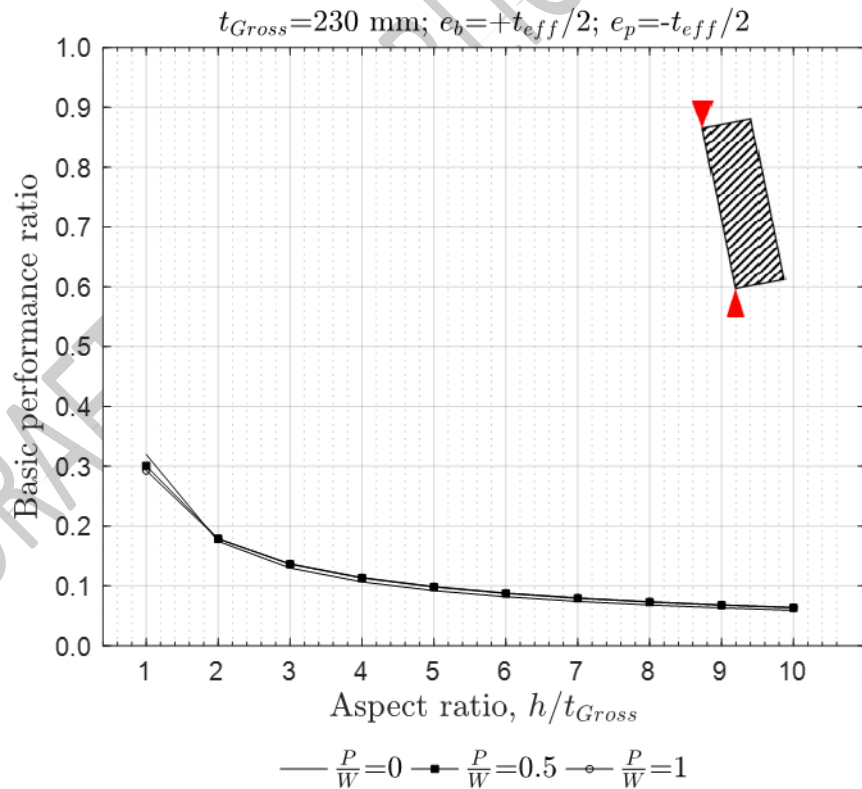
Figure C8C.4: 110 mm thick cantilever wall



(a) For $e_b = +t/2$ and $e_p = +t/2$ ($t_{Gross} = 230 \text{ mm}$)

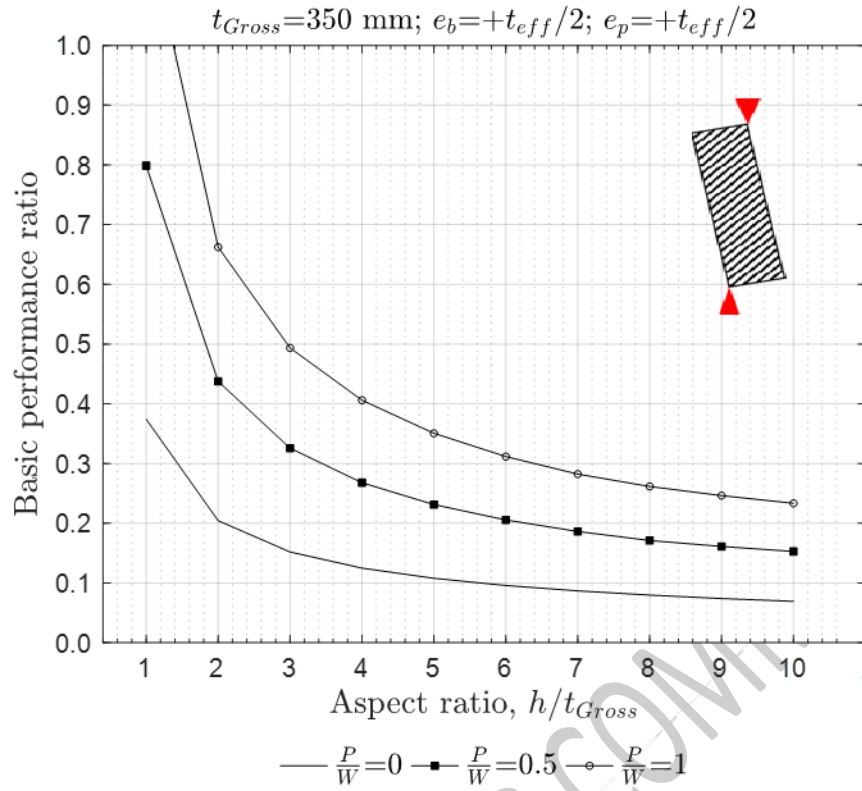


(b) For $e_b = +t/2$ and $e_p = 0$ ($t_{Gross} = 230 \text{ mm}$)

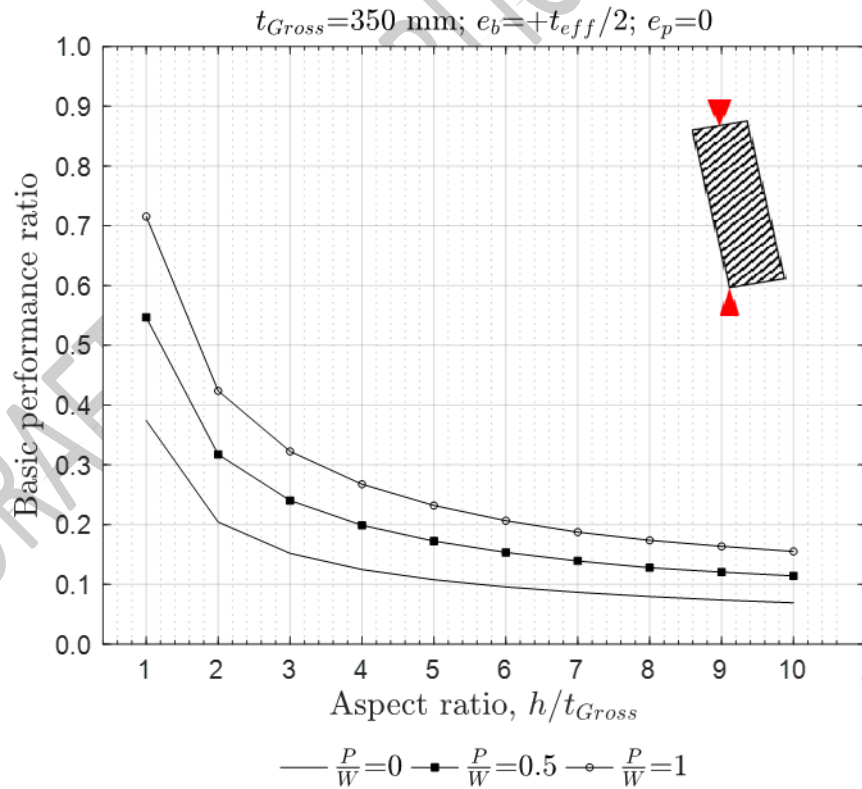


(c) For $e_b = +t/2$ and $e_p = -t/2$ ($t_{Gross} = 230 \text{ mm}$)

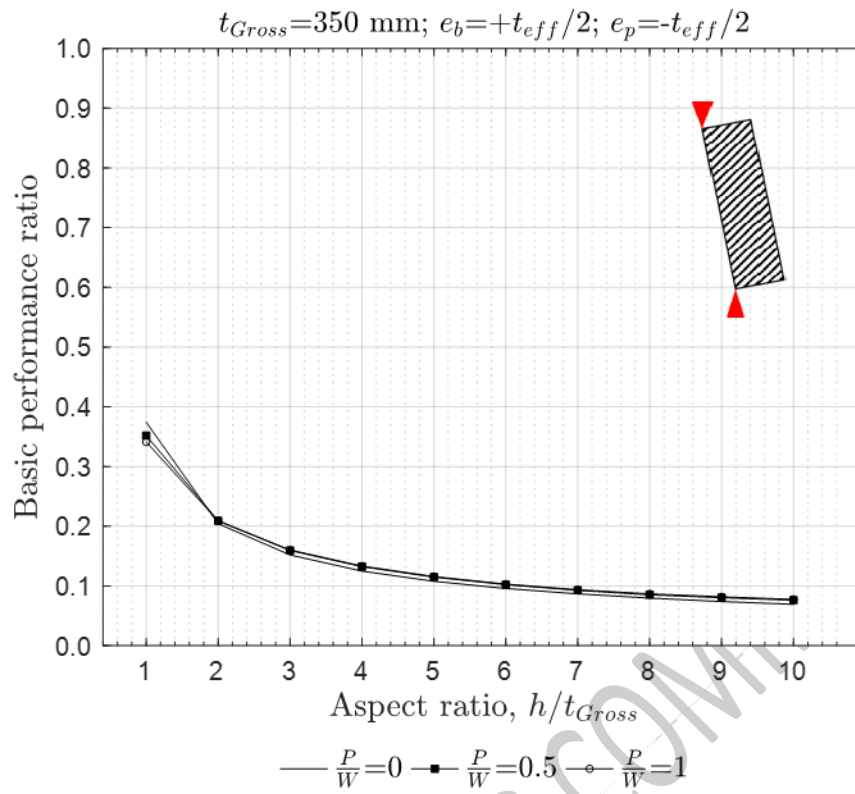
Figure C8C.5: 230 mm thick cantilever wall



(a) For $e_b = +t/2$ and $e_p = +t/2$ ($t_{Gross} = 350 \text{ mm}$)



(b) For $e_b = +t/2$ and $e_p = 0$ ($t_{Gross} = 350 \text{ mm}$)



(c) For $e_b = +t/2$ and $e_p = t/2$ ($t_{Gross} = 350 \text{ mm}$)

Figure C8C.6: 350 mm thick cantilever wall